An investigation of endoderm to mesoderm signalling in gut development

Thesis submitted for the degree of
Doctor of Philosophy
at the University of Leicester

by

Emma Jane Stringer (B.Sc.Hons. Liverpool)
Department of Biochemistry
University of Leicester

July 2008

Contents

Abbreviations

AIP	anterior intestinal portal
AJB	Alec Jeffrey's PCR Buffer
amp^R	ampicillin resistance
BLAST	Basic local alignment search tool
BM	basement membrane
BMP	bone morphogenetic protein
bp	base pairs
CBCs	crypt base columnar cells
CIP	caudal intestinal portal
cDNA	complementary DNA
CRC	colorectal cancer
C_T	threshold cycle
DIG	digoxigenin
DMEM	Dulbecco's Modified Eagle's Medium
DMSO	dimethyl sulphoxide
DNA	deoxyribonucleic acid
dpc	days post coitum
DSB	downstream binding site
DTA	diphtheria toxin A
DTT	dithiothreitol
ES cell	embryonic stem cell
EST	expressed sequence tag
FBS	foetal bovine serum
FRT	Flippase recognition target
h	hour(s)
HIEC	human intestinal epithelial crypt
Hsp90	heat shock protein 90
Hox	homeobox
ICM	inner cell mass
IMS	industrial methylated spirits

IP	intraperitoneal
LA	left arm
LB	Luria Bertani
LIF	leukaemia inhibitory factor
*lox*P	locus of crossover (x) in P1 bacteriophage
LRC	label retaining cell
M cells	microfold cells
MA	middle arm
MAPK	mitogen-activated protein kinase
MEFs	mouse embryonic fibroblasts
min	minute(s)
Neo^R	neomycin resistance
PBS	phosphate buffered saline
PCR	polymerase chain reaction
PFA	paraformaldehyde
qPCR	quantitative PCR
RA	right arm
RNA	ribonucleic acid
RT-PCR	reverse transcriptase PCR
S60	serine 60
sec	second(s)
SDS	sodium dodecyl sulphate
SSC	sodium chloride-sodium citrate
SSE	stratified squamous epithelium
TAE	tris-acetate-EDTA
TCFs	T-cell factors
TE	tris-EDTA
TM	tamoxifen
v/v	volume to volume
WT	wild type
w/v	weight to volume

Acknowledgements

I would first like to thank my supervisors Dr. Catrin Pritchard and Prof. Felix Beck for their invaluable advice and guidance throughout this project. Thanks also go to all the members of the Biomedical Services involved in this project and Jenny Edwards for her histology expertise. I would also like to express my gratitude to Dr Jacqueline Deschamps who has always been available for help and assistance. I would like to thank all members of Lab 3/43 both past and present. Particular thanks go to Vicki, Catherine, Susan, Linda, Alison, Kath and Katerina for their continued support, advice and offers of coffee! A special thank you to my Mum, Dad and my brother Dan for their immense support during the tough times. I finally want to thank Mark for his constant and unrelenting support. This thesis is dedicated to the memory of my Nan and Grandpa Stevenson.

Abstract

An investigation of endoderm to mesoderm signalling in gut development

Emma J. Stringer

It has been suggested that the intestinal endoderm is responsive to signals received from underlying mesoderm, indicating cross-talk between the layers. *Cdx2* mutant mice develop heterotopias of stomach-type epithelium within the paracaecal region of the intestine. They are therefore an ideal *in-vivo* model in which to study whether the loss of endodermal gene expression required for intestinal development leads to stomach-specific mesodermal gene expression.

In this study, *Sox2*, a stomach endoderm-specific marker, was used to detect gastric heterotopias in *Cdx2* mutant embryonic intestine using whole-mount *in-situ* hybridisation. The nature of the underlying mesoderm was investigated using a second marker, *Barx1,* which is known to be specifically expressed in the stomach mesoderm. RT-PCR was used to detect low levels of *Barx1* expression in $Cdx2^{+/-}$ caecum samples. Further investigation using *in-situ* hybridisation techniques indicated regions of *Barx1* expression in a similar distribution to the regions detected using the *Sox2* probe. This finding confirms that the mesoderm underlying the *Cdx2* mutant gastric heterotopias expresses a stomach-specific gene and therefore that the mesoderm is responsive to endodermal signals.

It has been suggested that $Cdx2^{+/-}$ mice do not develop gastric-type intestinal heterotopias postnatally. If proven, this would indicate that intestinal stem cell potential becomes limited at some point during development and prevents the epithelium responding to a postnatal loss of Cdx2 protein. A conditional *Cdx2* mouse model is required in order to investigate this hypothesis. The creation of this mouse model formed the second part of this project. Following creation of a targeting vector, transfection into ES cells and injection into blastocysts, chimeric mice were obtained. These mice were successfully bred for germline transmission.

1. Introduction

1.1 Anatomy of the adult gut

In the adult mouse, the gut is comprised of the oral cavity, pharynx, oesophagus, stomach, small intestine (encompassing the duodenum, jejunum and ileum), large intestine (including the caecum proximally) and colon (Figure 1.1).

Along the proximal-distal axis of the gut, the morphology of the tissue changes to meet the altering requirements of the digestive system. Overall, however, it can be generalised that the gut tube comprises of four layers. The inner most layer, adjacent to the lumen, is the mucosa. This consists for the most part of a simple columnar epithelial mucosal layer, the lamina propria (connective tissue containing glands) and the underlying connective tissue as well as the muscularis mucosa (a thin smooth muscle layer). Surrounding the mucosa is the submucosa, containing connective and vascular tissue along with the Meissner's plexus of nerves. This plexus regulates the digestive glands. The adjacent layer is the muscularis externa, including two smooth muscle layers (one circular and one longitudinal to the gut) and the Auerbach's plexus situated between them. This plexus regulates and controls gut motility. It is these muscle layers in combination with Auerbach's plexus that allow the peristaltic action of the gut. The outermost layer is the adventia which is a thin mesothelial layer (Figure 1.2) (Smith et al., 2000).

1.2 The developing embryo

1.2.1 Embryological origin of the germ layers

Three germ layers exist: the ectoderm, the endoderm and the mesoderm. The formation of the developing embryo varies across phyla; this discussion concentrates upon mammals.

In the mouse, by 6 days post coitum (dpc), the embryonic and extra-embryonic components of the egg cylinder can be distinguished. The egg cylinder is enveloped by a layer of primitive endoderm, although the appearance of this layer differs over the embryonic and extra-embryonic regions. The extra-embryonic part of the egg cylinder will go on to develop into the yolk sac, allantois, umbilical cord and other structures, but the development of these will not be discussed further. The embryonic component, at this point, is bilayered with both an outer endodermal layer and an

Figure 1.1 Basic anatomical layout of the adult mouse gut. (Adapted from Smith et al., 2000).

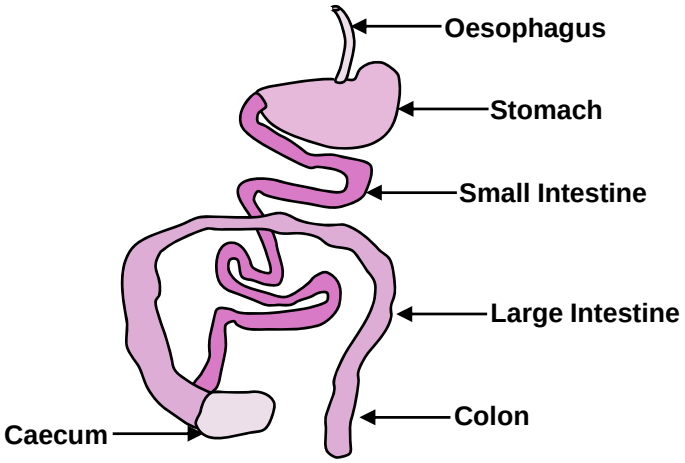

Figure 1.2 General Gut Histology. The diagram below demonstrates the different major layers within the length of the gut. This is, however, a basic summary as the layers change in morphology along the length of the gut. (Adapted from http://trc.ucdavis.edu/mjguinan/apc100/modules/Digestive/mammal/system1/system.html).

Unable to gain third party permission

inner ectodermal layer (the epiblast) (reviewed in Kaufman and Bard, 1999). It is the epiblast that will become the embryo and also contribute to some of the extra-embryonic membranes (Figure 1.3).

The formation of the primitive streak at 6.5dpc is the first indication of the future anterior-posterior axis of the developing embryo and signals the start of gastrulation. Gastrulation is defined as the time at which pluripotent cells of the epiblast divide, differentiate, and rearrange themselves into three distinct germ layers: ectoderm, mesoderm, and endoderm (reviewed in Wells and Melton, 1999).

The primitive streak remains an enigmatic region. It is known that epiblast cells adjacent to the streak will migrate through it, receiving cellular signalling information as they pass. The streak first appears in the posterior region of the developing embryo. The epiblast defines the region that will become the dorsal side of the embryo. Embryonic orientation is applied on this basis, despite the fact that the cells present will subsequently migrate away. The primitive streak slowly spreads towards the most distal region of the epiblast, where the cells condense.

The fate of the migrating cells is thought to be determined upon passage through the streak. The primitive streak migrates distally and as it does, a population of mesendodermal cells appears adjacent to the streak. The mesendoderm has the ability to form either endoderm or mesoderm, dependent upon cellular signalling received during migration through the streak (Kinder et al., 2001, Tada et al., 2005).

Some of these mesendodermal cells, of epiblast origin, migrate through the primitive streak to position themselves between the inner ectoderm and the outer primitive endoderm, thus forming the mesodermal layer (Figure 1.4) (reviewed in Beddington and Robertson, 1999). Two regions, however, at either end of the embryonic anterior-posterior axis, do not have an intervening layer of mesoderm, as these will become the buccopharyngeal and cloacal membranes positioned at either end of the gut tube (reviewed in Kaufman and Bard, 1999).

The definitive endoderm also arises from the mesendoderm (Figure 1.5) and gradually displaces the primitive endoderm (Figure 1.6). The definitive endoderm

Figure 1.3 Diagram of a 6dpc mouse embryo. The epiblast (light blue) can be seen enveloped in the visceral endoderm (yellow). (Taken from Wolpert et al., 1998). (A; anterior, P; posterior, Pr; proximal, D; distal)

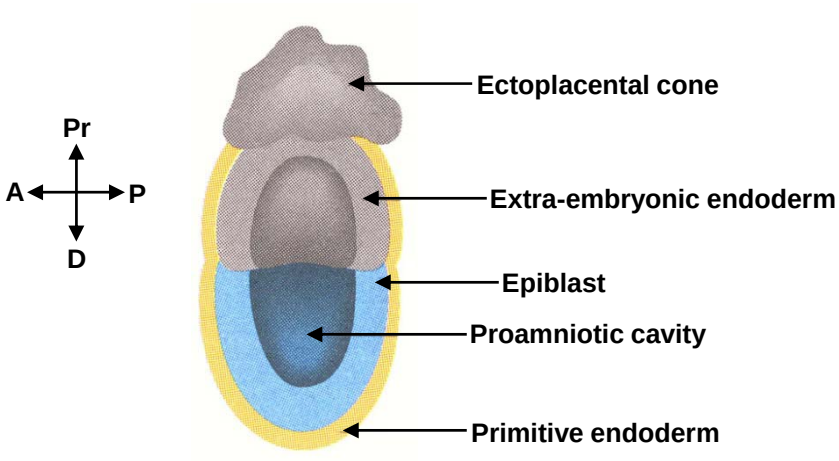

Figure 1.4 Diagram of a 6.5dpc mouse embryo. Black dotted arrows indicate the direction of cell movement. The mesoderm (red) can be seen to be spreading between the visceral endoderm (yellow) and epiblast (blue). The ectoderm is derived from the epiblast. (Adapted from Wolpert et al., 1998).

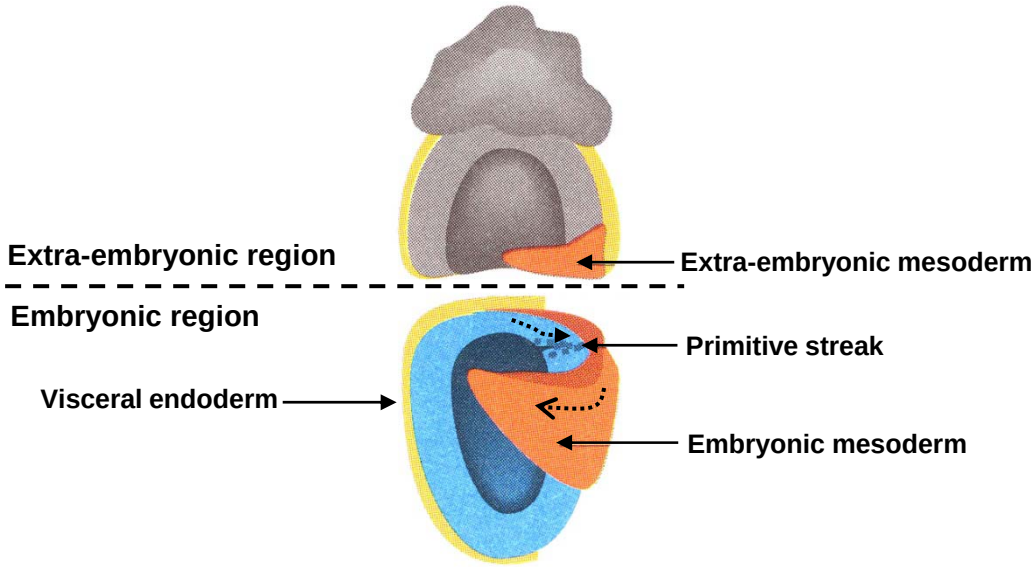

Figure 1.5 Diagram of germ layer movements at 7.5dpc in the mouse embryo. The arrows indicate the direction of cell movement, the arrow colour indicates the germ layer involved. (Taken from Wells et al., 1999).

Unable to gain third party permission

Figure 1.6 Diagram of a 8.5dpc mouse embryo. The node can be seen at the proximal region of the embryo, with the notochord precursors (brown) migrating anteriorly. The definitive endoderm (light yellow) can be seen migrating anteriorly, displacing the visceral endoderm (dark yellow). (Adapted from Wolpert et al., 1998). (A; anterior, P; posterior, Pr; proximal, D; distal)

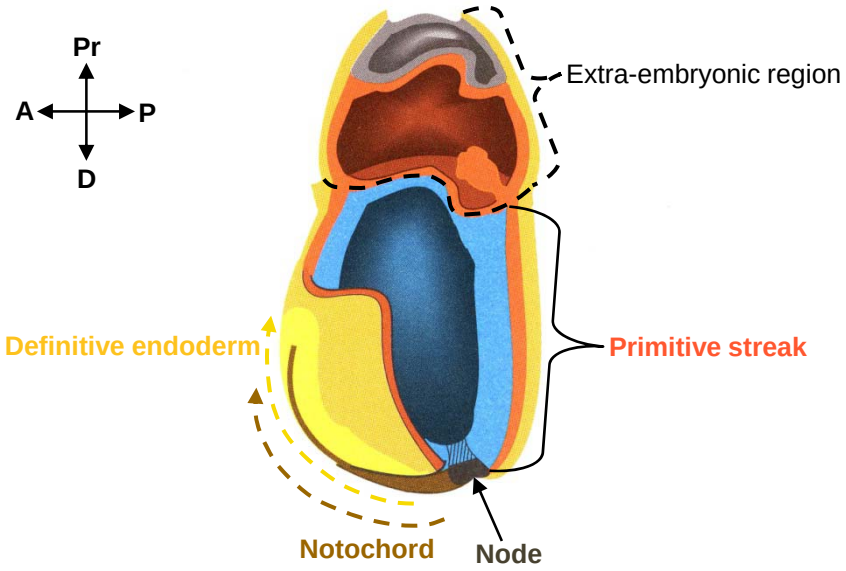

forms the gut and other tissues (Lawson and Pedersen, 1987). The controls involved in regulating the formation of mesoderm or definitive endoderm from the mesendodermal population of cells are largely unknown. It is suggested that the movement and subsequent displacement of the primitive endoderm is due to the accumulating definitive endodermal cells pushing the primitive layer anteriorly and laterally (reviewed in Tam et al., 2007).

1.2.2 Formation of the primitive gut

The developing gut is divided into three major sections: the foregut, the midgut and the hindgut. The foregut will eventually form the oesophagus, pharynx, stomach and proximal duodenum, the midgut will become the small intestine and a portion of the large intestine, and the distal colon will be formed from the hindgut. Other organs are derived from the same embryological origins, due to budding of the gut tube, such as the lower respiratory tract, liver, pancreas and gall bladder (reviewed in Kaufman and Bard, 1999), but these are not of major consideration within the objectives of this project.

The gut is made up of a heterogeneous combination of definitive endoderm, mesoderm and neural crest (reviewed in Beck et al., 2000). The initiation of gut development is signalled at 8.5dpc by a slight indentation within the developing head fold; the anterior intestinal portal (AIP) (reviewed in Wells and Melton, 1999). The AIP will develop into the foregut diverticulum (reviewed in Kaufman and Bard, 1999). At the caudal end of the embryo is the caudal intestinal portal (CIP), forming as an indentation within the developing tail fold (reviewed in Wells and Melton, 1999). At this point, although the endoderm appears morphologically homogenous, differences exist in the anterior-posterior direction (reviewed in Wells and Melton, 1999).

The layer of endoderm has been mapped to various tissue fates (Figure 1.7). Region I mapped to the yolk sac and ventral foregut (giving rise to the stomach and other tissues not related to this project). Region II mapped to the dorsal foregut endoderm, contributing to the oesophagus, stomach, duodenum and other tissues. Region III forms the small intestine as it mapped to the midgut/trunk endoderm and region IV mapped to the posterior trunk endoderm and hindgut, forming the large intestine (reviewed in Wells and Melton, 1999). The regional fate of the cells in the definitive

Figure 1.7 The tissue fates of the various regions of the embryonic endoderm. An image of a 7.5dpc embryo can be seen (A), with the endoderm peeled away from the body of the conceptus. The diagram to the right of this image (B) shows an idealisation of the same embryo. The endoderm can be seen as an enveloping layer around the epiblast/mesoderm/primitive streak core. The regions of embryonic endoderm have been labelled I-IV. The dotted arrows indicate tissue movements in later stages. The fates of these regions can been seen in the 8.5dpc embryo. Again, an image of the embryo can be seen on the left (C) with an idealised version on the right (D). Regions I-IV can be seen mapped to the endoderm of the future gut and the folding of the tissue layer at either end can be seen. The AIP and CIP invaginations are also indicated. (Adapted from Wells et al., 1999). (A; anterior, P; posterior, D; dorsal, V; ventral)

endoderm was determined from a combination of signals received from the primitive streak and adjacent germ layers. Many of the genes expressed in different regions are members of the Homeobox (*Hox*) or Parahox clusters (see section 1.6.1) (Duluc et al., 1997).

The AIP extends rostrally to become the foregut diverticulum, appearing to expand into the future cephalic region due to the migration and movement of tissue layers at this point. The AIP also extends posteriorly to merge with the future midgut region at which point the external opening narrows to become continuous with the yolk sac stalk. The CIP forms six hours later than the AIP and also expands. The two pockets then lengthen longitudinally towards the region of definitive endoderm between them. This region slowly folds ventrally at which point the midgut region can now be visualised (reviewed in Lewis and Tam, 2006, Kaufman and Bard, 1999).

In order for the folded midgut region to become an internalised tube, a crucial turning event occurs at 8dpc in the mouse embryo whilst the gut develops. Thus far, the embryonic endoderm, that will subsequently form the internal embryonic gut, is the ventral layer while the dorsal layer is the surface ectoderm containing the neural tube. The embryo therefore needs to turn so that the ectoderm becomes the exterior germ layer whilst the endoderm is internalised in order to form the gut tube. The embryo effectively 'rolls' about its midpoint in order to invert the germ layers but also to wrap itself in membranes. It takes until 9.5dpc for this process to be complete (reviewed in Kaufman and Bard, 1999, Wolpert et al., 1998).

The most rostral portion of the foregut is, at 8.5dpc, blind ending, but makes contact with an indentation on the surface of the embryo, the buccopharyngeal cavity. The foregut and buccopharyngeal cavity remain separated by the buccopharyngeal membrane, which breaks down at 9dpc (reviewed in Kaufman and Bard, 1999). Equally, at the most caudal region of the hindgut, the anal pit meets but remains separated from the hindgut by the cloacal membrane. At this point, the primitive gut has now formed a regionalised internal tube.

1.2.3 Morphological analysis of the developing gut

At 9.5dpc, the region to become the oesophagus remains unaltered, whilst the subsequent region, to become the stomach, dilates. The stomach is surrounded by a thick mesentery. At 10.5dpc the mesentery dorsal to the stomach hollows out at the right hand side as the intraembryonic coelom develops. This in-growth (bursa omentalis) expands, pushing the stomach round. Hence the stomach is no longer a central midline structure, and instead becomes a left-sided organ while retaining a central position at the junctions with the oesophagus and duodenum. The stomach then elongates further by 13.5dpc and becomes a transverse rather than longitudinal structure. The stomach in the mouse becomes sub-divided into regions by 13.5dpc (reviewed in Kaufman and Bard, 1999).

Once the embryo has turned, the midgut can be identified as a tube that will differentiate to form the caudal part of the duodenum, the jejunum, the ileum, the caecum, all of the ascending and most of the transverse large intestine. At this point the midgut remains open at the umbilical ring, where the embryo maintains maternal contact (reviewed in Kaufman and Bard, 1999).

From 8.5dpc, the umbilical ring narrows, but the gut remains connected to the yolk sac via the vitello-intestinal duct (reviewed in Beck et al., 1985). This only disappears as the midgut lengthens and protrudes out of the umbilical ring towards the umbilical cord, forming the physiological umbilical hernia. This occurs at 10.5dpc due to the rapid lengthening of the gut to allow regional differentiation along with the rapid expansion of the liver. The intestine returns to the abdomen at 15.5dpc, once the cavity has expanded enough to house all the necessary organs (reviewed in Kaufman and Bard, 1999).

The development of the hindgut is more complex because it also encompasses the development of the cloaca. For the purposes of this introduction, it is sufficient to say that the proximal part of the hindgut gives rise to the distal portion of the colon, while the distal part of the hindgut develops into the terminal colon, the rectum and the upper two-thirds of the anal canal. This occurs due to the hindgut diverticulum extending caudally into the pelvic region at 8dpc. This region then extends rostrally and caudally at 9.5dpc but the caudal region regresses by 12dpc. The anal pit meets

the primitive hindgut but the cloacal membrane between the two regions is maintained until 16.5dpc (reviewed in Kaufman and Bard, 1999).

1.2.4 Development of the gut tissue layers

The final stages of gut development occur in two steps. Firstly, the neonatal gut has to develop a proper identity along the anterior-posterior axis at which point cytodifferentiation occurs. Secondly, the gut has to undergo functional regionalisation at weaning in order to adjust to a change in diet (Duluc et al., 1994).

Initially the entire gut endoderm (including the future stomach) consists of an undifferentiated endoderm surrounded by undifferentiated mesoderm. Between these two layers lies a basement membrane (BM). Initially, this BM remains regular, only becoming interrupted as morphogenesis takes place (reviewed in Kedinger et al., 1998). From approximately 13-14dpc the endoderm becomes stratified while the lumen of the intestine is mostly obliterated. The alimentary tract continues to develop as a closed tube of pseudostratified epithelium surrounded by mesodermal cells. By 15dpc many intraepithelial vacuolar structures merge to reform the lumen and the epithelium has converted to a single-layered columnar epithelium in a wave from stomach to colon. The cells of the intestinal epithelium have an established polarity and can be distinguished as enterocytes at this point (Duluc et al., 1994, reviewed in Beck et al., 2000). As the tube is forming, the mesodermal cells encircling it proliferate and differentiate into the muscular and connective tissues surrounding the gastrointestinal tract (Duluc et al., 1994, reviewed in Beck et al., 2000).

By 18dpc, the mouse gastric mucosa contains short, solid infoldings (primordial buds). Within these buds are the precursors of stomach epithelial cells found in the mature organ (Karam et al., 1997).

The epithelium of the small intestine, meanwhile, develops protrusions into the lumen (the future villi) thought to be due to the proliferation of epithelial cells within the restriction of the surrounding muscle layer (reviewed in Stainier, 2005). At this point, cell cycling then becomes restricted to shallow pockets at the base of the projections (the future crypts) and cell diversity emerges within this stage (reviewed in Dauca et al., 1990). These cells then proliferate and cytodifferentiation occurs at the future villi,

although the villi do not fully extend and lengthen until just before birth. By 18.5dpc these processes are complete (reviewed in Stainier, 2005).

The crypts of Lieberkuhn, located in the intestines, develop postnatally from the shallow pockets. In the small intestine the villi express proteins suitable for the digestion and absorption of milk based nutrients within the first three weeks. The jejunum shows pinocytotic activity, the purpose of which is to transport intact maternal immunoglobulins into the circulatory system in the first week of life (reviewed in Henning, 1981). At the same time, the number of precursor cells in the stomach decreases by 22% as the cells begin to mature down stomach epithelial cell lineages (Karam et al., 1997).

The rodent gut shows re-differentiation at weaning, leading to the functional regionalisation seen in the adult gut; only at weaning do enzymes required for the breakdown and digestion of solid food begin to be expressed in the intestine (reviewed in Henning, 1981). Both lactase-phlorizin hydrolase and sucrase-isomaltase show highest levels of expression in the jejunum. Lactase expression peaks during the suckling period, while sucrase expression peaks post-weaning reflecting a change in diet (Fang et al., 2006).

1.3 Adult gut histology

1.3.1 Stomach

The histology of the stomach alters, depending upon the region in question. In the mouse, the stomach is divided into a region of stratified squamous epithelial type tissue and a glandular region. The region of stratified squamous epithelium is located in the anterior portion of the stomach (the fundus). The glandular region is comprised of a small mucous secreting area (the cardia), a central portion (the body), and the antrum followed by the pylorus that ends with the muscular pyloric sphincter (Figure 1.8). The fundus and body are referred to as the fundic region (reviewed in Fawcett, 1986, Smith et al., 2000).

The empty stomach forms longitudinal folds (rugae), which result from the contraction of the muscularis mucosa. The rugae flatten in the full stomach. All the regions contain furrows (gastric pits) in the surface epithelium (reviewed in Fawcett, 1986).

Figure 1.8 A transverse section of 18.5dpc embryonic mouse stomach was stained with haematoxylin and eosin. The regions of the stomach can be visualised in the embryonic organ, just prior to birth. This allows visualisation of all the regions on a single section. Scale bar = 500µm.

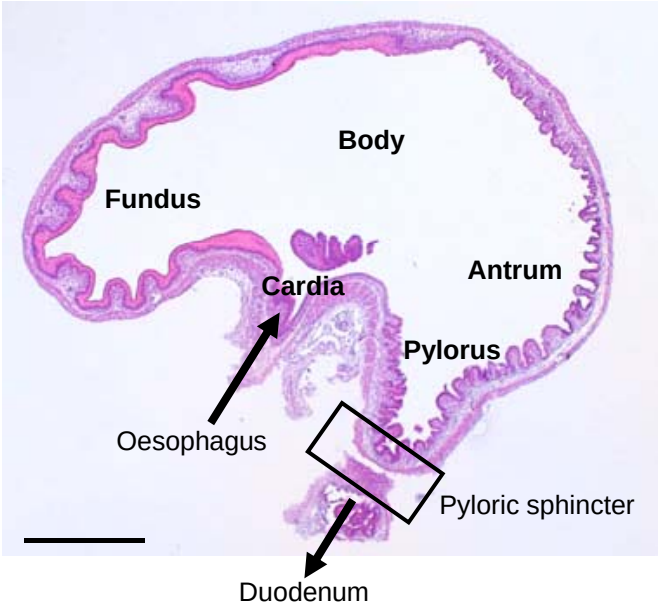

The gastric pits lead to gastric glands embedded in the lamina propria (Figure 1.9) (reviewed in Brittan and Wright, 2004). The gastric pits and the surface between them are lined with tall columnar epithelial cells. Surface mucous cells, found between the pits, are lost continuously into the lumen (reviewed in Fawcett, 1986).

The cardiac region contains relatively shallow gastric pits. Each pit leads to several cardiac glands embedded in the lamina propria, which are rich in mucous secreting cells with a few undifferentiated cells. Endocrine cells, secreting gastrin, are scattered between these (reviewed in Gartner and Hiatt, 2000, Fawcett, 1986).

The fundic region contains gastric glands. These glands are closely packed together, with a minority opening out at the base via slightly constricted necks. The gastric glands contain mucous neck cells, chief cells, oxyntic cells, endocrine cells and stem cells. The oxyntic cells produce hydrochloric acid and gastric intrinsic factor (to assist the ileum in absorbing vitamin B_{12}). The mucous neck cells (and the surface mucous cells) produce a mucous to protect the stomach lining from autodigestion. The chief cells are unique to the fundic region of the stomach. These cells secrete precursors of digestive enzymes, such as pepsin, rennin and lipase. The stem cells replace the epithelial lining and will be discussed in more detail later (reviewed in Gartner and Hiatt, 2000). Within the gastric glands are different regions. The point at which the gland meets the gastric pit is the isthmus region containing surface mucous cells and oxyntic cells. The adjacent region is the neck, containing mucous neck cells and oxyntic cells. The region closest to the base of the gland is the fundus, rich in chief cells interspersed with a few oxyntic and mucous neck cells. Mitotic activity in the gland appears to be confined to the neck region (reviewed in Fawcett, 1986, Brittan and Wright, 2004, Gartner and Hiatt, 2000).

The pyloric region of the stomach contains pyloric glands. These are deeper than any of the other stomach glands. The glands also have larger lumens and show more extensive branching. The pyloric glands, in comparison to the gastric glands of the fundic region, contain more mucous cells, less oxyntic cells and no chief cells. This is because the main role of the pyloric region is mucous secretion to neutralise the contents of the stomach prior to passage into the duodenum (reviewed in Brittan and Wright, 2004, Gartner and Hiatt, 2000, Fawcett, 1986).

Figure 1.9 A cross section of the stomach. The gastric pits in the mucosa lead down to the gastric glands buried deep in the lamina propria. The dotted lines indicate individual pits/ glands. (Adapted from http://www.lab.anhb.uwa.edu.au/mb140/CorePages/GIT/git.htm).

Unable to gain third party permission

1.3.2 Small intestine histology

The small intestine mucosa is folded into finger-like projections of the lamina propria (villi) that extend into the lumen (Figure 1.10). Surrounding the villi are numerous Crypts of Lieberkühn that are located in the mucosa, embedded into connective tissue (Figure 1.11) (reviewed in Potten et al., 1997). The small intestine is comprised, proximally to distally, of the duodenum, jejunum and ileum. The villi alter in number, morphology and length along the intestine to become fewer, shorter and wider (Figure 1.12) (reviewed in Gartner and Hiatt, 2000, Fawcett, 1986).

The small intestine epithelium comprises four cell types. These are the predominant enterocytes (absorptive cells), goblet cells (mucin secreting to protect the surface epithelium and ease chyme passage), peptide hormone secreting enteroendocrine cells and the Paneth cells (reviewed in Potten et al., 1997, Gartner and Hiatt, 2000, Fawcett, 1986). These are dispersed within a simple columnar epithelium. All the cells are produced in the lower region of the crypt and all except the Paneth cells migrate upwards in columns onto the villi as they mature, until they are shed from the villi tip into the lumen (reviewed in Potten et al., 1997). The Paneth cells, however, migrate downwards towards the base of the crypt. These cells contribute to innate immunity by sensing bacteria and bacterial antigens and discharging microbial peptides in response (Ayabe et al., 2000).

1.3.3 Large intestine histology

The large intestine is subdivided into the caecum, ascending and transverse colon, the rectum and anal canal. The large intestine has no villi but does contain Crypts of Lieberkühn in the lamina propria (Figure 1.13). The cells in the large intestine are similar to those found in the small intestine; goblet cells and enterocytes are both present, dispersed amongst columnar absorptive cells. The noticeable difference between the two tissues is the absence of Paneth cells in the large intestine and the abundance of goblet cells. The cells migrate to the intercrypt table at the top of the crypts, where the epithelium contains goblet cells and columnar cells but no enterocytes (reviewed in Gartner and Hiatt, 2000, Fawcett, 1986).

Figure 1.10 An electron microscope image of the surface of the small intestine. The villi can be seen as finger-like projections into the lumen of the intestine. (Taken from http://laser.phys.ualberta.ca/~egerton/SEM/fig21.jpg).

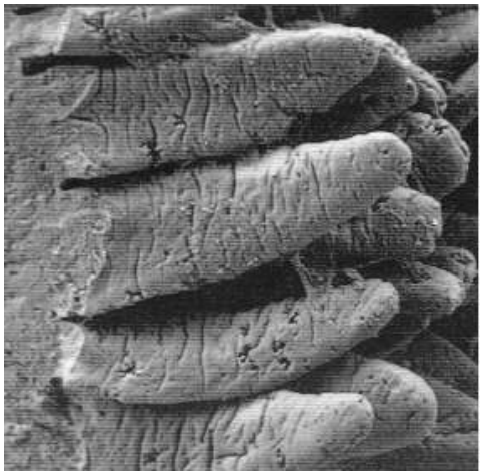

Figure 1.11 A cross section of the small intestine. The finger-like villi can be seen as mucosal projections of the lamina propria, into the lumen. The lamina propria also contains invaginations; the Crypts of Lieberkühn. (Adapted from http://medlib.med .utah.edu/WebPath /GIHTML/GI162.html).

Unable to gain third party permission

Figure 1.12 A comparison of the appearance of the villi between different regions of the small intestine. The images are all to equal scale. The villi can be seen to be getting shorter proximally (duodenum) to distally (ileum) along the length of the gut. Scale bars = 150µm. (Adapted from http://medlib.med.utah.edu/WebPath/GIHTML/GI162.html).

Unable to gain third party permission

Figure 1.13 A cross section of the large intestine. A single crypt is indicated by a dotted line. The crypts can be seen invading the lamina propria. (Adapted from http://www.lab.anhb.uwa.edu.au/mb140/Core Pages/GIT/git.htm).

Unable to gain third party permission

1.4 The intestinal crypt

1.4.1 Intestinal crypt maintenance

Both the large and small intestine generate new epithelial cells in the crypt (reviewed in Marshman et al., 2002). These cells migrate upwards, in straight vertical columns (Winton et al., 1988), towards the lumen whilst performing the function for which they were designed. In the large intestine, these cells are then lost at the intercrypt table. In the small intestine, the majority of cells travel up the crypt onto an adjacent villus, where they are then sloughed off the tip, while the Paneth cells migrate downwards (Figure 1.14) (reviewed in Marshman et al., 2002, Radtke and Clevers, 2005).

The tissue therefore has a polarity in that new cells are created by mitosis in the crypt and then move in a predetermined direction. In the mouse, the time taken for a cell to be created, perform its function and then be lost into the lumen is 5-7days. This linear movement means that the age of a cell (and therefore its position in the cell hierarchy) can be determined from its position along the crypt-villus axis (Figure 1.15) (reviewed in Marshman et al., 2002, Potten, 1998).

1.4.2 The intestinal crypt hierarchy

In the small intestine, the Paneth cells occupy cell positions 1-3 in the base of the crypt (i.e. the first three positions counting from the base upwards) and do not proliferate (Bjerknes and Cheng, 1981). The stem cells that regenerate the cells of the crypt are traditionally thought to be located at approximately position 4. These cells are interspersed with a few maturing goblet, enteroendocrine and columnar epithelial cells (Bjerknes and Cheng, 1981). In the large intestine, due to a lack of Paneth cells, the stem cells are located at the crypt base (reviewed in Potten and Loeffler, 1990, Marshman et al., 2002, Sancho et al., 2003).

It is thought that there are 4-6 actual steady state stem cells per crypt. These self renew throughout life and are responsible for crypt maintenance. The stem cell, upon division, generally produces one daughter cell and one stem cell (see section 1.5.3 for further discussion). The daughter cell enters the transit-amplifying cell population (located within the proliferative zone), of which there are approximately six generations. Cells in this population proliferate rapidly and are thought to become committed to differentiation into one cell lineage by the fourth generation. The transit-

Figure 1.14 A diagram of the process of cellular movements along the crypt-villus axis. The cells proliferate in the crypt via mitosis. The majority of these cells then differentiate as they migrate onto the villi before being lost at the villi tip, into the lumen of the gut. (Adapted from Radtke and Clevers, 2005).

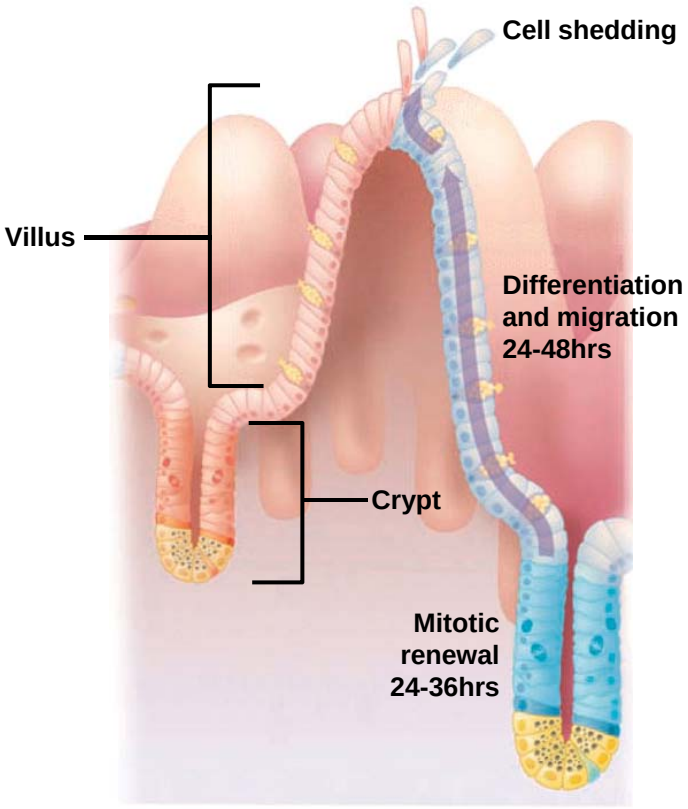

Figure 1.15 A diagram demonstrating the cellular components and positions in the crypts of the small intestine. The cells mature as they migrate upwards. The position of a cell along the crypt-villus axis therefore indicates its age and position in the cell hierarchy. The crypts of the large intestine are similar, except for an absence of Paneth cells at the base. (Adapted from Radtke and Clevers, 2005).

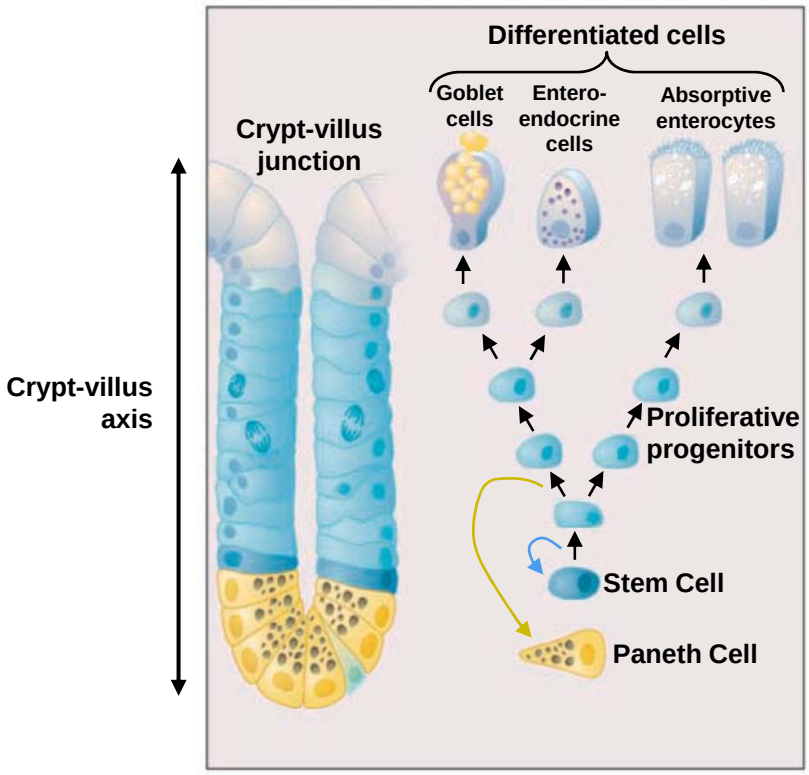

amplifying population is therefore divided into those cells with stem cell attributes (potential clonogenic stem cells) of which there is approximately 30-40 cells, and dividing transit cells which have no stem cell properties of which there are approximately 124 cells (Figure 1.16). In the base of the crypt in the small intestine, it is thought that there are approximately 30 differentiated, fully functioning, Paneth cells (reviewed in Potten, 1998, Marshman et al., 2002).

The crypts are monoclonal (i.e. all the cells comprising the crypt originate from the same stem cell) (see discussion in section 1.5.3), but the villi are polyclonal because more than one crypt supplies the cells for each villus (Schmidt et al., 1988). The cells mature as they migrate to the crypt-villus junction and are therefore fully mature and functioning upon entering the villi (reviewed in Heath, 1996). This differs in the large intestine where the cells proliferate in the bottom two-thirds of the crypt, while the mature cells reside in the top third and on the intercrypt table (reviewed in Marshman et al., 2002).

1.5 The intestinal stem cell

In 1990, the term ‘stem cell’ was defined as: ‘A proliferative cell that maintains its own numbers (self-maintenance) whilst dividing a large number of times during which it can produce daughter cells that are capable of differentiating down various lineages (pluripotency). It is also a cell that can alter its self-maintenance probability to ensure an expansion of stem cells numbers if required following injury (clonogenic capacity)’ (reviewed in Potten and Loeffler, 1990).

As an animal ages, slight division impairment of the stem cells is seen. This is thought to be due to a progressive accumulation of damage to the response pathways of the stem cells. The stem cells also undergo apoptosis much more readily. Martin et al showed that apoptosis levels, in the stem cell region, following 1Gy irradiation were much higher in older animals than young. They suggested that the stem cells had accumulated deoxyribonucleic acid (DNA) damage, leading to a lower apoptosis threshold in comparison to younger animals. The stem cells did, however, maintain a regenerative capacity despite impairment with age (Martin et al., 1998a, Martin et al., 1998b).

Figure 1.16 A diagram demonstrating the cell hierarchy in the small intestinal crypt. The Paneth cells (blue) are positioned at the base of the crypt. The actual stem cells are located at approximately cell position 4. The stem cells regenerate themselves and give rise to the transit-amplifying cell population (T_1-T_8). The first three generations of the transit cell population are potential clonogenic stem cells. These cells undergo a commitment to differentiation by the fourth generation and become dividing transit cells. The cells increase in generation from the crypt base up to the crypt-villus junction. (Adapted from Marshman et al., 2002).

1.5.1 Locating the intestinal stem cell

Until very recently, there has been no known marker for the intestinal stem cell. In order to determine the position of these elusive cells, less direct techniques have had to be employed (reviewed in Potten et al., 1997, Marshman et al., 2002, Potten, 1998). The majority of information regarding intestinal stem cells has concerned the small intestine.

The presence and actual number of stem cells in each crypt has been greatly debated. Various approaches have been adopted to determine the position of the stem cells. One such study involved labelling cells of the small intestinal crypt with tritiated thymidine (^{3}HTdR). The differentiated cells could therefore be tracked and appeared to originate from the crypt at approximately cell position 5. It was deduced that this was the position of the stem cells (Bjerknes and Cheng, 1981). This was further confirmed in 1989 by exposing the suspected stem cell region to a higher level of radioactivity than the rest of the small intestinal crypt. This resulted in a decrease in crypt survival. The stem cells were therefore deduced to be located within the region exposed to the highest level of radiation (Hendry et al., 1989).

The actual number of stem cells in the small intestine is still greatly debated. One investigation involved exposing mice to *N*-nitroso-*N*-ethylurea, known to induce lectin binding in intestinal epithelial cells, allowing them to be traced using lectin antibodies. The cells were tracked, and the data extrapolated to determine the region of origin. In this study, it was suggested that 4-6 cells were maintained long-term in the crypt and these were proposed to be the true stem cells. These were identified as being at position 4 in the crypt of the small intestine (above the Paneth cells) (Bjerknes and Cheng, 1999). Label-retaining experiments have also been performed to suggest that 4-6 cells are maintained long-term in the crypt and these are proposed to be the true stem cells. These label-retaining experiments involve the irradiation of the intestine to kill the majority of the stem cells, forcing them to regenerate. ^{3}HTdR was then injected and so any regenerating cells, including the stem cells, took up this label. The regenerated stem cells retained this label (the significance of which will be discussed in the next section) and were found to be positioned at approximately cell position four. There were approximately five label retaining cells (LRCs) in a crypt,

thought to be the stem cells (Potten et al., 2002), as expected from previous studies (Potten et al., 1978).

Recent research has now found that the stem cells of the gastrointestinal tract can be detected by labelling for expression of *Lgr5* (leucine-rich-repeat-containing G-protein-coupled receptor 5) (a Wnt target gene) (Barker et al., 2007). The labelled cells, thought to be stem cells but termed cycling crypt base columnar cells (CBCs) were found to be proliferating (shown by Ki67 labelling) and occasionally expressing M-phase marker phospho-histone H3, indicating that they cycled every 24hrs as expected for stem cells. Transgenic mice were produced whereby *Cre* expression was placed under the control of the *Lgr5* promoter, inducible by tamoxifen (TM). These mice were crossed to LacZ reporter mice (see section 6.1.2.3). TM administration led to genomic mutation of the majority of CBCs resulting in expression of LacZ whenever the *Lgr5* promoter was active. All progeny of the mutated CBCs expressed LacZ protein and so could be traced. LacZ was subsequently found in all cell types in the small intestine, extending from the crypt base, upwards onto the villi. In the large intestine, similar results were found, in that the LacZ labelled cells were of all lineages, forming ribbons from the crypt base up to the intercrypt table. This indicated that the CBCs have the ability to give rise to all cell types in the intestine, in a manner expected of the stem cells. The authors noted that it took longer for the large intestine to generate these ribbons and so concluded that the CBCs (suspected to be stem cells) must cycle at a slower rate in the large intestine. These CBCs, found to be expressing *Lgr5*, were located at the base of the large intestine, previously suggested as the site of large intestinal stem cells, and interspersed between the Paneth cells in the small intestine. This further confirmed the suspicion that the *Lgr5* expressing cells were in fact stem cells, although the position of these cells in the small intestine was slightly controversial in comparison to the previous data discussed above (Barker et al., 2007).

Current research has suggested that different stem cell populations exist in the intestinal crypt; this may explain the apparently conflicting results regarding the position of the adult small intestinal stem cells. Expression of a tamoxifen-inducible form of *Cre* from the *Bmi1* locus, in combination with a Cre-reporter strain of mouse, indicated that a population of cells expressing *Bmi1* were located at position 4+ in the

crypts of the adult small intestine (Sangiorgi and Capecchi, 2008). These cells were shown to proliferate, self-renew and give rise to all the cell lineages of the small intestine. Loss of these cells led to crypt death. The *Bmi1*-expressing cells proliferated more slowly that the *Lgr5*-labelled cells (Barker et al., 2007, Sangiorgi and Capecchi, 2008). The authors speculate that this may indicate that the intestine contains two populations of stem cells, a set more likely to enter into proliferation, located at the base of the crypt (the *Lgr5*-expressing cells) and a more quiescent set located above the Paneth cells (the *Bmi1*-labelled cells). It is thought that the stem cells may migrate between the two populations. *Bmi1*-expressing cells were, however, only found in the first 10 cm of the small intestine; this may indicate that the expression of different genes is required along the length of the intestine in order to maintain the sub-population of stem cells (Sangiorgi and Capecchi, 2008).

1.5.2 Protection of intestinal stem cell DNA

The small intestinal stem cells, in comparison to those found in the large intestine, show very few genetic defects. These defects are normally acquired over time and tend to lead to cancer induction or a decrease in the functional abilities of the cell.

The stem cell is most at risk of DNA mutation during mitosis, at which point replication induced errors can become evident. The small intestinal crypt contains a population of committed precursors that undergo approximately three divisions to produce both a short-lived precursor and another long-lived precursor (Bjerknes and Cheng, 1999). This, in theory, reduces the number of divisions the stem cell must undergo in order to maintain the crypt and therefore protects the stem cell DNA.

The integrity of the stem cell DNA in the small intestine is also maintained during mitosis by differential DNA strand segregation (Potten et al., 2002). It was shown by ^{3}HTdR labelling (as discussed in section 1.5.1) that the stem cells retain the ^{3}HTdR label for more than 12 rounds of cell division. The persistence of the label suggested that the replacement stem cell retains the original copies of the DNA and the daughter cell committed to differentiation receives the new copies. Any replication-induced errors created in the new copies of the DNA are therefore lost as the daughter cell (and all subsequent daughter cells from this) will be shed into the gut lumen in 5-7days (Potten et al., 2002). If random errors do occur in the template

stem cell DNA, the cell undergoes p53-dependent apoptosis to prevent the errors becoming propagated in the crypt (Merritt et al., 1994).

The stem cells of the large intestine have evolved differently and therefore do not undergo apoptosis as readily. This is possibly because the tissue is naturally exposed to many more DNA-damaging materials and so the loss of a stem cell following DNA damage would happen so regularly that the regeneration of the stem cells would pose more of a mutative risk to the tissue than the DNA mutagens (reviewed in Potten, 1998, Booth and Potten, 2000). In the large intestine, a different system is therefore utilised whereby the cells express an anti-apoptotic survival gene, B-cell leukaemia/lymphoma 2 (*Bcl-2*). This gene prevents the stem cell from entering apoptosis and instead forces it into a cell cycle check point system involving p53 and p21, prompting repair following DNA damage. Mutation of *Bcl-2* led to spontaneous apoptosis in the large intestine indicating it was *Bcl-2* that normally prevented this (Merritt et al., 1995). The large intestine, however, is therefore more prone to cancers than the small intestine (Merritt et al., 1995, reviewed in Potten, 1998).

1.5.3 Stem cell division

In order to maintain a crypt in normal equilibrium, the division of a stem cell must, in theory, be asymmetric. This means that upon stem cell division, one daughter cell will become a stem cell (self maintenance), while the other becomes a transit-amplifying cell. This can be reasoned in that if both cells became stem cells then the crypt would decrease in size, while if both cells became transit amplifying cells, the crypt would both lose a stem cell and increase in size (Loeffler et al., 1997, reviewed in Marshman et al., 2002).

This same outcome, however, could be reached following symmetric division. If one stem cell divides to create two more stem cells, and another stem cell divides to create two transit amplifying cells, the same outcome is achieved. Until recently, this was thought to be more likely because both the daughter cells are morphologically identical during mitosis and both are exposed to the same cytoplasmic and nuclear information. Therefore both cells would be expected to respond in the same manner (reviewed in Marshman et al., 2002).

However, the phenomenon of DNA-strand segregation suggests that the theory of asymmetric division is true and one daughter cell is designated to be the stem cell by retention of the original DNA strands (Potten et al., 2002). This has been confirmed mathematically to be the dominating type of cell division (Loeffler et al., 1997).

Symmetrical division of a stem cell has, however, been mathematically predicted to occur under certain circumstances (Loeffler et al., 1997). This type of cell division also explains how monoclonal crypts (i.e. all cells originate from the same stem cell) arise when the crypt is known to maintain a pool of stem cells (Li et al., 1994). A symmetrical division results in the spontaneous apoptosis of another stem cell in order to maintain crypt cell number. Over time, dependent upon the rate of stem cell division and the number of symmetrical divisions, the crypt will become monoclonal as all stem cells will have arisen from symmetrical divisions (Loeffler et al., 1997, reviewed in Booth and Potten, 2000).

In the small intestine, the process of stem cell division must be extremely tightly regulated as an erroneous single division could result in the loss or gain of between 64 and 128 cells. This would result in hypoplastic or hyperplastic crypts in older animals which are very rarely seen. The loss of a stem cell due to DNA damage is therefore rapidly replaced to prevent a hypoplastic crypt (reviewed in Marshman et al., 2002). To prevent hyperplastic crypts, there is a low level of stem cell apoptosis occurring normally, thought to be a tightly regulated, p53 independent, control mechanism. This process overcomes the effect of symmetric stem cell division by removing one of the older stem cells (Merritt et al., 1994, Merritt et al., 1995, reviewed in Potten, 1998, Marshman et al., 2002).

Stem cells in the large intestine rarely undergo spontaneous apoptosis (Merritt et al., 1995, reviewed in Potten, 1998). The result of this is that the regulation of stem cell number is not as tight because the stem cells express *Bcl-2*, as discussed previously (Merritt et al., 1995). The surplus stem cells are therefore not deleted and so hyperplastic crypts are frequently seen in older animals (reviewed in Marshman et al., 2002, Booth and Potten, 2000).

1.5.4 The intestinal stem cell niche

Although the stem cells reside at approximately position 4 in the small intestine, this is only an estimate on the basis that this tends to be the highest point of the Paneth cells. The actual position of the stem cells ranges between positions 2 and 7. The circumference of the crypt means that there are 16 cells at just position 4, of which a maximum of 4-6 can be stem cells. This means that there must be other cells positioned between them. The stem cells are therefore rarely adjacent, but still respond to signals from each other in order to maintain stem cell number. This is proposed to be via a diffusible factor creating a 'shell' around each stem cell (Figure 1.17). The cells may therefore respond to a gradient of this factor to determine a loss or gain of a stem cell that must be overcome (reviewed in Marshman et al., 2002, Potten et al., 1997).

The stem cells must also behave independently of their neighbouring epithelial cells. The control of this is greatly debated. The cells are either responding to an environment which 'permits' them to be stem cells (i.e. a niche), or they are intrinsically different to neighbouring epithelial cells. The phenomenon of DNA-strand segregation would suggest that they are intrinsically different, but the gradual loss of stemness in the cells as they migrate upwards would suggest that the environment does indeed have a role in the degree of stemness. This would mean that a stem cell 'niche' does exist (reviewed in Marshman et al., 2002, Potten et al., 1997).

Experimentally, the existence of a niche has been suggested. No single factor has been found to be solely responsible for this, but the Wnt pathway is thought to be involved. Tcf-4 (a member of the T-cell factor family) is a downstream member of the Wnt pathway; it complexes with β-catenin in order to function. *Tcf-4* knockout mice lost their crypt stem-cell population and died, suggesting it was required to maintain the stem cells (the genetic controls within the crypt are discussed further in section 1.7) (Korinek et al., 1998). The expression of a dominant-negative Tcf-4 in cells led to the loss of *Lgr5* expression. This suggests that *Lgr5* is a downstream Wnt target and as previously discussed in section 1.5.1, *Lgr5* is a possible marker for intestinal stem cells (Barker et al., 2007). These studies therefore suggest that the Wnt pathway is active in the stem cell region and therefore suggests that Wnt signals are involved in maintaining the stem cell niche.

Figure 1.17 The proposed ‘stem cell niche’. The stem cells (S) are dispersed within the base of the crypt, at an average of cell position 4. The Paneth cells (P) are located at the base. The Paneth cells mature as they migrate downwards (1p and 2p). The other cells mature as they migrate up the crypt, initially as potential clonogenic stem cells (1sc, 2sc and 3sc) then as differentiated, dividing transit cells (3 and 4). The proposed stem cell ‘shell’ of diffusible factors can be seen as concentric lines. (Adapted from Marshman et al., 2002).

Unable to gain third party permission

1.5.5 Intestinal stem cell potency

Embryonic stem cells (ES cells) have been found to be pluripotent (i.e. they have the ability to form all three germ layers). This has been shown in many species, including the human (Thomson et al., 1998).

Adult stem cells, however, are thought to be restricted, the level of which is currently unknown. Adult bone marrow stem cell experiments in the mouse showed that the bone marrow stem cells, when taken from a donor mouse and injected into an irradiated host, contributed to regions of the brain (Eglitis and Mezey, 1997), skeletal muscle (Ferrari et al., 1998), and liver (Petersen et al., 1999). Mesenchymal adult stem cells were manipulated in the laboratory to produce bone, cartilage, fat and muscle, depending on growth factors, cytokines, cell density, spatial organisation and mechanical forces (Pittenger et al., 1999). This indicated how specific the environment must be in order for a stem cell to perform a certain function and that the adult microenvironment is critical in controlling adult stem cell plasticity.

The adult intestinal stem cell is thought to be multipotent. This is based upon the fact that a single stem cell can regenerate the whole crypt following irradiation of all other stem cells. Each individual stem cell therefore has the capacity to differentiate into all cell types found within the crypt (reviewed in Potten et al., 1997).

The adult intestinal stem cell, however, may become restricted in comparison to the embryonic intestinal stem cell, the justification of which will be discussed in Chapter 6, but the degree of restriction cannot be currently studied with the mouse models available. This project hopes to address this by the creation of a conditional *Cdx2* knock-out mouse.

1.6 Developmental genetics

1.6.1 The homeobox genes

The signalling pathways involved in the development of the embryo are extremely vast and complex. As an introduction to these pathways, the homeobox genes will be focussed upon as the important genes involved in the development of the embryo with regard to the future gut.

All the homeobox genes contain a 180 base pair (bp) sequence (homeobox) that codes for a 60 amino-acid homeodomain; this is a sequence-specific DNA binding domain (McGinnis and Krumlauf, 1992). The homeobox genes code for transcription factors that regulate the target gene expression through their homeodomain (Scott et al., 1989). There are four homeobox gene clusters: EHGbox, *Hox*, NKL and Parahox.

There are 39 *Hox* genes, arranged in four clusters. The *Hox* genes are responsible for establishing anterior-posterior patterning and contribute to somite formation (Aulehla et al., 2003, reviewed in Deschamps and van Nes, 2005, Dubrulle and Pourquie, 2004). Parahox genes also exist, many of which play a major role in the development of the intestines.

1.6.1.1 Homeobox gene ancestry

The ancestral *Hox* gene cluster has been repeatedly duplicated in mammals via tandem and cluster duplications. Tandem duplications lead to expansion of the gene cluster upon the same chromosome (i.e. cluster growth). Cluster duplication leads to the entire cluster being replicated upon another chromosome to produce paralogs.

It has been shown ancestrally that one gene underwent tandem duplications on the same chromosome to produce three genes (the ArcheHox). Tandem duplications of these genes occurred to create three gene clusters (Figure 1.18). These clusters then underwent tandem duplications in order to expand, at which point one cluster underwent duplication and gene loss onto a different chromosome to create four gene clusters: EHGbox, Protohox, Proto-NKL and Parahox. Cluster duplication occurred to create exact cluster copies on another chromosome i.e. two chromosomes had exactly the same pattern of gene clusters. These then underwent cluster duplication and loss. The result of this was that 39 *Hox* genes were created within four clusters, along with four NKL clusters, four Parahox clusters and two EHGbox clusters, located on four chromosomes. Within these clusters are different groups of genes (Figure 1.18). The clusters were assigned letters (A-D) and each gene in the cluster was assigned a number (Scott, 1993). This means that, for example, *Hoxa3* is in the same position (position number 3) as *Hoxd3*, but on a different chromosome (a instead of d). This means the two genes are paralogs (reviewed in Pollard and Holland, 2000).

Figure 1.18 The ancestry of the homeobox genes. All the homeobox genes originated from a gene (yellow). This gene underwent numerous tandem and cluster duplications and gene losses (indicated on the diagram). The final clusters (EHGbox, Extended Hox, NKL and Parahox) can been seen, as can the paralogs of these clusters on different chromosomes (A, B, C, D). The ParaHox clusters are located on different chromosomes to the rest of the homeobox genes. The members of the homeobox gene clusters are shown above. (Taken from Pollard and Holland, 2000).

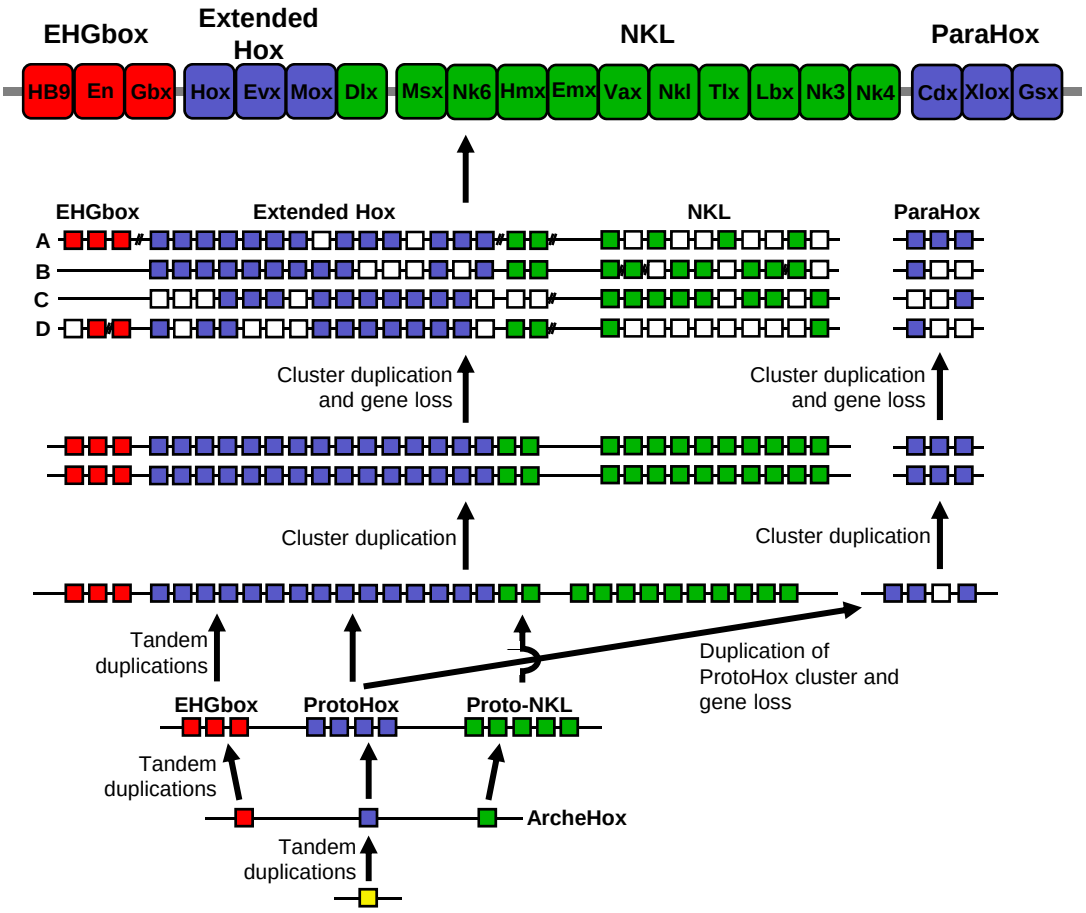

1.6.2 Signalling pathways during gastrulation

The *Hox* genes provide an overall expression pattern to the developing embryo, but many other genes are involved in the process of gastrulation.

Mix-like homeobox protein 1 (*Mixl1*) null embryos developed a normal mesoderm but the endodermal precursor cells failed to migrate through the primitive streak to form the definitive endoderm. This indicated that the two germ layers originating from the mesendodermal population of cells moved independently of each other and *Mixl1* function was required for endodermal migration (Tam et al., 2007).

How the mesendodermal cells decide between a fate of endoderm or mesoderm is unknown, as both arise from the epiblast and migrate through the primitive streak (Tam and Beddington, 1987). *Nodal* is known to have a primary role in the formation and maintenance of the primitive streak because the streak failed to form in mutants with curtailed *nodal* signalling activity (Conlon et al., 1994). Endoderm is more sensitive to attenuation of *nodal* signalling in comparison to mesoderm, but whether this involves *Mixl1* is unknown (Lowe et al., 2001, Liu et al., 2004). Elevated *nodal* expression, however, due to mutation of DR1-associated protein1 (*Drap1*) (involved in the negative feedback loop of *nodal*) led to an expanded primitive streak and excessive mesoderm (Iratni et al., 2002), indicating *nodal* signalling levels were crucial at this point for the development of the primitive streak and determination of the mesendodermal cells. *Wnt3* has also been highlighted as required for vertebrate axis formation as *Wnt3* mutants did not form a primitive streak, node or mesoderm (Liu et al., 1999).

Once the endoderm has exited the streak, differences in gene expression occur in the anterior-posterior direction. The anterior endoderm, consisting of the first cells to exit the primitive streak, expresses *Cerberus* (Bouwmeester et al., 1996) and haematopoietically expressed homeobox 1 (*Hex1*) (reviewed in Thomas and Beddington, 1996, Wells and Melton, 1999). The mid to hind-region expresses forkhead transcription factor A2 (*FoxA2*) (previously known as *Hnf3-β*) (Ang and Rossant, 1994). The posterior endoderm however, expresses caudal-type homeobox protein 2 (*Cdx2*) (Beck et al., 1995). The cells of the posterior endoderm also have a higher cell division rate. These differences are due to interactions between adjacent

structures and germ layers, which differ from the anterior to posterior position (reviewed in Wells and Melton, 1999).

1.6.3 Signalling pathways of the primitive gut

Many of the signalling pathways involve endoderm-mesoderm interactions which are crucial to the correct anterior-posterior patterning of the gut. A number of co-culture experiments have been performed in an attempt to determine the cross-talk occurring between the endoderm and mesoderm during gut development. Small intestine endoderm was co-cultured with a non-intestinal, heterologous group of mesodermal cells in the mouse. The small intestine endoderm was shown to contain the temporal and spatial information required to form intestinal mesenchymal concentric layers from heterologous skin fibroblasts (Duluc et al., 1994). The small intestinal mesenchyme, however, has some spatial and temporal control in that it could convert colonic endoderm to small intestine endoderm during co-culture experiments, although this did not occur in reverse (Duluc et al., 1994). These experiments, however, involved the use of intestinal endoderm and mesoderm that was determined although not yet differentiated and the tissue was xenografted under the skin or kidney capsule of nude mice (Duluc et al., 1994). This artificial system may account for some of the apparently conflicting results. These experiments do however highlight the complexities of the endoderm and mesodermal interactions involved in gut differentiation.

Sonic hedgehog (*Shh*) is expressed in the endoderm prior to formation of the AIP and CIP and continues to be expressed in regions of the gut into adulthood. Shh is thought to induce *Hox* expression in the hindgut mesoderm (Roberts et al., 1995). In the hindgut, endodermal *Shh* expression induces bone morphogenetic protein 4 (*Bmp-4*) and *Hoxd-13* expression in the adjacent posterior mesoderm, but this does not occur in more anterior mesoderm (Roberts et al., 1995). Mis-expression of *Hoxd-13* more anteriorly led to transformation of the adjacent developing midgut into hindgut in the chick (Roberts et al., 1998). Interactions between the two layers are therefore required to provide anterior expression boundaries to some of the *Hox* genes expressed along the length of the gut.

It has been suggested that fibroblast growth factor 4 (Fgf4) has a role in the anterior-posterior patterning of the gut tube during late gastrulation in the chick. The expression of *Fgf4* in the mesoderm is adjacent to the presumptive mid and hindgut domains but absent in the mesoderm adjacent to the future foregut. At early somite stages, expression levels remain high in the vicinity of the hindgut, but much lower adjacent to the posterior foregut and anterior midgut. The gut endoderm directly responds to Fgf4, expressed in the adjacent mesoderm. Over exposure of the endoderm to Fgf4 led to a more anterior expression of posterior endodermal genes such as *CdxB* (the chicken homolog to *Cdx2*) and pancreatic duodenal homeobox gene 1 (*Pdx1*) while more anterior endodermal gene expression (*Hex1* and *Nkx2.1*) was repressed (Dessimoz et al., 2006).

By 8.5dpc, at which point a gut tube can be visualised, gene expression along the anterior-posterior axis of the gut is mutually exclusive in different domains due to mesodermal *Hox* gene expression and expression of soluble factors, e.g. Fgf4. *Pdx1*, a Parahox gene, is expressed in the foregut/midgut boundary that will give rise to the duodenum and pancreas (Dessimoz et al., 2006). *Cdx2* and *Cdx4*, also Parahox genes, are expressed in the posterior midgut and hindgut that will form the small and large intestine (*Cdx4* is transiently expressed until 10dpc) (Beck et al., 1995, Gamer and Wright, 1993).

At 8.5dpc, various downstream targets of the Wnt pathway are expressed in the embryo. *Tcf1* is expressed in the primitive ectoderm, presomitic mesoderm and hindgut while *Tcf4* is found in the future hindgut. These factors are expressed at different time points in different tissues (Gregorieff et al., 2004), but gut specific expression is under consideration here. In *Tcf4/Tcf1* double null (*Tcf4*$^{-/-}$/*Tcf1*$^{-/-}$) embryos, by 8.5dpc the posterior gut endoderm did not express the endodermal markers *Sox17* and *Foxa1* and by 9.5dpc, the hindgut was completely absent due to a failure of the endodermal sheet to form a tube. These embryos also showed defects at the duodenal opening by 14.5dpc. Upon investigation, expression of a stomach endoderm specific marker, *Sox2* (see Chapter 3) was found to be expressed along the length of the intestine due to anteriorisation of the gastro-intestinal tract (Gregorieff et al., 2004). *Cdx2*, normally expressed in the intestinal endoderm at this stage (see section 1.8.4), was reduced to only partial expression,

indicating that the duodenum of the *Tcf4*$^{-/-}$/*Tcf1*$^{-/-}$ embryos has transformed into stomach (Gregorieff et al., 2004). Neither *Tcf4*$^{-/-}$ embryos alone (see section 1.7.2) or *Tcf4*$^{+/-}$/*Tcf1*$^{-/-}$ embryos (Gregorieff et al., 2004) showed this degree of abnormality. The compound mutation of both genes indicated functional redundancy of the downstream targets of the Wnt pathway, leading to these effects upon the caudal gut and the anterior transformation of the intestine.

Application of retinoic acid agonists and antagonists to the developing gut tube in *Xenopus* have been shown to be involved in the eventual rotation and looping of the gut (Lipscomb et al., 2006). The expression of H2.0-like homeobox (*Hlx*) has also been linked to the lengthening and looping of the intestine. *Hlx* is never expressed in the stomach but is present in the intestinal mesoderm from 9.5dpc onwards, but the purpose of expression at this stage is unknown (Lints et al., 1996). *Hlx*$^{-/-}$ embryos died at 15dpc. Upon investigation, amongst other defects in visceral organs, these animals had a small liver and shortened gut. The formation of the midgut umbilical hernia was also absent (Hentsch et al., 1996). The liver and gut are clearly reliant upon *Hlx* expression for expansion to normal proportions (Hentsch et al., 1996).

With regard to the stomach, a key homeobox gene, BarH-like homeobox-1 (*Barx1*), is detected in the mesenchyme from 9dpc until birth. This gene has been shown to be required for correct stomach development (Kim et al., 2007b). Barx1 functions by regulating sFrp1 and sFrp2, which are known to reduce local canonical Wnt activity. These signals act upon stomach endoderm to direct differentiation to a stomach phenotype (Kim et al., 2005). The role of *Barx1* in stomach development will be discussed in greater detail in Chapter 4. It has also been shown that *Wnt5a* and *Bmp-4* expression mark the most anterior region of the stomach (the fundus) in 11.5dpc mouse embryos (Smith et al., 2000). Posteriorly, *Six2* has been shown to be expressed in the stomach and *Nkx2-5* is expressed in the region of the pyloric sphincter in the mouse (see Chapter 4) (Smith et al., 2000). The data indicate that by 11.5dpc, if not before, the stomach has also developed regional gene expression patterns.

The *Hox* and ParaHox genes continue to be expressed in the endoderm and mesoderm of the developing gut of the mouse beyond 12.5dpc (reviewed in Beck et

al., 2000). The expression pattern of the *Hox* genes in the gut shows vague spatial co-linearity to the chromosomal *Hox* gene pattern, but the expression boundaries are not as well defined as those seen in patterning of the somites. The expression of the *Hox* genes (and the Nkx group of Parahox genes) is mostly limited to the mesoderm, with a few exceptions. The Parahox genes *Cdx2* and *Pdx1* are expressed in the gut endoderm into adulthood (Sekimoto et al., 1998, Kawazoe et al., 2002, Beck, 2002).

1.6.4 Signalling pathways involved in cytodifferentiation of the gut

At approximately 14.5-15.5dpc, as the epithelium converts from a pseudo-stratified epithelium to a columnar epithelium, Wnt signalling becomes evident. It has been shown that this signalling is limited to the postmitotic cells in the developing villi, not the intervillus cells. This is in contrast to the region of active Wnt signalling in the adult (see section 1.7.2) possibly due to different downstream Wnt targets being involved. This means that Wnt signalling may act in a different way during different embryonic and adult stages (Kim et al., 2007a).

Epithelial cell differentiation in the intestine has been demonstrated to be under the influence of interactions with the mesoderm. The mesenchymal cells near to the endodermal cells in the embryonic and perinatal gut express various soluble factors such as hepatic growth factors, neuregulin and keratinocyte growth factor (reviewed in Kedinger et al., 1998). These function via tyrosine kinase receptors expressed predominantly in epithelial cells. The fact that mesodermal cells express factors involved in epithelial cell behaviour suggests that the mesoderm plays a major role in the control and development of the gut epithelium (reviewed in Kedinger et al., 1998). Another example of this is the expression of the mesenchymal specific forkhead transcription factor 6 (*Fkh6*). Mice null for this factor showed increased epithelial cell proliferation. The number of dividing intestinal cells increased four-fold and so the proliferative zone expanded. This resulted in structural abnormalities of the stomach, duodenum and jejunum, due to abnormal crypt structure, formation of mucin-filled cysts and lengthened villi (Kaestner et al., 1997).

Interactions between the endoderm and mesenchyme have also been seen in the stomach. From 12.5dpc onwards, *Barx1*, a stomach mesodermal gene, functions via sFrp1 and sFrp2 to reduce local Wnt activity, acting upon the endoderm (Kim et al.,

2005). It has also been shown that glandular stomach mesenchyme was sufficient to cause tracheal endoderm to express pepsinogen (a stomach marker) (Hayashi et al., 1988). Equally, stomach endoderm in the mouse, could induce the formation of stomach-type smooth muscle in the adjacent mesoderm. The stomach endoderm was necessary for the mesoderm to achieve this (Takahashi et al., 1998).

It has been shown that *Gata4* inactivation in the intestine attenuates jejunal-specific gene products and instead induces expression of ileal-specific products. *Gata4* is therefore required for jejunal-ileal specification (Bosse et al., 2006).

The process of cytodifferentiation of some of the intestinal cells into secretory cells (Paneth, goblet and enteroendocrine cells) has been shown to be due, in part, to the expression of *Mtgr1*. The null mouse showed a progressive loss of these cells with a marked decrease at weaning. The progenitor cells were still present and so *Mtgr1* must be involved in the maturation of the secretory cells (Amann et al., 2005).

The mouse intestine remains responsive to various factors beyond birth and displays differentiation at weaning in response to a change in diet. It is the administration of factors such as thyroid hormones, glucocorticoids and epidermal growth factors, via the gut lumen, that abolish lactase-phlorizin hydrolase, leading to normal intestinal differentiation at weaning (Freund et al., 1990). This has been suggested to be due to regional and temporal expression of hepatocyte nuclear factor 1 (*Hnf-1*), *Cdx2* and *GATA* family members to activate sucrase in the midgut, while *Pdx1* and CREB-binding protein (*Cbp*) suppress it at the proximal and distal ends (Fang et al., 2006).

1.7 Gene expression and signalling in the adult gut

1.7.1 Anterior-posterior gene expression

The adult gut establishes an anterior-posterior pattern of gene expression, including Homeobox gene expression in the epithelium. Although research is not exhaustive, it has been shown that *Cdx1* and *Cdx2* (ParaHox genes) are found to be expressed in the intestine, although the two genes establish different areas of maximal expression within the intestine (section 1.8.5). Minor spatial colinearity of the *Hox* genes in the adult gut has also been detected. It has been shown that *Hox2.3* is expressed in the jejunum, while *Hox2.5* is expressed more distally in the ileum. *Hox1.3* is expressed

from the duodenum to colon, while *Hox1.7*, which is more distal on the chromosome, is expressed more distally, confined to just the colon. As previously discussed, the homeobox genes contain a DNA binding region and so regional expression of these genes along the gut axis may supply polarity and regional information leading to cellular differentiation via signalling pathways (James and Kazenwadel, 1991).

1.7.2 Proliferation-Differentiation control in the intestinal crypt

The anterior-posterior expression pattern of genes in the intestinal epithelium is thought to provide positional and cytodifferentiation information to the crypts of the intestine. The controls and signalling pathways within the crypt, however, are complex and based upon the theory that a 'niche' must be achieved within which the signals alter in a crypt-villus direction (or crypt-table direction in the large intestine). This will supply polarity to the crypt and aid cell migration and differentiation while maintaining 'stemness' of the stem cells and potential clonogenic stem cells (reviewed in Sancho et al., 2003). The majority of research has focussed upon the small intestine but it is not exhaustive. The information from various groups will be reported here as individual findings.

Wnt signalling is significant in the regulation of the intestinal crypt. It is suggested that the Wnt pathway in the intestine involves the stabilisation of β-catenin by Wnt signals (in combination with Frizzled and lipoprotein receptor-related proteins). This allows β-catenin to interact with T-cell factors (TCFs) in the nucleus. The interaction drives transcription of target genes. In the absence of Wnt, a degradation complex of proteins phosphorylates β-catenin, resulting in its ubiquitination and degradation by the proteosome (reviewed in Bienz and Clevers, 2000).

This pathway has been suggested to be involved in the proliferation/differentiation control of the crypt cells. Tcf4 is essential for maintaining a stem cell population in the small intestine. In *Tcf4*$^{-/-}$ embryos, the proliferating cells at the inter-villus region were lost as the villi form at 16.5dpc (Korinek et al., 1998). Equally, β-catenin has been found to accumulate in the transit amplifying cells of foetal small intestine epithelium (van Noort et al., 2002) and in the base of the adult crypts in both proliferative progenitors and the Paneth cells (van de Wetering et al., 2002, Batlle et al., 2002). Conditional knock-out of β-catenin in adult mice led to crypt ablation, highlighting the

absolute requirement of β-catenin to maintain the proliferative region (Ireland et al., 2004). The adenomatous polyposis coli (*Apc*) gene (part of the β-catenin degradation complex of proteins) represses proliferation as it functions as a negative regulator of β-catenin (Andreu et al., 2005, Korinek et al., 1998). Inactivation of *Apc* led to colorectal adenomas, due in part to an inability to regulate the β-catenin/Tcf4 pathway (Morin et al., 1997). *Apc* is therefore a tumour suppressor gene and has been defined as the 'gatekeeper' gene of the intestinal epithelium due to its ability to regulate proliferation/differentiation (Andreu et al., 2005). Transgenic expression of *Dickkopf-1* (*Dkk-1*), a Wnt inhibitor in mice led to a reduced intestinal proliferative compartment resulting in a loss of the crypts in the adult (Pinto et al., 2003). The combination of these findings has indicated a role for the Wnt signalling pathways in crypt proliferation.

β-catenin and Tcf functions have been investigated in colorectal cancer (CRC) cells. CRC cells accumulate Wnt mutations and so β-catenin and Tcfs become constitutively activated (van de Wetering et al., 2002). Constitutive activation of these factors led to expression of the same genes found to be normally expressed in the proliferating cells of the crypt. Equally, upon cessation of β-catenin and Tcf activity, the genes that subsequently became upregulated were the same genes as those found expressed in the differentiated cells of the crypt (van de Wetering et al., 2002). This suggested that β-catenin and Tcf (and therefore Wnt signalling) maintain cell proliferation at the base of the crypt. As the cells migrate away from this source, they become differentiated.

Cdx1 expression has also been found in the base of the adult crypt, coinciding with the region of proliferation. It has been suggested that *Cdx1* expression is lost as the cells undergo differentiation (Subramanian et al., 1998). The promoter region of *Cdx1* contains Tcf binding motifs and so it is regulated by β-catenin-Tcf complexes. *Cdx1* expression is therefore under the control of the Wnt pathway involved in maintaining cell proliferation in the crypt (Lickert et al., 2000).

Cdx2 protein, conversely, is found throughout the crypt and villus of the intestine but is either positively or negatively phosphorylated to modulate activity (section 1.8.5). This results in Cdx2 being functional in the region of the differentiated cells (Gross et

al., 2005). Sox9, a downstream transcription factor in the Wnt-β-catenin-Tcf4 cascade, has a repressive effect upon Cdx2, while having no effect upon Cdx1 (Blache et al., 2004). This finding highlights the complexities of the Wnt pathway in regulating the proliferation/differentiation control over crypt cells.

Recently, the Notch pathway has also been shown to maintain the proliferation status of the intestinal crypt cells. Mice in which the Notch cascade was blocked showed a conversion of proliferative cells to post-mitotic goblet cells (van Es et al., 2005). Constitutive activation of the Notch pathway inhibited differentiation in the proliferative cells (as opposed to causing hyper-proliferation) (Fre et al., 2005). This suggested that both the Wnt and Notch pathways play a role in maintaining the proliferative cell status in the crypt (van Es et al., 2005).

Epithelial-mesenchymal cross-talk has also been indicated in the proliferation/differentiation conversion of the intestinal epithelial crypt cells. The transcription factor, forkhead homolog 6 (*Fkh6*) is expressed in the mesenchyme of the adult gut (Kaestner et al., 1997). *Fkh6*$^{-/-}$ mice usually died in the first three weeks postnatally due to irregular positioning of dividing cells in the intestine. Those that did survive beyond this, by 50 days postnatally, showed expanded and disorganised crypts in the proximal small intestine, with an increase in the number of goblet cells present, scattered throughout the villi and crypt. *Fkh6* expression in the mesenchyme therefore negatively regulates proliferation in the epithelium and has some effects upon cell lineage (Kaestner et al., 1997). The phenotype of the *Nkx2-3*$^{-/-}$ mouse was similar to that of the *Fkh6*$^{-/-}$ mouse. *Nkx2-3* is expressed in the gut mesoderm from 9.5dpc onwards into adulthood but never the stomach (Pabst et al., 1997). The deletion of *Nkx2-3* led to hyperproliferation of the crypts. Cell lineage was not affected in these mutants however (Pabst et al., 1999). Fkh6 has been shown to upregulate the expression of *Bmp2* (expressed in the epithelium) and *Bmp4* (expressed in the mesenchyme), indicating that these could be downstream target genes in the regulation of cell proliferation (Kaestner et al., 1997, Pabst et al., 1999).

BMP (bone morphogenetic protein) signalling has been reported to inhibit intestinal stem cell activation and promote intestinal differentiation through restriction of the Wnt-β-catenin pathway (reviewed in He et al., 2005). BMP antagonists (Chordin-

like1, Gremlin1 and Gremlin2) are located in the base of the crypt to allow the epithelial stem cells to function (Kosinski et al., 2007). Gremlin1 has also been shown to activate Wnt signalling in intestinal epithelial cells (Kosinski et al., 2007). The Notch, BMP and Wnt pathways and downstream target genes, with regard to intestinal proliferation/differentiation, are intertwined and extremely complex.

1.7.3 Cell migration control in the adult intestinal crypt

The stem cells are traditionally thought to reside in the bottom third of the small intestinal crypt, above the Paneth cells. This means that cell migration is bi-directional and so some sort of control must exist to ensure that this occurs. The process of cell migration is closely linked to that of the proliferation/differentiation switch in the cells and so many of the processes are interlinked.

Wnt signalling has been suggested to be involved in the process of cell migration. The expression of EphB receptors and ephrin-B ligands in the crypt cells has been shown to be due to Wnt signals. The receptors (EphB2 and EphB3) are expressed in regions expressing β-catenin-Tcf (i.e. the base of the crypts) whilst the ligands are expressed in regions that do not express this complex (i.e. the differentiated cells) (Batlle et al., 2002). The ephrin ligands repel the Eph receptors; this ensures that the proliferative compartment remains near the crypt base (Batlle et al., 2002, van de Wetering et al., 2002).

1.7.4 Cell fate determination in the adult intestinal crypt

The proliferation-differentiation switch and the determination of cell fate are intertwined decisions involving the Notch pathway.

Notch signalling is important during cell fate determination in the intestine. Hairy and enhancer of split 1 (Hes-1) is a transcriptional repressor downstream of Notch signalling. It is required for the differentiation of enterocytes (Jensen et al., 2000). Hes-1 represses *Math-1* expression (Jensen et al., 2000). *Math-1* expression is required for commitment of cells to a secretory lineage (Paneth cells, goblet cells and enteroendocrine cells) (Yang et al., 2001). Neurogenin-3 (*Ngn-3*) is required to direct the secretory cells down the enteroendocrine lineage (Jenny et al., 2002).

The activation of the Notch signalling cascade has recently been directly linked to upregulation of *Hes-1* and therefore repression of *Math-1* and *Ngn3* (Fre et al., 2005). The Notch cascade system is involved in the secretory/absorptive cell fate decision. Constitutive activation of Notch signalling maintains the cells in a proliferative state (Fre et al., 2005).

Wnt signalling has also been shown to be involved in Paneth cell specification. Nuclear β-catenin is found in the Paneth cells and deletion of the *Apc* gene led to activation of the Wnt pathway and a subsequent increase in Paneth cell number (Andreu et al., 2005). The requirement for Wnt signalling in the specification of the Paneth cells has been confirmed in *Sox9* null mice. *Sox9* is a downstream target of the Wnt-β-catenin-Tcf4 pathway. The absence of *Sox9* led to a complete lack of Paneth cells or any evidence of markers for this lineage. All other intestinal cell lineages were present indicating that the stem cells were not affected (Mori-Akiyama et al., 2007).

1.7.5 Cell maturation in the crypt

Once the fate of a cell has been determined, further signals are required in order for the cell to mature and become fully functioning. Kruppel-like factor 4 (*Klf4*) mutant mice showed impaired maturation of the goblet cells in the colon (Katz et al., 2002). E74-like factor 3 (*Elf-3*) deficient animals showed abnormalities in the maturation of enterocytes and goblet cells (Ng et al., 2002).

1.8 Cdx2

1.8.1 Cdx2 chromosomal location and structure

The homeobox gene, *Drosophila caudal*, has three murine paralogs: *Cdx1* (Duprey et al., 1988), *Cdx2* (James and Kazenwadel, 1991) and *Cdx4* (Gamer and Wright, 1993). The *Cdx* genes are members of the ParaHox cluster that was derived from a common ancestor of the *Hox* genes (Pollard and Holland, 2000) (Figure 1.18). *Cdx1* is located on chromosome 18 (Johnson and Davisson, 1992) and *Cdx4* is located on the X chromosome (Horn and Ashworth, 1995). *Cdx2* has been mapped to chromosome 5 (Figure 1.19) (Chawengsaksophak and Beck, 1996). As previously described, homeodomain-containing proteins act as transcription factors.

Figure 1.19 The position and orientation of murine Cdx2 in relation to chromosome 5, in the 3' to 5' direction. The red blocks indicate exons, while the 'open' red boxes indicate untranslated regions upstream and downstream of the gene. The Cdx2 gene is transcribed in the 5' to 3' direction. Taken from ensembl (http://www.ensembl.org/index.html).

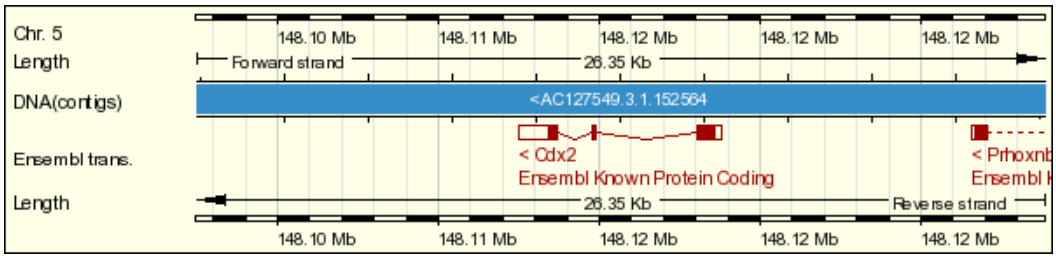

The murine *Cdx2* gene is transcribed in the 5' to 3' direction (Figure 1.19) and contains three exons and two introns (Figures 1.19 and 1.20). The mature *Cdx2* transcript consists of 2,145bp and the protein contains 311 amino acids (James et al., 1994). Exon 2 and part of exon 3 of *Cdx2* contains the homeobox sequence coding for the DNA binding part of Cdx2, the homeodomain (Suh et al., 1994). The homeodomain of Cdx1 and Cdx2 show significant homology suggesting that they overlap in biological activity. Transcriptional activation and repression from outside of the homeodomain may control differences in expression patterns between the two genes (James et al., 1994).

1.8.2 Cdx2 activation and signalling pathways

Cdx2 has transcriptional control over a number of genes in different tissues at various developmental and mature stages. In order for these spatial and temporal differences in *Cdx2* expression to occur, cell specific mechanisms of transcriptional control must exist (Xu et al., 1999). An example of this transcriptional control over Cdx2 is that it undergoes cell-type specific autoregulation. In cell lines that normally expressed *Cdx2*, the endogenous *Cdx2* promoter could be activated by a Cdx2 fusion protein transfected as an expression vector into the cell line. Transfection of the same construct into non-*Cdx2* expressing cells however did not activate the endogenous promoter; it remained repressed (Xu et al., 1999).

This difference in response to transfection of *Cdx2* in cells is due to the *Cdx2* promoter. It is the promoter that permits autoregulation; Cdx2 can bind to the TATA box and downstream binding site (DBS) of the proximal element of the murine *Cdx2* promoter. This region is conserved between mouse and human (Xu et al., 1999). Other transcription factors also bind to this region of *Cdx2*. It is therefore suggested that at low Cdx2 concentrations, *Cdx2* binds preferably to this region, accelerating transcription, while at higher concentrations, general transcription factors bind, resulting in repression of gene expression (Xu et al., 1999).

Oct1 has been shown to aid in autoregulation of *Cdx2*. This is due to the presence of an Oct binding site in the promoter region of *Cdx2*, first identified in the Caco-2 cell line. Oct1 binding to this site is involved in driving the expression of *Cdx2*, and also in

Figure 1.20 The murine *Cdx2* gene (A), mRNA (B) and protein (C). Key features of each variant are indicated on the diagram. *Cdx2* gene and transcript are adapted from a Vector NTI figure using data obtained from Ensembl (http://www.ensembl.org/index.html). Protein information is taken from Sanger (http://pfam.sanger.ac.uk/protein?acc=P43241). (E1-E3; Exon1-Exon3, UTR; untranslated region, N; N-terminal domain, C; C-terminal domain, ATG; start codon, TGA; stop codon).

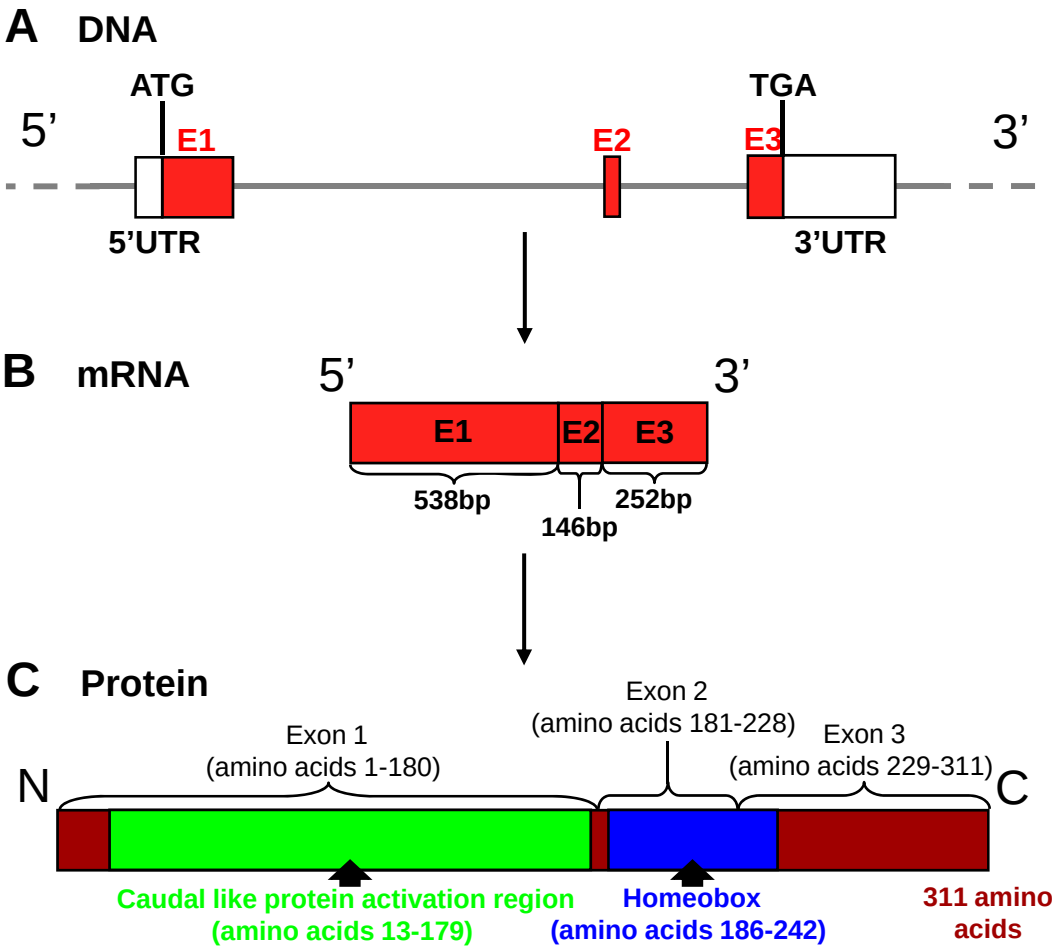

autoregulation of the gene. It is not currently known, however, if Oct1 interacts with other co-factors to mediate *Cdx2* expression (Jin and Li, 2001).

The expression of *Cdx2* in the intestine is also thought to be due to epithelial-mesenchymal interactions (Duluc et al., 1997). The basement membrane is located between the epithelial and mesenchymal regions of the intestine and is largely mesenchymal in origin. Laminin expressed at the basement membrane is thought to induce *Cdx2* expression. This was demonstrated in CaCo2-TC7 cells (spontaneously differentiating cells derived from the human adenocarcinoma clone). Culture of these cells, on a laminin coating, led to an overexpression of *Cdx2*. The resultant changes were the same as those reported in cells transfected with *Cdx2* RNA (Lorentz et al., 1997).

The downstream activity of Cdx2 is regulated in various ways. Fundamentally, Cdx2 is positively or negatively phosphorylated by different kinases. This leads to regions of Cdx2 activation along the crypt-villus (or crypt-table) axis of the intestine despite ubiquitous expression of the gene (see section 1.8.5). Following positive phosphorylation of the protein, Cdx2 can bind to promoter elements of other intestine-specific genes. The transcriptional activation of downstream genes occurs, in part, via enhancers, in a cell specific manner. Cdx2 has been shown to interact with co-activator proteins to mediate increased activity at the target enhancer (section 1.8.6) (Taylor et al., 1997).

The ability of Cdx2 to act via target enhancers means that Cdx2 may have transcriptional control over a vast number of genes, beyond those with Cdx2 binding sites in the promoter region (Taylor et al., 1997); these genes largely remain elusive.

1.8.3 Cdx expression in the developing embryo

Cdx2 expression is first detected at the 8-cell stage, with the protein present in the outer cells by the 16-25cell stage (the embryo is defined as a morula at this point following compaction). The embryo then develops into a blastocyst, at approximately 3.25dpc, prior to implantation (Strumpf et al., 2005).

The blastocyst is composed of a single epithelial layer (trophectoderm) surrounding a fluid-filled cavity (blastocoel) and inner cell mass (ICM). The ICM gives rise to the epiblast and primitive endoderm (see section 1.2.1). The trophectoderm comprises the extra-embryonic ectoderm. By this preimplantation stage (3.5dpc), *Cdx2* is expressed in the trophectodermal cells (Beck et al., 1995, Strumpf et al., 2005). By 4.75dpc *Cdx2* expression is only present in the polar trophectoderm and is thought to delineate it into different cell fates by 5.5dpc (Strumpf et al., 2005).

The requirement for *Cdx2* prior to implantation is confirmed by the pre-implantation lethality of *Cdx2* null (*Cdx2*$^{-/-}$) embryos (Chawengsaksophak et al., 1997). It was shown that these mutants failed to maintain a blastocoel. This was because *Cdx2* expression in the pre-implantation embryo leads to the downregulation of *Oct4* and *Nanog* in the outer cells of the blastocyst, allowing trophectodermal cells to develop. If *Oct4* and *Nanog* continue to be expressed in these cells, then they become committed to an ICM lineage and so the cells cannot maintain the internal pressure involved in blastocoel formation (Strumpf et al., 2005). The *Cdx2*$^{-/-}$ embryos could therefore develop to the early blastocyst stage, but *Cdx2* levels become critical beyond this in defining the trophectoderm (Strumpf et al., 2005).

Within the embryo, expression of *Cdx2* is first seen from 7.5dpc in the ectoderm, mesoderm and endoderm of the posterior region. It is also present at 8.5dpc in the caudal regions of the neural plate, neural tube and notochord (Beck et al., 1995). *Cdx1*, *Cdx2* and *Cdx4* demonstrate nested expression from the primitive streak stage (7.5dpc) in the neural tube and mesoderm, that is still present by 8.5dpc (Meyer and Gruss, 1993, Beck et al., 1995, Gamer and Wright, 1993). *Cdx1* is expressed most anteriorly, followed by *Cdx2*, then *Cdx4*. All three genes are expressed posteriorly. The *Cdx1* null phenotype showed anterior homeotic transformations of the vertebrae due to a posterior shift of anterior *Hox* gene expression domains. This would suggest the *Cdx* genes have a role in anterior-posterior patterning involving the *Hox* genes (Subramanian et al., 1995). *Wnt3a*$^{-/-}$ mice showed a similar phenotype. Upon investigation, the *Wnt3a* mutant embryos showed reduced expression of *Cdx1* in the primitive streak and tail bud region, suggesting that *Wnt3a* may mediate downstream *Cdx1* expression (Ikeya and Takada, 2001). *Cdx4* was also shown to be involved in

anterior-posterior patterning, but only in combination with mutations of *Cdx2*, due to redundancy between the *Cdx* genes (see below) (van Nes et al., 2006).

The crucial role of *Cdx2* in anterior-posterior patterning in *Cdx2*$^{+/-}$ mice is discussed in detail in section 1.8.7 but at this point it is suffice to state that they demonstrated an anterior homeotic shift. These mice, however, were haploinsufficient, not null. Tetraploid fusion was used in order to study the role of Cdx2 beyond implantation, in the *Cdx2*$^{-/-}$ embryos. The fusing of a wild-type tetraploid embryo and *Cdx2*$^{-/-}$ diploid embryo led to the wild-type tetraploid cells contributing to the extra-embryonic regions, while the *Cdx2*$^{-/-}$ diploid embryo developed within. The *Cdx2*$^{-/-}$ phenotype had therefore been 'rescued' and the role of Cdx2 in anterior-posterior patterning was then investigated (Chawengsaksophak et al., 2004).

Following 'rescue' by tetraploid fusion, it was found that Cdx2 was also required for the development of the subsequent foetal components of the placenta. The allantois, formed as an extra-embryonic outgrowth, was under-developed in these embryos and failed to fuse with the chorion. The yolk sac circulation was also abnormal, with the fine vessels replaced by coarse enlarged channels (Chawengsaksophak et al., 2004). The underdevelopment of these tissues due to a lack of *Cdx2* is thought to lead to the eventual death of the embryo at 11.5dpc.

In the wild type (WT) embryo, by 9.5dpc embryonic *Cdx2* expression is still strong in the regressing tailbud tissues. The neural tube, notochord and hindgut also stain strongly, but there is a sharp cut-off of expression proximal to the nascent intestine; the nascent stomach does not express *Cdx2* (Beck et al., 1995). In the 'rescued' *Cdx2*$^{-/-}$ animals, by 10dpc the cranial region had developed normally but the posterior region was grossly stunted due to a lack of Cdx2. This was apparent due to an absence of hind limb buds, and a reduced number of somites which were underdeveloped towards the caudal end. The neural tube also became irregular. In the oldest surviving embryos, the neural tube, notochord and endodermal gut tube extended to the posterior tip. The gut endoderm and splanchnopleuric mesoderm showed evidence of cell death (Chawengsaksophak et al., 2004). The truncated phenotype of these 'rescued' *Cdx2* homozygotes reflected that seen in *Fgfr1* mutants, but alterations in *Cdx2* expression were not investigated in these animals

(Partanen et al., 1998). The 'rescued' data suggests that *Cdx2* may act as a transducer of the Wnt and Fgf pathways, but the feed-back loops and controls involved are complex and so the exact interactions are not yet known (Chawengsaksophak et al., 2004).

By 12.5dpc, WT *Cdx2* expression is limited to just the gut endoderm and the very extreme tip of the neural tube (Beck et al., 1995). *Cdx1* is expressed from 7.5dpc along the length of the primitive streak but expression gradually declines and becomes limited to the posterior region until it is completely absent by 12dpc (Subramanian et al., 1995). *Cdx1* expression is first apparent in the endoderm of the gut at 12.5dpc and will continue to be expressed into adulthood (Duprey et al., 1988, Subramanian et al., 1995). At 12.5dpc, *Cdx4* is not expressed in the intestinal epithelium (Gamer and Wright, 1993).

Compound mutations of *Cdx1* and *Cdx2* mutant mice have indicated an element of redundancy between the genes. They demonstrated overlapping roles in anterior-posterior patterning and posterior axis elongation. The compound mutations revealed an increased severity in skeletal defects and a more extensive posterior shift of the *Hox* genes than seen in the single mutants. This indicated a functional redundancy of the two genes. The most severe phenotype was seen in $Cdx1^{-/-}/Cdx2^{+/-}$ mice. These mice demonstrated both an anterior transformation due to misexpression of the *Hox* genes and a posterior truncation.

Cdx1/Cdx4 and *Cdx2/Cdx4* compound mutations had shown that redundancy occurs between all the *Cdx* genes. $Cdx4^{-/-}$ null mutants appeared normal, it was only in combination with other *Cdx* mutations that a role for *Cdx4* became evident (van Nes et al., 2006). $Cdx1^{-/-}/Cdx4^{-/0}$ mutant embryos did not show significant anterior-posterior patterning impairment. $Cdx2^{+/-}/Cdx4^{-/0}$ mutant embryos, however, showed a more pronounced phenotype than $Cdx2^{+/-}$ mutants alone, with regard to both anterior-posterior patterning and posterior truncation (see section 1.8.7). This indicates the functional redundancy of *Cdx4*, only obvious upon loss of *Cdx2* (van Nes et al., 2006). *Cdx4* was also shown to be required for normal chorio-allantoic fusion during development; a minority of $Cdx2^{+/-}/Cdx4^{-/0}$ mutants failed to undergo this process. In those embryos where fusion occurred, the formation of the allantoic

vascular network failed to varying degrees. Only a small minority of mutants would therefore establish a placental labyrinth sufficient to support the foetus to survive to term. This phenotype was not seen in *Cdx2*$^{+/-}$ mutants, but was not as significant as that in 'rescued' *Cdx2*$^{-/-}$ embryos where all mutants died due to failure of allantoic outgrowth (van Nes et al., 2006). Of the *Cdx2*$^{+/-}$/*Cdx4*$^{-/0}$ that did survive to term, they all died of anal atresia, indicative of the role of the *Cdx* genes for posterior elongation and patterning (Young et al., paper in preparation). Overall, the contributions of the *Cdx* genes towards anterior-posterior patterning and truncations are not equal, because *Cdx1* and *Cdx4* contributions only became evident upon loss of another *Cdx* gene, whereas haploinsufficiency of *Cdx2* alone showed a phenotype. The compound loss of *Cdx4* and haploinsufficiency of *Cdx2* did however enhance the phenotype seen in *Cdx2*$^{+/-}$ mutants alone.

1.8.4 Cdx expression in the developing gut

Cdx2 expression in the gut endoderm has been reported from inception of the gut endoderm (Silberg et al., 2000) while Cdx1 protein is present by 12.5dpc; *Cdx1* expression is therefore absent in the gut endoderm during the earliest stages of gut development. At 13.5dpc, *Cdx1* expression is predominantly in the hindgut with lower levels of expression in the foregut and midgut (Silberg et al., 2000). At this point, *Cdx2* expression is exclusively in the foregut and midgut of the developing intestine (Beck et al., 1995, Silberg et al., 2000). *Cdx2* expression is continuous throughout the midgut loop and into the yolk sac stalk. Levels of *Cdx2* expression gradually decrease towards the rectum (Beck et al., 1995) (Figure 1.21). By 14.5dpc, the expression patterns do not alter from those seen at 13.5dpc, although the levels of *Cdx1* and Cdx2 expression increase generally during the transformation of the undifferentiated endoderm to a simple columnar epithelium (Silberg et al., 2000). By this stage *Cdx2* is primarily expressed in the future duodenum and midgut while *Cdx1* is primarily expressed in the future colon. The two genes display an overlapping region of strong expression in the midgut, defined at this point as being the loops of gut within the umbilical hernia (Beck et al., 1995).

The expression of *Cdx1* and *Cdx2* varies along the vertical intestinal axis. By 15.5dpc, *Cdx1* expression in the distal intestine is uniform along the crypt-villus axis while in the proximal colon it is predominantly expressed in the intervillus region that

Figure 1.21 *Cdx1* and *Cdx2* expression in the 13.5dpc gut. (A) A diagram indicating the position of the gastrointestinal tract in a 13.5dpc embryo. The midgut region can be seen projecting into the umbilical hernia. (B) The gastrointestinal tract shown as a linear tube in order to indicate regions of gene expression. (Adapted from www.med.unc.edu/embryo_images/unit-digest/digest_htms/digest030.htm).

Unable to gain third party permission

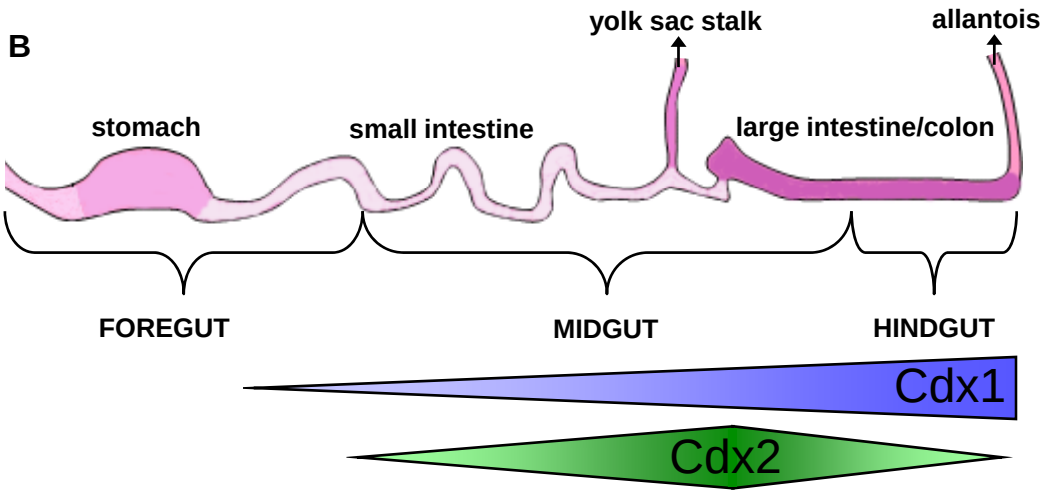

will develop into crypts (Silberg et al., 2000). *Cdx2* expression remains uniform along the vertical axis in all regions found to be expressing the gene (Silberg et al., 2000).

The abundance of *Cdx2* transcripts in the developing gut increases between 16dpc and 19dpc (James et al., 1994). This is the point at which the gut undergoes major developmental changes due to an inductive interaction between the endoderm and mesenchyme (reviewed in Dauca et al., 1990). At 18.5dpc there is no variation in vertical expression of *Cdx2* in the future distal jejunum, ileum and proximal colon (the region that will form the caecum and adjacent intestine) (James et al., 1994). In the proximal small intestine, *Cdx2* expression is heterogeneous in the intervillus region, with less staining at the villi tips (Silberg et al., 2000). *Cdx1* expression, by 18.5dpc was weak in the proximal intestine and strongest in the future distal jejunum, ileum, proximal and distal colon. Within these regions, expression was strongest in the intervillus regions, declining upwards onto the villi (Silberg et al., 2000).

Both *Cdx1* and *Cdx2* are expressed only in the endoderm, never the mesoderm and are completely absent in the stomach (James et al., 1994, Silberg et al., 2000).

1.8.5 Cdx2 expression in the adult gut

In the adult mouse, expression of *Cdx2* (and *Cdx1*) is restricted to the intestinal epithelium. By day 45 postnatally, *Cdx1* expression is highest in the crypt nuclei of the large and small intestine with diminished levels at the intestinal surface. Expression increases in an anterior-posterior direction, with the highest levels found from the distal jejunum to the distal colon (Subramanian et al., 1998, Silberg et al., 2000).

Cdx2 expression in the postnatal mouse increases from the duodenum to the proximal colon (James and Kazenwadel, 1991, Silberg et al., 2000, Subramanian et al., 1998) at which point *Cdx2* expression peaks then decreases towards the distal colon (Silberg et al., 2000). Within the regions of the colon expressing *Cdx2*, there is a 5-fold difference in *Cdx2* mRNA levels between the proximal (caecum) and more distal areas (James et al., 1994).

Cdx2 is expressed in the epithelium of the gut; it is completely absent from the underlying mesodermal layers. There is no vertical gradient of Cdx2 protein in the intestine. Cdx2 is thought to be required for the conversion of proliferating cells to a differentiation status as they migrate up the crypt. Cdx2 must therefore be functional only within defined regions and so mechanisms must exist that regulate Cdx2 function.

It has been shown that Cdx2 is differentially phosphorylated along the vertical crypt axis, suggesting that Cdx2 activity can be modulated by post-translational mechanisms. Cdx2 can be phosphorylated at serine 60 (S60) in the mitogen-activated protein kinase (MAPK) pathway. The S60 phosphorylated protein shows decreased transactivation and occurs most often in the proliferative compartment (Rings et al., 2001). Cyclin-dependent kinase 2 (Cdk2) was shown to be active in the proliferative compartment of the crypt and phosphorylates Cdx2 at serine 281 (Gross et al., 2005, Boulanger et al., 2005). Upon phosphorylation of Cdx2 by Cdk2, the protein is targeted for degradation and therefore cannot function (Boulanger et al., 2005, Gross et al., 2005). Conversely, p38 MAPK is phosphorylated and active in the differentiated cells of the intestine. Inhibition of p38 led to a decrease in sucrase-isomaltase expression (downstream of Cdx2). Upon investigation it was found that there was a decrease in binding of Cdx2 to the promoter of sucrase-isomaltase following p38 inactivation. Cdx3 (Cdx2 homologue in hamster) was found to directly interact with p38. The p38 was shown to be phosphorylating and therefore activating Cdx2 in the region of differentiating cells (Houde et al., 2001).

In the intestinal crypts, *Cdx1* expression is limited to the epithelial cells of the crypt, while Cdx2 functions predominantly in the villi due to differential phosphorylation with some overlap of the two functional proteins in the crypts (Boulanger et al., 2005, James et al., 1994, Silberg et al., 2000, Subramanian et al., 1998, Rings et al., 2001, Gross et al., 2005, Houde et al., 2001). Cdx1 is not differentially phosphorylated. It is suggested that positively phosphorylated Cdx2 is responsible for cellular differentiation and represses *Cdx1* expression in the upper regions of the small intestinal crypt (Lorentz et al., 1997). This is because *Cdx2* over-expressing cells demonstrated a downregulation of *Cdx1* and a decrease in *Cdx1* or overexpression

of *Cdx2* led to a decrease in proliferation. Cdx1 is required for proliferation via the Wnt pathway as previously discussed (Lorentz et al., 1997).

1.8.6 Cdx2 functions in the adult gut

In the adult, Cdx2 is known to regulate intestine specific genes such as sucrase-isomaltase (Suh et al., 1994), lactase-phlorizin hydrolase (Troelsen et al., 1997), carbonic anhydrase 1 (Drummond et al., 1996), Calbindin-D9k (Colnot et al., 1998, Lambert et al., 1996), and vitamin D receptor (Yamamoto et al., 1999). Some of the Cdx2 binding sites in the promoter regions of these genes are identical to each other and so Cdx2 must interact with various co-activator proteins to initiate differential gene expression.

CREB-binding protein (Cbp) has been found to be a co-activator protein of Cdx2. The interaction of these two proteins leads to the subsequent activation of sucrase-isomaltase expression in Caco-2 cells (Lorentz et al., 1999). Cdx2 has also been shown to interact with hepatic nuclear factor 1α (Hnf-1α). The co-operative binding of these two proteins to the lactase-phlorizin hydrolase (*Lph*) promoter leads to a synergistic upregulation of expression in the intestinal epithelium of the pig (Mitchelmore et al., 2000). The interaction of Cdx2 and Hnf-1α has also been found to be instrumental in the transcriptional control of liver fatty acid binding protein (Fabp1) (Staloch et al., 2005). The ability of Cdx2 to act synergistically with co-activators and to compete with other proteins may explain how the intestine achieves complex regional differences in gene expression.

Regional differences in expression levels of sucrase-isomaltase (*SI)* exist in the intestine. The *Cdx2* promoter has recently been shown to be responsive to combinations of the transcription factors Hnf-1α, Gata6, Tcf4 and β-catenin. Addition of these factors to non-*Cdx2* expressing cells led to expression of *Cdx2* and the subsequent expression of sucrase-isomaltase (*SI)* (Freund et al., Gastroenterology, in press). It has been shown previously that the expression of *SI* relies upon the interaction of Gata-4 with some of these factors. *Gata-4* expression decreases from a high level in the proximal small intestine, to complete absence in the colon. This creates a spatial control over the expression of *SI*, causing the regional differences in SI expression seen in the intestine (Krasinski et al., 2001).

The role of Cdx2 in the renewal of the intestinal epithelium along the crypt-villus unit has been investigated recently. It has been found that conditional expression of *Cdx2* in undifferentiated intestinal crypt cells led to a decrease in proliferation despite the absence of the *Cdx2* co-activators Gata-4 and HNF-1. These cells, however, failed to differentiate (Escaffit et al., 2006). This indicated that co-activators are required to interact with Cdx2 in order for differentiation to occur, although Cdx2 does not require these factors to inhibit proliferation. This data suggested Gata-4 and HNF-1 are such factors (Escaffit et al., 2006).

A decrease in *Cdx2* expression enhances the migration of intestinal cells (Gross et al., 2007). This is reflected in the finding that *Cdx2*$^{+/-}$ intestine responded quicker to abrasive damage than wild type tissue due to the ability of the epithelial cells to migrate to the villi faster in the absence of Cdx2 (Calon et al., 2007). This phenotype reflected that seen in *Smad3*$^{+/-}$ mice. Cdx2 protein interacts with Smad3 protein to synergistically activate *Smad3* transcription, therefore *Cdx2* inactivation leads to *Smad3* inactivation and so the same phenotypic outcome is achieved (Calon et al., 2007). The role of Cdx2 in the migration of intestinal cells has implications in colon cancer (see section 1.8.8).

The role of *Cdx2* in determining the fate of the intestinal epithelial cells has been indicated by microarray analysis. Expression of *Notch1* and *Deltex1* is upregulated in *Cdx2* expressing cells in comparison to non-*Cdx2* expressing cells (Uesaka et al., 2004). Both these genes are members of the intestinal Notch pathway. As discussed in section 1.7.4, this pathway is critical for the determination of cell fate in the intestinal epithelium. It was also shown by microarray analysis that *Cdx2* expression induced the expression of E2F3 (an E2F transcription factor member); this gene is also thought to be involved in cell fate determination in epithelial cells (Uesaka et al., 2004).

1.8.7 Cdx2$^{+/-}$ *heterozygous and Cdx2*$^{-/-}$ *chimeric mice experimental data*

The *Cdx2*$^{+/-}$ mouse demonstrated haploinsufficiency; the extreme phenotype seen in the *Cdx2*$^{-/-}$ mouse, however, led to embryonic death, as previously discussed in section 1.8.3. The *Cdx2*$^{+/-}$ mouse has therefore been extensively studied because the

haploinsufficiency permitted embryonic survival and provided a key insight into other functions of Cdx2, for example, the role within the gut.

In order to create a null *Cdx2* allele a conventional knockout was performed. This involved replacing all the *Cdx2* exons (apart from a small region of exon 1) with a positive selection cassette. The functional homeodomain (mostly contained within exon 2) had therefore been removed rendering *Cdx2* null in that allele (Figure 1.22) (Chawengsaksophak et al., 1997). This construct was electroporated into ES cells that were subsequently screened for presence of the positive selection cassette. Those clones that had correctly undergone homologous recombination were used to create chimeric mice from which germ line transmission was achieved (see section 1.9) (Chawengsaksophak et al., 1997). The *Cdx2*$^{-/-}$ embryos resulting from *Cdx2*$^{+/-}$ intercrosses were embryonic lethal (see section 1.8.3). The heterozygotes, however, demonstrated a phenotype to varying degrees.

The *Cdx2*$^{+/-}$ mice on the 129SV background displayed a shortened, kinked tail and a decrease in neonatal weight in comparison to wild type litter mates (Figure 1.23). The weight difference was thought to be due to the requirement of Cdx2 by the placenta in order to develop normally. *Cdx2*$^{-/-}$ mice 'rescued' by tetraploid fusion failed to undergo chorio-allantoic fusion to produce a functional placental labyrinth because Cdx2 is required for the posterior elongation of the extra-embryonic mesoderm from which the allantois is derived (Chawengsaksophak et al., 2004). The *Cdx2*$^{-/-}$ embryos also displayed abnormal yolk sac circulation. Reduced *Cdx2* expression in the *Cdx2*$^{+/-}$ mice was adequate to permit survival but led to placental insufficiency and therefore growth retardation (Chawengsaksophak et al., 1997).

The vertebrae of the *Cdx2*$^{+/-}$ mice were morphologically altered. The *Cdx2*$^{+/-}$ vertebrae C6 (cervical 6), C7 and T3 (thoracic 3) displayed the morphological features of the immediately cranial vertebrae of the WT controls, i.e. an anterior homeotic shift. The ribs of the *Cdx2*$^{+/-}$ mice also displayed an anterior homeotic shift in that the second-most anterior rib was occasionally fused to the most-anterior rib or an additional true rib was present at the distal end of the sternum (Chawengsaksophak et al., 1997). The 'rescued' *Cdx2*$^{-/-}$ embryos demonstrated a more severe phenotype due to the complete absence of Cdx2; these embryos

Figure 1.22 Generation of a *Cdx2* null allele. Homologous recombination occurred between the endogenous *Cdx2* locus and the targeting vector at the sites marked with a blue 'X'. Most of exon1 and all of exons 2 and 3 (represented by red boxes) were therefore replaced by a *neo*^{R} cassette. This resulted in a null *Cdx2* allele. (Restriction enzyme sites: B, *Bam*HI; E, *Eco*RI; H, *Hind*III; N, *Not*I; S, *Sac*I; X, *Xba*I). (Adapted from Chawengsaksophak et al., 1997).

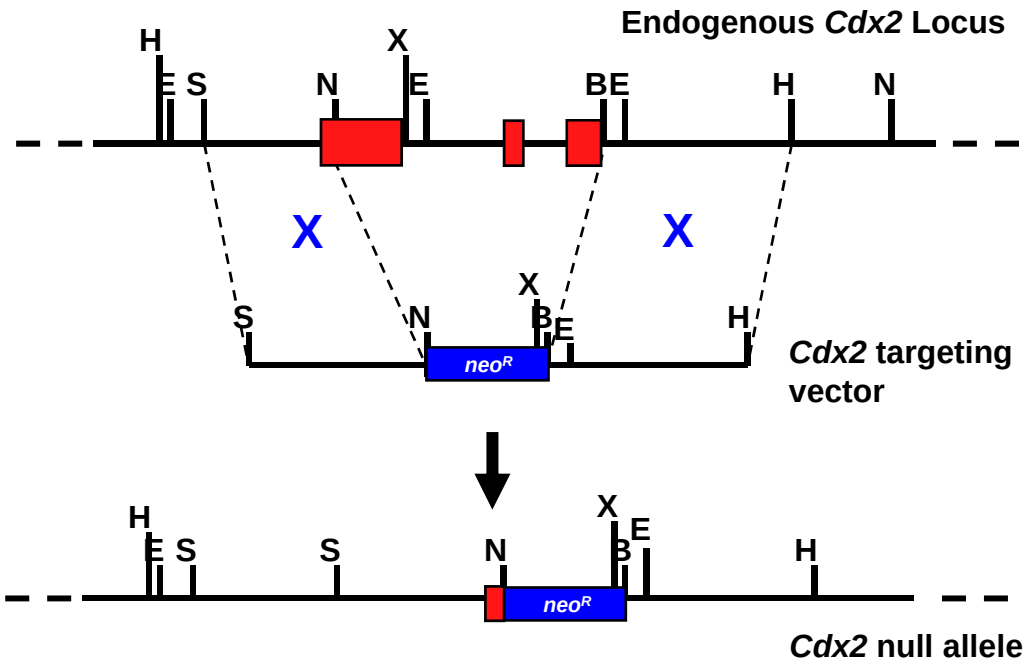

Figure 1.23 The phenotype seen in 3 week old *Cdx2*$^{+/-}$ heterozygous mice. The mouse on the right is wild type. The four mice on the left demonstrate the varying penetrance of *Cdx2* haploinsufficiency in the mutant mouse. The shortened body and kinked tail are indicative of an anterior-posterior shift of vertebrae and posterior truncation. (Taken from Chawengsaksophak et al., 1997).

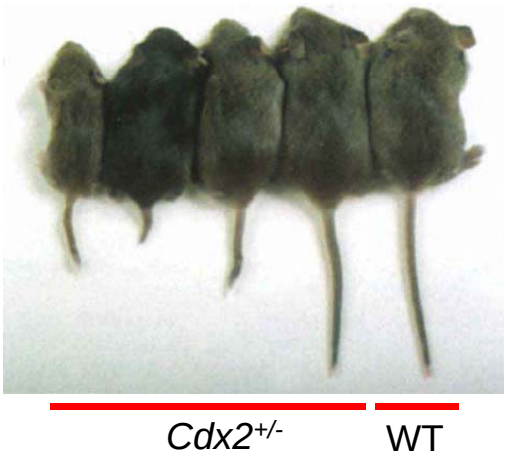

showed a grossly curtailed posterior region due to the requirement of Cdx2 for posterior elongation (see section 1.8.3) (Chawengsaksophak et al., 2004).

Within the gut of the *Cdx2*$^{+/-}$ mice on both a 129SV and C57/BL6 background, multiple gastric heterotopias were found, with the majority located in the proximal colon (the caecal and paracaecal regions) (Chawengsaksophak et al., 1997). This is the site at which *Cdx2* expression is highest (James et al., 1994, Silberg et al., 2000). The tissue adjacent to these heterotopic lesions continued to express *Cdx2* while the lesions did not; there was, however, no loss of heterozygosity in any of these cells (Chawengsaksophak et al., 1997). The lack of Cdx2 protein is therefore thought to be due to haploinsufficiency of Cdx2 protein levels. It has been proposed that a threshold of Cdx2 is required in order for the gene to be functional. Some cells meet this threshold and so develop normally; others fail to do so and so heterotopias develop. What causes this difference in individual cells is not known; it is thought to be due to epigenetic factors or random secondary mutations. The development of gastric lesions in regions of *Cdx2* haploinsufficiency is fundamental evidence of the requirement of Cdx2 to control the fate of the epithelial stem cells down an intestinal cell lineage. Without Cdx2, the cells revert to a 'default' stomach phenotype (Beck et al., 1999).

Upon investigation, these lesions were found to contain gastric-type epithelium containing intercalary growth. The intercalation is thought to be due to discontinuity between the ectopic gastric and normal colonic epithelia. The tissue attempts to overcome this by epimorphic regeneration. Upon sectioning of lesions removed from adult colon, stratified squamous epithelium (SSE), typical of forestomach was seen, followed by an ordered sequence of cardia, body, antrum/pylorus, small intestine and then the host colon. This occurred in an anterior-posterior direction on either side of the SSE (Figures 1.24 and 1.25) (Beck et al., 1999). The SSE was seen in the colon of newborn *Cdx2*$^{+/-}$ mice but intercalation was not histologically evident. Only by four weeks old could gastric body tissue be histologically detected in the intercalated lesions of the *Cdx2*$^{+/-}$ mice. The polyp-like shape formed because of the lack of space in which the intercalation was occurring (Beck et al., 1999).

Figure 1.24 A section through a *Cdx2*$^{+/-}$ caecal polyp. The intercalation demonstrated within the polyps can be clearly seen in this section; not all gastric regions can be visualised due to the orientation of the polyp during sectioning. (GBo, gastric body; GA, gastric antrum/pylorus; SI, small intestine; C, colon). (Taken from Chawengsaksophak et al., 1997).

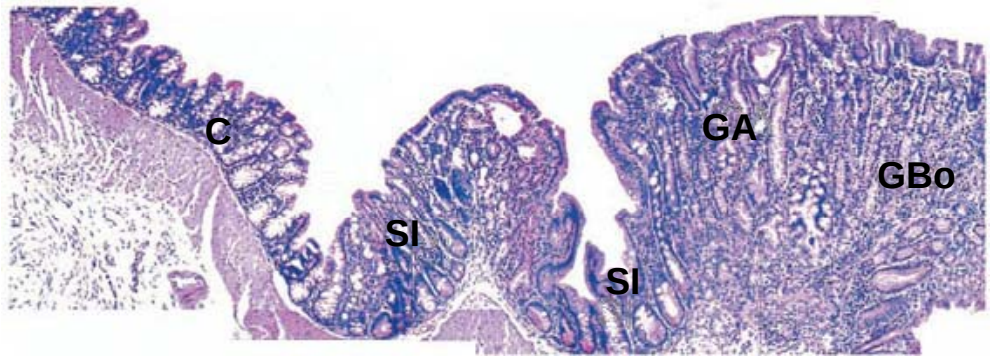

Figure 1.25 An idealised diagram of the intestinal polyps in *Cdx2* mutant mice. The section in figure 1.24 only shows a few of the gastric regions found in the polyps. Serial sections of various samples have revealed that the polyps demonstrate intercalation of all the normal gastrointestinal regions from stratified squamous epithelium (SSE) of the stomach, to the normal colonic tissue, as shown in this diagram. Adapted from a diagram by Prof. Felix Beck.

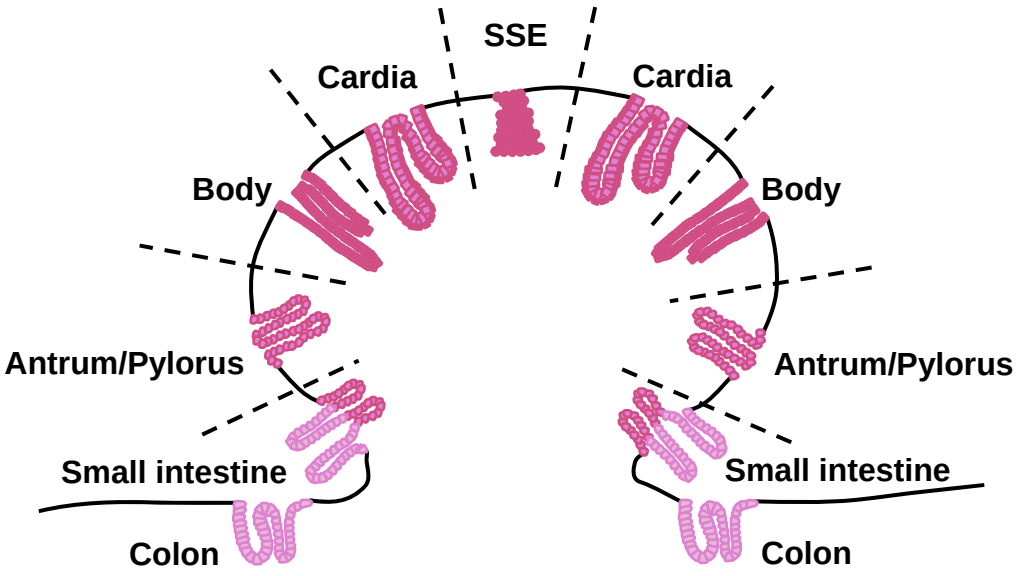

These intercalated lesions could also be detected in chimeric (*Cdx2*$^{-/-}$//WT) mice, created by injection of *Cdx2*$^{-/-}$ female ES cells into 3.5dpc blastocysts (Beck et al., 2003). The *Cdx2*$^{-/-}$ cells engrafted into random regions of the blastocyst and so contributed to various regions of the adult mouse. The anterior-homeotic shift seen in *Cdx2*$^{+/-}$ mice was not seen in *Cdx2*$^{-/-}$//WT mice because the *Cdx2*$^{-/-}$ cells were sparsely distributed. *Cdx2*$^{-/-}$ cells did, however, engraft in the intestine resulting in the formation of a lesion containing gastric-type epithelium. These heterotopias were identical to those found in the *Cdx2*$^{+/-}$ mice but were truly *Cdx2* null. The origin of the cells within the heterotopias was traced by Y-chromosome painting because the *Cdx2*$^{-/-}$ cells were female, injected into male hosts. This meant that the ability of the *Cdx2*$^{-/-}$ cells and surrounding colon to form different tissue types within the lesion was determined (Beck et al., 2003). It was found that the mesoderm was always male in origin, i.e. WT. It was found that host tissue contributed only to the villus-like peripheral regions of the heterotopic lesion and the colon itself; the *Cdx2* null cells did not contribute to these regions. The gastric regions of the lesions, however, were formed solely from the *Cdx2*$^{-/-}$ cells. This may have been due to the surrounding host colon reverting to a small intestine phenotype upon detection of adjacent gastric pyloric tissue and so the *Cdx2*$^{-/-}$ epithelium would not need to form small intestine as the host colon had already done so (Beck et al., 2003).

1.8.8 The role of Cdx2 in cancer

Intestinal heteroplasia is the transdifferentiation of epithelial cells of the stomach or oesophagus to an intestinal cell type, expressing intestinal genes. This leads to dysplasia and then carcinoma (Silberg et al., 2002). Barrett's oesophagus is an example of intestinal-type metaplasia in the oesophagus where the normal squamous epithelium converts to a simple columnar mucosa (cardia-type mucosa) (Vallbohmer et al., 2006). *Cdx2* was found to be expressed in increasing levels from the cardia-type mucosa stage until full Barrett's oesophagus was achieved. It is not currently known whether expression of *Cdx2* is causative or a by-product of intestinal metaplasia in the oesophagus, but the gene is intrinsically involved in intestinal differentiation (Vallbohmer et al., 2006).

In general, intestinal metaplasia is known to be induced partly by environmental factors that in combination with unknown genetic factors, leads to a clinical situation

(Mutoh et al., 2002). A *Cdx2* mutant mouse has provided a model in which to study intestinal metaplasia in the stomach. Ectopic expression of *Cdx2* in the gastric mucosa of a transgenic mouse (expressing *Cdx2* under the control of a parietal cell specific promoter, H^+/K^+-ATPase) led to a change in the gastric mucosa from day 18 postnatally. At this point, the proliferative region of some of the glands was found to be in the base as opposed to the expected isthmus region. These glands were expressing *Cdx2*. By day 244, all the oxyntic cells had disappeared and the majority of the epithelial cells expressed *Cdx2* in intestinal-like crypts. The crypts were composed of large numbers of goblet cells, enteroendocrine cell and enterocytes but Paneth cells were absent. These regions were expressing intestine-specific genes, but other intestine-specific factors required for the development of Paneth cells were thought to be absent. By definition, Cdx2 appeared to be able to induce intestinal metaplasia (Mutoh et al., 2002).

Mutoh et al later found that the intestinal metaplasia progressed to invasive gastric adenocarcinoma when the transgenic mice were culled at later stages (Mutoh et al., 2004b). Upon investigation, it was found that *APC* (known to assist the degradation of β-catenin and therefore prevent proliferation) and/or *p53* (part of the apoptosis pathway) were mutated in the majority of intestinal metaplasia of these mice. These mutations, over a long duration, led to adenocarcinoma (Mutoh et al., 2004b). This was solely as a result of initial ectopic *Cdx2* expression, although it was not known whether the *APC* and *p53* mutations were randomly occurring or whether *Cdx2* expression had a direct effect upon these genes (Mutoh et al., 2004b).

The above research focused upon ectopic *Cdx2* expression from foetal stages. In pathological situations, genetic alterations occur randomly in regions formerly differentiating as stomach. Although it has been shown that ectopic *Cdx2* expression can lead to gastric adenocarcinoma in the laboratory, it is still unknown whether this occurs pathologically or whether *Cdx2* expression is a downstream consequence.

Cdx1 transgenic mice have also been shown to develop intestinal metaplasia. In these mice stomach specific expression of *Cdx1* was driven by the same promoter as that used previously to drive ectopic *Cdx2* expression in the parietal cells (H^+/K^+-ATPase; see above). Initially the cells expressed both H^+/K^+-ATPase and *Cdx1* but

H^+/K^+-ATPase expression was gradually lost in the gastric fundic mucosa. Eventually *Cdx1* was diffusely expressed and the parietal cells disappeared completely; the gastric mucosa was replaced completely by intestinal metaplasia. *Cdx1* induced metaplasia displayed all four intestinal cell types, unlike *Cdx2* induced metaplasia. The proliferating cells were located all over the crypt and possibly due to this, the metaplastic mucosa was much thicker than that reported in the *Cdx2* transgenic mice (Mutoh et al., 2004a).

In the colon, the loss of *Cdx2* expression can have opposing effects, dependent upon the initial cause of tumourigenesis (Calon et al., 2007). The loss of *Cdx2* can be disadvantageous because *Cdx2* demonstrates the qualities of a tumour-suppressor gene (Bonhomme et al., 2003). $Cdx2^{+/-}$ mice were therefore hypersensitive to carcinogenesis following a chemically induced or random mutation because this occurred in a background haploinsufficient for *Cdx2*. Excessive proliferation is normally suppressed by *Cdx2* (Bonhomme et al., 2003). The combination of $Apc^{+/\Delta 716}/Cdx2^{+/-}$ mutations led to an increase in the number of colonic heterotopias present in the intestine of mice, in comparison to single mutations alone, indicating that the two genes interact in forming aberrant lesions in the colon (Aoki et al., 2003). In intestinal carcinogenesis arising from chronic inflammation however, reduced *Cdx2* expression is advantageous. This is because a lack of Cdx2 increases cell motility and proliferation in the gut epithelium and so inflammation can be rapidly alleviated, preventing a chronic situation arising (Calon et al., 2007).

Once colorectal cancer (CRC) has become established the loss of *Cdx2* indicates an enhanced risk of the cancer disseminating and metastasising (Gross et al., 2007). The expression of *Cdx2* becomes reduced and heterogeneous during the progression of CRC, but the gene remains intact (Ee et al., 1995, Kaimaktchiev et al., 2004, Subtil et al., 2007). The reduction in *Cdx2* expression appears to be due to the cells undergoing an epithelial-mesenchymal transition, one of the first stages of metastasis. This leads to an upregulation of, amongst other genes, *Snail* and *Slug* (Gross et al., 2007). These two repressors have a direct effect upon the *Cdx2* promoter leading to its downregulation. It is the downregulation of *Cdx2*, not the upregulation of Cdx2 repressors, that has a direct effect upon increasing cell migration (Gross et al., 2007).

1.9 Manipulating the mouse embryo

1.9.1 Embryonic stem cells

Pluripotent ES cells are derived from the inner cell mass of a 3.5dpc blastocyst. ES cells were first successfully cultured in 1981 (Martin, 1981, Evans and Kaufman, 1981). ES cells are cultured by growing them on a layer of mitotically inactivated feeder cells (mouse embryonic fibroblasts, MEFs). The MEFs provide the ES cells with the nutrients required to maintain the pluripotent capacity of the cells and to provide anchorage to the ES cells. The ES cells are grown in the presence of leukaemia inhibitory factor (LIF) additional to that produced by MEFs to ensure differentiation of the cultured cells is suppressed (Smith et al., 1988).

Exogenous DNA can be incorporated into the cultured ES cells by electroporation. This involves applying a high voltage electrical pulse to a suspension of ES cells and DNA. This allows the exogenous DNA to enter the cells and to become incorporated into the endogenous DNA (Reiss et al., 1986).

1.9.2 Gene targeting in ES cells

Homologous recombination between exogenous and endogenous DNA following electroporation allows the manipulation of the gene of interest. Targeting vectors are designed to include the exogenous DNA and a positive selectable marker, flanked by homologous DNA sequences. Homologous recombination will therefore occur at the two homologous regions, replacing the endogenous region on the chromosome with the exogenous DNA (Figure 1.26). This event is reasonably rare, and so a positive selectable marker is used to isolate any ES cells which have incorporated the vector. These clones can then be investigated further for homologous recombination events.

The neomycin resistance gene (*neo*^{R}) is commonly used as a positive selectable marker. It confers resistance to the antibiotic geneticin (G418). ES cells grown in the presence of G418 will survive if the *neo*^{R} cassette has recombined into the endogenous DNA following electroporation. This will isolate all clones containing the cassette, whether recombination was homologous or random integration has occurred. The clones must then be screened for homologous recombination, normally performed by polymerase chain reaction (PCR).

Figure 1.26 Homologous recombination during gene targeting. Usually a replacement targeting vector is designed in which a positive selection cassette such as *neo*^{R} is included within the mutated region of interest. Homologous recombination will occur between regions of homology on either side of the exogenous DNA. This will result in a targeted locus containing the positive selection cassette along with the mutated version of the original exon. This targeting event in ES cells will allow the cell to survive selection for the presence of the *neo*^{R} cassette and therefore indicate any ES clones containing homologous recombination events. The use of a negative cassette such as DTA will help ensure any ES cells containing random targeting events do not survive as they will express the diphtheria toxin A.

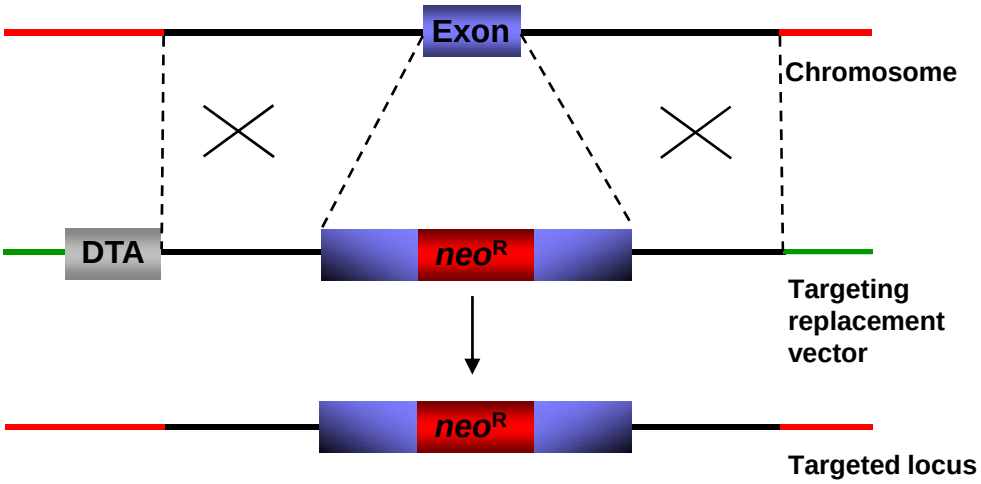

A diphtheria toxin A (*DTA*) cassette can be used for negative selection, to reduce the number of clones surviving random integration events. The diphtheria toxin contains two fragments, A and B. DTA is the N-terminal region of the diphtheria toxin, 22kDa in size. The presence of DTA in eukaryotic cells leads to an inhibition of protein synthesis and subsequent cell death (Collier and Kandel, 1971, Gill and Dinius, 1971). Random integration events involving the transfer of the *DTA* cassette into the endogenous DNA will therefore lead to cell death (Figure 1.26).

The use of a dual system involving both positive and negative selectable markers therefore reduces the number of surviving colonies containing incorrect targeting events.

1.9.3 Generation of transgenic mice

Once the targeting event in ES cells has been achieved, transgenic mice can be generated. The targeted ES cells are injected into 3.5dpc blastocysts, recovered via micromanipulation techniques from a mouse. The injected blastocysts are then transferred into the uterus of a surrogate pseudo-pregnant female. If the pregnancy is successful, neonates are born approximately 16 days later. These neonates will be chimeras if the targeted ES cells have successfully become incorporated into the host blastocyst (Bradley et al., 1984).

Coat colour can be used to identify chimeras. The ES cells containing the targeted event are obtained from a mouse of a specific fur colour (e.g. white) and transferred into a host blastocyst of a different fur colour (e.g. black). The subsequent mice will therefore be black with regions of white fur if they are chimeras containing ES cells incorporated into the skin (see Figure 1.27). Ear or tail samples are normally also taken from mice that do not appear externally chimeric to ensure that they are truly WT and not that the targeted ES cells have simply not been incorporated into the skin.

Germline transmission is required in order to create a mouse line transmitting the mutated allele. Most ES cells originally used are male in origin and so female chimeras are less likely to transmit the ES cell targeted event through the germline. Male chimeras are therefore mated to wild-type females. The females are normally

Figure 1.27 Generation of transgenic mice from ES cells. (A) Targeted albino coat colour ES cells are usually microinjected into a black coat colour 3.5dpc blastocyst. (B) Blastocysts are transferred to surrogate female. (C) Chimeric pups are produced containing cells derived from both the original injected ES cells and the host blastocyst. (D) Chimeras are mated with WT C57/BL6 mice. (E) F1 progeny are produced. Successful germline transmission can be detected by coat colour. Agouti coloured offspring will have transmitted the targeted ES cells, whereas black coloured offspring originate from the host blastocyst.

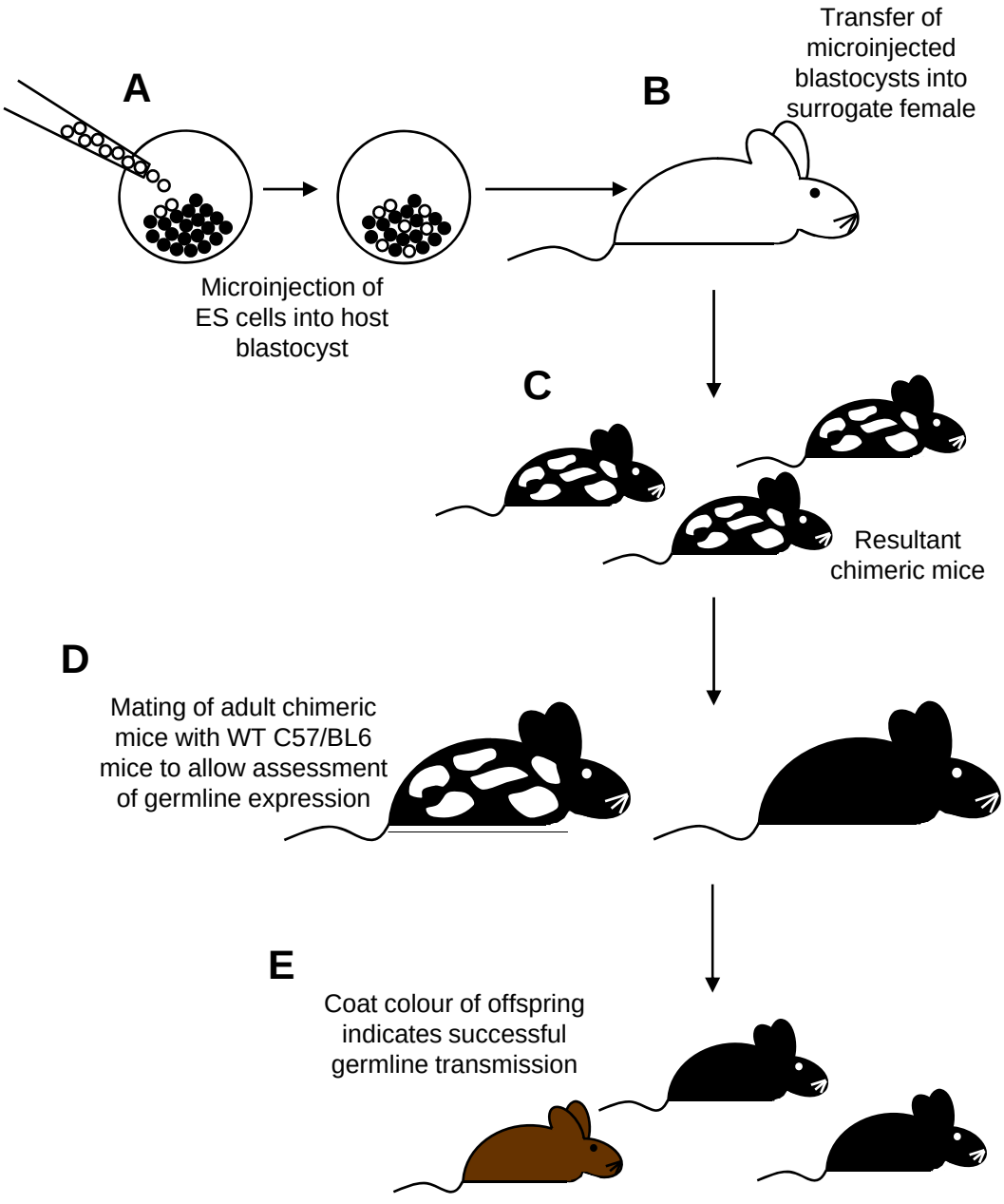

C57/BL6 as these mice are black and therefore successful germline transmission is indicated by the coat colour of the offspring (Figure 1.27). These offspring will be heterozygous for the mutation and can be used to set up a breeding colony.

1.10 Conditional gene targeting systems

1.10.1 The Cre-LoxP inducible system

In many situations, the generation of inherent null mutants leads to an embryonic lethal phenotype, for example *Cdx2*$^{-/-}$ mutants; these failed to survive despite 'rescue' via tetraploid fusion (as previously discussed). This meant that the function of the gene beyond its requirement for embryonic survival could not be investigated. To circumvent this problem, systems have been created whereby the gene, or a portion of the gene, can be conditionally 'knocked out'. These systems provide spatial and temporal control over loss-of-function studies.

One system utilises Cre-mediated recombination; the Cre-*Lox*P system. Cre recombinase is a 38kDa integrase transcribed from the cyclization recombination (*Cre*) gene of P1 bacteriophage. Cre recognises and mediates site-specific recombination between locus of crossover (x) in P1 bacteriophage (*lox*P) sites. The *lox*P sequences are found naturally in bacteriophage and are used for maintenance of the phage genome as a unit copy plasmid in the lysogenic state of the life cycle (Hoess et al., 1982, Hoess and Abremski, 1984, reviewed in Nagy, 2000).

The *lox*P site consists of a 34bp sequence. This contains two 13bp inverted repeats with an 8bp non-palindromic spacer sequence in the centre (see Figure 1.28) (Torres and Kuhn, 1997). The direction of the spacer sequence determines the *lox*P sequence orientation. The direction of the two *lox*P sites determines the nature of the recombination event (Figure 1.29) (Hoess et al., 1982, Hoess and Abremski, 1984).

This system can be used to conditionally inactivate genes by positioning the functional region of the gene in question between two *lox*P sites in the same orientation. This arrangement will permit normal transcription of the gene. Addition of Cre recombinase will cause excision of the region between the two *lox*P sites, thus rendering the gene null (Nagy, 2000). The use of this system will be discussed further in Chapter 6.

Figure 1.28 Sequence of a *lox*P site. This consists of a 34bp sequence containing a non-palindromic spacer flanked on either side by an inverted repeat. (Adapted from Hoess et al. 1982).

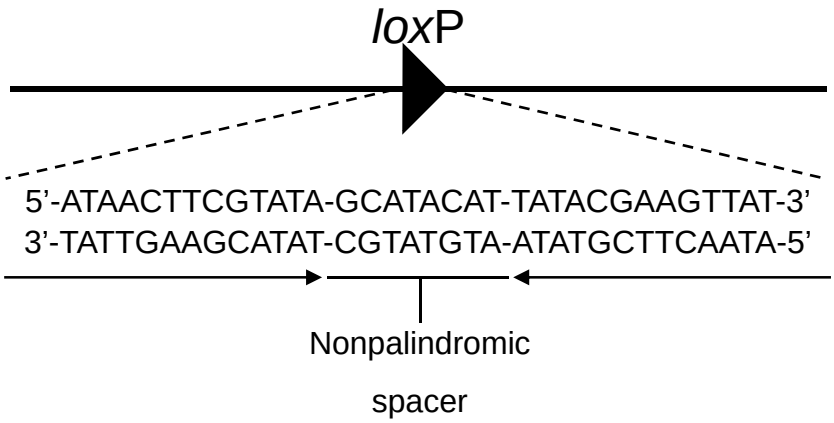

Figure 1.29 Possible Cre-mediated recombination events. (A) If both *lox*P sites are in the same orientation then recombination will occur resulting in excision of the flanked region, leaving one remaining *lox*P site. (B) If the *lox*P sites are in different orientations, then recombination will occur between the two sites, reversing the orientation of the flanked region. (Adapted from Nagy, 2000).

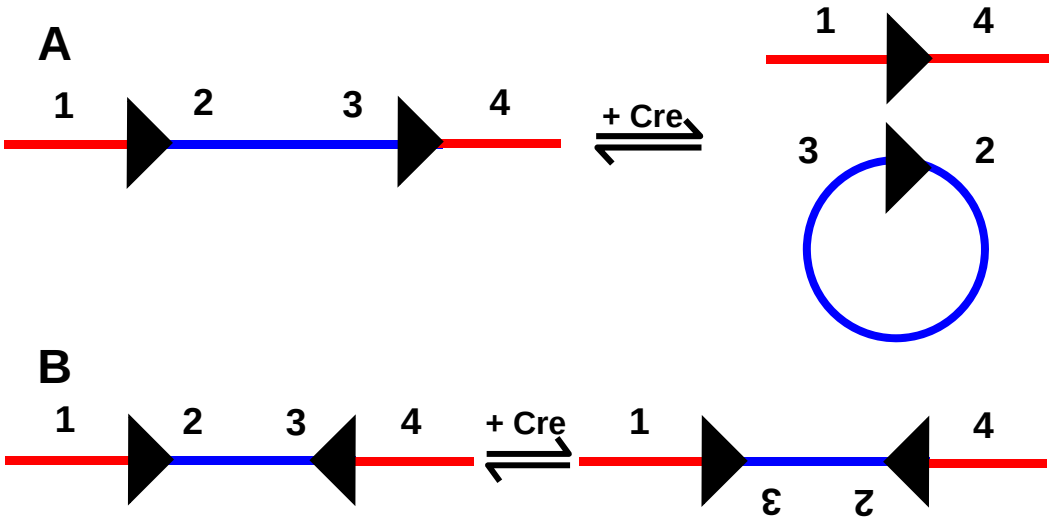

1.10.2 The Flp-FRT system

A separate system to the Cre-*LoxP* technique is available, the Flp-*FRT* system. This allows the use of multiple site-specific recombinase systems to be used during the same genetic strategy.

Some targeting vectors contain two regions that need to be deleted. One region may be the functional portion of a gene that must be selectively deleted to create a conditional knock-out mouse. Flanking this region with *lox*P sites permits inducible Cre-mediated recombination. Other regions may be advantageous to ubiquitously delete prior to the creation of transgenic mice, for example the neo^R cassette used during positive selection of ES clones. Flanking both regions with *lox*P sites leads to numerous outcomes following addition of Cre (Figure 1.30). Use of another recombination system, such as Flp-*FRT*, removes this problem (Figure 1.31).

This system is found in *Saccharomyces cerevisiae* and is thought to aid the amplification of the plasmid in the yeast nucleus (Zhu et al., 1995). The system comprises of two Flippase recognition target (*FRT*) sites that undergo recombination upon the addition of Flippase recombinase (Flp). The *FRT* site contains two 13bp inverted repeat sequences surrounding an 8bp spacer sequence (Figure 1.32) (McLeod et al., 1986). The inverted repeat sequences are homologous to those in *lox*P (Hoess and Abremski, 1984). The use of this system will be discussed further in Chapter 6.

1.11 Aims

This thesis is concerned with two aspects of gut development. Firstly, the relationship between the endoderm and mesoderm during development and secondly whether intestinal stem cell potency is reduced postnatally.

As mentioned above, co-culture experiments have shown that undifferentiated mesoderm will develop intestinal characteristics when exposed to intestinal endoderm. Intestinal mesoderm, however, has also been shown to cause the alteration of colonic endoderm to small-intestinal endoderm, although this does not occur in reverse (see section 1.6.3) (Duluc et al., 1994). The fact that these results were gained by xenograft of co-cultures into nude mice, which is a fairly artificial

Figure 1.30 Possible outcomes following Cre-mediated recombination in triple *lox*P constructs. The positive selection cassette is not required beyond selection of ES clones and may hinder gene transcription in the transgenic animal. The initial requirement is therefore the removal of this cassette. In systems utilising three *lox*P sites, the desired outcome is the type 2 deletion, i.e. the exon remains flanked by *lox*P sites while the selection cassette is excised out. Two other outcomes are however possible. The entire region between the outer two *lox*P sites may be excised (type 1 deletion), or the exon alone may be excised leaving the selection cassette intact (type 3 deletion). Either outcome is unwanted as both render the gene inherently null.

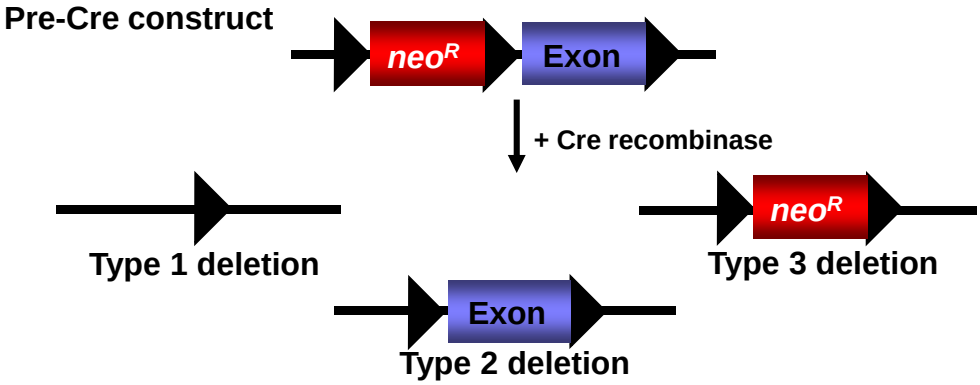

Figure 1.31 A dual recombination strategy. The Flp/*FRT* system works in a similar manner to the Cre/*Lox*P system. Flanking the positive selection cassette with *FRT* sites allows excision of the cassette following addition of Flippase recombinase with only one possible outcome. The exon is then flanked by *Lox*P sites ready for Cre-mediated recombination.

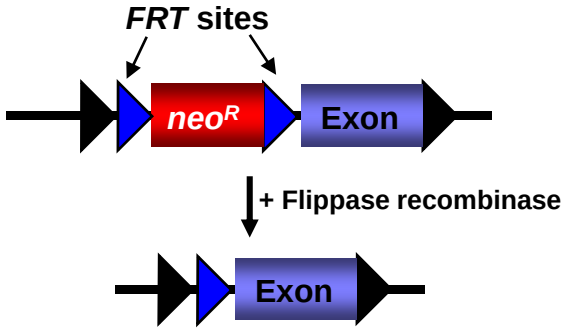

Figure 1.32 Sequence of a *FRT* site. A 34bp sequence consisting of a non-palindromic spacer flanked on either side by an inverted repeat. (Adapted from McLeod et al., 1986).

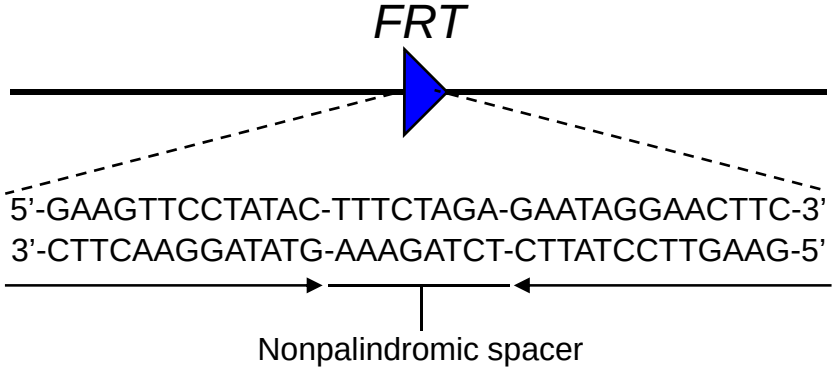

environment, may explain some of the conflicting findings. A completely *in-vivo* system would provide more conclusive information.

Cdx2 mutant mice permit the investigation of endoderm-mesoderm interactions, prior to determination of the gut layers, in an *in-vivo* environment. It is known that the loss of intestinal endoderm-specific Cdx2 protein leads to the development of gastric heterotopias, i.e. endodermal *Cdx2* expression is fundamental for the development of intestine epithelium, without which default stomach epithelium develops. It is not known, however, if the mesoderm is responsive to these altered endodermal signals or remains as intestine.

It is hypothesised here that the mesoderm responds to the endoderm, downstream of *Cdx2* expression. This is thought to be the case because endodermal *Cdx2* expression occurs at the initiation of intestinal development. Following the commencement of this project, *Barx1*$^{-/-}$ mice were used to show that loss of expression of a mesoderm-specific gene causes the morphological alteration of stomach epithelium. This demonstrated that the endoderm is responsive to mesodermal signals but still did not indicate whether the original signal was endodermal in origin as hypothesised (Kim et al., 2007b). If the *Cdx2* hypothesis is accurate, stomach mesoderm-specific genes would be expressed in the absence of endodermal *Cdx2* in the intestine of *Cdx2* mutant mice (Figure 1.33). The aims of this thesis were to test this hypothesis by:

- The identification of nascent areas of heterotopias in the *Cdx2*$^{+/-}$ heterozygous and *Cdx2*$^{-/-}$ chimeric gut with the aim of determining the ideal developmental stage in which to investigate these regions further.

- The use of PCR techniques to identify stomach-mesoderm specific gene expression in *Cdx2*$^{+/-}$ heterozygous gut.

- The use of *in-situ* hybridisation techniques to investigate the nature of aberrant stomach-mesoderm specific gene expression in the *Cdx2*$^{+/-}$ and *Cdx2*$^{-/-}$ gut.

- The generation of a mouse line where *Cdx2* is flanked by *lox*P sites introduced by gene targeting in ES cells with the aim of generating a conditional knockout mouse for *Cdx2.* The potential of the intestinal stem cells to respond to an alteration in epithelial gene expression occurring after the initial development of the intestine can then be investigated. This will also indicate whether the mesoderm has become restricted to intestinal-type tissue and at what stage this has occurred.

Figure 1.33 Diagram illustrating the hypothesis to explain the relationship between the endoderm and mesoderm with regard to *Cdx2* in the intestine. It was shown in *Barx1*$^{-/-}$ mice that the mesoderm signals to the endoderm (red arrows). It was hypothesised that the initial signal (*Cdx2*) originates in the intestinal endoderm (blue arrows). This signal is received by the mesoderm (depicted on the left) causing expression of unknown intestinal-mesoderm specific genes (indicated by yellow box). The mesodermal signal is received by the endoderm, confirming the development of intestinal epithelium. In the absence of Cdx2 (depicted on the right), the mesoderm expresses unknown stomach-mesoderm specific genes (indicated by blue box). This signal is received by the endoderm and so stomach epithelium develops.

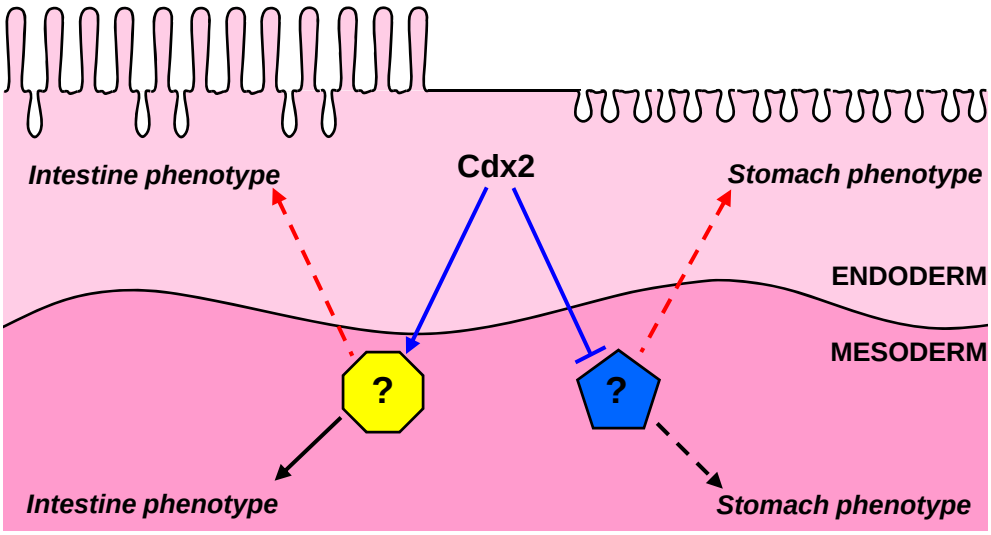

2. Materials and Methods

The H_2O used in all methods (including those requiring RNase-free H_2O) was always MilliQ water, dispensed into sterile containers.

2.1 Molecular Biology

Unless otherwise stated, all chemicals were obtained from Fisher and all restriction endonucleases were supplied by New England Biolabs.

2.1.1 Plasmids

The plasmids used were:

- pBluescriptSKII+ (pBSSKII+) (Stratagene; Figure 2.1A)
- pGKNeoF2L2DTA (gift from A. Connor, Fannie C. Rippel Transgenic Facility, Cambridge, UK; Figure 2.1B)
- pGKNeoF2L2DTAΔNcoI (gift from S. Munson, GENETA, University of Leicester, UK; Figure 2.1C)
- pBS-Barx1 (gift from P. Sharpe, Craniofacial Department, King's College London, UK; Figure 2.1D)
- pBS-Hoxb-1 (gift from J. Deschamps, Hubrecht Institute, Royal Netherlands Academy of Arts and Sciences, Netherlands; Figure 2.1E)

ESTs were supplied by MRC Geneservice as I.M.A.G.E. Clones:

I.M.A.G.E. Ids: 6335394 (*Csl;* Figure 2.2A)
932297 (*Nkx2-5*; Figure 2.2B)
6413283 (*Sox2*; Figure 2.2C)

2.1.2 Ethanol precipitation

0.1x volume of 3 M NaOAc (pH 5.5) and 2x volumes 100% [v/v] ethanol were added to the DNA sample. The solution was placed at -20˚C overnight or -80˚C for 2 hours (h) to aid precipitation of the DNA. The solution was then centrifuged at 13,000 rpm, 4˚C for 10 min. The supernatant was discarded and the pellet washed with 70% [v/v]

Figure 2.1 Plasmid maps. (**A**) pBSSKII+ (MCS= multiple cloning site) (**B**) pGKNeoF2L2DTA (**C**) pGKNeo F2L2DTAΔNcoI (**D**) pBS-Barx1 (**E**) pBS-Hoxb-1

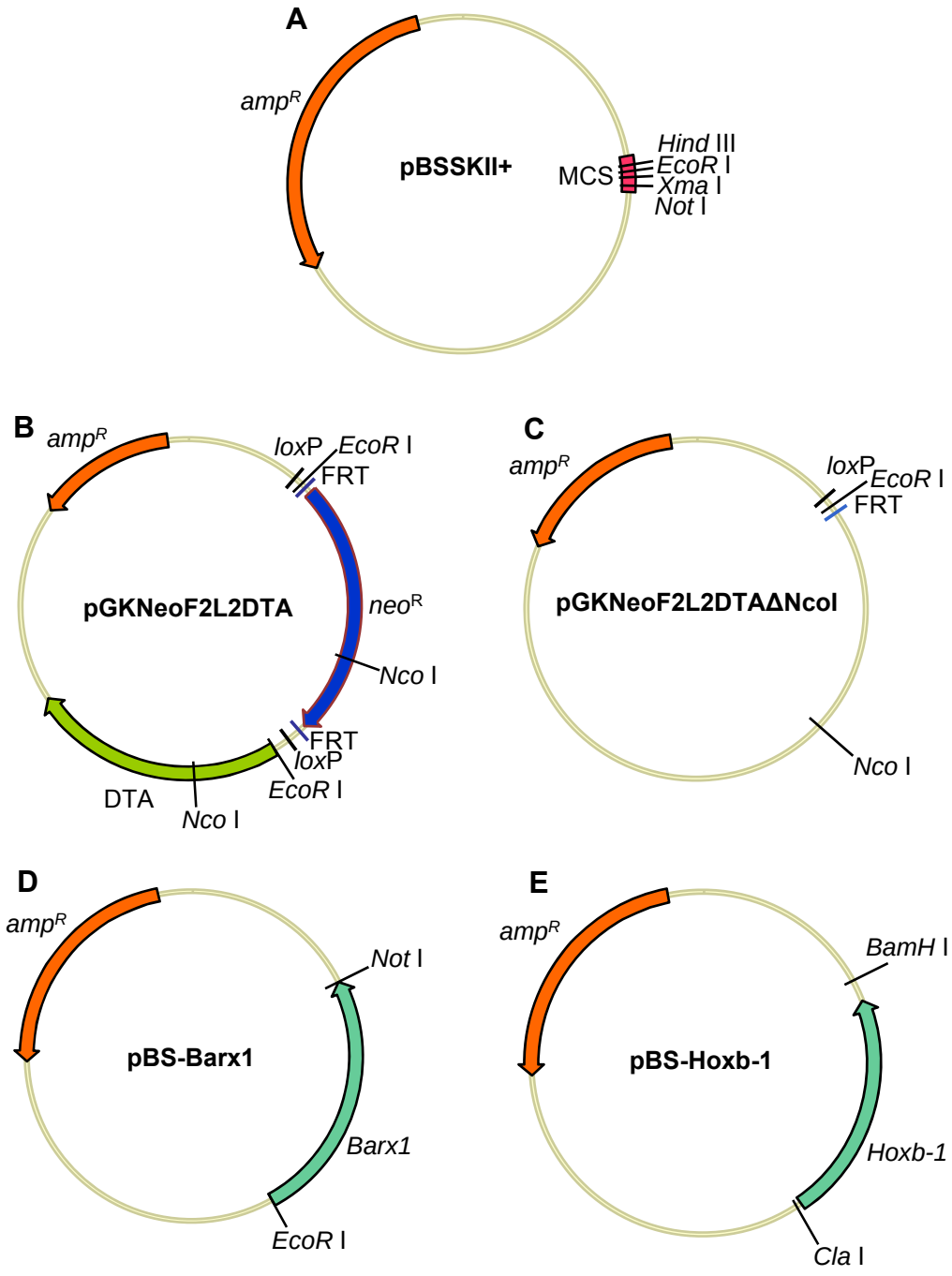

Figure 2.2 I.M.A.G.E. EST plasmid maps. (A) I.M.A.G.E. 6335394 (Csl) (B) I.M.A.G.E. 932297 (Nkx2-5) (C) I.M.A.G.E 6413283 (Sox2)

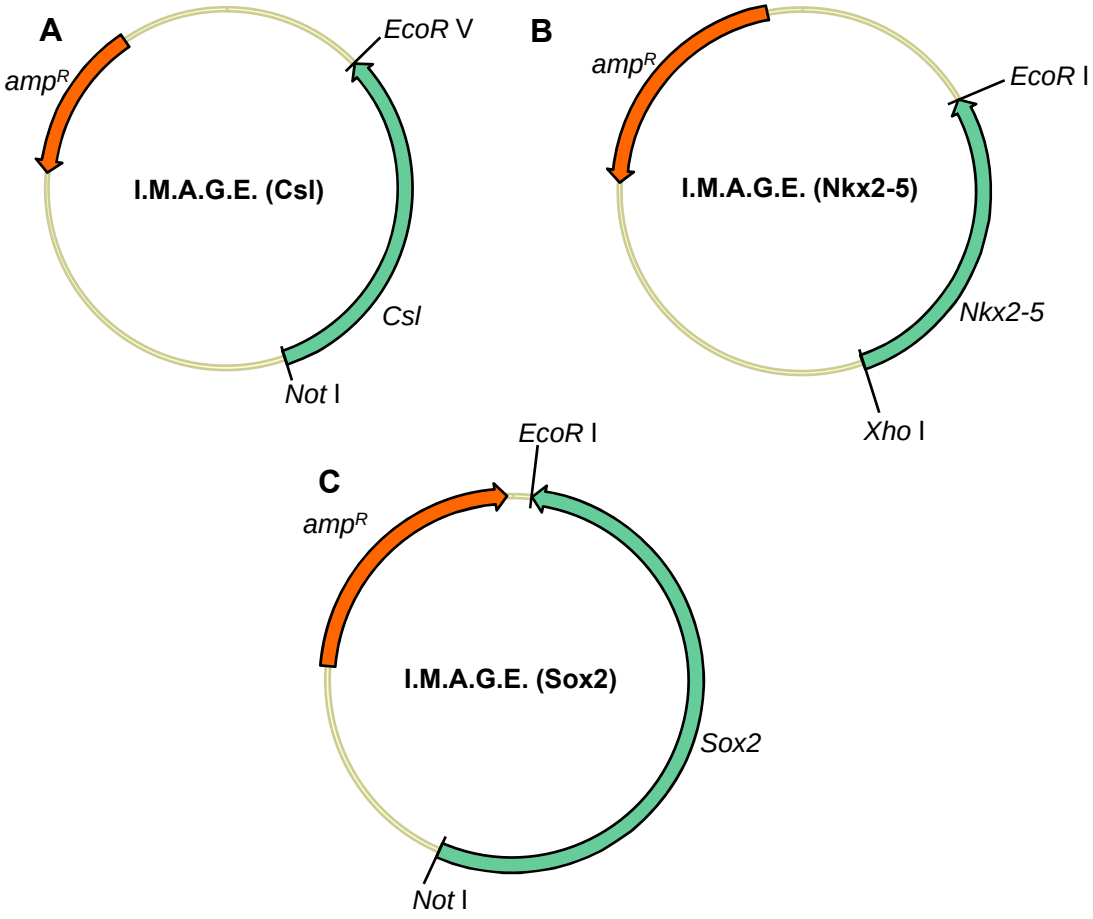

ethanol. The tube was again centrifuged at 13,000 rpm, 4˚C for 5 minutes (min) and the supernatant discarded. The DNA pellet was then air dried and resuspended in an appropriate volume of TE (10mM Tris [pH 8.0], 1mM EDTA [pH 8.0] [Fisher]) or H_2O.

2.1.3 Small-scale restriction enzyme digest of DNA

For analytical purposes, DNA obtained from a minipreparation was used (see section 2.1.11). 1 unit of restriction enzyme was added to a mixture containing 10 µl of DNA and 1x restriction enzyme buffer (supplied by the enzyme manufacturer at 10x concentration). The reactions were incubated at the optimal temperature recommended by the manufacturer for 1 h.

2.1.4 Large-scale restriction enzyme digest of DNA

For cloning purposes, 10 µg of plasmid DNA (obtained from a maxipreparation or caesium chloride preparation; sections 2.1.12 and 2.1.13) was added to a tube containing 1x restriction enzyme buffer (supplied by the manufacturer) and the required enzyme (1 µl enzyme per 5 µg DNA). This was incubated at the optimal temperature as recommended by the manufacturer, for at least 2 hours assessed by agarose gel electrophoresis.

2.1.5 Agarose gel electrophoresis

Pure agarose (Roche) was melted in 1x TAE (40 mM Tris base, 1 mM EDTA [pH 8.0] [Fisher]) to obtain a 1% [w/v] agarose solution, to which 1 µg/ml ethidium bromide was added. Gels were electrophoresed in 1x TAE. 5x loading dye (30% [v/v] glycerol [Fisher], 0.5% [w/v] Orange G) was added to the samples if required. The samples were loaded into the wells of the gel. 5 µl of a 1kb Plus DNA ladder™ (Invitrogen) was loaded alongside the samples to indicate the size of the DNA bands produced. Gels were electrophoresed at 100 V and DNA bands visualised using a Bio-Rad gel documentation system.

2.1.6 Purification of gel fragments

The required DNA band was extracted from the agarose gel using a clean scalpel blade. The DNA was purified from the gel using a QIAquick Gel Extraction Kit (Qiagen). The method used was as per the manufacturer's protocol.

2.1.7 Removal of 5' phosphate groups from linearised plasmid DNA

Following restriction digest of the DNA sample, calf intestinal alkaline phosphatase (CIP; New England Biolabs) was added to the digest reaction (0.5 µl enzyme per 5 µg DNA in reaction) and incubated at 37˚C for 15 min. To deactivate the enzyme, 5 mM EDTA was added to the reaction and the mixture incubated at 75˚C for 10 min.

2.1.8 Removal of small fragments following restriction enzyme digestion

A QIAquick Nucleotide Removal Kit (Qiagen) was used as per the manufacturer's protocol in order to remove <10mers from >40bp double-stranded DNA fragments following restriction enzyme digest.

2.1.9 Ligation of DNA fragments

A spectrophotometer (Eppendorf BioPhotometer) was used to determine the concentration of DNA in each sample of vector and insert. In order to determine the volume of linearised vector required for the ligation (on the basis that 50 ng of insert DNA will be used), the equation below was used:

$$\frac{(\text{insert size}) \times 50}{(\text{vector size})} \times \frac{3}{1} = \text{amount of vector}$$

(N.B. Insert and vector size are in Kb)

The equation takes into consideration the size of the fragments involved in the ligation and assumes a 3:1 ratio of insert to vector. The resulting value is the amount, in ng, of vector DNA required for a ligation with 50ng insert DNA.

The calculated amount of insert and linearised plasmid were added to 1.5µl of 10x T4 ligase buffer (supplied with enzyme) along with 1µl T4 DNA ligase (Roche), in a total volume of 15µl. This was incubated at room temperature for 4 hours.

2.1.10 Transformation of competent DH5α E.coli

One aliquot (50 µl) of DH5α library competent cells (Invitrogen) was thawed on ice and transferred to a polypropylene tube. 10ng of plasmid or ligation mix were gently mixed with the cells and the tube incubated on ice for 30 min. The tube was heat

shocked at 42ºC for 45 sec then placed back on ice for 2 min. 500 µl of S.O.C. media (Invitrogen; 2% [w/v] tryptone, 0.5% [w/v] yeast extract, 10 mM NaCl, 2.5 mM KCl, 10 mM $MgCl_2$, 10 mM $MgSO_4$, 20 mM glucose) was added to the tube and placed in a 225 rpm shaking incubator at 37ºC for 1 h. 25 µl of bacteria containing the plasmid (or 400 µl of bacteria containing the ligation mix) was spread onto a Luria Bertani (LB) agar plate (1.5% [w/v] agar bacteriological [Oxoid], 1% [w/v] bactotryptone [Oxoid], 0.5% [w/v] bactoyeast extract [Oxoid], 17 mM NaCl [Fisher]) containing 50 µg/ml ampicillin. The plate was inverted and incubated at 37ºC overnight.

2.1.11 Minipreparation of plasmid DNA from bacteria

A single colony was picked from an LB agar plate and transferred to 5 ml of LB media (1% [w/v] bactotryptone [Oxoid], 0.5% [w/v] bactoyeast extract [Oxoid], 17 mM NaCl [Fisher]) containing 50 µg/ml antibiotic. The tube was placed in a 225 rpm shaking incubator at 37ºC overnight. 1 ml of the subsequent bacterial culture was centrifuged at 13,000 rpm for 1 min. The supernatant was removed and the bacterial pellet resuspended in 100 µl of resuspension buffer (P1; 50 mM Tris-HCl [pH8.0], 10 mM EDTA (Fisher), 100 µg/ml ribonuclease [RNaseA; Promega]). 200 µl of lysis buffer (P2; 0.2 M NaOH [Fisher], 1% [w/v] sodium dodecyl sulphate [SDS; Melford]) was added and the tube gently inverted several times. 150 µl of neutralisation buffer (P3; 5M KOAc, [pH5.5]) was added and the tube inverted several times rigorously. The tube was then centrifuged at 13,000 rpm for 5 min. The supernatant was transferred to a fresh tube and 500 µl 100% [v/v] ethanol was added and mixed. The DNA was then precipitated by centrifugation at 13,000 rpm for 10 min at 4ºC. The supernatant was discarded and the pellet washed with 70% [v/v] ethanol. The tube was again centrifuged at 13,000 rpm for 1 min at 4ºC then the supernatant discarded. The resultant pellet was air dried then resuspended in 50 µl TE (10mM Tris [pH 8.0], 1mM EDTA [pH 8.0] [Fisher]) containing 50 µg/ml RNaseA.

2.1.12 Maxipreparation of plasmid DNA from bacteria

2 ml of a 5 ml overnight bacterial culture was used to inoculate a sterile flask containing 500 ml of LB media and 50 µg/ml antibiotic. The flask was placed in a 225 rpm shaking incubator at 37˚C overnight. The bacteria were then harvested and the plasmid DNA extracted using an EndoFree Plasmid Maxi Kit (Qiagen) as per the manufacturer's manual.

2.1.13 Caesium chloride preparation of plasmid DNA from bacteria

2 ml of a 5 ml bacterial culture was used to inoculate a sterile flask containing 400 ml of LB media and 50 µg/ml ampicillin. The flask was placed in a 225 rpm shaking incubator at 37˚C overnight. The bacteria were harvested by centrifugation at 6,000 rpm, 4˚C for 10 min (Sorvall Evolution RC centrifuge using a SLA-1500 rotor). The supernatant was discarded and the pellet resuspended in 10 ml P1 buffer. 20 ml P2 buffer was then added and the tube inverted gently several times. 15 ml of P3 buffer was finally added and the tube inverted again. The tube was then centrifuged at 9,000 rpm, 4˚C for 15 min. The supernatant was filtered (Miracloth; Calbiochem) into a fresh tube and 50 ml 100% [v/v] ice cold isopropanol was added to precipitate the DNA. The tube was centrifuged for 15 min at 9,000 rpm. The supernatant was discarded, the tube inverted and the DNA pellet allowed to air dry. The pellet was resuspended in 6 ml TE and transferred to a polypropylene tube containing 6 g CsCl (Invitrogen). Once the CsCl had dissolved, 275 µl of 10 mg/ml ethidium bromide was added to the tube. The tube was then centrifuged at 4,000 rpm for 5 min. The resultant clear solution was syringed into two quick seal Ultra Centrifuge tubes (Beckman). The tubes were heat sealed and centrifuged at 100,000 rpm, 20˚C for 16 h (Beckman Optima^{TM} Max-E Ultracentrifuge). The lower plasmid band was extracted from the tube via syringe and retained in a fresh tube. The DNA was extracted from this by addition of an equal volume of water-saturated isobutanol to the tube, followed by vigorous shaking and removal of the upper aqueous layer. This was repeated until the upper layer became clear at which point the upper layer was removed and the lower layer retained. The DNA was precipitated by addition of 2x volume H_2O and 2x total volume 100% [v/v] ethanol. The tube was then centrifuged at 11,000 rpm (Sorvall Evolution RC; SS-34 rotor) for 15 min and the supernatant discarded. The DNA pellet was washed with 70% [v/v] ethanol and centrifuged at 11,000 rpm for 5 min. The supernatant was discarded, the pellet air dried and then resuspended in 250 µl TE.

2.1.14 Specialised techniques for pGKCdx2 large scale preparation

The plasmid pGKCdx2 required a specialised technique in order to create a large scale preparation. XL10-GoldR Ultracompetent Cells (Stratagene) were transformed as per the manufacturer's protocol with 10ng pGKCdx2 plasmid and plated out overnight at 37˚C. Numerous individual colonies were selected from the LB agar

plate and each was used to inoculate 5 ml of Terrific broth (1.3% [w/v] bacto-tryptone [Oxoid], 2.6% [w/v] yeast extract [Oxoid], 0.4% [v/v] glycerol in 900 ml H_2O then autoclaved; added to 0.17 M KH_2PO_4, 0.72 M K_2HPO_4 in 100 ml autoclaved prior to mixing). The 5 ml broths were then grown overnight in a 225 rpm shaking incubator at 37˚C. The more confluent broths were combined the next morning to create a bacterial suspension suitable for use with the EndoFree Plasmid Maxi Kit (Qiagen).

2.1.15 Primer synthesis and DNA sequencing

Primers were designed with the aid of Primer3 (http://frodo.wi.mit.edu/). If primers were required to have restriction sites added to allow cloning of the PCR product, then the New England Biolabs (NEB) catalogue was consulted as to how many nucleotides, in addition to those constituting the restriction site, were required to make primer annealing more efficient. The primers were then synthesised by Invitrogen. All DNA sequencing was performed by the Protein and Nucleic Acid Chemistry Laboratory (PNACL), University of Leicester, UK.

2.1.16 Lysis of mouse tissue for genotyping

A small ear sample, removed for identification purposes, was used for genotyping adult mice whilst the tail was removed from embryos for the same purpose. If embryos resulting from chimeric litters were to be genotyped then both a tail sample and a toe sample were taken to ensure chimerism was thoroughly investigated. The samples were lysed by adding 70 µl of 0.05 M NaOH to the tube and then placing them at 95˚C for 15 min. The samples were neutralised using 7 µl of 1 M Tris [pH7.5] before PCR.

2.1.17 Lysis of cells to extract genomic DNA

The media was removed from fully confluent ES clones grown on a 12-well cell culture plate. The clones were washed with phosphate buffered saline (PBS; 136 mM NaCl, 8 mM Na_2HPO_4, 2.7 mM KCl, 1.5 mM KH_2PO_4). 500 µl of DNA lysis buffer (50 mM Tris [pH7.6], 1 mM EDTA, 100 mM NaCl, 0.2% [w/v] SDS) containing 100 µg/ml of freshly added proteinase K was added to each well of the plate. The clones were then incubated at 37˚C for 16 h (or 60˚C for 3 h). The lysates were each transferred to a separate eppendorf and 1 ml of 100% [v/v] ethanol was added. The tubes were inverted several times then placed at -20˚C overnight (or -80˚C for 2 h). The tubes

were centrifuged at 13,000 rpm for 10 min and then the supernatant was carefully removed. 1 ml of 70% [v/v] ethanol was added and the tubes were again centrifuged at 13,000 rpm for 10 min and the supernatant removed. The DNA pellets were allowed to dry at room temperature for 15 min then resuspended in 250 µl TE. Incubating the DNA samples at 60˚C for 30 min aided dissolving of the DNA.

2.1.18 Standard polymerase chain reaction (PCR)

Reddymix PCR Master Mix (Abgene) was used for most PCR reactions. Primers (Table 2.1) were added to 18 µl Reddymix, at a final concentration of 0.5 pmol/µl. DNA was added to a final concentration of 10 pg–1 µg.

Alternatively, PuReTaq™ Ready-to-go PCR beads (Amersham) were used. Each bead was rehydrated in 21 µl H_2O and primers (Table 2.1) added at a final concentration of 0.5 pmol/µl. 1 µl of DNA sample or plasmid was added to the mixture.

If the PCR was to be used to generate DNA fragments that would eventually be used for creating transgenic mice, then a High fidelity Taq DNA polymerase was used. A master mix was made containing 1 x Alec Jeffreys Buffer (AJB; 11.1x stock: 2 M Tris-HCl [pH8.8], 1 M $(NH_4)_2SO_4$, 1 M $MgCl_2$, 100% [v/v] 2-mercaptoethanol, 10 mM EDTA [pH8.0], 100 mM dATP, 100 mM dCTP, 100 mM dGTP, 100 mM dTTP, 10 mg/ml BSA), 2% [v/v] dimethyl sulphoxide (DMSO), 0.5 pmol/µl primers (Table 2.1) and 0.175 units/µl High fidelity Taq DNA polymerase (Roche) in a final volume of 140 µl. 14 µl of genomic DNA (200 µg/ml) was added to the master mix as a template. This mixture was divided into PCR tubes containing 25µl of mixture per tube.

Regardless of which method was used, each PCR sample was overlaid with a drop of mineral oil and the tubes were placed in a G-Storm™ PCR machine. The PCR conditions used are indicated below:

Initial denaturation of DNA at 95˚C for 5 min followed by a number of cycles (Y; Table 2.1) consisting of three steps:

Table 2.1 A list of primers used in this project.

Primer Name	Sequence 5' to 3'	Annealing Temp (X)	Number of Cycles (Y)	Purpose
T3	AAT TAA CCC TCA CTA AAG GGA GA	N/A	N/A	Sequencing
T7	TAA TAC GAC TCA CTA TAG GGA GA	N/A	N/A	Sequencing
OCP66	CGT GCA ATC CAT CTT GTT CA	65˚C	35	Sequencing
OCP174	AGG TCG GTG TGA ACG GAT TTG	55˚C	30	RT-PCR
OCP175	TGT AGA CCA TGT AGT TGA GGT CA	55˚C	30	RT-PCR
Cdx2-P1	AGG GAC TAT TCA AAC TAC AGG AG	61˚C	35	PCR
Cdx2-P2	ATA TTG CTG AAG AGC TTG GCG GC	61˚C	35	PCR
Cdx2-P3	TAA AAG TCA ACT GTG TTC GGA TCC	61˚C	35	PCR
OES2	ATA AGA ATG CGG CCG CGG ACA GCG CTC AGT CCC CAG GG	61˚C	35	PCR/sequencing
OES5	CCA TCG ATG AAT TCC AGG GCA GGA CTT TGT GTG TGG TAC TGG TG	65˚C	35	PCR
OES7	TGC CGC TAA GCT TAT GGA TCA GAG AGC TGT AAG G	55˚C	35	PCR
OES9	CTC TGG AAT TCT GAA AGA GCG GCA AAA ACA ACT GGA CAC TCA AGG	65˚C	35	PCR/sequencing
OES10	GTG CCT ACG CGG CCG CGC TAC CTG CTT TTC TTC TTC CA	60˚C	35	PCR
OES11	TCC TGC CCG CGG CCG CTG AGT GCT ATC TCC ATG TTG TCA G	60/61˚C	35	PCR/sequencing
OES12	TAT AAG CTT TGC CTC TGG CTC CTG TAG TT	55˚C	35	PCR
OES14	CTG ACC CAG CCA AAG ACC	58˚C	30	RT-PCR
OES15	GTA GCT GGG GTA GGG GTA GG	58˚C	30	RT-PCR
OES23	GCC TGA GCC AGT TAC AGG TG	60˚C	30	RT-PCR
OES24	GTC TCC GCT GGC TTC TCT GT	60˚C	30	RT-PCR
OES25	GTC TCC TTG GCA CGC TCT T	N/A	N/A	Sequencing
OES26	TAG CAC TTG TTG CCA GAA CG	61˚C	30	RT-PCR
OES27	AAG CCG CTC TTC TCT TTT CC	61˚C	30	RT-PCR
OES29	TGT AGC CTC GAC TTG GCT TT	N/A	N/A	Sequencing
OES30	TCC TAG CCA GGA CAG GAG AA	55˚C	35	PCR
OES31	GGG TTC CGG ATC CAC TAG TTC	55˚C	35	PCR
OES34	TCG CCT TCT TGA CGA GTT CT	55˚C	35	PCR
OES35	AGG GAC AGG AAG TCC AGG TT	55˚C	35	PCR

Step 1: 95˚C for 30 sec

Step 2: X˚C for 30 sec (Table 2.1; Note: PCR to genotype *Cdx2* mutant mice requires 1 min)

Step 3: 72˚C for 1 min per Kb of product

A final extension at 72˚C for 10 min

2.1.19 Isolation of RNA from mouse tissue

Tissue was washed in PBS then immediately transferred to RNAlater (Invitrogen) in pieces no bigger than 3 mm^3. The tissue was stored at -20˚C until required.

An RNeasy kit (Qiagen) was followed as per the manufacturer's protocol for RNA extraction from tissue using a rotor-stator homogeniser. Once the RNA had been extracted, a 1 µl aliquot was used for any DNA based PCR reactions that were required in order to genotype the sample, prior to DNase treatment. A DNA-free kit (Ambion) was then used as per the manufacturer's protocol in order to remove this DNA contamination. The rigorous DNase-treatment method was followed and repeated to ensure complete DNA removal.

2.1.20 Reverse transcriptase polymerase chain reaction (RT-PCR)

RNA samples prepared from mouse tissue were quantified using a spectrophotometer and the $OD^{260/280}$ value was ensured to be >1.6. An equal amount of RNA was used for each reverse transcription reaction in order to ensure samples were comparable.

Superscript III^R (Invitrogen) was used for the reverse transcription reaction in order to make complementary DNA (cDNA). The samples used for RNA extraction were extremely small and so in order to maximise the amount of comparable RNA, the sample with the lowest RNA concentration was used undiluted. All other samples were adjusted so as an equal amount of RNA was included, diluted in H_2O to a total volume of 11 µl. To this, 1 µl each of 50 µM oligo(dT) (Promega) and 10 mM dNTP mix (Promega) was added and the mixture incubated at 65ºC for 5 min then cooled on ice for 1 min. A master mix comprising of 2 µl 10x RT buffer, 4 µl 25mM $MgCl_2$, 2 µl 0.1 M DTT, 1 µl Superscript III^R (Invitrogen) and 1 µl RNAsin (Promega) was

added to the RNA mixture and incubated at 50ºC for 50 min. The reaction was terminated by heating at 85ºC for 5 min. 1 µl of the cDNA was used in PCR reactions.

2.1.21 Semi-quantitative reverse transcriptase PCR

The PCR reaction used for semi-quantitative PCR analysis was followed using primers according to Table 2.1 and section 2.1.18, dependent upon which gene was being investigated. 1 µl of each cDNA sample was used and 15 µl of the PCR reaction was loaded onto an agarose gel for electrophoresis.

2.1.22 Restriction enzyme digest of genomic DNA

Genomic DNA was prepared as described in section 2.1.17. The digest reaction mixture contained approximately 5 µg genomic DNA, 30 µl of the appropriate 10x restriction digest buffer, 10 units of the appropriate restriction enzyme, 2.5 mM spermidine and 100 µg/ml RNaseA. The total volume was made up to 300 µl with water. The reaction was carried out at 37 ºC for at least 16 h.

2.1.23 Southern blot analysis

Genomic DNA was digested (section 2.1.22) and ethanol precipitated (section 2.1.2). The DNA pellet was resuspended in 20 µl of 1:1 TAE and 5x loading dye. Samples were then electrophoresed at 20 V through a 0.8% agarose gel overnight. The gel was post-stained in 1 µg/ml ethidium bromide for 1 h. The gel was then soaked in 0.25 M HCl for 5 min, rinsed in H_2O, then soaked in 0.4 M NaOH for 30 min. Sponges were positioned in a deep tray and 0.4 M NaOH added, up to the level of the sponges so that they were saturated. A piece of gel blotting paper (Schleicher & Schuell) cut to the same size as the gel was placed on top of the sponges, upon which the gel was placed. A piece of Zeta-probe GTgenomic tested blotting filter (Biorad) the same size as the gel was rinsed in H_2O then soaked in 0.4 M NaOH for 10 min. This was then positioned on top of the gel. Three pieces of 3MM paper (Whatman), again cut to the size of the gel, were soaked in 0.4 M NaOH and placed on top of the Zeta-probe membrane. It was ensured that no air bubbles became trapped between any layers. The gel/paper stack was then surrounded by Nescofilm and clingfilm to ensure no NaOH seeped around the gel rather than through it. A stack of paper towel was placed on top of the gel/paper to a height of 20 cm and a 100 g weight gently placed on top. This was then left overnight. The filter was then

immersed in 2x sodium chloride-sodium citrate (SSC; dilution of 20x stock: 3 M NaCl, 0.3 M $Na_3C_6H_8O_7$ [pH7.0]) for 1 min. The filter was then orientated and baked at 80˚C for 2 h, wrapped in 3MM paper. This was performed by V. Aldridge, Biochemistry Department, University of Leicester.

2.1.24 Probe radio-labelling, hybridisation and post-hybridisation washes

The baked filter was placed in a tube with 20 ml Church buffer (0.5 M NaH_3PO_4 [pH 7.2], 7% [w/v] SDS, 0.5M EDTA [pH8.0]) and prehybridised at 65˚C in a revolving oven for 3 h. To label the probe, 50 ng DNA (neo probe; supplied by S. Munson, GENETA, University of Leicester) in TE to a total volume of 45 µl was denatured by incubating the solution at 95˚C for 5 min then immediately placing it on ice for 2 min. The solution was briefly centrifuged and transferred to a labelling bead (Ready-To-Go DNA labelling beads, Amersham Biosciences). 5 µl of [α-^{32}P] dCTP nucleotide (Amersham Biosciences) was added to the reaction and the tube incubated at 37˚C for 30 min to allow labelling of the DNA. A ProbeQuant G-50 micro column (GE Healthcare) was used to remove unincorporated nucleotides. The column was first pre-centrifuged at 3,000 rpm for 1 min to resuspend the resin. The labelled probe was then gently applied to the centre of the column. The column was centrifuged at 3,000 rpm for 2 min and the purified sample was eluted into a tube below. The labelled probe was heated to 95˚C for 10 min and then placed on ice for 2 min. The buffer in the tube with the pre-hybridised filter was replaced with 13 ml of fresh Church buffer and the purified probe added. The filter was then hybridised at 65˚C overnight in a rotating hybridisation oven.

The filter was washed for 20 min with 50 ml of 0.2x SSC (20x stock: 3 M NaCl, 0.4 M citric acid) in 0.1% [v/v] SDS at 65˚C. This was repeated for a total of five times. The filter was wrapped in cling film and exposed to Biomax MR1 film (Kodak) for 1 week.

2.2 Cell Culture

All reagents were obtained from Invitrogen and all procedures were performed in a tissue culture hood unless otherwise stated.

2.2.1 Maintenance of MEFs

A single aliquot of MEFs containing approximately 1 x 10^6 cells was thawed by transferring the vial to a 37˚C waterbath until the cells had almost completely thawed. They were then added to a tube containing 4 ml of feeder growth media (Dulbecco's Modified Eagles Medium [DMEM] with L-glutamine and 4500 mg/l L-glucose, supplemented with 10% [v/v] foetal bovine serum [FBS] [Sigma], 0.1% penicillin-streptomycin) and centrifuged at 1250 rpm for 5 min. The supernatant was discarded and the cell pellet resuspended in 5 ml of feeder growth media. The cell suspension was transferred to a 10 cm cell culture plate and an additional 5 ml of feeder growth media was added. The cells were then incubated at 37˚C in a 10% CO_2 humidified atmosphere. The media was replaced every other day until the cells reached confluency. At this stage they were trypsinised as follows: the media was aspirated and the cells washed with 5 ml PBS. 3 ml of 0.05% [v/v] trypsin in PBS was added and the plate incubated at 37˚C for 5 min, agitated, then left for a further 5 min. 6 ml of feeder growth media was added to the plate and the cell suspension was gently pipetted up and down to create a single-cell suspension.

The cells were then split equally between three cell culture plates and media added to make a total volume of 10 ml per plate. The plates were then incubated at 37˚C, 10% CO_2 in a humidified atmosphere and the media replaced every other day until confluence was achieved. The MEFs were then split again and the whole procedure repeated until the required number of cells was achieved.

2.2.2 Mitomycin C treatment of MEFs

2 µg/ml mitomycin C in H_2O (Sigma) was added to the media of 80% confluent cells and the plate returned to the incubator for 3 h. The mitomycin C media was then removed and the cells washed three times with PBS. The mitomycin C media and initial PBS wash were disposed of as per guidelines. The MEFs were then ready to be frozen down as stocks to use as feeder cells for ES cell cultures (see below).

2.2.3 Freezing down stocks of MEFs and feeder cells

The media was aspirated from a confluent 10 cm plate of MEFs and the cells were washed with PBS. Alternatively, feeder cells were prepared and washed with PBS following mitomycin C treatment (see above). The plate was then trypsinised (section 2.2.1). All the cell suspensions from all the trypsinised plates were transferred to a single tube. A 1 in 10 dilution of the suspension was used to determine the total number of cells in the single-cell suspension, using a haemocytometer. The cell suspension was then centrifuged at 1250 rpm for 5 min and the supernatant removed. The cells were resuspended in enough freezing media (45% [v/v] MEF growth media, 45% [v/v] FBS, 10% [v/v] DMSO [Sigma]) to achieve a concentration of 1 x 10^6 cells/ml. The cell suspension was then transferred as 1 ml aliquots into cryovials. The vials were rapidly transferred to polystyrene containers and stored at -80˚C. A single aliquot contained enough MEFs to use for future expansions whilst an aliquot of feeder cells was sufficient to support a 10 cm cell culture plate of confluent ES cells.

2.2.4 Thawing of feeders from frozen stocks

1 ml aliquots of feeder cells were thawed in the same way as MEFs (see section 2.2.1). A single aliquot containing 1 x 10^6 cells was sufficient for one 10 cm plate. The cells were then incubated overnight with feeder growth media at 37˚C in a 10% CO_2 humidified atmosphere prior to the addition of ES cells.

2.2.5 Maintenance of embryonic stem (ES) cells

The ES cell growth media used to support the ES cells was routinely warmed to 37˚C before being used. The ES cell line (E14.1a) originated from a 129/Ola mouse strain. In order to maintain the line, any plates upon which the cells were to be grown had to first be coated with sterile 0.1% [w/v] gelatin for 5 min. The plate was then seeded with an aliquot of feeder cells, ideally 16 h prior to addition of ES cells. A single vial of ES cells was thawed at 37˚C and transferred to a tube containing 5 ml of ES cell growth media (DMEM with L-glutamine and 4500 mg/l D-glucose, supplemented with 15% [v/v] FBS, 0.01% penicillin/streptomycin, 1 mM non-essential amino acids, 10 mM sodium pyruvate, 115 µM β-mercaptoethanol [Sigma], 2 ml recombinant leukaemia inhibitory factor [LIF; ES Cell Facility, University of Leicester, UK]). The cell suspension was centrifuged at 1250 rpm for 5 min and the supernatant discarded.

The ES cell pellet was resuspended in 10 ml of ES cell growth media and the suspension transferred to the 10 cm plate containing the feeder cells, having first removed the feeder growth media from the plate. The cells were left overnight at 37˚C, 10% CO_2 in a humidified atmosphere. The media was replaced each day until the cells reached 70% confluency.

Once the cells were confluent they were trypsinised as follows: the media was aspirated and the cells washed with 5 ml PBS. 3 ml of 0.05% [v/v] trypsin in PBS was added and the plate incubated at 37˚C for 5 min, agitated, then left for a further 5 min. 6 ml of ES cell growth media was added to the plate and the cell suspension was gently pipetted up and down to create a single-cell suspension.

The cells were then split equally between three cell culture plates (gelatine-treated and seeded with feeder cells 12 h prior to use) and media added to make a total volume of 10 ml per plate. The plates were then incubated at 37˚C, 10% CO_2 in a humidified atmosphere and the media replaced every other day until 70% confluency was achieved, at which point the cells were passaged again until the desired number of cells was achieved.

2.2.6 Electroporation of ES cells

The media was aspirated from 70% confluent cells and the cells were trypsinised (see section 2.2.1). The 6 ml cell suspensions from each plate were then combined in a single tube. The cell number was determined using a 1 in 10 dilution of the cell suspension and a haemocytometer. The single-cell suspension was then centrifuged at 1250 rpm for 5 min and the supernatant removed. The cells were washed with PBS, centrifuged once again and then the PBS aspirated. Enough PBS was then added to create a cell suspension with a concentration of between 5 x 10^7 and 1 x 10^8 cells per 1.6 ml. 1.6 ml of the cell suspension was divided between two electroporation cuvettes (Bio-Rad). 30 µg of DNA (linearised, ethanol precipitated and resuspended in no more than 50 µl of water) was added to each cuvette and gently mixed. The cuvettes were placed in a Gene Pulser equipped with a capacitance extender (Bio-Rad) and electroporated at 0.24 V and 500 µFD. The cells from both cuvettes were then combined in 12 ml of ES cell growth media and transferred onto three fresh 10 cm cell culture plates, previously prepared with

gelatine and feeder cells as described. The total volume of ES cell growth media was made up to 10 ml per plate and the cells incubated overnight at 37˚C, 10% CO_2 in a humidified atmosphere. The next day, the media on the cells was replaced with ES cell growth media containing 300 µg/ml of G418 (Invitrogen). The G418 containing media was replaced each day, for approximately four days, until clones had formed.

2.2.7 Selection of resistant ES cell clones

A 48-well cell culture plate was gelatinised and seeded with feeder cells 24 h prior to ES cell clone selection. The feeder growth media in the 48-well plate was then replaced with 0.5 ml of ES cell growth media, ready to be seeded with ES clones. A 96-well plate was also prepared with 30 µl of 0.1% [v/v] trypsin in PBS in each well. The 10 cm plate containing the ES cell clones was washed twice with PBS and then 15 ml of PBS was added to the plate for picking. Each clone was picked under a microscope in a volume of 10 µl of PBS. The clone was transferred to a well of the 96-well plate containing trypsin. The plate was incubated at 37˚C, 10% CO_2 in a humidified atmosphere for 10 min. After incubation, the plate was agitated before 60 µl of ES cell growth media was added to each well. The contents of the well were then gently pipetted up and down to achieve a single-cell suspension before the contents were transferred to a single well of the 48-well plate. Once all the wells had been seeded with an ES clone, the plate was incubated at 37˚C, 10% CO_2 in a humidified atmosphere. The media was replaced each day until the cells reached confluency.

2.2.8 Freezing down and seeding for DNA analysis of ES clones

Once the ES clones on the 48-well plate had reached confluency, the media was aspirated and the cells washed with PBS. 80 µl of 0.05% [v/v] trypsin in PBS was added to each well and the plate incubated at 37˚C, 10% CO_2 in a humidified atmosphere for 10 min. 60 µl of FBS was added to 40 wells of a 96-well cell culture plate while a 12-well plate was gelatinised as previously described. 2.5 ml of ES cell growth media was then added to each well of the 12-well plate. The incubated cells were gently pipetted up and down to achieve a single-cell suspension. 60 µl of this suspension was transferred to a well of the 96-well plate and mixed gently; these cells would be frozen down. The remaining cells were used to seed a well of the 12-well plate to use for DNA analysis. 100 µl of 2x freezing mix (40% [v/v] ES cell growth

media, 40% [v/v] FBS, 20% [v/v] DMSO) was added to each well of the 96-well plate, mixed gently and then rapidly transferred to a polystyrene box at -80˚C. Approximately 40 clones were transferred into a single 96-well plate to minimise the exposure of the cells to DMSO prior to freezing.

2.2.9 Thawing and expansion of selected ES clones

Selected ES clones, frozen in 96-well plates, were thawed at 37˚C and each was immediately transferred into the well of a gelatinised 24-well plate containing feeder cells and 2 ml of ES cell growth media. After 24 h, the media was replaced and 150 µg/ml G418 added to maintain selection pressure. Once confluency was achieved, the cells were treated with 0.25 ml of 0.05% [v/v] trypsin in PBS and incubated at 37˚C, 10% CO_2 in a humidified atmosphere for 5 min. 0.5 ml of ES cell growth media was added to the plate and the cells gently pipetted up and down to achieve a single-cell suspension. This was transferred to a single well of a gelatinised 6-well plate containing feeder cells and 6 ml of ES cell growth media was added containing 150 µg/ml G418. Once confluent, 1 ml of 0.05% [v/v] trypsin in PBS was added to the plate and incubated at 37˚C, 10% CO_2 in a humidified atmosphere for 5 min, agitated, then incubated for a further 5 min. 3 ml of ES cell growth media was added to the plate and the cells gently pipetted up and down to achieve a single-cell suspension. This was transferred to a 10 cm gelatinised plate containing feeder cells and the media topped up to 10 ml. The selected ES cell clones were then treated as normal ES cells.

2.2.10 Freezing of ES clones

The plates containing the cells to be frozen were trypsinised (section 2.2.1). All the cell suspensions from all the trypsinised plates were transferred to a single tube. A 1 in 10 dilution of the suspension was used to determine the total number of cells in the single-cell suspension, using a haemocytometer. The cell suspension was then centrifuged at 1250 rpm for 5 min and the supernatant removed. The cells were resuspended in enough freezing media (45% [v/v] ES cell growth media, 45% [v/v] FBS, 10% [v/v] DMSO [Sigma]) to achieve a concentration of 1 x 10^6 cells/ml. The cell suspension was then transferred as 1 ml aliquots into cryovials. The vials were

rapidly transferred to polystyrene containers and stored at -80˚C for up to a week prior to transfer to liquid nitrogen storage.

2.2.11 Generation of transgenic mice

The preparation of ES cells for injection was performed by J. Meisura and S. Munson (GENETA, The University of Leicester, UK). Selected ES cells were grown until 70% confluency was achieved. The cells were then trypsinised as previously described (section 2.2.1) and 5 ml of growth media added. The cell suspension was then centrifuged at 1250 rpm for 5 min. The resultant cell pellet was resuspended in 500 µl injection media (DMEM with 4500 mg/l L-glucose, supplemented with 10% [v/v] FBS, 0.01% penicillin/streptomycin, 20 mM L-glutamate, 10 mM sodium pyruvate). The cells were injected into donor blastocysts and implanted into a pseudo-pregnant foster mother under PPL 80/1933 by the Division of Biomedical Services, The University of Leicester, UK. The foster mother was culled by cervical dislocation at defined time points if chimeric embryos were required.

2.3 Histology

Unless otherwise stated, all chemicals were obtained from Fisher.

2.3.1 Tissue fixation

The required tissue was dissected from the animal, washed in PBS and transferred to 20x volume of 4% [w/v] paraformaldehyde (PFA). The tissue was left overnight on a shaking incubator. The tissue was then transferred to 70% [v/v] ethanol and stored at 4ºC until required.

Occasionally, methacarn fixative (60% methanol [v/v], 30% chloroform [v/v], 10% glacial acetic acid [v/v]) was used. The tissue was first washed in PBS and transferred to methacarn fixative overnight on a shaker. The tissue was then placed in two washes of 100% ethanol [v/v] for 30 min each. Samples were put into fresh 100% ethanol [v/v] for long term storage at 4˚C.

2.3.2 Tissue processing

Extremely small samples were positioned in 2% agarose in H_2O prior to processing. Tissues were impregnated with wax using a Shandon Citadel 2000 following the manufacturer's protocol. This was performed by J. Edwards (MRC, Leicester). Once processed the tissues were embedded in a paraffin wax block.

2.3.3 Preparation of glass slides for tissue sections

Uncoated glass microscope slides (Raymond Lamb) were placed in polyacetal racks and soaked overnight in 5% [v/v] Decon. The slides were washed in hot H_2O for 30 min then rinsed in H_2O five times, for 5 min each. The slides were dried in a 60ºC oven. The racks containing the slides were submerged for 1 min in subbing solution (2% 3-aminopropyltriethoxysilane in acetone), then into two tanks of acetone for 1 min each. The racks were then transferred to two tanks of H_2O and then placed back into the oven to dry before use.

2.3.4 Sectioning of wax-embedded tissue samples

Paraffin blocks were stored at 4ºC prior to use. The blocks were sectioned using a Leica RM2135 microtome and the sections floated onto a 40ºC waterbath prior to transferring onto a slide. The slides were placed in a polyacetal rack and left to dry at 37ºC overnight.

2.3.5 Dewaxing and rehydration of sections

The racks of slides were placed in two consecutive tanks of xylene and left for 10 min in each tank. The racks were transferred to two tanks of 100% [v/v] ethanol for 10 min per tank and then placed in 70% ethanol for 10 min. The racks were finally placed in H_2O at which point the sections were rehydrated.

2.3.6 Immunohistochemical analysis of paraffin sections

The Cdx2 antibody works best upon tissue sections fixed in methacarn fixative (Chawengsaksophak et al., 1997). Following fixation, processing and sectioning, the sections were dewaxed in xylene for 10 min then dehydrated in methanol for 2 min. The sections were then incubated in 2% [v/v] hydrogen peroxide in methanol, for 15 min. The slides were rehydrated through an alcohol series consisting of 100%, 100% and 70% [v/v] ethanol for 10 min per stage and finally rinsed in PBS. The sections

were blocked in 10% [v/v] goat serum in PBS containing 0.3% [v/v] titronX-100 for at least an hour. The sections were then incubated in 2% [v/v] goat serum in PBS for 10 min. The Cdx2 antibody (raised in rabbit) was pipetted onto the sections at a dilution of 1:400 in 2% goat serum [v/v] in PBS and left overnight at 4˚C. The sections were washed for 30 min with multiple changes of PBS. The secondary antibody (Polyclonal Swine Anti-Rabbit Immunoglobulins/Biotinylated; Dako) was subsequently pipetted onto the sections. The secondary antibody was diluted 1:500 in 2% [v/v] goat serum and the sections incubated for 30 min then washed with PBS with multiple changes over 30 min. The tertiary antibody (Streptavidin/HRP; Dako) was diluted 1:500 in 2% [v/v] goat serum and the sections incubated for 30 min, then washed multiple times with PBS over 30 min. The antibody was detected using a Vector DAB kit (Vector Labs).

2.4 Whole mount gene expression analysis using digoxigenin-labelled RNA probes

This whole mount *in-situ* hybridisation protocol is based upon a protocol used by the Hubrecht Laboratory, Utrecht, Netherlands, supplied by J. Deschamps. Unless otherwise stated, all chemicals were obtained from Fisher.

2.4.1 Synthesis of DIG-labelled RNA probe

All chemicals and plasticware were certified RNase-free prior to use. RNase Away (Invitrogen) was used to wipe all pipettes and surfaces to ensure they were RNase free. 10 µg of DNA was linearised and ethanol precipitated prior to commencing. The DNA pellet was resuspended in 10 µl TE and stored at -20˚C until required.

20 µl of reaction mix (1x transcription buffer [supplied with polymerase], 10 mM dithiothreitol [DTT; Invitrogen], 1x DIG RNA Labelling Mix [Roche], 1.5 µg linearised plasmid, 40 units RNasin^{R} [Promega], 20 units appropriate polymerase [Promega] made up in H_2O) was incubated at 37˚C for 2 h. This was then diluted to 50 µl with 1x transcription buffer at which point a 0.5 µl aliquot was electrophoresed on an RNase-free 1% [w/v] agarose gel containing 0.5 µg/ml ethidium bromide to ensure a ribonucleic acid (RNA) band could be seen along with the DNA template band. 2 µl of DNase I (20 units; Promega) was added to the mixture and then incubated at 37˚C for 30 min. Another 0.5 µl aliquot was electrophoresed on an RNAse-free 1% [w/v]

agarose gel containing 0.5 µg/ml ethidium bromide to ensure that the DNA template band was no longer present. The mixture was held on ice whilst the gel was electrophoresed. If the DNA template band was still visible, the mixture was incubated at 37˚C for a further 15 min. The following reagents were then added to the mixture: 50 µl H_2O, 1 µl of 10 mg/ml yeast tRNA, 8 µl 5 M LiCl, 300 µl 100% [v/v] ethanol. The mixture was left at -20˚C overnight to precipitate the RNA probe. The tube containing the probe was then centrifuged at 13,000 rpm, 4˚C for 15 min. The supernatant was removed and the pellet washed with 70% [v/v] ethanol and re-spun. The supernatant was removed once again and the pellet dried on the bench for 30 min. The RNA probe was resuspended in 20-50 µl of 1:1 TE/formamide (Invitrogen). If the original agarose gel showing both the RNA band and DNA template band indicated that the yield RNA was 10x that of the input DNA, then 50 µl of TE/formamide was used. The probe was then stored in aliquots at -80˚C.

2.4.2 Pretreatment and hybridisation of embryonic tissue

RNase-free conditions and treatments were maintained throughout the procedure. The uterus was dissected from a pregnant mouse and transferred to PBS where it was kept on ice until all the embryos had been processed. 10.5dpc embryos were removed from the uterus and processed as whole embryos. 12.5-18.5dpc embryos were dissected from the uterus and kept in ice cold PBS whilst the gut was dissected under PPL 80/1933. The tail was removed for genotyping and processed as described in section 2.1.16. The full length of the gut, from the stomach to the colon, was removed and fixed overnight in 4% [w/v] PFA in 2 ml glass vials. The tissue remained in the glass vials for the duration of the experiment. The sample was twice washed for 5 min in PBT (1:1000 dilution Tween20 in PBS). The samples were then dehydrated through a methanol series (25%, 50%, 75% [v/v] in PBT) for 5 min each. The tissue was then transferred to 100% [v/v] methanol for 5 min before fresh 100% [v/v] methanol was added for long term storage at -20˚C.

When the tissue was required for hybridisation, it was first rehydrated through the same methanol series as above, in reverse and finally twice washed for 5 min in PBT. Following this, the samples were transferred to 200 µl of 10 µg/ml proteinase K (Invitrogen) in PBT and then permeabilised in 800 µl fresh proteinase K in PBT for 15 min at room temperature. The proteinase K was then removed and replaced with 2

mg/ml glycine in PBT for 5 min. This was exchanged for fresh 2 mg/ml glycine in PBT for a further 5 min. The samples were then rinsed twice, for 5 min each, in PBT at room temperature. The tissue was then re-fixed in fresh 4% [w/v] PFA containing 0.2% [v/v] glutaraldehyde for 20 min at room temperature. The PFA was replaced with 300 µl prehybridisation buffer (50% formamide [Invitrogen], 5x SSC [pH4.5], 2% blocking powder (Roche), 0.1% Tween20, 0.5% CHAPS [Invitrogen], 50 µg/ml yeast tRNA, 5 mM EDTA, 50 µg/ml heparin, made up in H_2O and dissolved at 65˚C) and the tissue allowed to settle on the bottom of the glass vial. The buffer was then removed and 400 µl fresh prehybridisation buffer was added to the vial and incubated at 70˚C for at least 1 h. The buffer was then replaced with 300 µl of prewarmed prehybridisation buffer, to which 2 µl of probe was added. The probe was left to hybridise to the tissue overnight at 70˚C, with gentle rocking.

2.4.3 Post-hybridisation washes and antibody incubation

All solutions were prepared and prewarmed in advance. Embryo powder was prepared as follows: 12.5-14.5dpc embryos were homogenised in a minimum volume of ice-cold PBS, to which four volumes of ice-cold acetone was added, mixed and incubated on ice for 30 min. The tube was then centrifuged at 13,000 rpm for 10 min, the supernatant removed and the pellet washed with ice-cold acetone and re-spun. The pellet was then spread out on a clean plastic surface, allowed to air dry then ground into a fine powder. The resultant powder was stored at 4˚C.

The DIG antibody needed first to be prepared. 10% [v/v] sheep serum (Invitrogen) in TBST with levamisole (0.14 M NaCl, 2.7 mM KCl, 25 mM Tris/HCl [pH7.5], 0.1% Tween20, 2 mM levamisole) was incubated at 70˚C for 30 min to inactivate any endogenous alkaline phosphatase activity. 15 mg of embryo powder was added to 2.5 ml TBST with levamisole and also incubated at 70˚C for 30 min. The embryo powder suspension was then vortexed for 10 min at room temperature before being cooled on ice. To this, 250 µl of heat-inactivated 10% sheep serum was added. 5 µl of anti-DIG coupled to alkaline phosphatase (Roche) was added to the tube and incubated at 4˚C with gentle shaking for at least 4 h. Meanwhile, the hybridisation buffer was removed from the tissue and replaced with 800 µl of prehybridisation buffer. The samples were washed for 10 min at 70˚C, after which 400 µl 2x SSC (pH4.5) was added to the buffer and incubated for 10 min, followed by another two

400 µl aliquots of 2xSSC 10 min apart, so a total of 1200 µl of 2x SSC had been added to the 800 µl of prehybridisation buffer and incubated for a total of 30 min. The solution was then removed from the tissue and two washes of 0.1% CHAPS in 2x SSC at 70˚C for 30 min each were performed. The tissue was then digested for 1 h in 100 µg/ml RNaseA, 0.1% CHAPS in 2x SSC at 37˚C. This was then twice replaced with maleic acid buffer (100 mM maleic acid, 150 mM NaCl, pH7.5 using NaOH) for 10 min at room temperature, then twice for 30mins at 70˚C, so the tissue was washed for a total of 4 times with maleic acid buffer. The samples were then washed for 10 min at room temperature with PBT before this was replaced with TBST with levamisole for two washes of 10 min each at room temperature. The tissue was then pre-blocked with 900 µl of 10% heat inactivated sheep serum for 2-3 h at room temperature with gentle shaking.

Following incubation, the anti-DIG mixture was centrifuged at 3,000 rpm for 10 min at 4˚C. The supernatant was transferred to a fresh tube and diluted to 10 ml with ice-cold heat inactivated 1% sheep serum in TBST with levamisole. The anti-DIG mixture was then kept on ice. The blocking serum was removed from the tissue and replaced with 300 µl of the anti-DIG mixture, which was then removed. 700 µl of fresh anti-DIG mixture was then added to the samples and incubated overnight at 4˚C with gentle shaking.

2.4.4 Post antibody washes and detection

The anti-DIG mixture was replaced with TBST with levamisole and the tissue washed for 5 min three times at room temperature. The tissue was then washed 5 times for 1 h each with TBST with levamisole, then left in TBST with levamisole overnight on a shaker.

2.4.5 Development of signal

The tissue was washed three times for 10 min each at room temperature with NTMT (100 mM NaCl, 100 mM Tris/HCl [pH9.5], 50 mM $MgCl_2$, 0.1% Tween20). The samples were then rinsed in 300 µl BM purple solution (Roche), which was then replaced with 700 µl fresh BM purple and the tissue incubated at room temperature, in the dark, until the colour had developed to the required intensity.

2.4.6 Processing of tissue

Once the colour reaction had developed to a required intensity, the tissue was again twice washed in NTMT at room temperature for 10 min per wash. The experiment remained in the dark as much as possible. The samples were then placed in PBT containing 10 mM EDTA. The tissue remained in this solution whilst being photographed. If the tissue was to be sectioned to histologically examine the region of staining, then the sample was re-fixed for 1 h in 4% PFA with 0.2% glutaraldehyde. The sample was then transferred to PBT containing 10 mM EDTA and washed for 30 min. The tissue was then ready for paraffin wax embedding. Following embedding and sectioning, tissue was either mounted unstained, or stained with haematoxylin and eosin or Nuclear Fast Red (Sigma) according to the manufacturer's protocol until the desired level of colour was achieved.

2.5 Gene expression analysis upon tissue sections using radio-labelled RNA probes

All reagents were obtained from Fisher unless otherwise stated. The original protocol that this method is based upon was obtained from Prof. P. Sharpe, The Craniofacial Department, King's College, London, UK.

2.5.1 Synthesis of a 35S radiolabelled RNA probe

All plasticware and pipette tips were certified RNAse free and RNAse Away was used to wipe down surfaces and pipettes prior to use. It was ensured that all reagents were RNAse-free before being used to generate the RNA probe. A master mix was created containing the following reagents; 5 µl 5x reaction buffer (supplied with polymerase), 0.5 µl 1 M DTT (Invitrogen), 1.2 µl each of 10 mM GTP, 10mM ATP and 10mM CTP (Invitrogen), 1 µl 50 µM UTP, 0.5 µl RNasin^{R} (Promega), 7 µl 35S UTP (Amersham). The mixture was divided into two tubes in order to generate two probes. To each tube 3.2 µl of 1 µg/µl DNA (linearised, ethanol precipitated and resuspended in TE) was added along with 0.5 µl of the appropriate polymerase (Promega). The tubes were incubated at 37˚C for 40 min, after which another 0.5 µl of polymerase was added and the tubes again incubated for a further 1 h. 1.25 µl of DNAse solution (2.5 µl RNasin^{R}, 5 µl 10 mg/ml yeast tRNA, 2.5 µl 1 M DTT, 2.5 µl RNase-free DNAse1 [Promega]) was then added to each tube. The contents were incubated at 37˚C for 10 min. 294 µl of precipitation solution (160 µl H_2O, 4 µl 1 M DTT, 4 µl 5 M

NaCl, 20 µl 3 M NaOAc [pH5.2], 400 µl 100% [v/v] ethanol) was added to each tube and then inverted gently several times before leaving the tubes at -20˚C overnight to allow the RNA to precipitate. The tubes were centrifuged at 13,000 rpm for 10 min at 4˚C and the supernatant carefully removed. The pellets were then washed with 10 mM DTT in 100% [v/v] ethanol and re-centrifuged at 13,000 rpm for 5 min. The supernatant was removed and the pellet left on the bench to dry for 20 min. The pellet was resuspended in 25 µl of 50 mM DTT in sterile H_20 and vortexed briefly. The tubes were then incubated at 60˚C for 1 min, vortexed briefly once again then transferred onto ice. 1 µl of the probe was removed for analysis on a TBE-urea gel before the tubes were transferred to -80˚C for storage for up to 1 month.

2.5.2 Preparation of tissue sections for hybridisation

The tissue was dissected, positioned in agarose then embedded in wax as previously described (section 2.3). The tissue was sectioned at 8 µm 1 day prior to hybridisation, onto Histobond™ (Raymond Lamb) slides. The sections were then left at 37˚C overnight to dry.

The sections were placed into polyacetal racks then dewaxed in Histoclear (Raymond Lamb) twice for 15 min each. The sections were then rehydrated through an ethanol series of 100%, 95%, 90%, 80%, 60% and 30% [v/v] ethanol for 2 min each then placed in H_2O twice for 2 min each. The sections were placed in 2% HCl (Fisher) for 20 min followed by 2x SSC for 5 min. The tissue was digested in 5 µg/ml Proteinase K (Invitrogen) in prewarmed buffer (0.1 M Tris/HCl [pH8.0], 50 mM EDTA) at 37˚C for 10 min. The racks were then transferred to 2 mg/ml glycine (Fisher) in PBS for 2 min and then washed twice in PBS for 1 min per wash. The sections were then re-fixed in 4% PFA for 20 min before being washed for 2 min in PBS. 625 µl acetic anhydride (Sigma) was rapidly added to 250 ml 0.1 M triethanolamine (Sigma) and stirred with a flea before the racks were added and left for 10 min. The sections were then washed with PBS for 5 min and then H_2O for 2 min. The ethanol series used previously was then repeated in reverse in order to dehydrate the sections. The sections were then dried in the racks for at least 1 h under tinfoil.

2.5.3 Hybridisation of radiolabelled probe to sections

The total number of sections was noted and the amount of required probe was calculated for this number, plus an additional two sections as surplus. The amount of probe to be used per section was calculated so as 1x 10^6 counts of radioactivity was applied to each section. The calculation was therefore:

$$\frac{1{,}000{,}000}{\text{scintillation count}} \times (\text{number of sections}) + 2 = \text{amount of probe}$$

The amount of hybridisation buffer (50% formamide, 10% dextran sulphate [Sigma; taken from 50% frozen stock], 50 mM DTT, 0.5 mg/ml yeast tRNA, 0.3 M NaCl, 20 mM Tris/HCl [pH8.0], 5 mM EDTA, 1x Denharts [Sigma] in H_2O) required was 100 µl per section, plus the surplus two sections. The calculated amount of probe was added to this amount of buffer and the mixture incubated at 80˚C for 2 min then placed on ice. 100 µl of the probe mixture was pipetted onto each section, gently cover-slipped and transferred to a slide chamber containing tissue soaked with formamide solution (2x SSC, 50% formamide). The chambers were sealed and incubated in a hybridisation oven at 55˚C overnight.

2.5.4 Post-hybridisation washing of sections

All solutions were prewarmed before use and the washes were performed in a hybridisation oven containing a rocking shelf. Each coverslip was removed from the section in a minimal amount of wash solution (2x SSC, 50% formamide, 10 mM DTT) at 55˚C. The slides were loaded into a polyacetal rack and placed in wash solution for 15 min at 55˚C. This was replaced with fresh wash solution and incubated at 55˚C for 20 min. The wash solution was again replaced and the sections washed at 65˚C for 20 min. The slides were then washed twice with RNase buffer (0.5 M NaCl, 10 mM Tris [pH8.0], 1 mM EDTA [pH8.0]) at 37˚C for 15 min each. RNaseA (Sigma) was then added to fresh RNase buffer at a concentration of 0.04 mg/ml and the sections incubated in this at 37˚C for 30 min. The slides were then rinsed with more RNase buffer at 37˚C for 15 min. This was then replaced with two changes of wash solution incubated at 65˚C for 20 min each time. The sections were transferred to 0.1x SSC containing 8 mM DTT at 65˚C for 20 min, then fresh 0.1x SSC containing 8mM DTT at room temperature for 5 min. The sections were placed in ammonium acetate (0.3

M ammonium acetate, 70% [v/v] ethanol) at room temperature for 2 min, then 95% [v/v] ethanol, followed by 100% [v/v] ethanol for 2 min each. The slides were then left to dry at room temperature for at least 1 h, under tinfoil. The control sections were exposed to Biomax MR1 film overnight to ensure that a signal could be seen and the probe had therefore hybridised.

2.5.5 Exposing sections to emulsion

A water bath was set up in a dark room at 45˚C containing 7.5 ml of 2% [v/v] glycerol in a tube. The remainder of the protocol was performed under a safe light. Ilford K5 Nuclear Emulsion (Agar Scientific) shreds were added to the 2% [v/v] glycerol until 15 ml total volume was reached. The emulsion was left to melt into the glycerol for 10 min. The lid was then placed on the tube and the tube gently inverted to mix the solution. This was then gently transferred to a glass coplin jar and allowed to settle. The sections were dipped into the emulsion one at a time and the slide backs wiped firmly with a paper towel. The slides were then placed flat, emulsion side up, on a tin lid and left to dry in the dark for 2 h. The slides were then put into polyacetal racks and placed in a tin with a desiccation packet. The tin was sealed and the slides left at 4˚C for 10 days.

2.5.6 Developing the radiolabelled sections

After 10 days, the tins were opened in the dark room under a safe light. The racks of slides were first placed in Kodak D-19 developer for 4 min, then 1% [v/v] acetic acid for 30 s. The slides were then washed in water for 30 s and placed into two washes of 30% [w/v] sodium thiosulphate for 4 min each. Finally the slides were placed in water at which point they could be exposed to light. The water was replaced numerous times over an hour before the sections were counter-stained with 1% [v/v] Giemsa's solution for 1 min. They were then washed with water and dried at 37˚C overnight. The sections were then mounted with DPX.

3. Identification of Nascent Heterotopias in the Cdx2 Mutant Gut

3.1 Introduction

3.1.1 The phenotype of Cdx2$^{+/-}$ heterozygous and Cdx2$^{-/-}$//WT chimeric mice

In chapter 1, the intestinal phenotype of the *Cdx2*$^{+/-}$ and *Cdx2*$^{-/-}$//WT mice was introduced. In summary, the mice demonstrate regions of gastric heterotopias developing in the intestine (Chawengsaksophak et al., 1997, Beck et al., 2003). These heterotopias are most frequent in the region shown to express the highest levels of *Cdx2* (i.e. the caecum) (James et al., 1994, Silberg et al., 2000).

The origin of the cells in the gastric heterotopias was investigated in the *Cdx2*$^{-/-}$//WT chimeric mice. Upon investigation it was found that the gastric heterotopias occur where *Cdx2*$^{-/-}$ cells had engrafted in the intestine. The underlying mesoderm was of host origin (Beck et al., 2003). The heterotopic lesions in the *Cdx2*$^{+/-}$ mice retained heterozygosity but did not express Cdx2 protein. The surrounding normal intestine contained Cdx2 protein. Therefore the mice are haploinsufficient for *Cdx2* (Chawengsaksophak et al., 1997).

3.1.2 Stomach endoderm-specific expression of Sox2

SRY-related HMG box 2 (*Sox2*) is involved in maintaining the undifferentiated, pluripotent state of stem cells within the epiblast (Avilion et al., 2003). The requirement of Sox2 by the inner cell mass is shown in *Sox2*$^{-/-}$ embryos. These embryos die prior to gastrulation, but can be rescued by an injection of WT ES cells. This results in an embryo consisting of only WT cells and a few redundant *Sox2*$^{-/-}$ cells that are completely non-functional (Avilion et al., 2003).

Sox2 is expressed at different levels in the endoderm of many foregut-derived organs, such as the tongue, oesophagus, trachea, proximal lung and stomach (Ishii et al., 1998, Que et al., 2007). *Sox2* is expressed at 9.5dpc in all endodermal cells of the foregut although by 10.5dpc protein levels are higher dorsally in the future oesophagus than ventrally in the future trachea. As the oesophageal endoderm becomes multilayered and develops into stratified squamous epithelium, *Sox2* levels are higher in the endodermal cells adjacent to the basal lamina (Que et al., 2007). *Sox2* expression in the developing stomach initially extends to the junction with the

duodenum. Expression levels in the distal stomach (body and antrum/pylorus) gradually decrease until 18.5dpc where a sharp boundary of expression is present between the stratified and glandular regions of the stomach (Que et al., 2007).

It is thought that Sox2 promotes the formation of stratified squamous epithelium as opposed to glandular epithelium hence the gradual decrease of expression in the distal stomach. It has been shown that *Sox2* is co-expressed with *p63* in the basal cells of the oesophagus and forestomach and a reduction of Sox2 in hypomorphic mutants led to a downregulation of *p63* and *K14* expressing cells, suggesting that Sox2 regulates transcription of these genes. Equally, Sox2 is thought to repress proximal stomach expression of genes required for the correct function of the glandular distal region such as mucin genes and trefoil-factor peptides. Sox2 therefore maintains the regional differences in the endoderm of the stomach (Que et al., 2007).

3.2 Aims

The nature of the mesoderm underlying the region of heterotopic stomach endoderm developing in the *Cdx2* mutant intestine is investigated here. It was not known if the underlying mesoderm remained intestine-specific or responded to the overlying stomach-type epithelium by expressing stomach mesoderm-specific genes. This information could not be determined histologically and so tissue-specific gene expression was investigated. The relevant genes are generally only expressed during development and so tissue-specific gene expression was not investigated postnatally. The aim of this chapter was to devise a method of detecting the gastric heterotopias, as they cannot be found by histological techniques. Subsequently the aim was to determine the optimal embryonic time-point at which to further investigate the nature of the mesoderm underlying the heterotopias using gene expression techniques. *Sox2* was chosen as a marker for stomach endoderm for this purpose.

3.3 Results

3.3.1 Genotyping to identify Cdx2$^{+/-}$ heterozygotes and Cdx2$^{-/-}$//WT chimeras

Cdx2$^{+/-}$ heterozygous embryos were obtained from timed matings between *Cdx2*$^{+/-}$ and C57/BL6 mice. The *Cdx2*$^{+/-}$ embryos were phenotypically indistinguishable from WT when on the C57/BL6 background. The embryos therefore had to be genotyped

to identify mutants. Primer pair P1 and P3 was used to identify the WT *Cdx2* allele. All embryos contained this allele and so this PCR acted as a control for the sample. Primer P2 annealed to the neo^R cassette found in the $Cdx2^{-/-}$ allele and so pairing of this primer with P1 produced a larger PCR product than P1 and P3 combined (Figure 3.1A). All three primers were added to the same PCR reaction. The heterozygous animals were identified as producing two bands on the agarose gel. The WT band was 443bp in size, the mutant band was 636bp (Figure 3.1B) (Chawengsaksophak et al., 1997).

The $Cdx2^{-/-}$//WT chimeras were identified in the same manner; primers P1 and P3 annealed to the WT host *Cdx2* alleles while P1 and P2 annealed to the $Cdx2^{-/-}$ alleles of the engrafted cells, producing bands on an agarose gel of the same size as shown in Figure 3.1B (data not shown). These animals were created by injecting $Cdx2^{-/-}$ cells into WT hosts and so if $Cdx2^{-/-}$ cells had successfully incorporated into the blastocyst then both PCR products were visible on an agarose gel. Two samples were taken from chimeric embryos to increase the probability of chimeric cells being present.

3.3.2 Determining a whole-mount technique suitable for detecting gene expression

A technique was required that was suitable for use on whole-mount intestine to allow screening of the whole organ for gastric heterotopias. The most appropriate technique was to use digoxigenin (DIG)-labelled RNA probes, detected using a magenta chromogenic probe that could be visualised under a light microscope. In order to set up this technique, pBS-HoxB-1, known to be successfully used by another group for creating DIG-labelled RNA probes, was used initially as a control for the technique.

The plasmid pBSHoxb-1 (supplied by J. Deschamps, Hubrecht Institute, Royal Netherlands Academy of Arts and Sciences, Netherlands) contained some of the sequence of the *Hoxb-1* gene (Figure 3.2A). The plasmid was linearised with *Cla* I and the antisense probe created using T7 polymerase (Figure 3.2B). Linearisation of the plasmid prevents unnecessary transcription of backbone vector. A sense probe was not used at this point because this probe was used as an indicator that the technique was working. The reaction mixture containing both probe and DNA

Figure 3.1 Genotyping to identify the *Cdx2* null allele. (A) The *Cdx2*$^{+/-}$ heterozygous and *Cdx2*$^{-/-}$//WT chimeric animals possess both the WT allele and the null allele. WT animals do not possess the null allele. The primers P1 and P3 can be used as a control for the samples. The primer P2 will anneal to the *neo*^{R} cassette and so in combination with P1, this primer set can be used to identify *Cdx2* mutant animals. (Devised by Chawengsaksophak et al., 1997). (B) *Cdx2*$^{+/-}$ genotyping results. DNA from 14.5dpc embryos from a C57/BL6 x *Cdx2*$^{+/-}$ mating were genotyped using primers P1, P2 and P3. Embryos 4, 5 and 7 were *Cdx2*$^{+/-}$, the remainder were all WT.

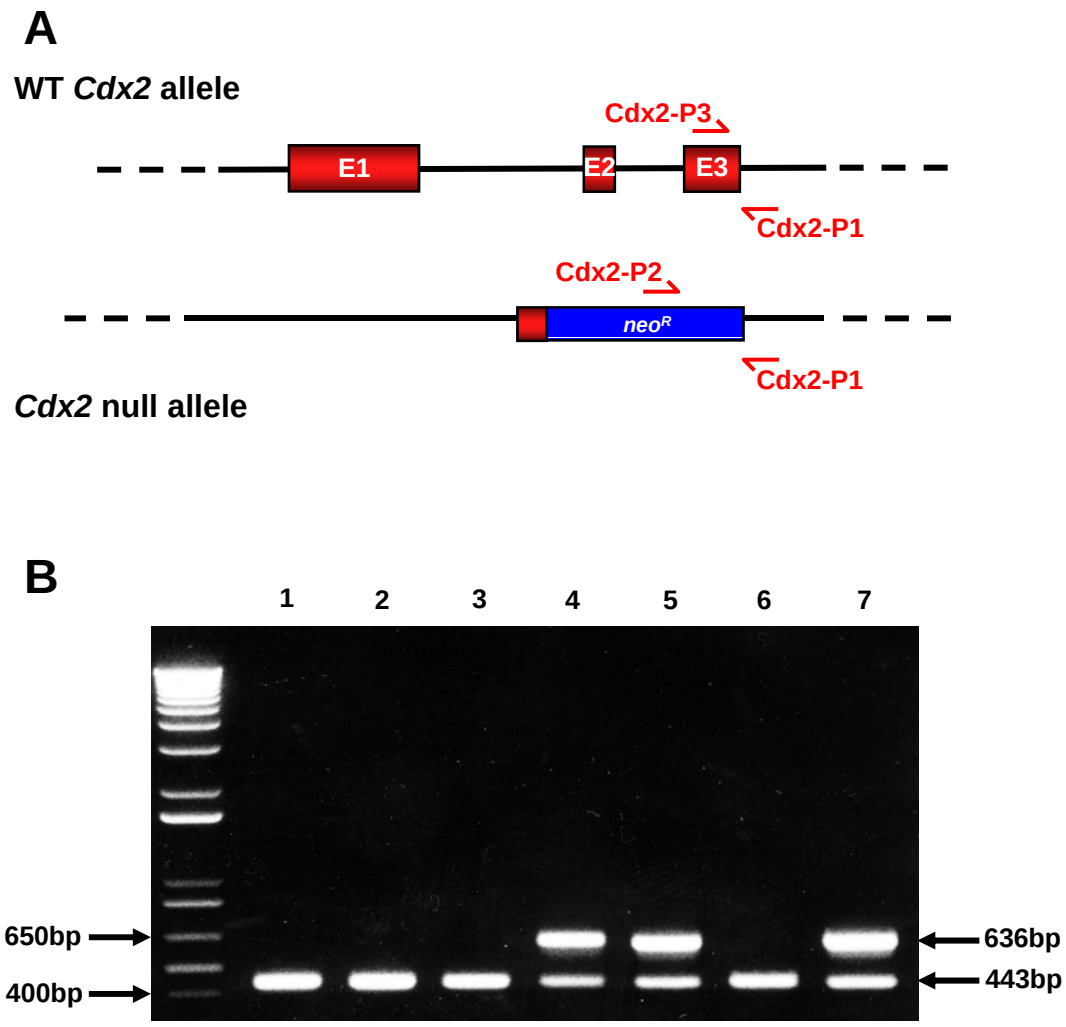

Figure 3.2 Establishing the technique of *in-situ* hybridisation. The pBS-Hox-B1 plasmid (A) was digested with *Cla* I before being used as a template to create the DIG-labelled RNA anti-sense probe. Transcription of the probe using T7 polymerase therefore ended at the *Cla* I site (B). Following transcription using T7 polymerase, the reaction mixture was electrophoresed on an agarose gel (C). The lower band at approximately 1.1Kb was the RNA probe generated from the DNA template. The template could be seen at approximately 4Kb.

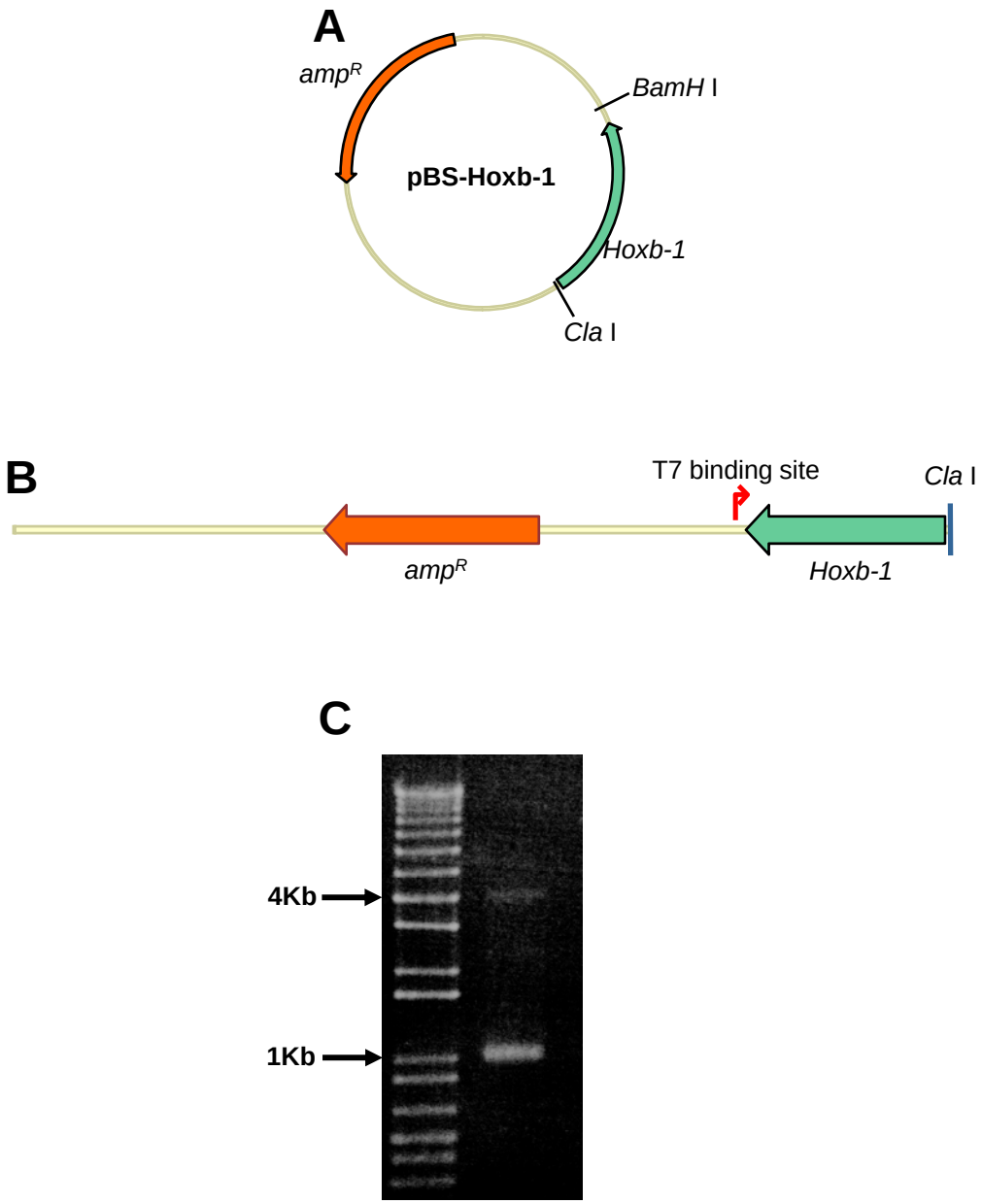

template was electrophoresed on an agarose gel to check the integrity of the reaction prior to DNase digestion (Figure 3.2C). The *in-situ* hybridisation technique was subsequently performed upon 10.5dpc embryos in an attempt to reproduce published data (Studer et al., 1998). The experimental expression pattern of *Hoxb-1* did indeed reproduce the findings in the paper by Studer et al., (Figure 3.3), confirming that the technique worked in my hands.

3.3.3 Confirming I.M.A.G.E. clone suitability for identifying Sox2 expression

Having established the technique, *in-situ* hybridisation with a *Sox2* probe was attempted. The *Sox2* antisense DIG-labelled RNA probe was generated by linearisation of the I.M.A.G.E. clone with *EcoR* I followed by transcription using T3 polymerase (Figure 3.4A). The control sense probe was generated following linearisation with *Not* I and transcription using T7 polymerase (Figure 3.4B).

Whole mount *in-situ* hybridisation using these probes was initially performed on WT 12.5dpc embryonic gut. The I.M.A.G.E. clone worked well as a template for creating the *Sox2* probe. The use of the antisense probe confirmed that *Sox2* expression is limited to the endoderm of the stomach and is completely absent in the intestine (Figure 3.5A and B). The expression of *Sox2* in the stomach endoderm at different developmental stages was investigated in subsequent *Cdx2*$^{+/-}$ samples (see below). The stomach of a 14.5dpc *Cdx2*$^{+/-}$ embryo hybridised with the *Sox2* antisense probe was sectioned in order to confirm staining in the endoderm (Figure 3.5C). The WT intestine did not contain any regions of ectopic *Sox2* expression, despite leaving the chromogenic probe to develop overnight and careful microscopic examination of the gut (Figure 3.6).

3.3.4 Identifying heterotopic endoderm in the Cdx2$^{+/-}$ *and Cdx2*$^{-/-}$ *gut*

12dpc *Cdx2*$^{+/-}$ gut strongly expressed *Sox2* in the endoderm of the stomach and the oesophagus (Figure 3.7B). *Sox2* was not ubiquitously expressed in the intestine; the caecal tissue of the same sample showed a scattering of very small *Sox2* expressing regions in the tip of the caecum (Figure 3.7C). No other regions of *Sox2* expression could be photographed with the equipment available but microscopic regions were visible under a dissection microscope. These regions were found in the distal ileum just proximal to the caecum.

Figure 3.3 Comparison of published data to experimental results with the *Hoxb-1* DIG-labelled RNA probe. (A) Published image of a 9.5dpc WT embryo indicating *Hoxb-1* gene expression detected using DIG-labelled RNA probe (Taken from Studer et al., 1998). (B) Experimental image of a 10.5dpc WT embryo indicating *Hoxb-1* gene expression detected in the same manner. In both images, gene expression was located in the tailbud and in the region of the presumptive rhombomere 4 (indicated by arrowhead).

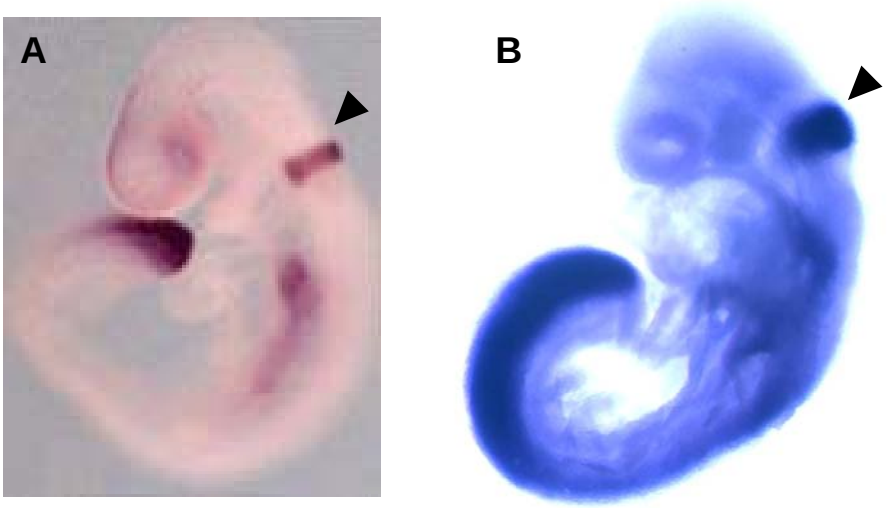

Figure 3.4 Alternative restriction enzyme and polymerase binding sites resulting in transcription of sense or antisense probes for *Sox2*. (A) The *Sox2* plasmid was restriction enzyme digested with either *EcoR* I or *Not* I. (B) Generation of the *Sox2* antisense probe by linearisation with *EcoR* I and probe generation with T3 polymerase. (C) Generation of the *Sox2* control sense probe using T7 polymerase following linearisation using *Not* I.

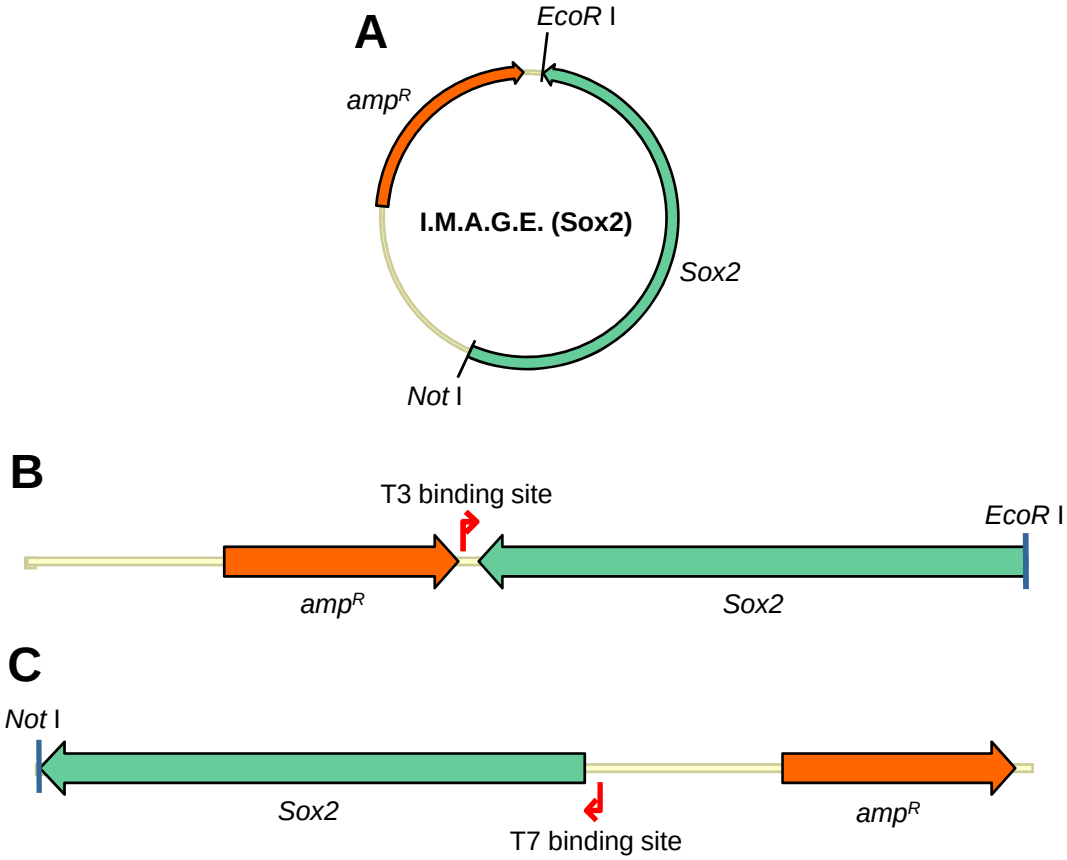

Figure 3.5 *Sox2* expression in WT embryonic gut. (A) 12.5dpc WT embryonic tissue hybridised with *Sox2* antisense probe. The inner endodermal layer was clearly labelled for *Sox2* expression while the outer mesodermal layer was absent for gene expression (shown by dotted line). Faint expression was also seen in the oesophagus. The intestine did not have detectable *Sox2* expression, commencing at the site of the arrowhead. (B) 12.5dpc WT embryonic tissue hybridised with the *Sox2* sense probe showed a complete absence of signal. (C) Section of 14.5dpc embryo stomach following whole-mount *in-situ* hybridisation with a DIG-labelled *Sox2* antisense RNA probe. The inner endodermal layer expressed *Sox2* as indicated by the purple colour. There was incomplete penetration of the colour, possibly due to tissue density. The outer mesoderm was absent for *Sox2* expression. The section was cut at 8µm and photographed under brightfield. White scale bars = 1mm, black scale bar = 200µm..

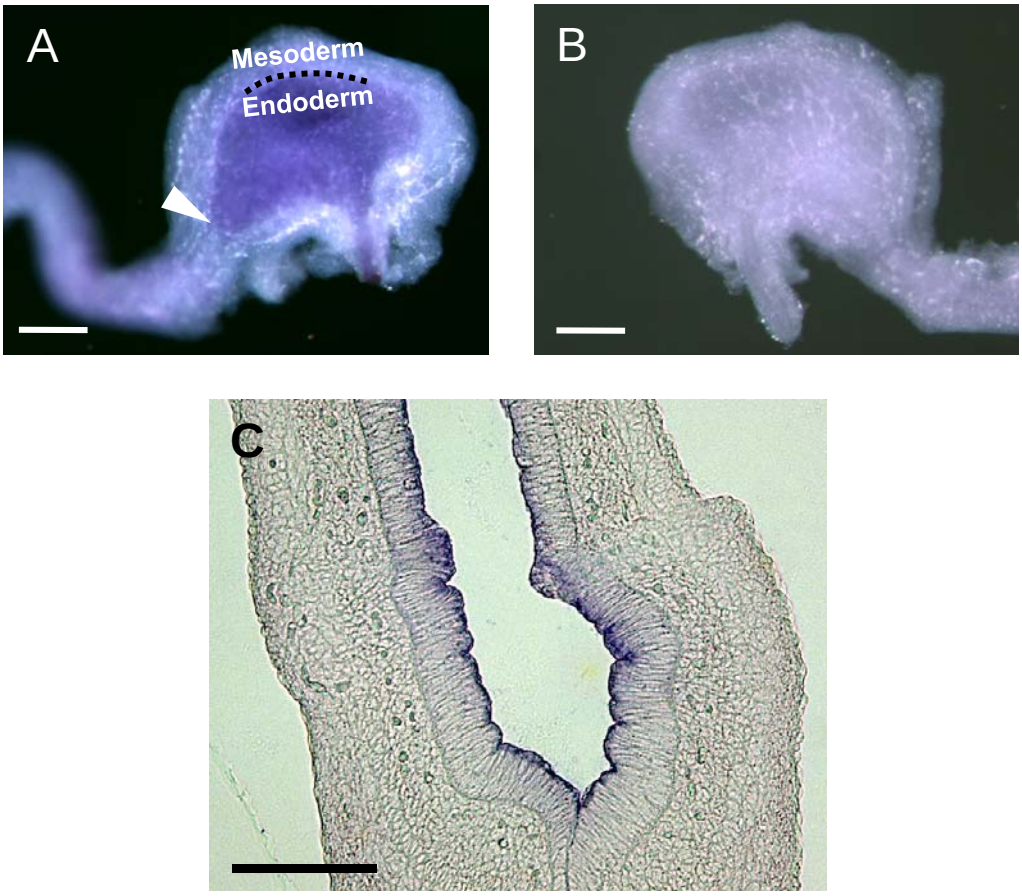

Figure 3.6 WT 14.5dpc gut hybridised with *Sox2* antisense RNA probe. The stomach showed strong expression of *Sox2* as expected. The caecum, enlarged on the right, did not express *Sox2*; this is the region in the *Cdx2*$^{+/-}$ animals where gastric heterotopias are most common. *Sox2* was not expressed in any other regions of the gut upon close examination under a dissection microscope. Scale bar = 1mm

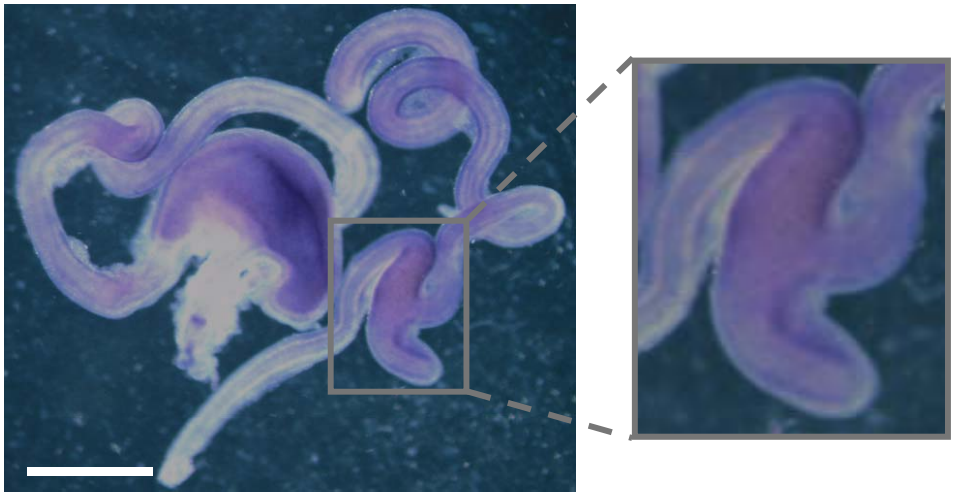

Figure 3.7 *In-situ* hybridisation of 12dpc tissue using a *Sox2* RNA probe. (A) WT control sample using a *Sox2* sense RNA probe (B) *Cdx2*$^{+/-}$ sample hybridised with a *Sox2* antisense RNA probe indicated *Sox2* expression in the endoderm of the stomach and oesophagus. (C) The caecum of the same sample had numerous regions of *Sox2* expression indicated by arrowheads where possible. (N.B: figure 3.7A is the same image as that used in figure 3.12A because both experiments were performed at the same time and so only one control was included. This image is included twice for continuity). Scale bars = 1mm

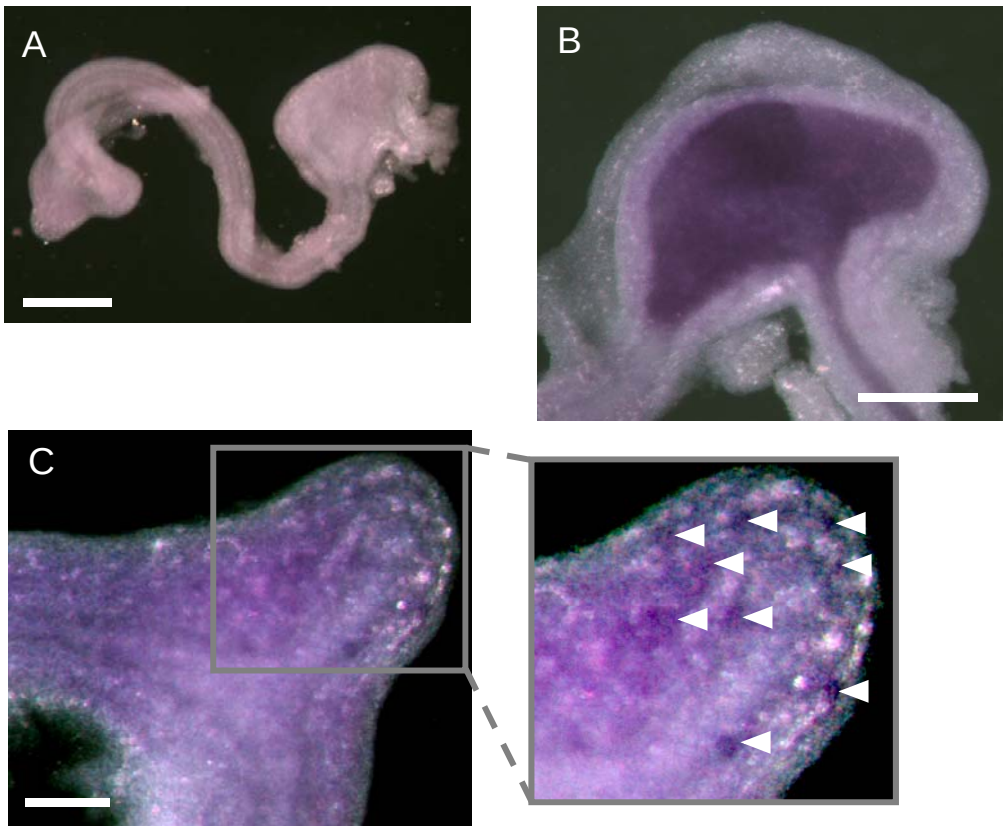

Cdx2$^{+/-}$ stomach at 12.5dpc also showed strong *Sox2* expression in stomach endoderm and extremely strong expression in the oesophageal endoderm (Figure 3.8B). *Sox2* expression was absent in the majority of the intestine. Strong discrete regions of expression were however detected in the proximal intestine (Figure 3.8B) and future jejunum (Figure 3.8C). The majority of *Sox2* expressing regions were found in the caecum and paracaecal endoderm (Figure 3.8D). The positions of the ectopic regions were clearly seen in the endoderm of the gut as the lumen could be visualised at this developmental stage.

As with previous samples, the 14.5dpc *Cdx2*$^{+/-}$ sample demonstrated strong *Sox2* expression in the stomach endoderm, but by this stage expression was absent in the oesophagus. Numerous ectopic *Sox2* expressing regions were detected along the length of the gut, in particular the future jejunum (Figure 3.9C) and caecal/paracaecal region and the future ileum (Figure 3.9D).

By 15.5dpc *Sox2* expression in the distal stomach endoderm was decreasing (Figure 3.10B). Only a few regions of ectopic *Sox2* expression were found in the midgut region (Figure 3.10C). The same was seen at 16.5dpc where only the anterior region of the stomach endoderm expressed *Sox2* (Figure 3.11B). The strength of the magenta colour was much fainter at this stage in the stomach, although on close examination ectopic regions of expression were still detected in the midgut of the *Cdx2*$^{+/-}$ sample (Figure 3.11C).

12 and 14.5dpc *Cdx2*$^{-/-}$//WT chimeric samples were also investigated alongside the *Cdx2*$^{+/-}$ 12dpc sample. Stomach and oesophageal endodermal *Sox2* expression was as expected. The 12dpc sample also showed numerous regions of ectopic *Sox2* expression in the intestine (Figures 3.12C and D), some of which were too small to photograph with the equipment available. The 14.5dpc *Cdx2*$^{-/-}$//WT chimeric caecum did not contain any ectopic *Sox2* expressing regions.

3.4 Conclusion

The results obtained using pBSHoxb-1 to create an RNA probe confirmed that the technique of whole-mount *in-situ* hybridisation using a DIG-labelled RNA probe was working successfully in the laboratory. The I.M.A.G.E. clone identified as containing

Figure 3.8 *In-situ* hybridisation of 12.5dpc tissue using a *Sox2* RNA probe. (A) WT control sample using a *Sox2* sense RNA probe (B) *Cdx2*$^{+/-}$ sample hybridised with a *Sox2* antisense RNA probe indicated *Sox2* expression in the endoderm of the stomach and oesophagus. A small region of ectopic *Sox2* expression was detected in the intestine indicated by an arrowhead. (C) A region of the future jejunum of the same sample, with regions of *Sox2* expression indicated by arrows. (D) The caecum and paracaecal region of the same *Cdx2*$^{+/-}$ sample demonstrated numerous regions of *Sox2* expression mostly indicated by arrowheads. Scale bars = 1mm

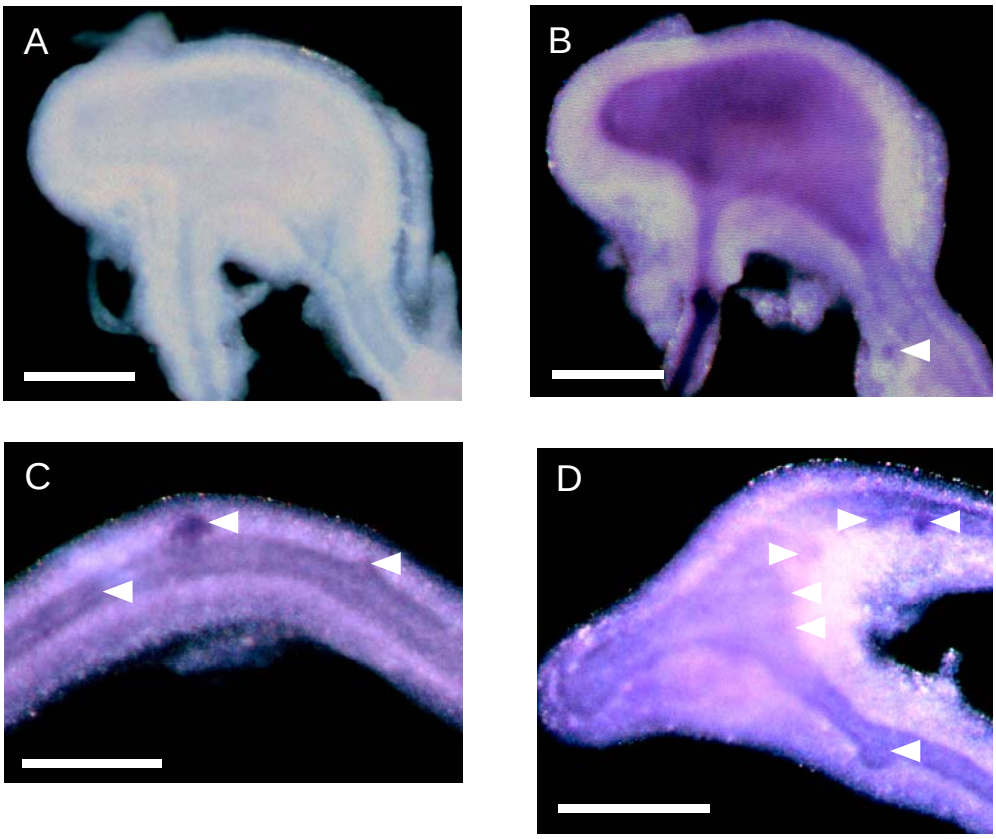

Figure 3.9 *In-situ* hybridisation of 14.5dpc tissue using a *Sox2* RNA probe. (A) WT control sample using a *Sox2* sense RNA probe (B) *Cdx2*$^{+/-}$ sample hybridised with a *Sox2* antisense RNA probe indicated *Sox2* expression in the endoderm of the stomach. The oesophagus was absent for *Sox2* expression. (C) The gut of the *Cdx2*$^{+/-}$ 14.5dpc sample, with a region of the small intestine highlighted. This region contained areas of *Sox2* expression indicated by arrowheads. (D) The mid and hindgut of the same sample with *Sox2* expressing regions highlighted with arrowheads. Scale bars = 500µm.

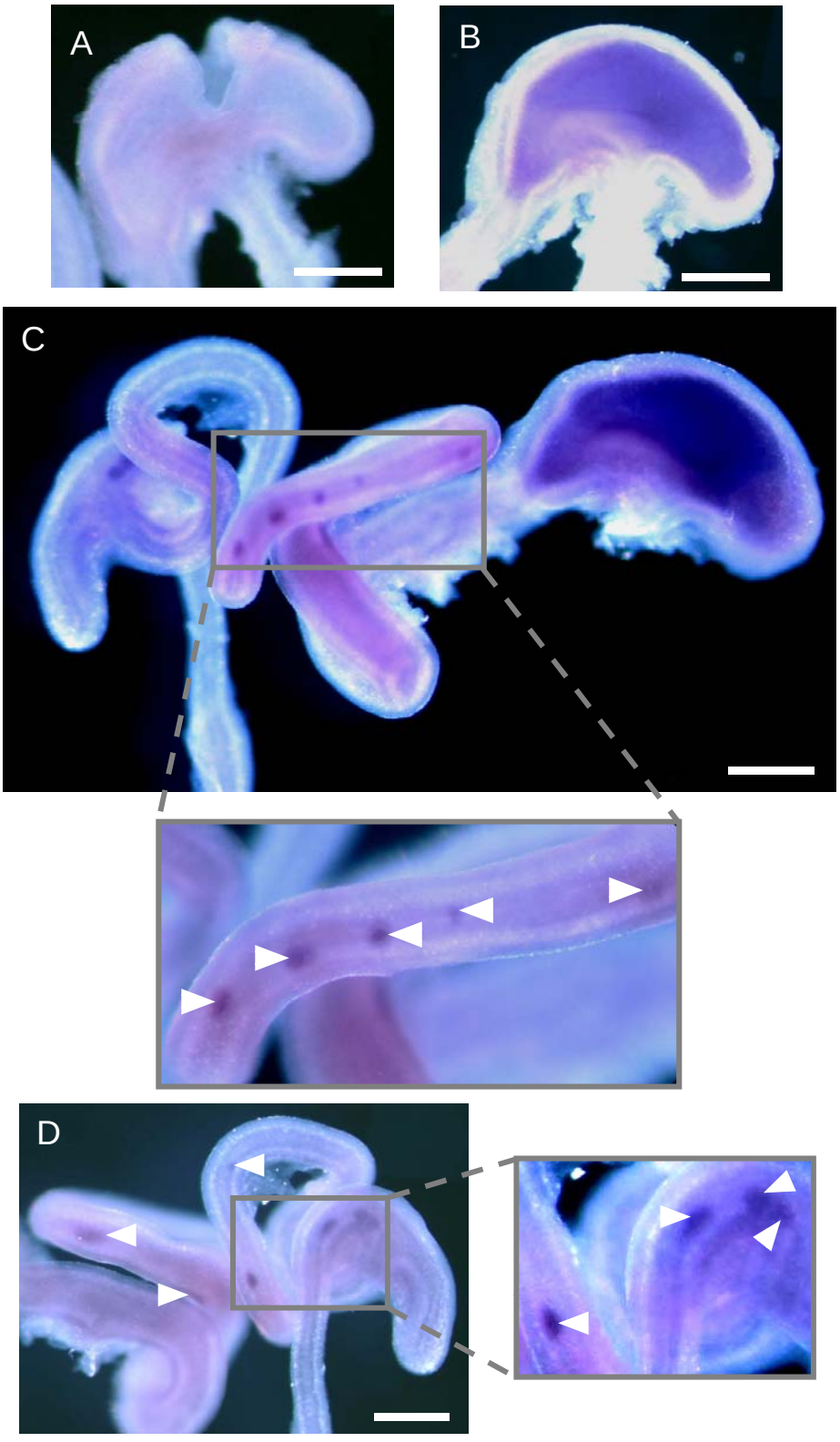

Figure 3.10 *In-situ* hybridisation of 15.5dpc tissue using a *Sox2* RNA probe. (A) WT control sample using a *Sox2* sense RNA probe (B) *Cdx2*$^{+/-}$ sample hybridised with a *Sox2* antisense RNA probe indicated *Sox2* expression in anterior regions of the stomach endoderm. (C) The midgut of the same sample indicated two regions of *Sox2* expression highlighted by arrowheads. Scale bars = 1mm.

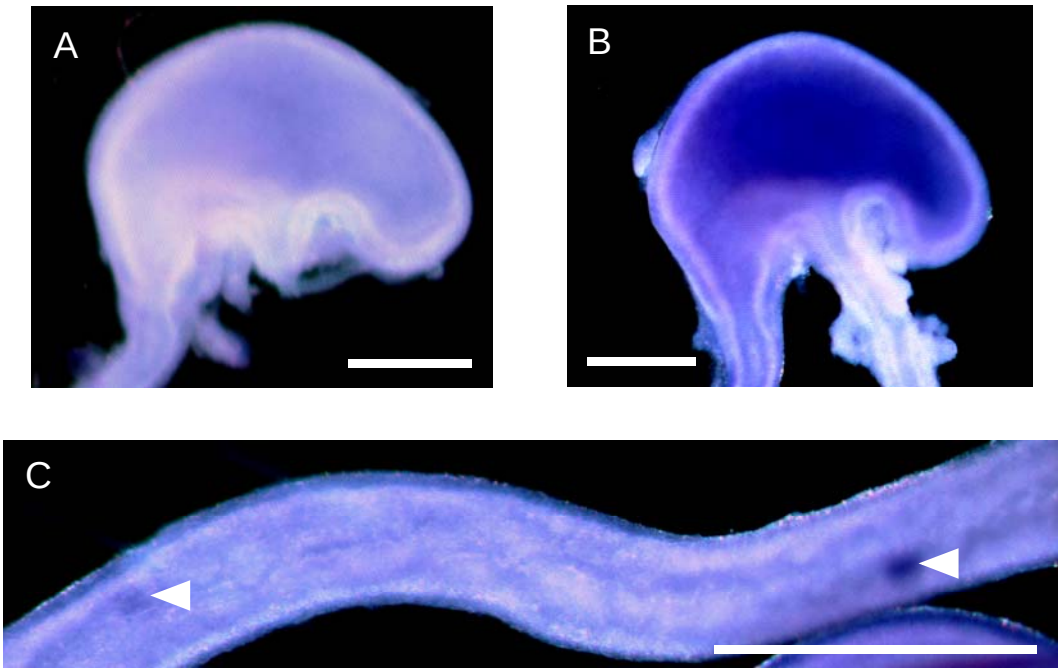

Figure 3.11 *In-situ* hybridisation of 16.5dpc tissue using a *Sox2* RNA probe. (A) WT control sample using a *Sox2* sense RNA probe (B) *Cdx2*$^{+/-}$ sample hybridised with a *Sox2* antisense RNA probe indicated faint *Sox2* expression predominantly in the anterior regions of the stomach endoderm. (C) A region of the future jejunum of the same sample indicated three regions of *Sox2* expression highlighted by arrowheads. The region indicated by the black arrowhead may have been one large ectopic area or two smaller adjacent regions. Scale bars = 1mm

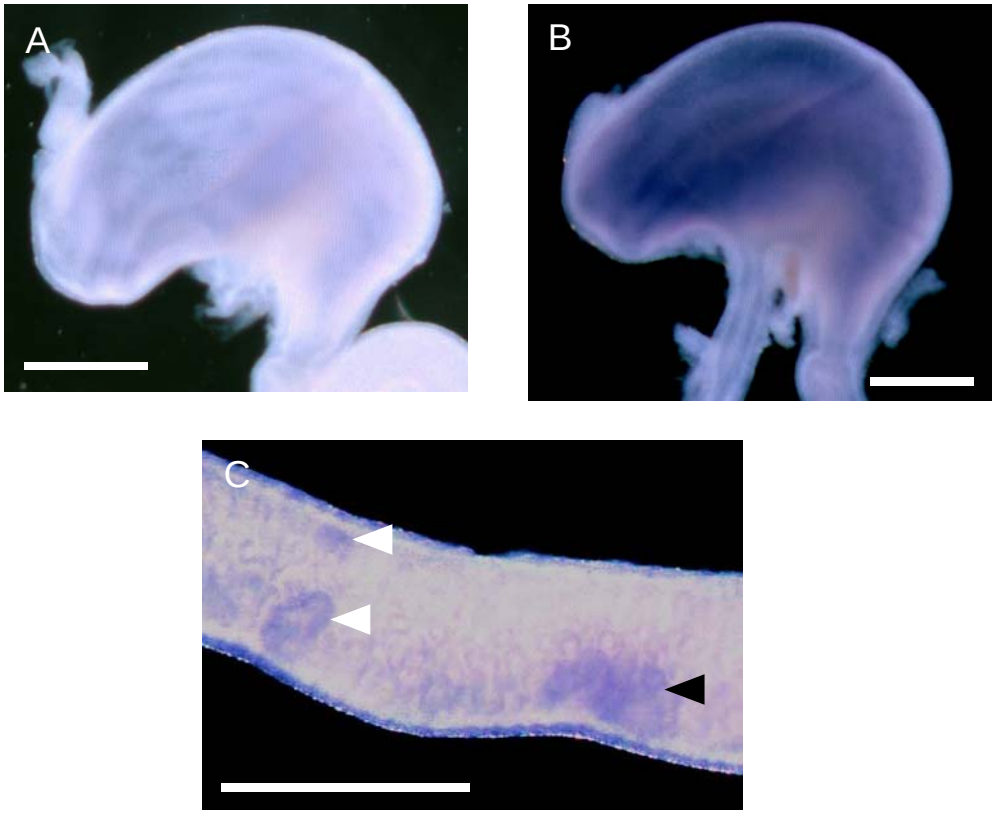

Figure 3.12 *In-situ* hybridisation of 12dpc tissue using a *Sox2* RNA probe. (A) WT control sample using a *Sox2* sense RNA probe (B) *Cdx2*$^{-/-}$//WT chimeric sample hybridised with a *Sox2* antisense RNA probe indicated *Sox2* expression in the stomach endoderm and oesophagus. (C) The proximal small intestine of the same sample indicated small but defined regions of *Sox2* expression highlighted by arrowheads. (D) The hindgut of the *Cdx2*$^{-/-}$//WT sample with numerous regions of *Sox2* expression indicated by arrowheads where possible. (N.B: figure 3.12A is the same as that used in figure 3.7A because both experiments were performed at the same time and so only one control was included. This image is included twice for continuity). Scale bars = 500µm

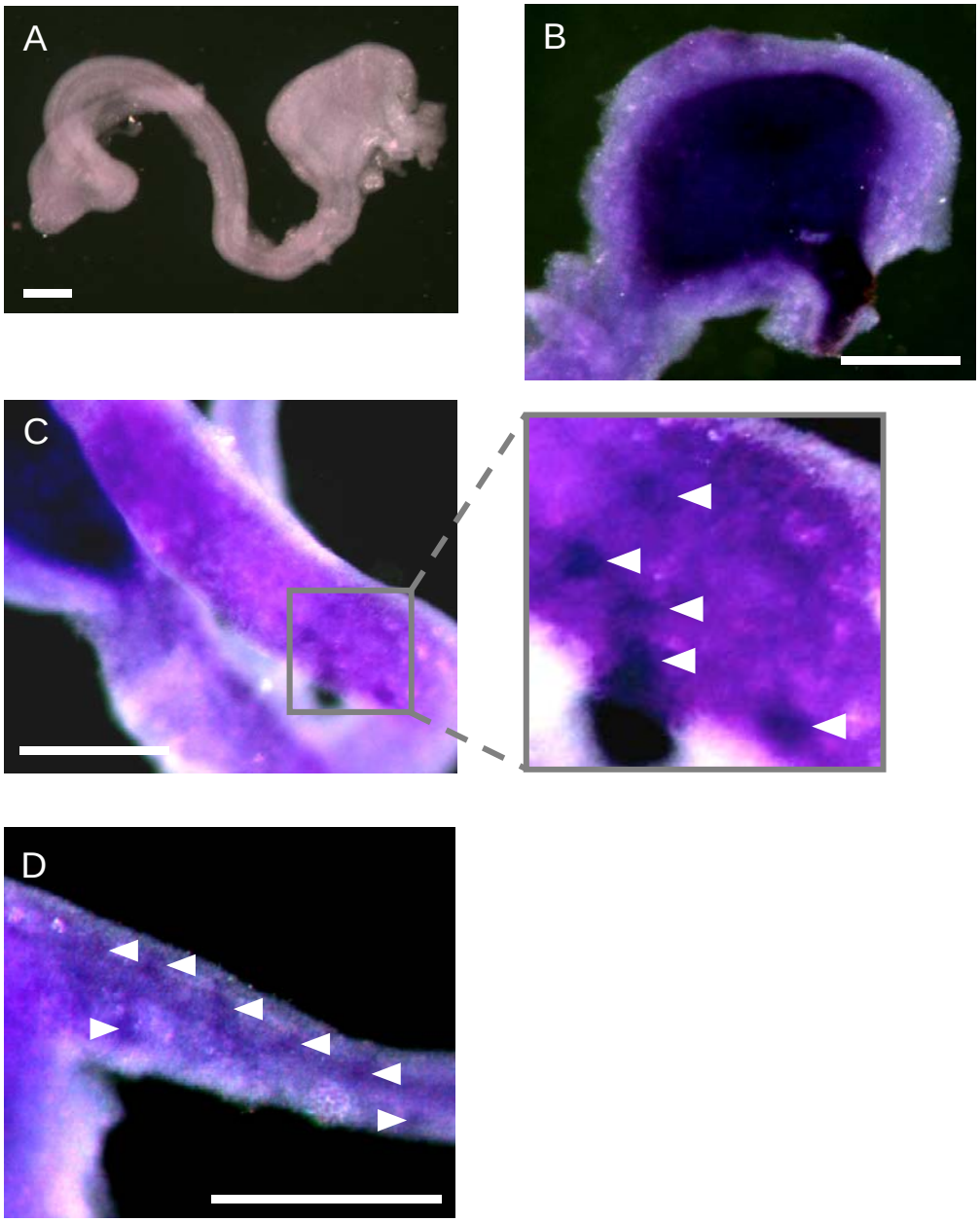

Sox2 sequence was also found to perform well as a template for creating *Sox2* RNA sense and antisense probes. The expression of *Sox2* in the stomach reflected that found by Que et al., 2007. The *Sox2* probe was therefore used on *Cdx2*$^{+/-}$ and *Cdx2*$^{-/-}$ //WTtissue to identify regions of ectopic *Sox2* expression.

The age of the embryos investigated was predicted by plug date and mothers carrying litters at 12.5, 14.5 and 16.5dpc were obtained. It is known that determining embryonic age using plug dates can be slightly inaccurate and so Theiler staging was used to confirm that some embryos were older or younger than expected, resulting in 12, 12.5, 14.5, 15.5, and 16.5dpc embryos being used. Only two chimeric samples were obtained that were suitable for this technique. This was due to a limited number of chimeric litters.

Regions of ectopic *Sox2* expression in the developing gut of *Cdx2*$^{+/-}$ mice were identified at all available embryonic stages from 12dpc to 16.5dpc. Only the 12dpc *Cdx2*$^{-/-}$//WT chimeric sample contained regions of ectopic *Sox2* expression; the 14.5dpc *Cdx2*$^{-/-}$//WT sample did not. The most likely explanation for this is that *Cdx2*$^{-/-}$ cells had not engrafted into the 14.5dpc *Cdx2*$^{-/-}$//WT intestine.

Sox2 expression is specific to the foregut endoderm. It is not normally expressed in the intestine. *Cdx2*$^{+/-}$ and *Cdx2*$^{-/-}$//WT mice are known to develop heterotopic regions of stomach-epithelium type tissue in the paracaecal region due to haploinsufficiency or complete absence of Cdx2. The *Cdx2* mutant embryos contain small regions of *Sox2* expression in the intestine. These *Sox2* expressing regions are adjacent to the intestinal lumen (i.e. endodermal) and are focussed mainly in the paracaecal region where *Cdx2* expression is normally highest. These regions are therefore determined to be developing heterotopic lesions of gastric epithelium (gastric heterotopias). The embryos also appeared to be developing heterotopic lesions in the region of the future jejunum. This region, however, is not generally observed to develop heterotopias in adult *Cdx2*$^{+/-}$ mice. Reasons for this are unknown but it may be that overriding mechanisms occur later in development to prevent these small regions of gastric heterotopia developing further.

Once it had been determined that these *Sox2* expressing regions were indicative of heterotopic lesions, the ideal embryonic age at which to investigate them further was then determined. Between 12-12.5dpc the ectopic regions of Sox2 expression are too small to be successfully photographed with the available equipment. The tissue is also extremely delicate. This time-point was therefore determined not optimal.

Between 15.5 and 16.5dpc heterotopic lesions can still be identified but normal stomach endodermal *Sox2* expression is harder to detect. It is suspected that not all gastric heterotopias are therefore being visualised at this point, suggested by the fact that both the 15.5 and 16.5dpc samples appear to contain fewer heterotopic lesions than earlier samples. The most likely explanation is that not all lesions can be detected at this age due to increased tissue density, but it cannot be ruled out that these two samples inherently contained fewer heterotopic lesions. It was therefore decided that although the visible regions of *Sox2* expression in these older embryos were larger, the tissue was too dense for full investigation and some heterotopic regions may not be detectable.

In the 14.5dpc gut, normal *Sox2* expression is both ubiquitous and strong in the stomach endoderm and appears to be decreasing or absent in the oesophagus. The gastric heterotopia is easily detected due to the lower density of the tissue but it is not as difficult to handle as younger gut. It was therefore decided that for the purpose of this investigation, 14.5dpc *Cdx2* mutant embryonic gut would be focussed upon.

In conclusion, it has been demonstrated that the *in-situ* hybridisation technique works and *Sox2* expression can be used to detect gastric heterotopias in the intestine of $Cdx2^{+/-}$ heterozygous and $Cdx2^{-/-}$//WT embryos. The optimal embryonic age at which to detect these heterotopias is 14.5dpc.

4. Investigating the interaction of the epithelial and mesodermal layers of the gut in *Cdx2* mutant mice using PCR techniques

4.1 Introduction

Having identified regions of *Sox2* expression in the developing intestine of *Cdx2*$^{+/-}$ and *Cdx2*$^{-/-}$//WT embryos, the nature of the underlying mesoderm needed to be determined. Reverse transcriptase PCR (RT-PCR) was chosen as the most suitable method to provide initial information regarding expression of mesodermal genes, although certain criteria had to be used to select genes suitable as tissue markers. PCR could only ever be used to detect aberrant gene expression because normal tissue would always be present in the *Cdx2* mutant intestine. The genes under investigation would therefore have to be normally expressed in stomach mesoderm but never intestine. *Sox2* has previously been shown to be ideal for detecting stomach endoderm from 12.5dpc onwards and so the mesodermal genes selected would also have to be expressed at a similar time-point to permit co-localisation (discussed in chapter 5). Three genes were identified as matching this criteria; *Nkx2-5*, *Csl* and *Barx1*.

4.1.1 Stomach mesoderm specific Nkx2-5

Nkx2-5 is a homologue of the Drosophila homeobox gene *Tinman* (reviewed in Harvey, 1996). In the mouse, *Nkx2-5* is first expressed at 7.5dpc. Transcripts are detected during various stages in development in the heart, pharyngeal endoderm, tongue, spleen and stomach. The visceral mesoderm capping the distal end of the stomach expresses *Nkx2-5* at 11.5dpc. By 14.5dpc this *Nkx2-5* positive distal region forms a ring around the stomach corresponding to the region of the future pyloric sphincter (Lints et al., 1993).

Transgenic mice were created where the expression of *Cre* recombinase was directed by expression of *Nkx2-5* (*Nkx2-5/Cre* mice)(Moses et al., 2001). These mice were crossed to Rosa26 reporter (*R26R*) mice. *R26R* mice express β-galactosidase (β-gal) in the presence of Cre. This can be detected by the presence of LacZ (see section 6.1.2.3). *Nkx2-5/Cre;R26R* mice therefore highlighted *Nkx2-5* expressing

cells via X-gal staining of the LacZ protein. The original purpose of these mice was to direct *Cre* expression to cardiac progenitor cells (as *Nkx2-5* is expressed in all cells with a cardiac specific fate) but it also provided information regarding the spatial and temporal expression of *Nkx2-5* (Moses et al., 2001). With regard to expression of *Nkx2-5* in the stomach, these mice confirmed previous findings that *Nkx2-5* is expressed in the stomach mesoderm at 10.5-13.5dpc in embryos and not the intestine (Moses et al., 2001).

In the chick, *Nkx2-5* is expressed in the mesoderm of the pyloric sphincter at embryonic stage HH 21, equivalent to 10.5dpc in the mouse (Buchberger et al., 1996, Smith and Tabin, 1999, Theodosiou and Tabin, 2005). Repression of endogenous *Nkx2-5* in the chick led to an alteration in the endodermal phenotype of the pyloric sphincter. In these animals the pyloric sphincter endoderm had a keratinized layer similar to that seen in the gizzard (the equivalent organ to the anterior stomach) (Smith et al., 2000). Equally, ectopic expression of *Nkx2-5* in the gizzard led to development of pyloric sphincter-like epithelium (Theodosiou and Tabin, 2005). Mesodermal *Nkx2-5* therefore has an effect upon endodermal development.

4.1.2 Stomach mesoderm specific Chisel

Chisel (*Csl*) is a downstream target of Nkx2-5 and is therefore downregulated in *Nkx2-5* null mutants (Palmer et al., 2001). *Csl* transcripts are detected in the atria and ventricles of the heart, in all skeletal muscles and the pulmonary veins. The involvement of *Csl* in the development of the heart has been extensively studied. *Csl* is also found in the smooth muscles of the stomach but not the intestine (Palmer et al., 2001). Although scientific data regarding stomach *Csl* expression is limited, *Csl* could be a useful marker to indicate whether the mesoderm underlying the epithelial heterotopia is expressing stomach mesoderm-specific genes.

The expression of *Csl* in the smooth muscle of the stomach is seen in both embryonic and neonatal stages. *Csl* is not expressed in the endodermal layer of the stomach. Both *Csl* transcripts and protein, however, are absent in adult stomach

tissue, indicating that expression is transient and limited to embryonic development (Palmer et al., 2001).

4.1.3 Stomach mesoderm specific Barx1

BarH-like homeobox-1 (*Barx1*) is a homologue of *Drosophila* BarH1. In the embryo, it is expressed in the head and neck mesenchyme, the proximal fore and hindlimbs and the wall of the developing stomach (Tissier-Seta et al., 1995) (as discussed in section 1.6.3). In the mouse, by 9.5dpc, *Barx1* expression can be detected in the stomach although the precise region of expression cannot be determined (Tissier-Seta et al., 1995). Only by 11.5dpc can expression of *Barx1* be localised to the mesoderm, not the epithelial layer of the stomach (Kim et al., 2005). *Barx1* expression peaks at 13.5dpc, but is barely detectable by 16.5dpc; by neonatal stages it cannot be detected (Kim et al., 2005, Tissier-Seta et al., 1995). It is not expressed in the intestine at any point (Kim et al., 2005, Tissier-Seta et al., 1995).

The role of mesenchymal expression of *Barx1* upon stomach endoderm has been tested via co-culture techniques. 12.5dpc mouse stomach mesenchyme was treated with *Barx1*-specific siRNAs prior to co-culture with stomach endoderm (Kim et al., 2005). The resultant culture was found to be expressing genes normally found in the intestine epithelium (including *Cdx2*). Forced expression of *Barx1* in intestinal co-culture experiments led to downregulation of intestinal epithelium specific genes and upregulation of a stomach epithelial marker, Mucin 1 (*Muc1*) (Kim et al., 2005). This indicated that *Barx1* expression has a role in endodermal-mesenchymal interactions and cell fate.

Microarray analysis of *Barx1*-siRNA treated stomach mesenchymal cells indicated a downregulation in *sFrp1* and *sFrp2* (secreted Frizzled-related protein) expression. In co-culture experiments involving stomach mesoderm, epithelium and *Barx1*-siRNA, forced expression of *sFrp1* and/or *sFrp2* returned gene expression back to that seen in normal stomach epithelium. *sFrp1* and *sFrp2* are therefore the predominant downstream targets of Barx1 (Kim et al., 2005). The Barx1/sFrp pathway downregulated the Wnt pathway, confirmed by the finding that forced *Dkk1* expression (a Wnt antagonist) in co-culture experiments produced the same result as

forced sFrp expression. It was deduced that inhibition of canonical Wnt signalling is crucial for stomach epithelium specification. Wnt signalling in the stomach is therefore confined spatially and temporally by the time and position of *Barx1* expression (Kim et al., 2005).

Barx1$^{-/-}$ mice, on a 129SV background, die at 13dpc due to unknown reasons (Kim et al., 2005). Prior to this, the stomach is shrunken and malformed while the intestine develops normally. The lining within the stomach is infolded and disorganised. These mice could not be fully investigated because cytodifferentiation of the gut occurs beyond 13dpc (Kim et al., 2005). Breeding the *Barx1*$^{-/-}$ mice onto a C57/BL6 background rescued the lethal phenotype and null mutants subsequently died postnatally following respiratory distress due to cleft palate; probably due to the requirement of *Barx1* during branchial arch development (Kim et al., 2007b).

The stomach of the *Barx1*$^{-/-}$ mutants was reduced in size and remained as a midline structure. The anterior gastric lining appeared to show some gastric features, while the posterior region appeared to contain villi (Kim et al., 2007b). Histological and immunohistochemical techniques confirmed that the proximal region of the stomach was shortened and contained blurred squamous-glandular and fundic-antral boundaries. The gastric-duodenal junction shifted anteriorly into the stomach itself, but remained defined despite the lack of the pyloric sphincter (Figure 4.1). It would therefore appear that gastric size, shape, regionalisation and pyloric sphincter formation are regulated by the mesenchymal expression of *Barx1*. The role of Barx1 in controlling Wnt signalling in the stomach epithelium was confirmed in these mice (Kim et al., 2007b).

4.2 Aims

The heterotopias developing in the *Cdx2* mutant intestine contain stomach-epithelium type tissue. The original instructive signal in these heterotopias is endodermal in origin (i.e. a loss of endodermal expression of *Cdx2*). It was not known whether the mesoderm underlying these regions responds to signals from the heterotypic endoderm and therefore expresses stomach mesoderm-specific genes. The aim of this chapter was to identify a gene that was normally expressed in the stomach

Figure 4.1 The *Barx1*$^{-/-}$ stomach in comparison to wild type. The *Barx1*$^{-/-}$ stomach fails to expand and rotate. The stomach also demonstrates a gastrointestinal homeotic shift; the stomach-intestinal boundary is shifted anteriorly. The characteristic regions of the stomach are less defined and also demonstrate an anterior shift. It was therefore deduced that *Barx1* is required for correct stomach formation. (Taken from Kim et. al., 2007).

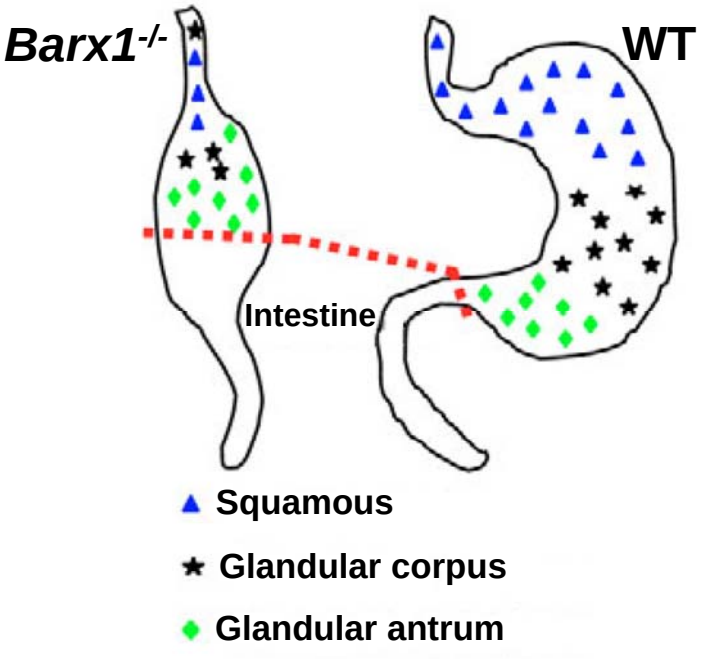

mesoderm and completely absent in the intestine. The expression of this gene was then investigated in the *Cdx2* mutant intestine using RT- PCR techniques.

4.3 Results

4.3.1 Selecting suitable RT-PCR primers

Primer pairs needed to be designed so that each primer annealed to a different exon and therefore spanned an intron. This would mean that a different sized PCR product would be seen if primers were annealing to contaminating genomic DNA as opposed to cDNA transcribed from mRNA (Figure 4.2 and 4.3). The ability to detect genomic DNA contamination is crucial for the purpose of RT-PCR; it ensures that the DNA product is solely due to the amount of cDNA present and the band intensities can therefore be compared. The primers were designed so that they span the exons closest to the polyA tail of the mRNA. This was because oligo(dT) primer was used for the reverse transcription reaction to create the cDNA and so cDNAs from this end of the gene should be in abundance. *Nkx2-5* (Figure 4.2) and *Barx1* (Figure 4.3) RT-PCR primers were designed in this manner. The *Csl* gene comprises only one exon (Figure 4.4) and so it was decided that the expression of this gene would not be investigated further unless RT-PCR for *Nkx2-5* and *Barx1* expression failed to provide any conclusive results. This was because genomic contamination of samples could not be unequivocally ruled out using primers designed for this gene.

Sox2 RT-PCR was to be used as a positive control for any samples found to be expressing *Barx1*, as this would indicate the presence of gastric heterotopias. The primer sequences for RT-PCR of the *Sox2* gene were obtained from a paper (Wislet-Gendebien et al., 2005) and designated OES26 and OES27. The product from a PCR using the *Sox2* RT-PCR primers with 14.5dpc WT stomach cDNA was sent for sequencing. The results confirmed that the PCR product mapped to the *Sox2* gene. The amount of *Sox2* expression detected by RT-PCR in control stomach samples was, however, relatively low. This meant that either the primers were inefficient or *Sox2* expression was inherently low in the stomach. Redesigning of the primers did not yield a product at all and so OES26 and OES27 continued to be used. *Gapdh* expression was used as a loading control. The primers OCP174 and OCP175 had been previously optimised in this laboratory for this purpose.

Figure 4.2 *Nkx2-5* primer annealing sites. The *Nkx2-5* gene contains two exons (E1 and E2). Primers OES14 and OES15 were designed to anneal to different exons and therefore span an intron. (A) Primers annealing to genomic DNA contamination. If genomic DNA is contaminating the cDNA sample, then a product 1.8Kb in size would be seen on the gel. (B) Primers annealing to cDNA. If the primers have correctly annealed to the cDNA then a smaller product would be seen due to the intron being spliced out.

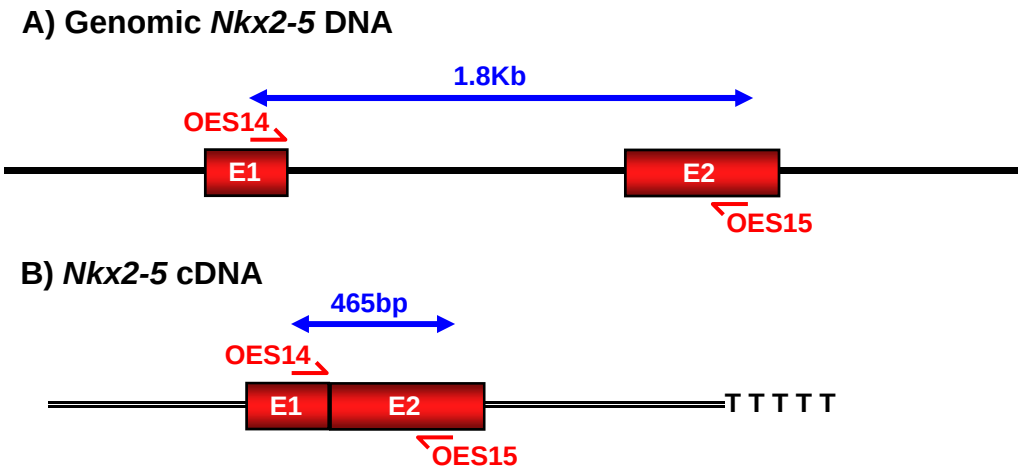

Figure 4.3 *Barx1* primer annealing sites. The *Barx1* gene contains four exons (E1-4). Primers OES23 and OES24 were designed to anneal to different exons and therefore span an intron. (A) Primers annealing to contaminating genomic DNA. If genomic DNA is contaminating the cDNA sample, then a product of 532bp would be seen on the gel. (B) Primers annealing to cDNA. If the primers have correctly annealed to the cDNA then a smaller product of 180bp would be seen due to the intron being spliced out. The primers were designed to anneal to exons closest to the polyA tail of the transcript.

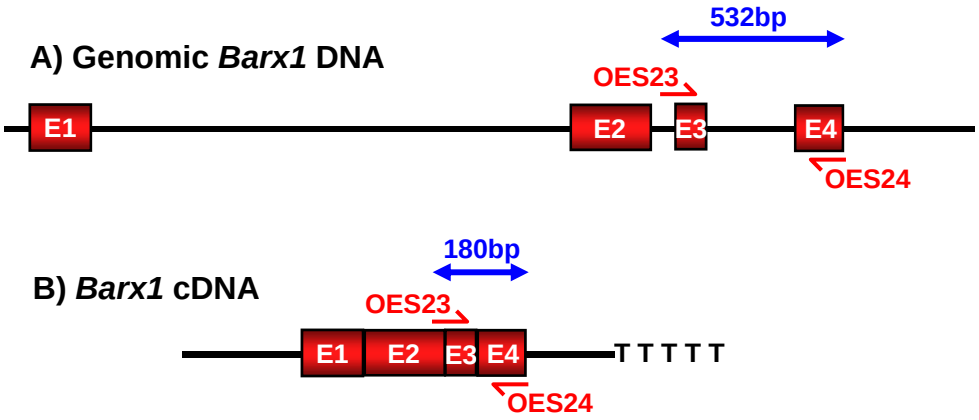

Figure 4.4 The *Csl* gene. *Csl* is comprised of only one exon and so a primer pair could not be designed to span an intron for use in rtPCR.

4.3.2 Optimising RT-PCR primers for detection of Nkx2-5

A RT-PCR was performed upon 14.5dpc gut cDNA samples using *Nkx2-5* specific primers OES14 and OES15. When the resultant PCR products were electrophoresed upon an agarose gel, numerous bands were seen for all samples (Figure 4.5). *Nkx2-5* should only be expressed in the stomach sample with an expected band size of 465bp. However numerous bands were observed and all samples gave products with the primers. These primers were not suitable for RT-PCR because they did not amplify a single target sequence and so the use of *Nkx2-5* RT-PCR was not pursued further.

4.3.3 Investigating Barx1 expression in Cdx2 mutant caecum using RT-PCR

Primers OES23 and OES24 were designed for RT-PCR of the *Barx1* gene. The product from a PCR using OES23 and OES24 with 14.5dpc WT stomach cDNA as a template was extracted from an agarose gel. This DNA product was sequenced with primer OES25. Primer OES25 anneals just within the PCR product and so the whole product was sequenced. The sequencing results confirmed that the PCR product mapped to *Barx1* and so the primers were specific and therefore suitable for RT-PCR.

Numerous *Cdx2*$^{+/-}$ heterozygous caecal/paracaecal samples were investigated in comparison to WT littermates. The results of these studies are summarised in Table 4.1A. Initially, 14.5dpc samples were focussed upon. RNA and the subsequent cDNA were successfully produced from eight 14.5dpc *Cdx2*$^{+/-}$ embryos. *Barx1* expression in six of these *Cdx2*$^{+/-}$ caecum samples was compared to that of WT caecum. Three of these six comparisons indicated no *Barx1* expression in either the *Cdx2*$^{+/-}$ or WT caecum sample. Two *Cdx2*$^{+/-}$ samples, when compared to WT caecum, indicated higher levels of *Barx1* expression in the *Cdx2*$^{+/-}$ sample than the WT sample. However, unexpectedly, low *Barx1* expression was detected in the WT samples and was possibly due to a low level of PCR contamination (Figures 4.6 and 4.7). Adjustment of exposure levels allowed the difference in *Barx1* expression levels between the *Cdx2*$^{+/-}$ and WT caecum sample to be emphasised (Figure 4.7). *Sox2* expression was investigated in these samples, the purpose of which was to confirm that stomach endoderm and therefore a heterotopia was present in the sample. Only

Figure 4.5 *Nkx2-5* RT-PCR primers using 14.5dpc WT gut cDNA. A band at 465bp indicated expression of *Nkx2-5*. This should only be detected in the stomach sample but numerous bands were seen for all cDNA samples. The lack of a single band meant that these primers were not suitable for use in semi-quantitative RT-PCR. (l.int; large intestine, s.int; small intestine).

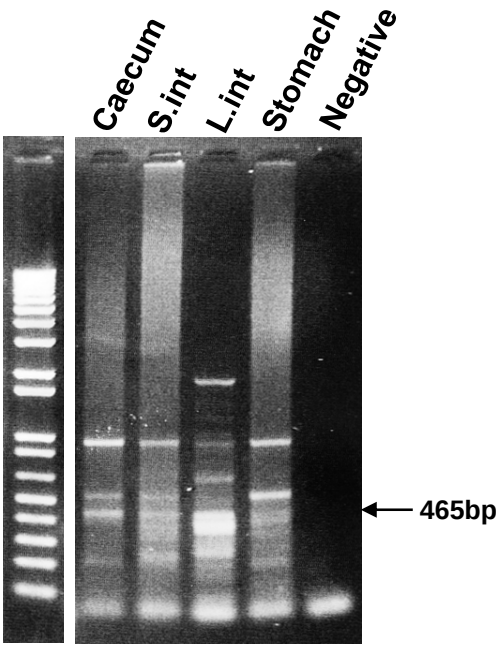

Table 4.1 A summary of *Barx1* expression in embryonic caecum, detected by RT-PCR. The result for *Barx1* expression shown in column 'A' corresponds to the genotype also shown in column 'A' and the same with column 'B'. *Cdx2*$^{+/-}$ data is shown in Table (A), *Cdx2*$^{-/-}$//WT data is shown in Table (B). The corresponding PCR results are shown in the figures indicated. (+; expression, ++; stronger expression, –; no expression).

A

Embryonic Age (dpc)	Genotype A	Genotype B	*Barx1* Expression A	*Barx1* Expression B	*Sox2* Expression A	*Sox2* Expression B	Figure Number
14.5	WT	*Cdx2*$^{+/-}$	-	-			
14.5	WT	*Cdx2*$^{+/-}$	-	-			
14.5	WT	*Cdx2*$^{+/-}$	-	-			
14.5	WT	*Cdx2*$^{+/-}$	+	++	-	-	4.6
14.5	WT	*Cdx2*$^{+/-}$	+	++	-	+	4.7
14.5	WT	*Cdx2*$^{+/-}$	+	-			
14.5	*Cdx2*$^{+/-}$	*Cdx2*$^{+/-}$	+	-			4.8
16.5	WT	*Cdx2*$^{+/-}$	-	-			
16.5	WT	*Cdx2*$^{+/-}$	-	+			4.9
19.5	WT	*Cdx2*$^{+/-}$	-	-			
19.5	WT	*Cdx2*$^{+/-}$	-	-			
19.5	WT	*Cdx2*$^{+/-}$	-	-			

B

Embryonic Age (dpc)	Genotype A	Genotype B	Barx1 Expression A	Barx1 Expression B	Sox2 Expression A	Sox2 Expression B
14.5	WT	*Cdx2*$^{-/-}$ //WT	-	-		
14.5	WT	*Cdx2*$^{-/-}$ //WT	-	-		
16.5	WT	*Cdx2*$^{-/-}$ //WT	-	-		
16.5	WT	*Cdx2*$^{-/-}$ //WT	-	-		

Figure 4.6 *Barx1* and *Sox2* expression in 14.5dpc *Cdx2*$^{+/-}$ caecum in comparison to WT caecum. *Barx1* expression was detected in both samples, but the level of expression in the *Cdx2*$^{+/-}$ caecum sample was higher. *Sox2* expression was not detected in either sample, possibly because the PCR was not sensitive enough. A stomach sample acted as a *Barx1* and *Sox2* positive control and *Gapdh* as a loading control.

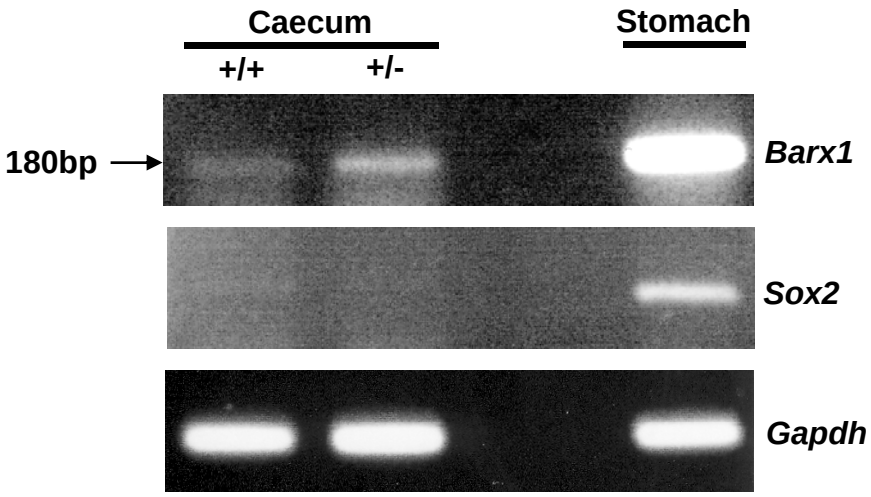

Figure 4.7 *Barx1* and *Sox2* expression in another 14.5dpc *Cdx2*$^{+/-}$ caecum in comparison to WT caecum. (A) Again, *Barx1* RT-PCR products were more strongly detected in the *Cdx2*$^{+/-}$ sample compared to the WT sample. *Sox2* expression was also detected in the *Cdx2*$^{+/-}$ but not in the WT caecum. A stomach sample again acted as a *Barx1* and *Sox2* positive control and *Gapdh* as a loading control. (B) Following shorter exposure of the photograph, the higher level of *Barx1* expression in the *Cdx2*$^{+/-}$ caecum in comparison to the WT caecum was more clearly seen. The images of *Sox2* and *Gapdh* expression are the same in both versions.

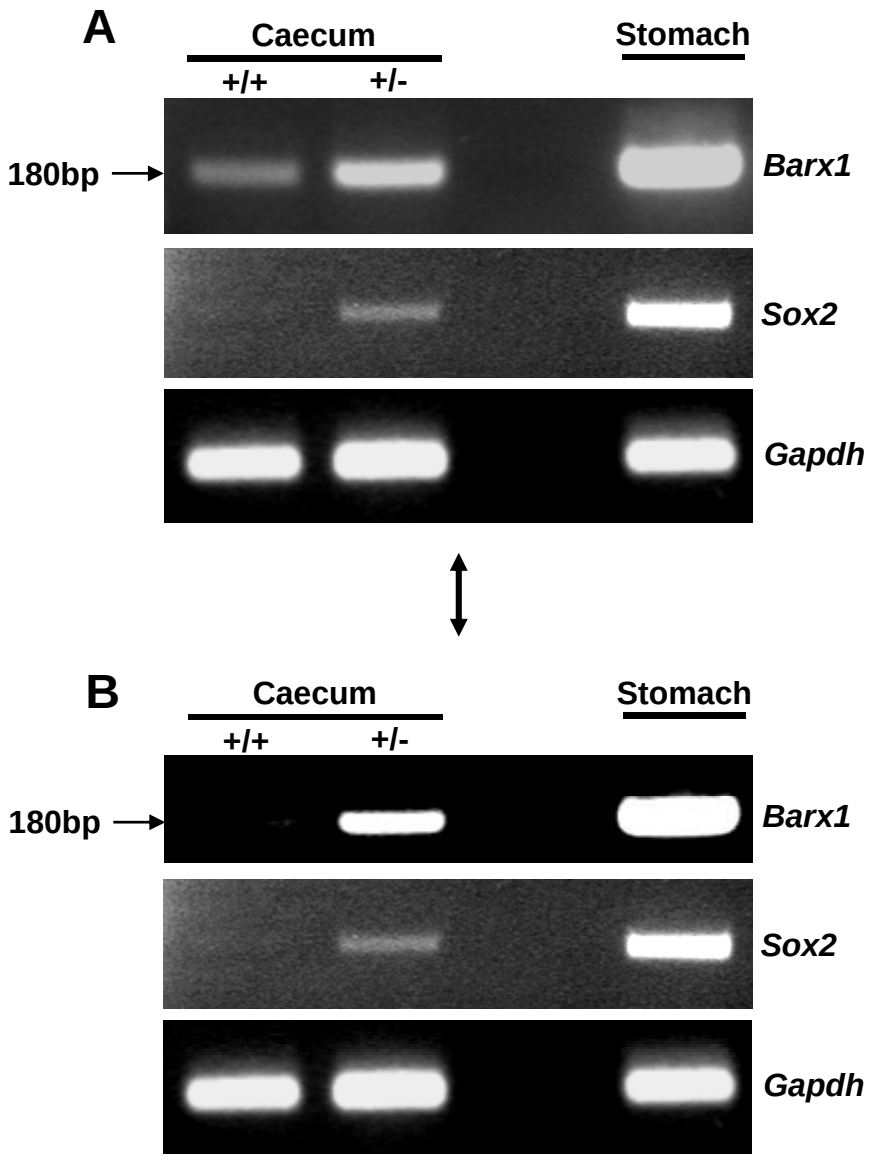

one 14.5dpc *Cdx2*$^{+/-}$ sample indicated expression of *Sox2* (Figure 4.7). The reason for this inconsistency is not clear but as previously discussed, this may be because amounts of *Sox2* transcripts are below detectable levels or that this particular PCR is inefficient. One 14.5dpc WT sample indicated expression of *Barx1* whilst the *Cdx2*$^{+/-}$ sample did not; this was deemed to be due to contamination. In further experiments liver controls were included to hopefully indicate any sample contamination. If contamination of the liver sample was detected then the result was ignored. Two 14.5dpc *Cdx2*$^{+/-}$ caecum samples were then compared to each other; unfortunately a WT sample was not available at the time. The comparison of the two *Cdx2*$^{+/-}$ samples indicated that one sample expressed *Barx1* whilst the other did not (Figure 4.8), highlighting the varying levels of *Barx1* expression between *Cdx2*$^{+/-}$ caecum samples.

Barx1 expression in two 16.5dpc *Cdx2*$^{+/-}$ caecum cDNA samples was also compared to WT caecum (summarised in Table 4.1A). One comparison indicated no *Barx1* expression in either sample. The other 16.5dpc *Cdx2*$^{+/-}$ sample indicated *Barx1* expression whilst the WT caecum did not (Figure 4.9). *Sox2* expression was investigated in these samples but no bands could be detected including for the stomach positive controls indicating a problem with the *Sox2* PCR. When *Barx1* expression in a 19.5dpc *Cdx2*$^{+/-}$ caecum sample was compared to that of WT samples, *Barx1* was not detected in either sample; this was repeated for three different *Cdx2*$^{+/-}$ caecums (summarised in Table 4.1A) but in all cases, no *Barx1* expression could be found.

Cdx2$^{-/-}$//WT chimeric tissue was also investigated. *Barx1* expression was assessed in 14.5dpc and 16.5dpc chimeric caecum samples in comparison to WT samples. All chimeric samples failed to demonstrate *Barx1* expression in the caecum (summarised in Table 4.1B).

4.3.4 Investigation of normal Barx1 expression levels in the stomach

It has been previously reported that expression of *Barx1* decreases from 13.5dpc and becomes absent beyond 16.5dpc (Kim et al., 2005). Following the use of embryonic stomach tissue up to 19.5dpc as a positive control for *Barx1* expression, the gene was strongly expressed much later than expected. RT-PCR for *Barx1* was therefore

Figure 4.8 *Barx1* expression in two 14.5dpc *Cdx2*$^{+/-}$ caecum samples. The sample on the left expressed *Barx1* but the sample on the right did not, indicating a variance between individual caecums. A stomach sample acted as a *Barx1* positive control and liver samples acted as negative controls. *Gapdh* expression was used as a loading control.

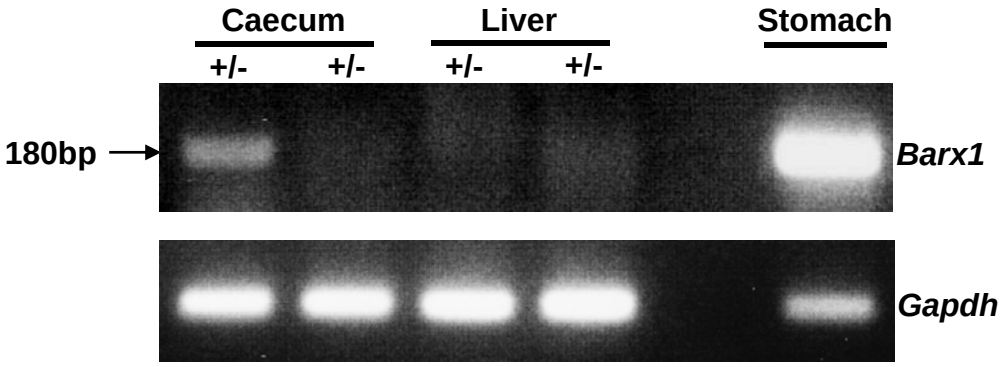

Figure 4.9 *Barx1* expression in a 16.5dpc *Cdx2*$^{+/-}$ caecum. *Barx1* expression was detected in the *Cdx2*$^{+/-}$ caecum but not in the WT caecum. A stomach sample acted as a positive control while liver samples were used as negative controls to help ensure no contamination was occurring. *Gapdh* expression was used as a loading control.

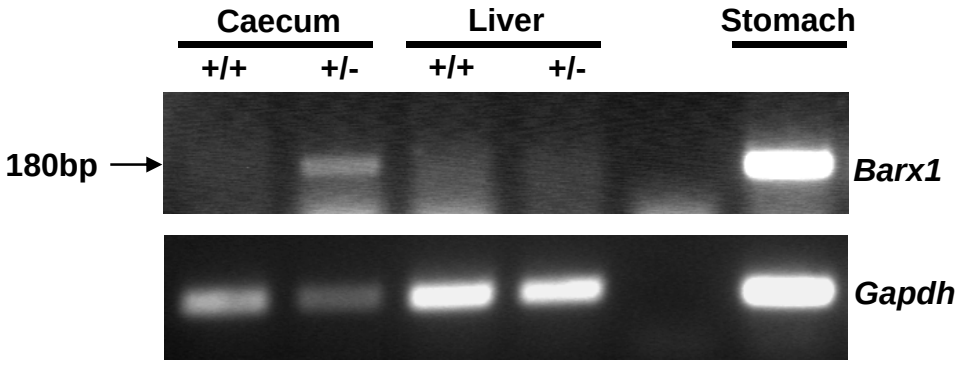

performed on stomach cDNA generated from 14.5, 16.5, 19.5dpc, 1 day old and weaned animals. Tissue from a weaned mouse has undergone cytodifferentiation of the gut epithelium; this means that all genes solely involved in stomach development would therefore no longer be required by this stage, including *Barx1*.

The results indicated that *Barx1* expression levels in the stomach do not appear to drastically alter between 14.5dpc and post weaning (Figure 4.10). This is not in agreement with the findings reported by Kim et al. (2005). The primer sequences used by Kim et al. are not known, but OES23 and OES24 were shown to specifically detect *Barx1* expression. It is also extremely unlikely that the results seen here are due to contamination issues because the level of gene expression is high and the liver and intestine controls were negative. These results are therefore considered to be accurate; one reason for the apparently conflicting findings is that there may be strain differences; Kim et al. used 129SV mice while this study used C57/BL6 mice.

4.4 Conclusion

The purpose of this chapter was to detect aberrant mesodermal gene expression within the intestine of *Cdx2* mutant mice. Any expression of stomach mesoderm-specific genes is indicative of a mesodermal response to heterotypic endoderm.

In chapter 3 it was deduced that the size of the gastric heterotopias were extremely small and the total volume of the intestine in comparison was extremely large. It was therefore decided that RT-PCR should focus upon the *Cdx2* mutant caecum. This was because the majority of heterotypic lesions develop here and so the ratio of ectopic tissue to normal intestine should be higher and therefore more detectable by PCR. RT-PCR upon embryonic caecum however proved technically difficult due to the size of the sample providing only a limited amount of cDNA. This was confounded further by sensitivity problems with the *Sox2* primers despite redesigning them.

12.5dpc caecal samples were too small to successfully extract RNA and so were not used. RNA was successfully extracted from 14.5, 16.5 and 19.5dpc $Cdx2^{+/-}$ caecum samples but the total volume extracted was extremely small and so only one reverse

Figure 4.10 *Barx1* expression in WT stomach. The liver and intestine samples had no detectable expression of *Barx1* as expected. There was no notable difference in *Barx1* expression levels between any of the stomach samples, including that from a weaned mouse.

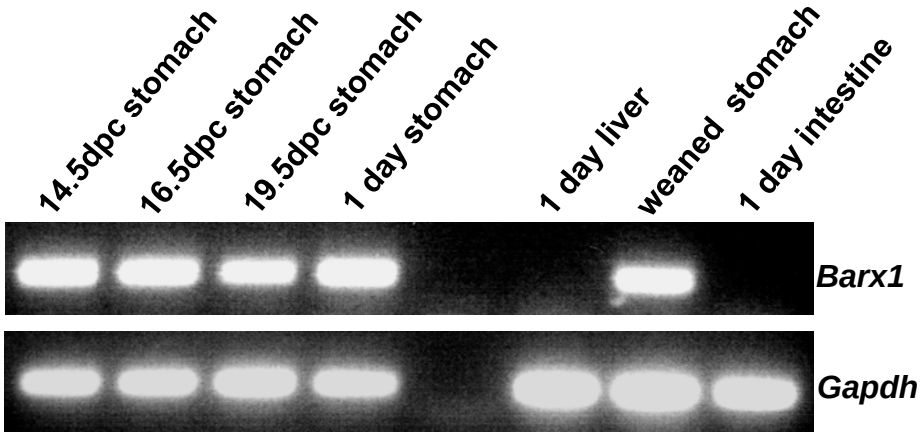

transcriptase reaction could be performed from one RNA sample. A normal control for RT-PCR is a reaction without any reverse transcriptase. A subsequent PCR product is then indicative of genomic contamination as no cDNA is present in the sample. The low yield of RNA from embryonic caecum samples meant this could not be performed and so the use of primers spanning introns became instrumental in detecting any genomic contamination.

Following problems with the use of *Nkx2-5* RT-PCR primers, RT-PCR for *Barx1* was adopted as the best method of determining mesodermal tissue-type. In spite of a low cDNA yield, *Barx1* expression was investigated in numerous caecum samples. A few WT caecum samples (3 in 11) unexpectedly expressed *Barx1*; one reason for this may have been contamination and so a liver control, which does not express *Barx1*, was included in an attempt to highlight any further contamination issues. If a liver sample was shown to be contaminated then the result was ignored. A few *Cdx2*$^{+/-}$ samples (4 in 13) did express *Barx1*, three of which indicated stronger expression than that detected in the WT comparison. The fourth sample was compared to another *Cdx2*$^{+/-}$ sample.

Sox2 RT-PCR was performed as a positive control. However, it proved highly variable in the *Cdx2*$^{+/-}$ samples, even though results from Chapter 3 clearly showed *Sox2* expression in many samples by *in-situ* hybridisation. The reason for this is not clear but may suggest that *Sox2* transcripts are very low in the heterotopias compared to *Barx1* or that the PCR is inefficient. Of the two successful *Sox2* RT-PCRs upon *Barx1* positive *Cdx2*$^{+/-}$ caecum, *Sox2* was only detected in one sample; this indicated that stomach endoderm (i.e. gastric heterotopia) was present in this sample. The *Cdx2*$^{-/-}$*//*WT samples failed to indicate any *Barx1* expression despite confirmation that *Cdx2*$^{-/-}$ cells had engrafted in the sample. Reasons for this inconsistent finding could be that some of the *Cdx2*$^{+/-}$ samples did not contain heterotopic regions (hence one *Cdx2*$^{+/-}$ sample being *Barx1* positive while the other in the comparison was negative); this however was not the case in the chimeric samples where engraftment was confirmed. Another reason could therefore be that heterotopic number was extremely low and so low levels of *Barx1* transcripts were undectable in a high volume of intestinal transcripts.

Although *Barx1* was not detected in all the *Cdx2* mutant samples and did not always correlate with *Sox2* expression, the general trend gained from these results is that *Barx1* was present on some occasions. This evidence suggests that the mesoderm is expressing stomach-specific genes in response to an alteration in endodermal gene expression. Although alone this is not conclusive, it provides encouragement to investigate *Barx1* expression further using other techniques to clarify the findings discussed here.

As a separate finding, this study has shown that *Barx1* continues to be expressed in the stomach beyond weaning. *Barx1* expression in the stomach has previously been shown to decrease beyond 13.5dpc to become completely absent at birth. The reasons for the conflicting findings are unclear but may be due to strain differences. This information has implications for use of the techniques adopted in this thesis for investigation into endoderm-mesoderm signalling in adult intestine following conditional alterations in gene expression (see Chapter 6 and Discussion).

5. Investigating the interaction of the epithelial and mesodermal layers of the gut in *Cdx2* mutant mice using *in-situ* techniques

5.1 Introduction

The aberrant expression of stomach mesoderm-specific *Barx1* in *Cdx2*$^{+/-}$ embryonic caecum detected by PCR has been suggested in Chapter 4. The purpose of this chapter was to use *in-situ* techniques to confirm that the mesoderm was responding to overlying stomach-specific signals and indicate the exact nature of this expression in relation to stomach-endoderm specific *Sox2* expression.

5.1.1 Role of Barx1 in the odontogenic code

Barx1 has been shown to be fundamental in the patterning of the jaw. This involves a highly complex interaction between the endoderm and mesoderm, resulting in regionalisation of gene expression. The role of Barx1 in the odontogenic code is discussed here because developmental signalling pathways tend to be frugal; the functions and pathways involving Barx1 in jaw development may be conserved more distally in the foregut. The odontogenic code results in regionalisation of *Barx1* expression and function; a similar regionalisation may occur in the gastric heterotopias.

Teeth develop from specialised thickenings, at 11dpc in the mouse. These thickenings occur in the upper and lower jaw epithelium and adjacent mesenchyme (papilla and follicle). The epithelium invaginates into the mesenchyme which consequently condenses around it. This leads to the formation of the tooth bud at 13.5dpc. The epithelium then extends further into the mesenchyme, wrapping itself around the condensed region to form a cap by 14.5dpc. By 16dpc this has formed into a bell-shaped tooth germ that will eventually completely enclose the condensed mesenchyme by 18dpc. Cytodifferentiation occurs at the bell stage (see Figure 5.1). The enamel knot, developing at the tip of the bud is thought to act as a ‘signalling centre’ to control this process (reviewed in Tucker and Sharpe, 2004). The type of murine tooth that will develop varies dependent upon the position along the jaw; monocuspid incisors form proximally and multicuspid molars form distally.

Figure 5.1 A schematic representation of tooth development. An epithelial thickening occurs in the future mandible at 11.5dpc, marking the site of tooth development. By 13.5dpc the dental mesenchyme has condensed resulting in a tooth bud, followed by a cap structure a day later. At 18.5dpc, cytodifferentiation has occurred in the bell-like structure, resulting in a fully formed tooth by day 35 post-partum (P35). (Adapted from Tucker and Sharpe, 2004).

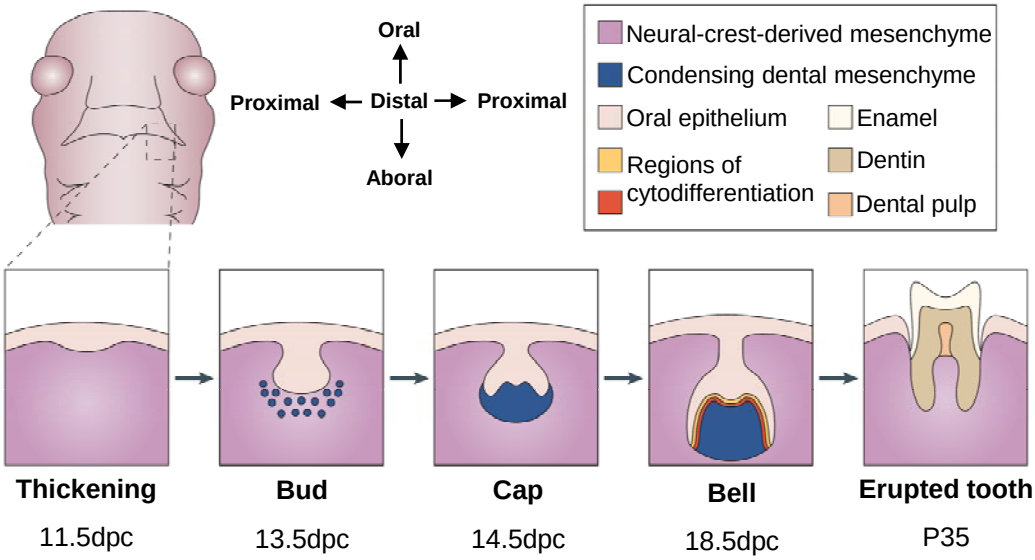

Barx1 expression is detected in the jaws of the mouse during development. Faint expression is first seen at 9.5dpc in the jaw primordia region. By 11.5dpc this expression becomes much stronger in the proximal region of the mesoderm of the mandibular process and is never detected in the distal region (the front of the future jaw) (Kim et al., 2005, Tissier-Seta et al., 1995). The mesenchyme surrounding the dental lamina of the first upper and lower molars generally expresses *Barx1* at 12dpc. By 13.5dpc this label condenses to strong expression in the future dental papilla and follicle and remains less specific in the surrounding mesenchyme. Expression of *Barx1*, by 16.5dpc, is confined to the papilla of the molars and is absent from the rest of the head at this stage (Tissier-Seta et al., 1995). The epithelium never expresses *Barx1*, nor does the distal jaw region that will develop into incisors (Tissier-Seta et al., 1995). Barx1 is only expressed in the region of the developing molars.

Correct development of the teeth is dependent upon proximal-distal gene expression patterns in the jaw. The epithelial expression of *Fgf8* in the proximal region of the jaw allows expression of mesenchymal *Barx1* and distal-less homeobox genes (*Dlx1* and *Dlx2*). *Bmp4* expression in the distal region of the epithelium represses *Barx1* expression, while allowing expression of other mesenchymal genes such as msh-like homeobox genes (*Msx1* and *Msx2*) (Tucker et al., 1998). Bmp4 activity was repressed via Noggin implants, leading to ectopic expression of *Barx1* in presumptive incisor mesenchyme. This caused the development of molar-like teeth instead of incisors (Tucker et al., 1998). *Barx1* is therefore instrumental in the development of multicuspid teeth. The mesenchyme is responsive to such epithelial signals until 10.5dpc. The response of the mesenchyme varies between the upper (maxillary) and lower (mandibular) jaws possibly due to expression of different *Dlx* genes in the two regions. The cause of this difference is unknown, but the mesenchyme of the two jaws is thought to be fundamentally different because the overlying epithelial layers appear to be functionally interchangeable between the jaws (Ferguson et al., 2000).

Within proximal-distal regions, gene expression varies in the oral-aboral direction. This is thought to occur in part due to the progressive loss of ability of the mesenchyme to respond to epithelial signals. Within the distal regions, the most

aboral area loses this ability first and so is able to express genes normally repressed by Fgf8. The tooth-forming oral domain (gingiva) therefore expresses LIM homeobox (*Lhx*) genes while the lower aboral domain (alveolar process) is positive for Goosecoid (*Gsc*), normally repressed by Fgf8. These domains are defined by the proximal-distal gene expression pattern that is already determined (Tucker et al., 1999). These expression patterns 'build-up' to form an extremely complex orthodontic code (see Figure 5.2). Within this code, the tooth buds will become initiated. The teeth will develop into different shapes depending upon the combination of genes present along the jaw. The orthodontic code, within which *Barx1* is fundamentally involved, therefore controls the correct patterning, number and formation of teeth (reviewed in Tucker and Sharpe, 2004).

5.2 Aims

Expression of *Barx1* had been identified in the *Cdx2* mutant intestine using RT-PCR but its precise location was unknown. Alongside the RT-PCR study, the use of *in-situ* techniques was used. The reason for using this technique was to identify expression of a stomach-mesoderm specific gene in relation to endodermal *Sox2* expression and an absence of Cdx2 protein. This would unequivocally confirm that the mesoderm directly underlying the stomach-type epithelium is receiving and responding to signals in order to express stomach mesoderm-specific genes. The aims of this chapter were therefore to identify a gene suitable for these techniques and to investigate whether this gene co-localised with *Sox2* expression and absence of Cdx2 in the endoderm.

5.3 Results

5.3.1 Identifying a Barx1 plasmid suitable for RNA probe templates

A plasmid was required that contained a region of the DNA sequence of *Barx1*. This would confirm the findings from Chapter 4 and also provide insight into the location of expression in relation to *Sox2*.

The *Barx1* plasmid (pBS-Barx1) was obtained from Prof. P. Sharpe (Craniofacial Department, King's College London, UK). The *Barx1* antisense RNA probe was generated by linearisation of the plasmid with *EcoR* I (Figure 5.3A) followed by

Figure 5.2 The odontogenic code. The various genes involved in the orthodontic code are expressed in specific regions. These regions are defined by upstream genetic regulation leading to a highly complex pattern of gene expression. Tooth buds form in response to the orthodontic code. The type of tooth that will form (in the mouse these are incisors or molars) is specified by the genetic code present at the position along the jaw. (Adapted from Tucker and Sharp, 2004).

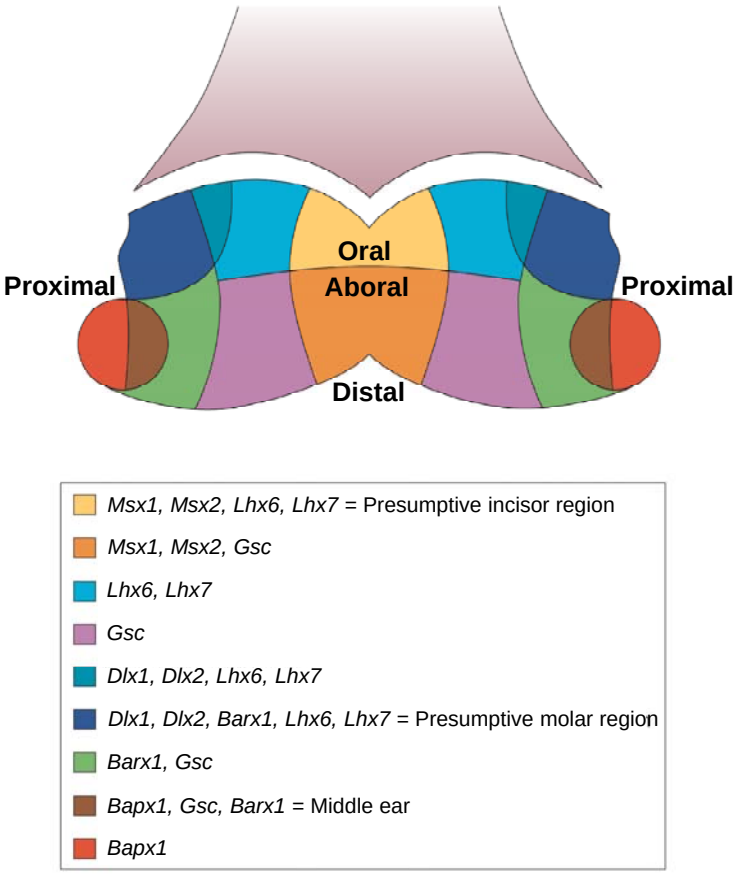

Figure 5.3 Alternative restriction enzyme and polymerase binding sites in pBS-Barx1. The plasmid (A) was linearised with restriction enzymes to create the antisense or sense probe. (B) Generation of the antisense probe. The plasmid was linearised with *EcoR* I and the antisense probe generated with T7 polymerase. (B) Generation of the control sense probe. The probe was transcribed using T3 polymerase following linearisation of the plasmid with *Not* I.

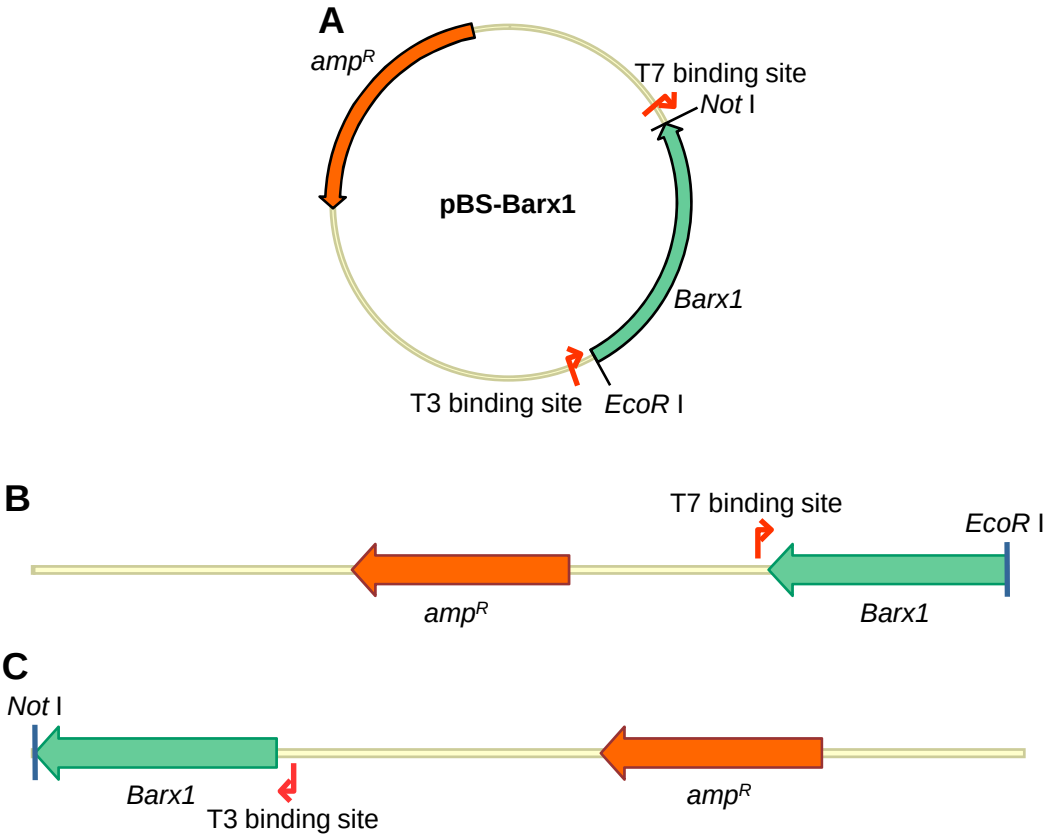

transcription using T7 polymerase (Figure 5.3B). The sense probe was generated following linearisation with *Not* I and transcription using T3 polymerase (Figure 5.3C).

5.3.2 Confirming pBS-Barx1 suitability for detecting stomach mesoderm using in-situ techniques

Whole mount *in-situ* hybridisation using *Barx1* sense and antisense DIG-labelled probes was performed upon WT 14.5dpc embryonic gut. The use of the antisense probe confirmed that *Barx1* expression is limited to the mesoderm of the stomach and is completely absent in the intestine (Figure 5.4). The development of colour was monitored and indicated that *Barx1* expression is strongest in the posterior region of the stomach (Figure 5.4B and C). A WT 14.5dpc stomach hybridised with the *Barx1* antisense probe was sectioned to confirm staining in the mesoderm (Figure 5.5).

5.3.3 Detecting ectopic Barx1 in Cdx2 mutant intestine using whole-mount in-situ techniques

Two 12.5dpc *Cdx2*$^{+/-}$ samples were hybridised with the *Barx1* antisense DIG-labelled RNA probe. The stomach showed extremely strong *Barx1* expression while the oesophagus and intestine, as expected, did not (Figure 5.6 and data not shown). Both samples contained small ectopic regions of *Barx1* expression in the intestine but these were too small to be successfully photographed. The same probe was used on 14.5dpc *Cdx2*$^{+/-}$ gut and all three samples indicated regions of *Barx1* expression in the intestine (Figures 5.7, 5.8 and 5.9). The majority of the *Barx1* positive regions were found in the distal small intestine and caecum and appeared to be mesodermal. Only one 16.5dpc *Cdx2*$^{+/-}$ sample was investigated. It was found to contain a single region of *Barx1* expression in the small intestine following hybridisation with the *Barx1* antisense probe, although this region was extremely faint probably because the tissue is too dense at this stage for complete probe penetration (Figure 5.10). For this reason, no further tissue was investigated at later stages.

Similar results were obtained in *Cdx2*$^{-/-}$//WT samples. Again, the 12.5dpc samples both contained *Barx1*-expressing regions that were too small to photograph successfully. One 14.5dpc chimeric sample contained a very strong region of *Barx1*

Figure 5.4 14.5dpc WT gut hybridised with *Barx1* antisense probe. (A) The entire WT 14.5dpc gut following overnight colour incubation. The WT intestine and oesophagus had no *Barx1* expression. (B) The stomach 4 hr after incubation in the chromogenic probe. The posterior region developed a coloured signal first while the anterior region (*) did not express *Barx1*. (C) The same sample after incubation overnight. *Barx1* expression was detected throughout the stomach mesoderm but it remained strongest in the posterior region. When the regions indicated in (B) and (C) are expanded on the right, it can be seen that the colour is developing in the mesoderm of the stomach. Scale bars = 2mm.

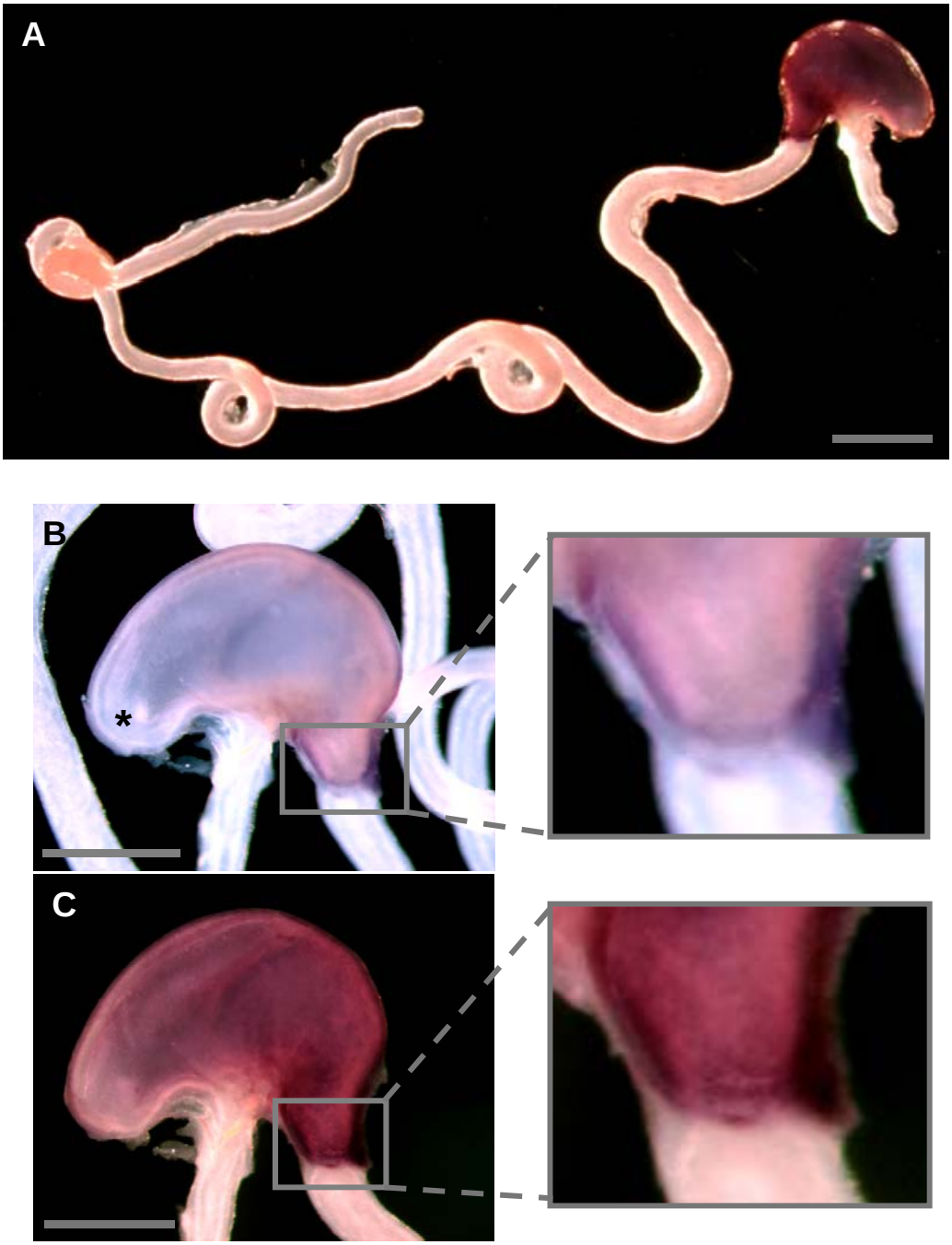

Figure 5.5 14.5dpc WT gut hybridised with *Barx1* antisense probe. Following the development of a coloured signal, the tissue was embedded in wax and sectioned at 8 µm. The outer mesoderm is stained strongly for *Barx1* expression; the tissue was thought to be too dense for the probe to penetrate the inner mesodermal layers. *Barx1* is not expressed in the endoderm. Scale bar = 200µm.

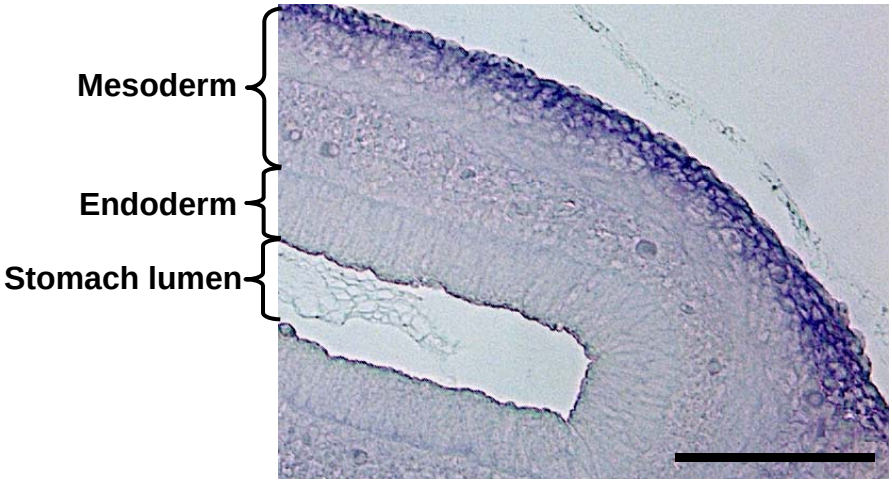

Figure 5.6 12.5dpc *Cdx2*$^{+/-}$ stomach hybridised with *Barx1* antisense probe. The stomach mesoderm expresses *Barx1* strongly. There were also small regions of *Barx1* expression in the intestine; there were too small to successfully photograph. The dotted line indicates the outline of the stomach against the background. Scale bar = 500µm.

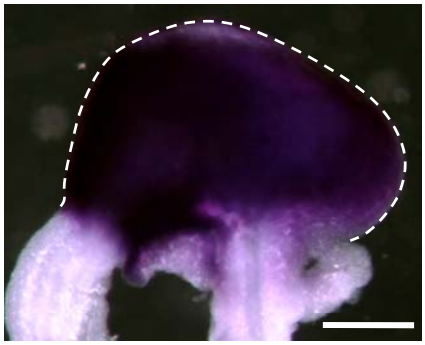

Figure 5.7 14.5dpc *Cdx2*$^{+/-}$ gut hybridised with *Barx1* probe. (A) WT stomach hybridised with *Barx1* sense probe as a control. (B) *Cdx2*$^{+/-}$ stomach hybridised with the antisense probe. The stomach mesoderm expresses *Barx1* strongly, as expected. (C) The intestine of the *Cdx2*$^{+/-}$ sample. Ectopic regions of *Barx1* expression can seen in the distal small intestine and the caecum (indicated by arrows). Scale bars = 1mm.

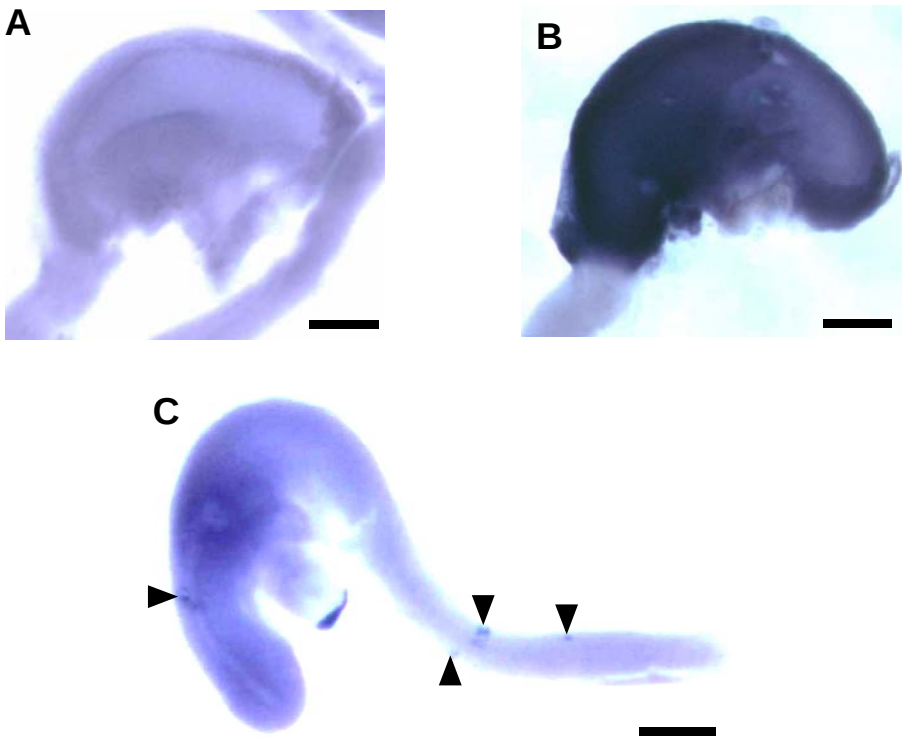

Figure 5.8 14.5dpc *Cdx2*$^{+/-}$ gut hybridised with *Barx1* DIG-labelled RNA probes. (A) WT 14.5dpc gut hybridised with *Barx1* sense DIG-labelled RNA probe. (B) *Cdx2*$^{+/-}$ stomach labelled with *Barx1* antisense DIG-labelled RNA probe; the stomach expresses *Barx1* strongly; the intestine and oesophagus do not. (C) The future jejunum of the *Cdx2*$^{+/-}$ sample. A region of *Barx1* expression is detected, indicated by an arrow. (D) The caecum of the same sample. Three regions of *Barx1* expression are detected, indicated by arrows. (E) The duodenum and distal small intestine of the *Cdx2*$^{+/-}$ sample. Three regions of *Barx1* expression are detected, indicated by arrows. (F) WT 14.5dpc gut hybridised with *Barx1* antisense probe. There are no regions of ectopic *Barx1* expression in this control sample. The caecum of the sample is focussed upon as this was the region in *Cdx2* mutant mice normally found to contain ectopic areas of *Barx1* expression. (N.B: (A) is the same image as that shown in figure 5.11A because both experiments were performed at the same time and so a single control was used). Scale bars = 1mm in all panels.

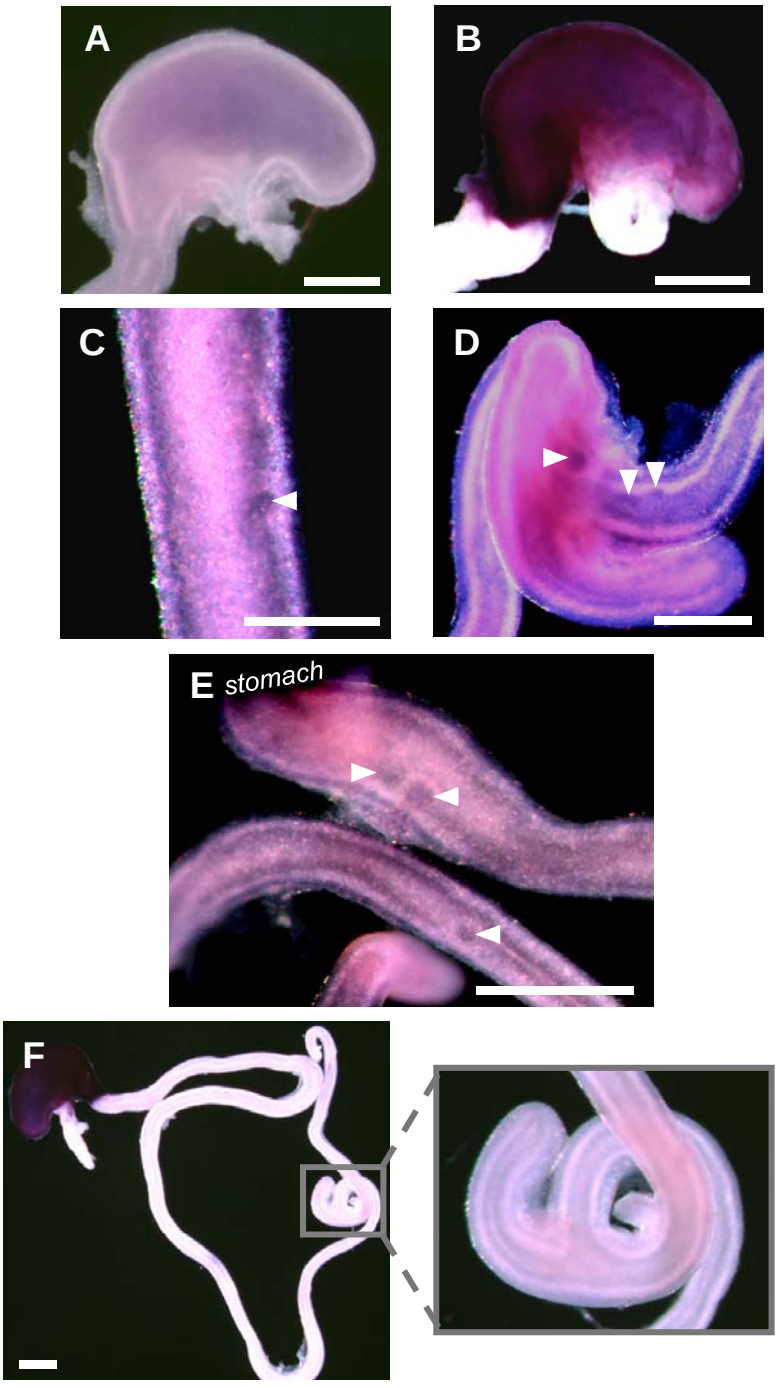

Figure 5.9 14.5dpc *Cdx2*$^{+/-}$ gut hybridised with *Barx1* DIG-labelled RNA probe. (A) WT 14.5dpc gut hybridised with *Barx1* sense DIG-labelled RNA probe. (B) *Cdx2*$^{+/-}$ stomach labelled with *Barx1* antisense DIG-labelled RNA probe. The stomach strongly expresses *Barx1,* the intestine does not. The oesophagus was lost during dissection but the remnants did not express *Barx1*. (C) The distal midgut and caecum of the *Cdx2*$^{+/-}$ sample. Four regions of ectopic *Barx1* expression are detected although they are very faint, indicated by arrows. Scale bars = 500µm.

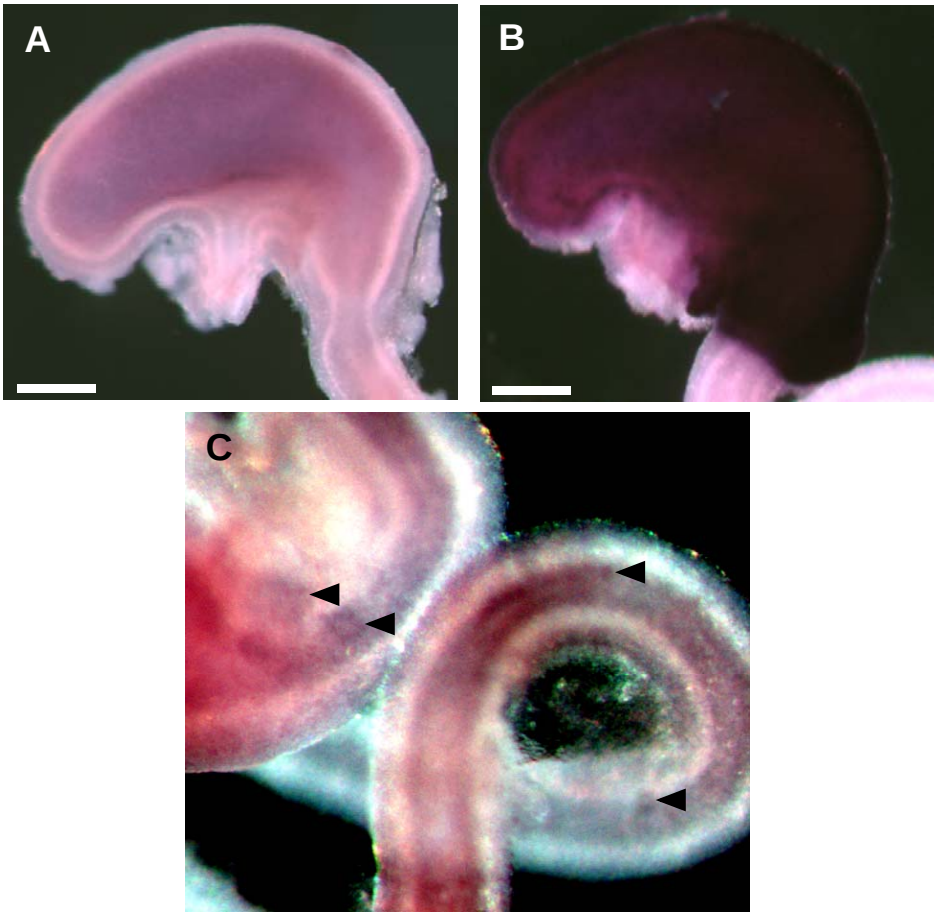

Figure 5.10 16.5dpc gut hybridised with *Barx1* DIG-labelled RNA probes. (A) WT 16.5dpc stomach hybridised with *Barx1* sense DIG-labelled RNA probe. (B) *Cdx2*$^{+/-}$ stomach labelled with *Barx1* antisense DIG-labelled RNA probe. The stomach expresses *Barx1* strongly*;* the intestine and oesophagus do not. (C) The midgut region of the *Cdx2*$^{+/-}$ sample, indicating one region of faint *Barx1* expression (indicated by arrow). (D) WT 16.5dpc gut hybridised with *Barx1* antisense probe; the intestine does not contain any regions of *Barx1* expression. (E) The caecum of the sample in (D) is expanded to emphasise absence of ectopic *Barx1* in WT gut. (N.B: figure (A) is the same image as that used in 5.13A because both experiments were performed at the same time and so a single control was used). Scale bars = 1mm unless otherwise stated.

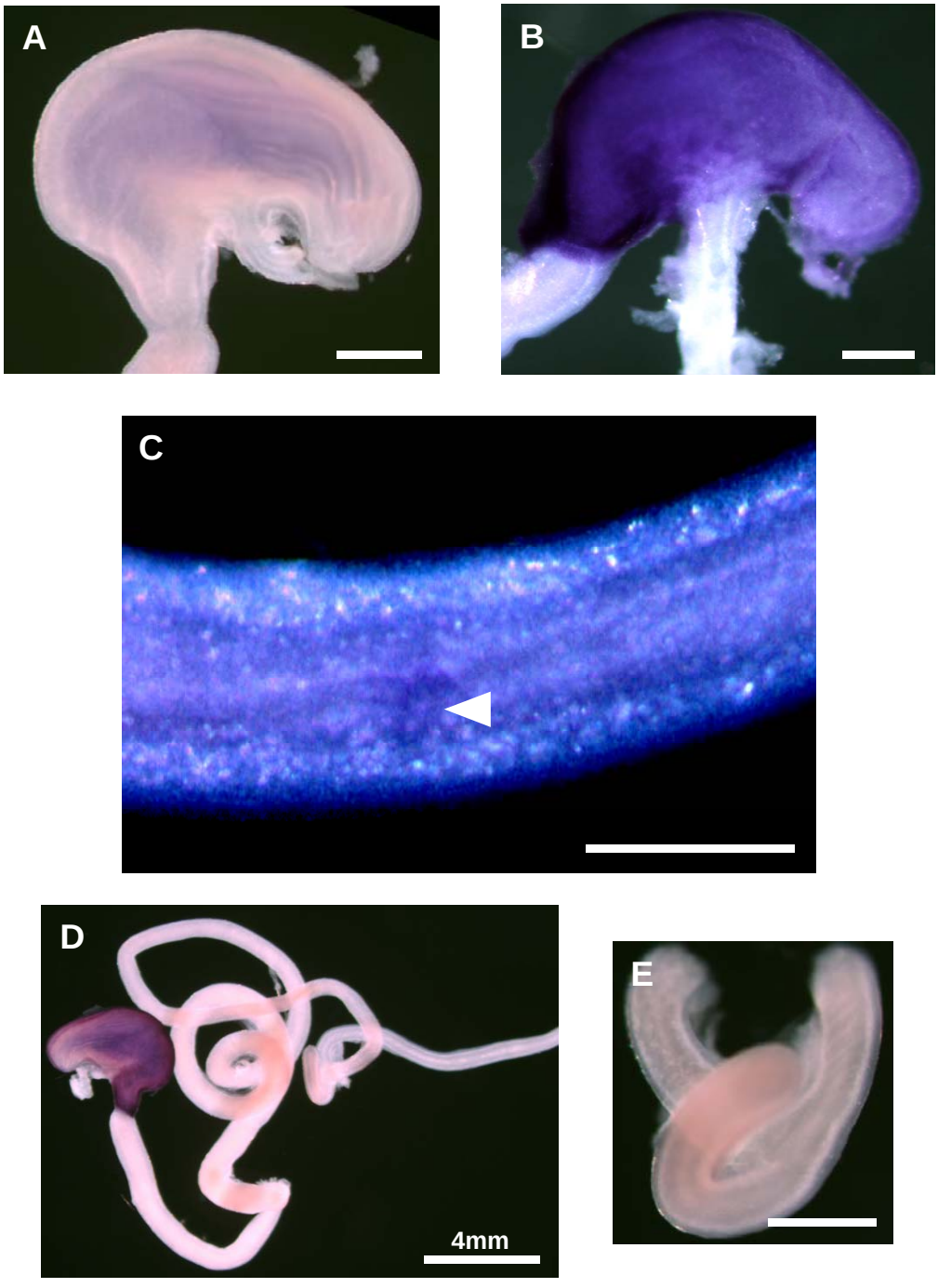

expression in the duodenum (Figure 5.11), but another sample did not contain any ectopic regions of *Barx1* expression (data not shown).

The large region of strong expression in the 14.5dpc chimeric sample was excised out and sectioned in order to investigate regional expression further. This was stained with nuclear fast red and photographed (Figure 5.12). This confirmed that the region of *Barx1* expression is confined to the mesoderm. A 16.5dpc chimeric sample also contained a faint region of expression (Figure 5.13).

5.3.4 Co-localising Sox2 and Barx1 in the Cdx2 mutant intestine

The ectopic expression of *Barx1* and *Sox2* in the *Cdx2* mutant gut had to be co-localised to confirm that the expression of *Barx1* was directly underlying that of *Sox2*. Ideally, the expression of both genes would be investigated on the same tissue section. One approach would have been to detect the nascent heterotopic lesions using whole mount *in-situ* hybridisation for *Sox2* then section these regions to investigate expression of *Barx1*. One problem with this approach was that the regions detected by whole mount *in-situ* hybridisation were very small and the purple stain was generally not strong enough to visualise following sectioning. Another approach would have been to use dual labels on a single section, i.e. each RNA probe could be detected with a different chromogenic probe (co-labelling). On this basis, *in-situ* hybridisation on stomach sections using a DIG-labelled RNA probe was attempted (using a protocol by N. Pringle, Richardson Lab, Wolfson Institute for Biomedical Research, London). However, despite numerous attempts and various adjustments, this technique did not work for unknown reasons.

S^{35} radiolabelled *Barx1* and *Sox2* antisense probes were, however, successfully hybridised to and detected on serial sections of *Cdx2* mutant caecum. Stomach from the same sample was sectioned and used as a control for both the antisense and sense probes (Figure 5.14). This approach was limited as co-localisation upon single sections was not possible and so serial sections had to be used.

Co-localisation of *Barx1* and *Sox2* was observed in some *Cdx2* mutant caecums but not others; some samples indicated no expression of either gene, others only

Figure 5.11 *Barx1* labelling of 14.5dpc *Cdx2*$^{-/-}$//WT chimeric embryonic gut. (A) WT gut hybridised with *Barx1* sense control probe. (B) *Cdx2*$^{-/-}$//WT 14.5dpc gut labelled with *Barx1* antisense probe. The chimeric sample shows one region of *Barx1* labelling in a thickened area midway along the small intestine indicated by a box. (C) An expansion of image (B) indicated by the grey box. (N.B: (A) is the same image as that used in figure 5.8A because both experiments were performed at the same time and so a single control was used). Scale bars = 500µm.

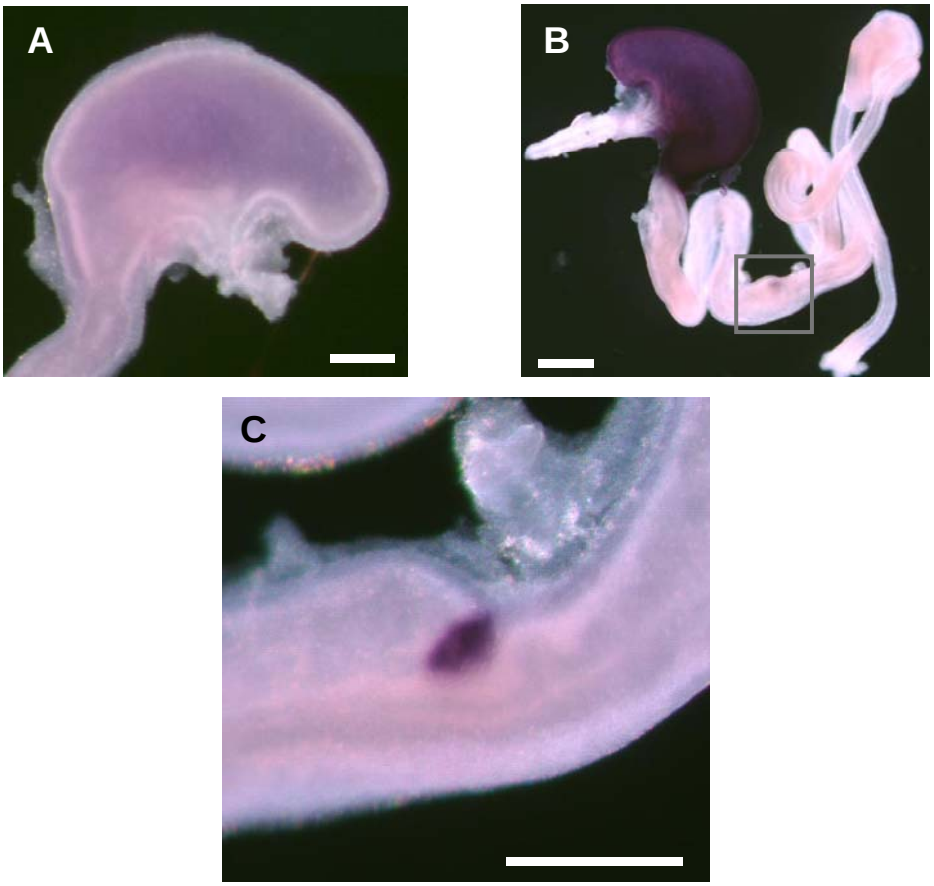

Figure 5.12 Sections of ectopic *Barx1*-expressing region. The region of *Barx1* expression shown in figure 5.11 was substantial enough to be sectioned at 7µm and stained with Nuclear Fast Red (A) or haematoxylin and eosin (B). The region of *Barx1* expression can be seen and is indicated by the grey box; it is confined to the mesoderm. Scale bars = 100µm.

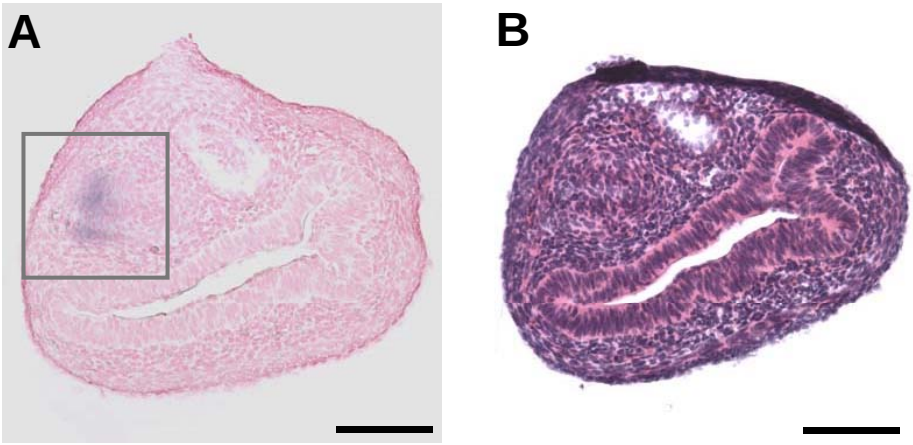

Figure 5.13 16.5dpc *Cdx2*$^{-/-}$//WT gut hybridised with *Barx1* DIG-labelled RNA probes. (A) WT 16.5dpc stomach hybridised with *Barx1* DIG-labelled sense probe. (B) *Cdx2*$^{-/-}$ //WT stomach hybridised with *Barx1* DIG-labelled antisense probe. The stomach strongly expresses *Barx1*, the intestine and remnants of the oesophagus do not. (C) The future jejunum of the same sample. A faint region of ectopic *Barx1* expression can be detected, indicated by an arrow. (N.B: figure (A) is the same image as that used in 5.10A because both experiments were performed at the same time and so a single control was used). Scale bars = 1mm.

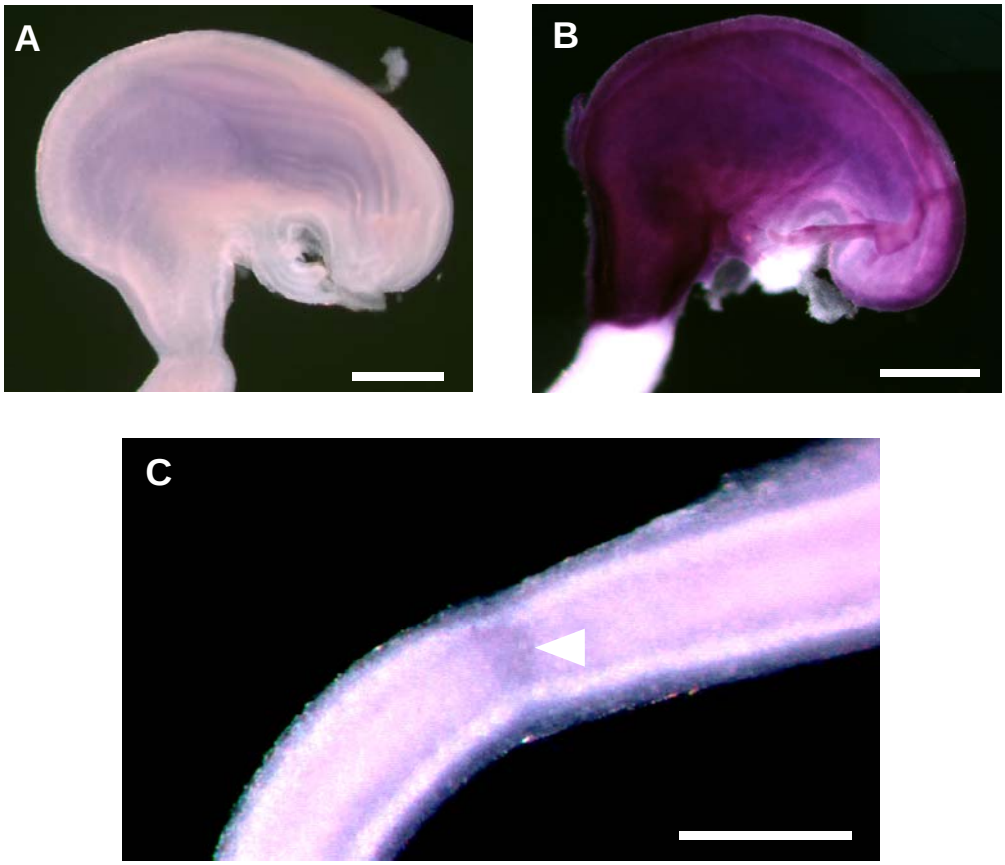

Figure 5.14 Serial sections of 18.5dpc stomach hybridised with radiolabelled probes as a control. (A-D) Serial sections of stomach indicating hybridisation of *Barx1* and *Sox2* sense and antisense probes. The sections were visualised with both brightfield (top panels) and darkfield (bottom panels) microscopy. Scale bars = 100µm.

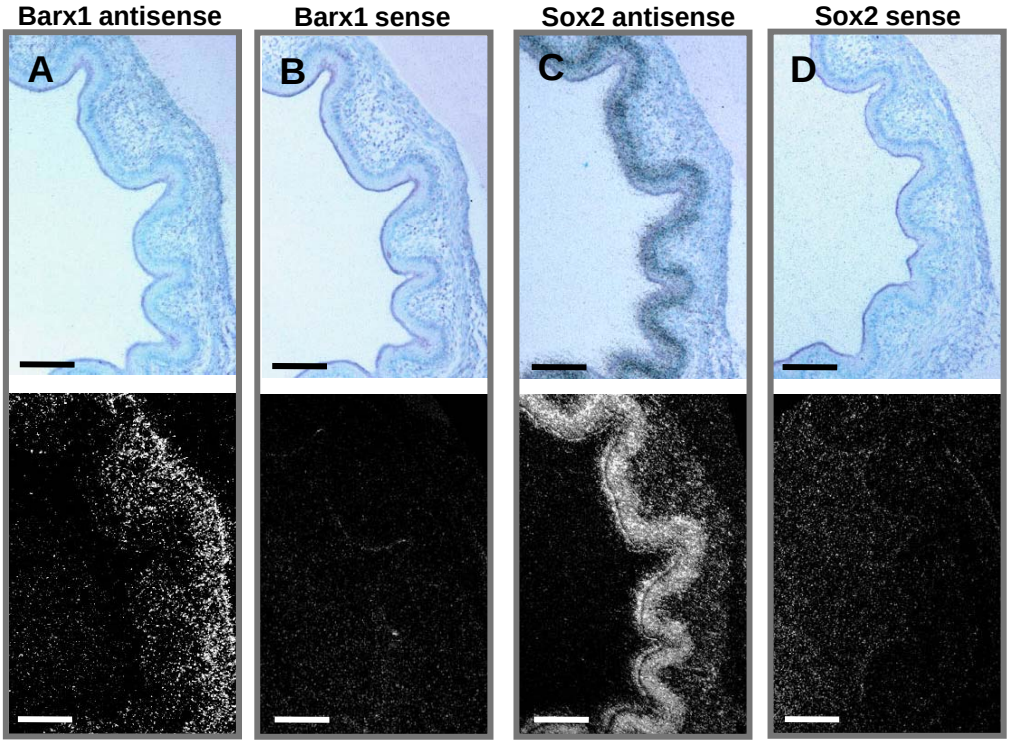

expressed *Sox2*. The expression of *Sox2* and *Barx1* in a 14.5dpc *Cdx2*$^{+/-}$ caecum was investigated first. The caecum indicated a region of *Sox2* expression that was strictly confined to the endoderm. This was demonstrated on two sections but *Barx1* expression could not be detected on the flanked serial section (Figure 5.15). The same result was also found in an 18.5dpc *Cdx2*$^{+/-}$ caecum (Figure 5.16). This technique was also performed on another two 14.5dpc *Cdx2*$^{+/-}$ caecum samples but no regions of *Sox2* or *Barx1* expression were detected.

Co-localisation was found in a 16.5dpc *Cdx2*$^{+/-}$ sample. Again, the stomach was successfully used as a control for the sense and antisense probes, producing results similar to those shown in Figure 5.14. Two caecum sections demonstrating endodermal expression of *Sox2* flanked a serial section demonstrating *Barx1* expression. The region expressing *Barx1* was extremely small but it was located in the mesoderm underlying the ectopic *Sox2* expression (Figure 5.17).

Co-localisation of *Sox2* and *Barx1* was also investigated in *Cdx2*$^{-/-}$//WT caecum. An 18.5dpc caecum failed to show any *Sox2* or *Barx1* expressing regions but co-localisation was demonstrated in a 14.5dpc *Cdx2*$^{-/-}$//WT caecum (Figure 5.18, 5.19 and 5.20). This sample was fixed in methacarn and so the sections were also suitable for immunohistochemistry with the Cdx2 antibody. The caecum demonstrated numerous regions of endodermal *Sox2* expression, many of which had adjacent regions of mesodermal *Barx1* expression. When a serial section was incubated with the Cdx2 antibody in immunohistochemistry (Figure 5.19C), all the endoderm absent for Cdx2 protein was expressing *Sox2,* while endoderm not expressing *Sox2* contained Cdx2 protein (Figure 5.19B compared with 5.19C).

5.4 Conclusion

The RT-PCR performed in Chapter 4 demonstrated the suitability of *Barx1* for *in-situ* hybridisation experiments. Although *Barx1* is most strongly expressed in the distal stomach, the development of a coloured signal rapidly becomes extremely strong and ubiquitous in the stomach mesoderm following hybridisation of a DIG-labelled *Barx1* RNA probe. This, combined with the fact that *Barx1* is expressed in the

Figure 5.15 Radiolabelled serial sections of 14.5dpc *Cdx2*$^{+/-}$ gut. (A) Serial section 20 of the caecum hybridised with *Sox2* antisense probe. A *Sox2* expressing region of endoderm can be seen, indicated by a box; an expanded view of this can be seen to the right. (B) Serial section 25 hybridised with *Barx1* antisense probe. There was no *Barx1* expression in the region expressing *Sox2*. (C) Serial section 27 hybridised with *Sox2* antisense probe. The same region as that in section 20 was still expressing *Sox2* and so section 25 definitely contained a heterotopic region that did not express *Barx1*. The arrowhead provides orientation in the serial sections. All scale bars are 100µm.

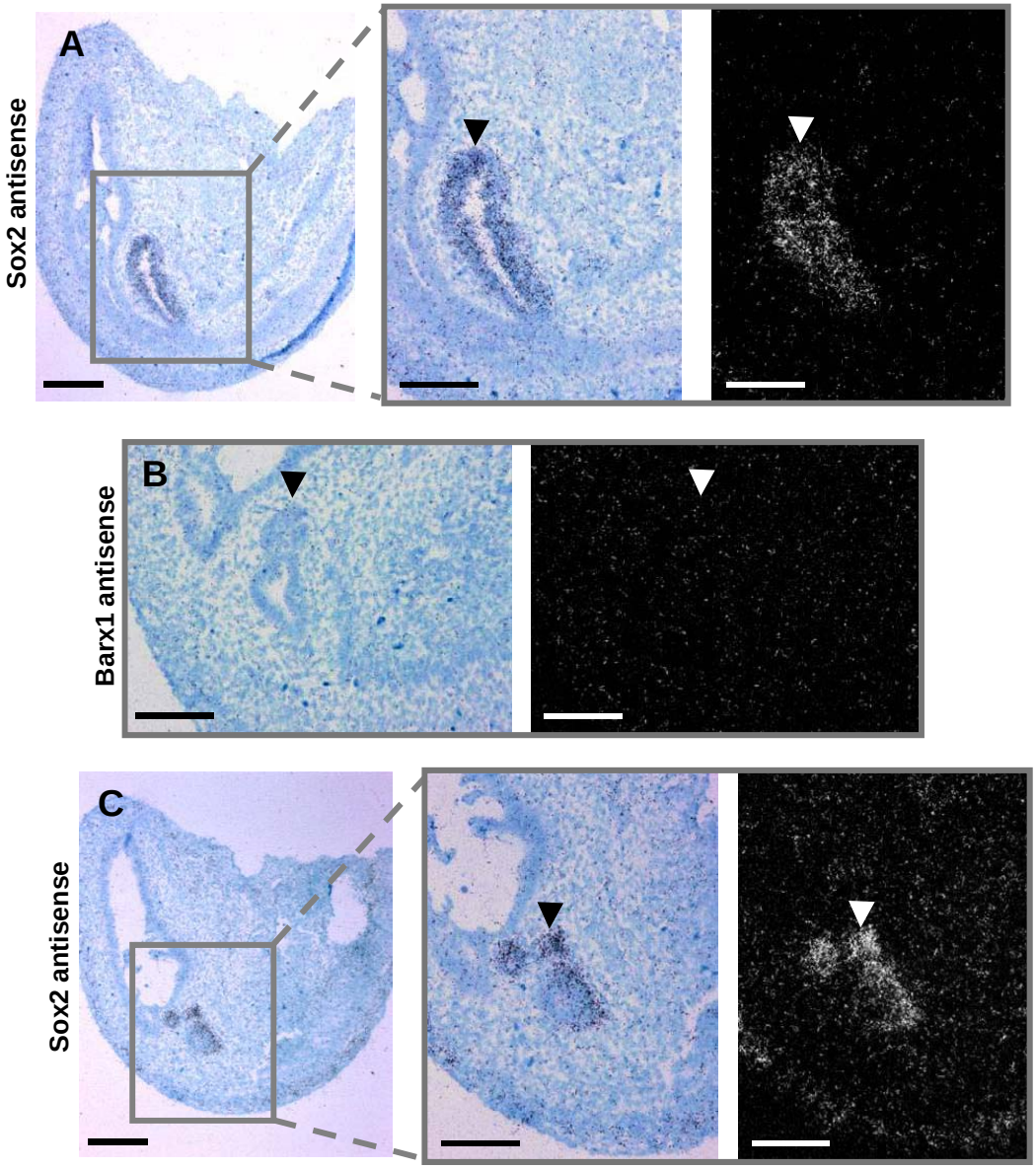

Figure 5.16 Serial sections of 18.5dpc *Cdx2*$^{+/-}$ gut hybridised with radiolabelled probes. (A) Serial section 50 of the caecum hybridised with *Sox2* antisense probe. A *Sox2* expressing region of endoderm can be seen, indicated by a box; an expanded view of this can be seen to the right. (B) Serial section 59 hybridised with *Barx1* antisense probe. There was no *Barx1* expression in the region expressing *Sox2*. (C) Serial section 60 hybridised with *Sox2* antisense probe. The same region as that in section 50 was still expressing *Sox2;* indicated by a box and expanded to the right. Section 59 therefore definitely contained a heterotopic lesion absent for *Barx1*. The arrowhead provides orientation in the serial sections. All scale bars are 100µm.

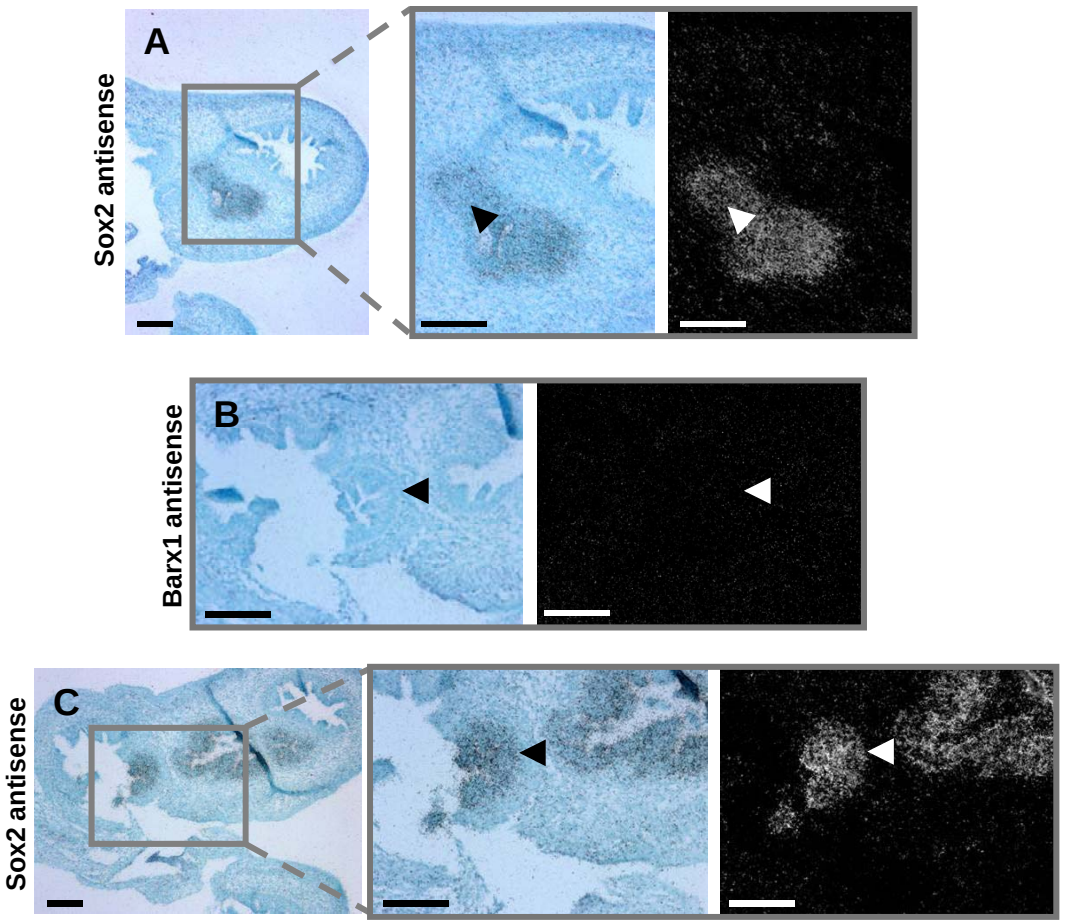

Figure 5.17 Serial sections of 16.5dpc *Cdx2*$^{+/-}$ gut hybridised with radiolabelled probes. (A) Serial section 102 of the caecum hybridised with *Sox2* antisense probe. A *Sox2* expressing region of endoderm can be seen, indicated by a box; an expanded view is shown to the right. (B) Serial section 108 hybridised with *Barx1* antisense probe. There is a small region of mesodermal *Barx1* expression in the region underlying *Sox2* expression, in line with the arrowhead. (C) Serial section 109 hybridised with *Sox2* antisense probe. The same region as that in section 50 was still expressing *Sox2* and so section 108 definitely contained a heterotopic region. Subsequent sections did not demonstrate *Barx1* expression. The arrowhead provides orientation in the serial sections. All scale bars are 100µm.

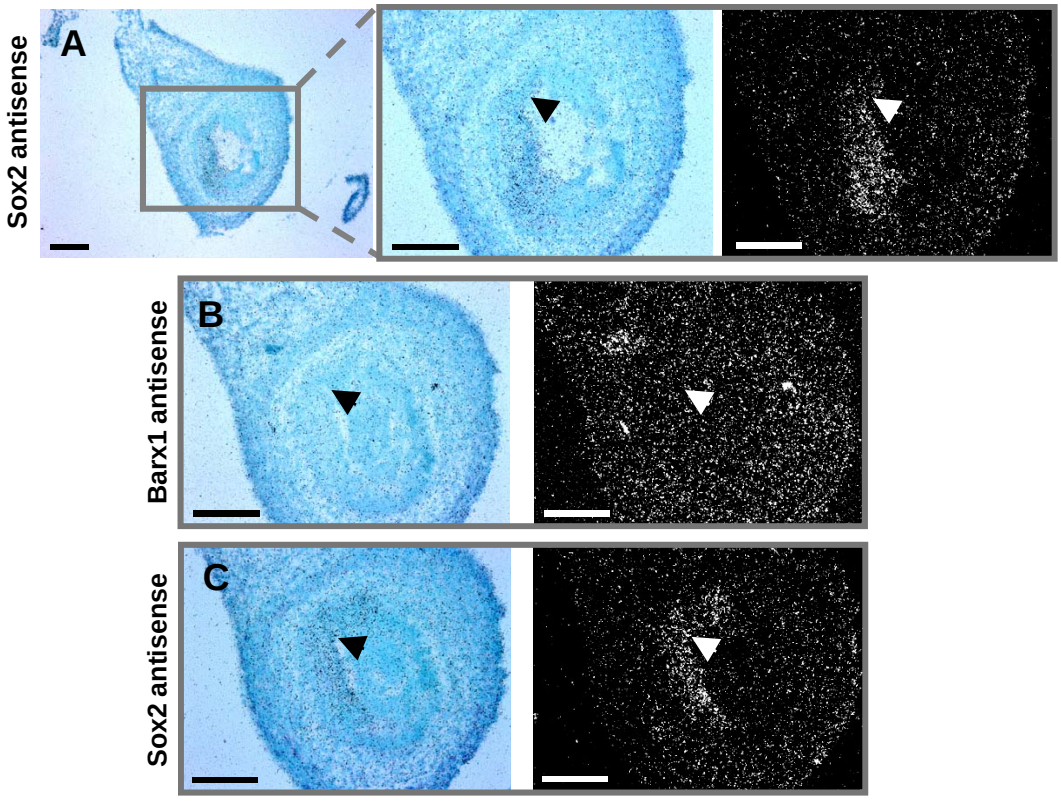

Figure 5.18 Serial sections of 14.5dpc *Cdx2*$^{-/-}$/WT gut hybridised with radiolabelled probes. (A) Serial section 27 of the caecum hybridised with *Barx1* antisense probe indicated a region of expression in line with the arrowhead. Another region of expression that may have been present is indicated by the box. (B) Serial section 28 contains a *Sox2* expressing region in the endoderm overlying the region of *Barx1* expression, in line with the arrowhead. Another region of *Sox2* expression possibly corresponds with the second possible region of *Barx1* expression indicated in section 27. (N.B; figure 5.18, 5.19 and 5.20 are the same experiment, separated to make reference easier). All scale bars are 100µm.

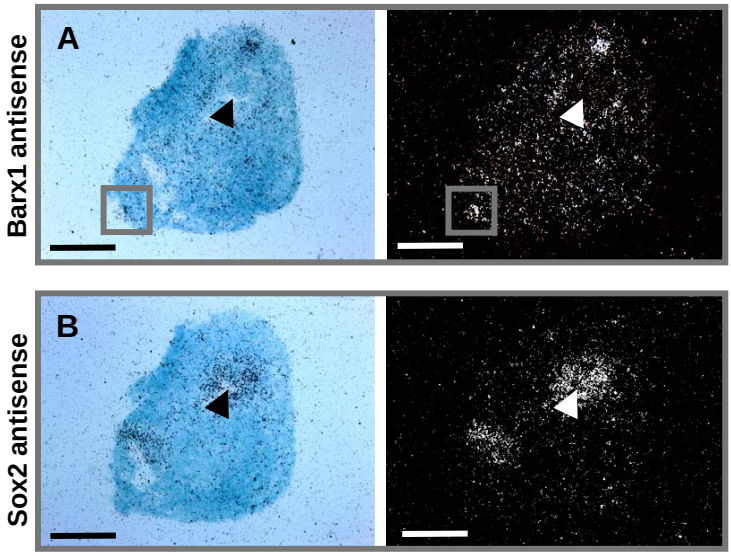

Figure 5.19 Serial sections of 14.5dpc *Cdx2*$^{-/-}$//WT caecum hybridised with radiolabelled probes. (A) Serial section 60 hybridised with *Barx1* antisense probe. There are two regions of *Barx1* expression indicated by arrowheads; these underlie regions of *Sox2* expression shown in (B). (B) Serial section 61 hybridised with *Sox2* antisense probe. Multiple regions of endoderm are expressing *Sox2*, but not all. (C) Section 63 stained with Cdx2 antibody. The regions expressing *Sox2* in (B) were absent for Cdx2 and vice versa. This section can be compared to all other sections with reference to the arrowheads. (D) Serial section 65 of the caecum hybridised with *Barx1* antisense probe. A region of *Barx1* expression can be seen. (E) Serial section 66 contained various regions of endodermal *Sox2* expression. The arrows provide orientation and reference between sections. (N.B; figures 5.18, 5.19 and 5.20 are the same experiment). Scale bars = 200µm.

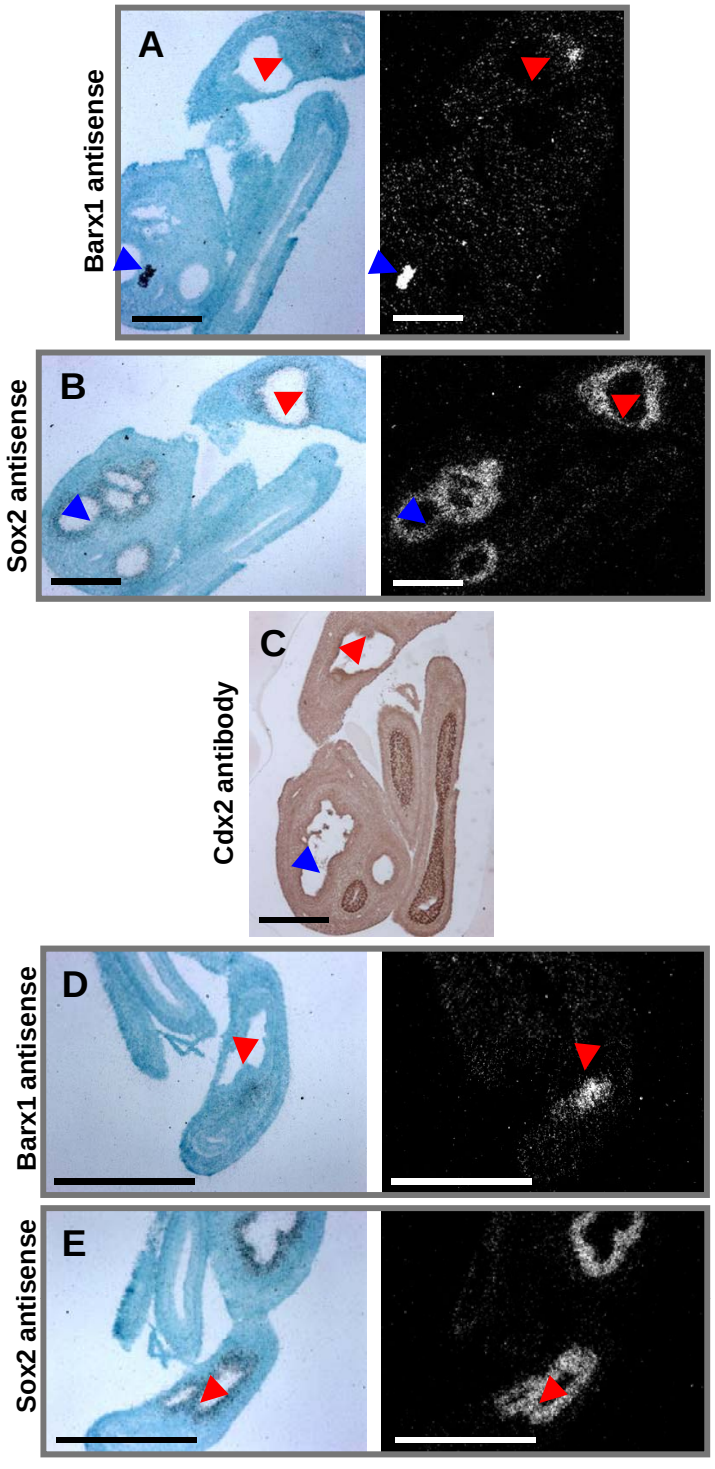

Figure 5.20 Serial sections of 14.5dpc *Cdx2*$^{-/-}$//WT caecum hybridised with radiolabelled probes. (A) Serial section 80 and (C) serial section 85 hybridised with *Barx1* antisense probe. Two regions of expression are detected. (B) Serial section 81 and (D) serial section 86. Both were hybridised with *Sox2* antisense probe. One region of *Barx1* expression (highlighted by red box) does not initially appear to underlie *Sox2* expression. Subsequent serial sections, however, indicated that *Sox2* expression was present. (N.B; figures 5.18, 5.19 and 5. 20 are the same experiment). Scale bars = 200µm.

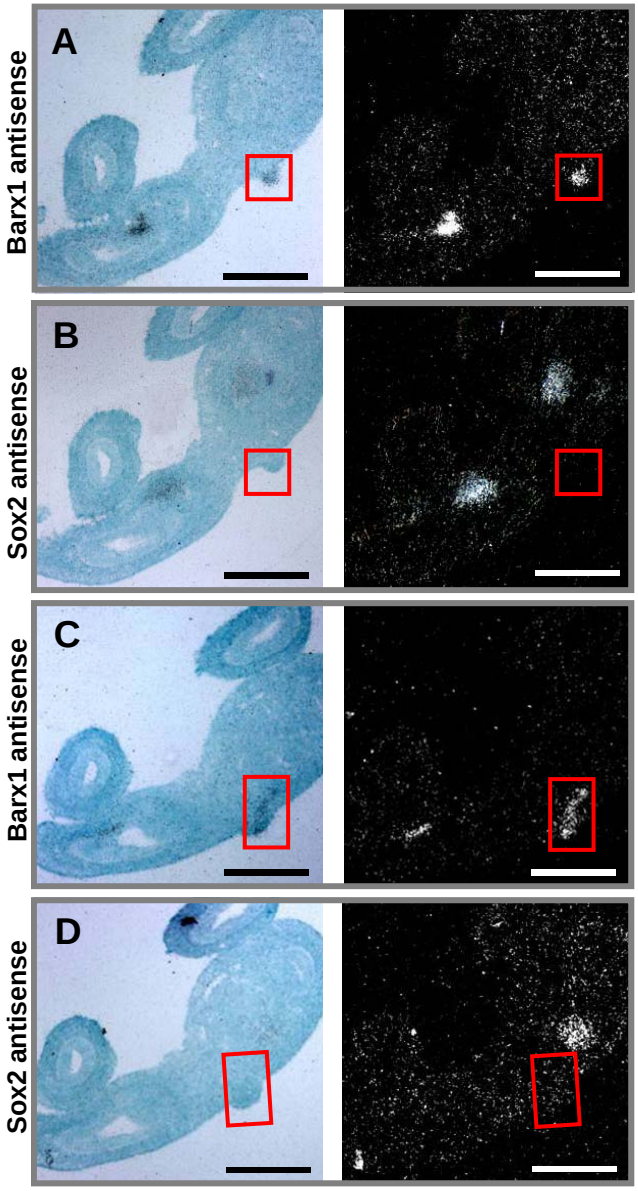

stomach from relatively early stages, confirms that the investigation of intestinal ectopic *Barx1* expression in *Cdx2* mutant embryos is the best approach at this stage.

The whole-mount examination of *Barx1* expression in the intestine of the *Cdx2*$^{+/-}$ embryos indicated that small regions of intestinal mesoderm were expressing stomach-mesoderm specific *Barx1*. The 12.5dpc samples were too small to be successfully photographed with the available equipment, but all samples investigated from 12.5dpc to 16.5dpc contained at least one region of *Barx1* expression. These areas were in a similar distribution and number to those shown with the *Sox2* DIG-labelled RNA probe; small discrete regions, generally focussed around the caecum and paracaecal area, with occasional regions found more proximally and distally. This suggested that the *Barx1* and *Sox2* regions were co-localising.

In the *Cdx2*$^{-/-}$//WT embryos, the distribution and number of lesions could not be compared to the heterozygous *Sox2* results because the position of the heterotopic regions in these mice was due to the position of engraftment of the *Cdx2*$^{-/-}$ cells and is therefore not comparable. A small number of samples did not appear to contain *Barx1* expressing regions in the intestine, possibly due to failure of engraftment in this organ. A number of samples however did demonstrate aberrant *Barx1* expression in the intestine. Again, the 12.5dpc samples were too small to photograph with the equipment available, but a faint region was found in the 16.5dpc *Cdx2*$^{-/-}$//WT sample. This region is thought to be faint because of the increasing density of the tissue that the probe must penetrate and the possible decrease in expression of *Barx1* by this developmental stage. A 14.5dpc *Cdx2*$^{-/-}$//WT sample, however, displayed a single region of extremely strong *Barx1* expression in the proximal midgut region. This area was sufficiently large to excise from the intestine and section transversely in order to confirm mesodermal *Barx1* expression.

The ectopic expression of *Barx1* and *Sox2* had to be co-localised in order to confirm that it is the mesoderm underlying the heterotopic lesions that is expressing stomach-specific *Barx1*. Ideally, the expression of the two genes would have been co-localised upon the same section. Co-labelled *in-situ* hybridisation with DIG-labelled *Barx1* and *Sox2* antisense probes was attempted on stomach sections but despite numerous

attempts and various adjustments, this technique did not work. The use of radiolabelled probes for the same purpose was already shown to be successful upon test samples. *In-situ* hybridisation using radiolabelled probes is also highly sensitive; this criterion is extremely important when the relative size of the heterotopias within the intestine is considered. The use of radiolabelled probes did however mean that serial sections had to be taken because dual expression could not be shown on the same section as that previously labelled by whole mount in-situ hybridisation with a DIG-labelled probe.

Two samples; a 16.5dpc *Cdx2*$^{+/-}$ caecum and a 14.5dpc *Cdx2*$^{-/-}$//WT caecum demonstrated co-localisation of ectopic *Sox2* and *Barx1* expression in conjunction with loss of Cdx2 protein in the *Cdx2*$^{-/-}$//WT sample. These samples consistently indicated that the region of *Barx1* expression lay under the *Sox2* expressing endoderm. Some regions of *Sox2* expression did not overly *Barx1* expressing mesoderm. There are two possible explanations for this. 1) One possibility is that *Barx1* expression is not always present underlying the heterotopias; this would explain the number of *Cdx2* mutant caecum samples that did not express *Barx1* following RT-PCR. 2) Very small regions of *Barx1* expression may have been missed in some samples. At present, it cannot be distinguished which of these is correct.

Sox2 expression in the normal stomach endoderm is ubiquitous at the developmental stages studied here. The ectopic gastric endoderm (assumed to express ubiquitous *Sox2)* is likely to be demonstrating regional expression of other genes due to tissue intercalation. The presence of *Barx1* only within small areas of the mesoderm underlying *Sox2* expression indicates that *Barx1* expression may be regional within the heterotopic lesion. The ectopic expression of *Barx1* is due to altered endodermal signals; regionalisation of this expression is likely to be due to regional development of gastric endodermal gene expression. *Barx1* is expressed most strongly in the posterior region of the stomach mesoderm and so it may be this area of the lesion that expresses detectable mesodermal *Barx1*.

It is postulated that during normal gut development a feedback control mechanism exists involving unknown factors. This is based on the fact that *Barx1*$^{-/-}$ mice

demonstrate an anterior shift of *Cdx2* expression (Kim et al., 2007b) and so Barx1 must normally repress this. Findings from this project indicate that a loss of Cdx2 protein in the endoderm of paracaecal regions leads to expression of mesodermal *Barx1.* Therefore this would suggest Cdx2 must normally repress *Barx1* expression. The role of Barx1 in regionalisation of the stomach may be similar to the role of Barx1 in creating the orthodontic code, as homeobox genes are known to display conserved functions at different sites in the developing embryo. This is supported by the finding that Bmp4 represses *Barx1* in the jaw (Tucker et al., 1998) and this appears to be reflected in the stomach; Bmp4 is found in the proximal region (Smith et al., 2000) while *Barx1* expression is strongest in the distal region of the stomach.

The limitations of this chapter are that only one stomach mesoderm-specific gene was investigated. Further studies of other stomach and intestine specific genes both endodermal and mesodermal would provide further insight into the signalling pathways that appear to be causing regional *Barx1* expression (or possibly no *Barx1* expression at all in some cases) in the mesoderm underlying the *Cdx2* gastric heterotopias.

Overall, however, this project has addressed the interactions of the endoderm and mesoderm in the intestine with respect to two fundamental genes; *Cdx2* and *Barx1*. Data from this project along with that from others (Kim et al., 2007b) has emphasised the mutual exclusivity of these two genes in the stomach and intestine. The controls involved in dictating these anterior-posterior regions of expression are little understood but are clearly crucial; FGF signalling has been suggested to be involved, as discussed in chapter 1 (Wells and Melton, 2000, Dessimoz et al., 2006). Previous work has shown that a loss of Cdx2 protein leads to gastric heterotopias within the midgut endoderm. With reference to the original aim of this project, the findings of this chapter lead to the conclusion that the mesoderm underlying the gastric heterotopic lesion, detected by *Sox2* expression, does respond to signals induced in the endoderm by a loss or haploinsufficiency of Cdx2. The mesoderm conforms to these signals by expressing a stomach-mesoderm specific gene, *Barx1*. This has been proven, even if *Barx1* expression is not consistent in all samples for reasons requiring further investigation. The inductive signal is received from the earliest

stages possible, prior to any differentiation of the tissue. This cross-talk and inductive behaviour of the endoderm has never been demonstrated at this level before.

6. Generation of a conditional *Cdx2* mouse line

6.1 Introduction

6.1.1 Evidence that intestinal stem cell potential becomes restricted postnatally

Previous observations suggested that *Cdx2*$^{+/-}$ mice do not develop heterotopias postnatally. An average of 1.67 heterotopias were found to develop in the paracaecal region of each *Cdx2*$^{+/-}$ mouse; this number did not increase with age (Figure 6.1) (Beck et al., 1999). There are two explanations for this observation. 1) The factors causing the loss of Cdx2 embryonically do not occur postnatally. 2) The intestinal stem cells lose potency postnatally and so do not respond to a loss of Cdx2. It is hypothesised that the second suggestion is correct. This is because it is thought that the loss of function of *Cdx2* is caused by the intervention of epigenetic factors or random mutations, resulting in the gastric heterotopias. There is no reason why these interventions do not occur postnatally. On this basis, if the stem cells retained the multipotency seen embryonically, then the development of lesions would continue into adulthood upon the loss of function of *Cdx2*. The observation that the number of heterotopias does not increase with age therefore suggests that the intestinal stem cells have undergone a degree of alteration at a point during gestation and are no longer able to respond to a loss of *Cdx2*. The adult intestinal stem cells may therefore be intrinsically different to the embryonic stem cells. The stage at which this may occur and to what degree is unknown. These theories may be investigated further by the creation of a mouse line containing a conditional knock out of *Cdx2*.

6.1.2 Conditional gene targeting systems

6.1.2.1 The Cre-LoxP inducible system

The requirement for a conditional gene knock out system is sometimes necessary, for example the study of the function of a gene beyond its requirement for embryonic survival. Such a system is also useful in order to induce a genetic change in a 'normal' animal to permit the study of the cellular response to such an alteration. An example of this is the response of intestinal stem cells to a loss of *Cdx2* in the adult, as discussed above.

Figure 6.1 The number of gastric heterotopias in *Cdx2*$^{+/-}$ mice of various ages. The red line indicates a line of best fit through the average values. The slope of this line is not statistically different to zero, i.e. the number of heterotopias present in the *Cdx2*$^{+/-}$ paracaecal region does not increase with age. The number in brackets indicates the sample size at each monthly time point. (Adapted from Beck et al. 1999).

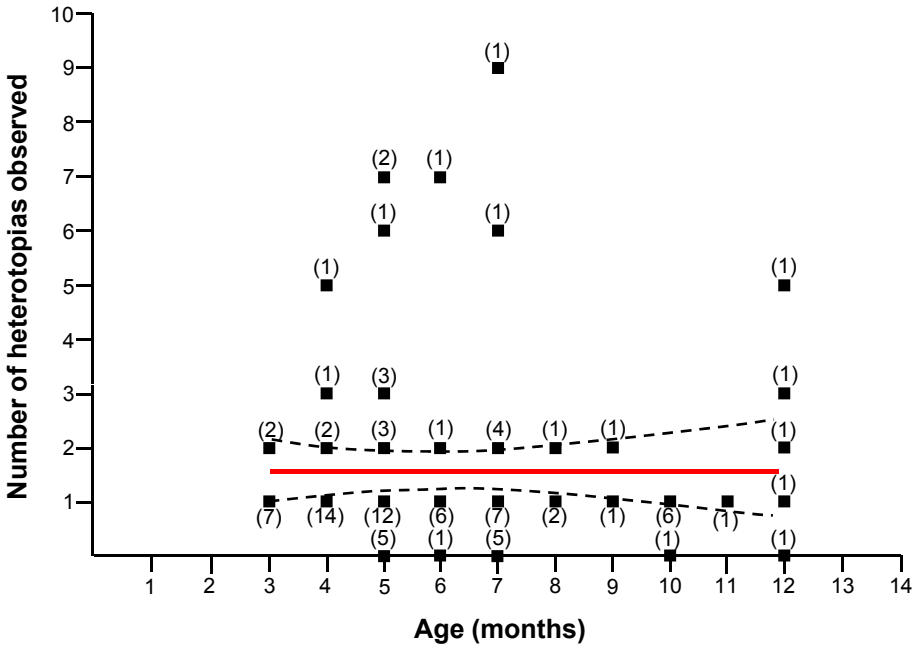

Currently, the best system to achieve conditional knock-out is the Cre-*Lox*P system. This involves the use of Cre to recognise and mediate site-specific recombination between *lox*P sites, as discussed in section 1.10.1. The addition of Cre to a transgenic mouse line carrying the gene in question, flanked by *lox*P sites, leads to excision or modification of that gene rendering it 'null'. Prior to addition of Cre, the mouse will express the target gene as normal (Nagy, 2000). The spatial and temporal expression of Cre is dependent upon the Cre recombinase expressing strain to which the transgenic mice are crossed.

6.1.2.2 Cre recombinase expressing strains

Various strains are available that express *Cre* in different regions and under different controls. Within this project, the purpose of the expression of Cre recombinase is to cause recombination between two *lox*P sites, rendering *Cdx2* null. This system must be inducible and so inducible *Cre* expressing strains will therefore be considered here.

There are two fundamental approaches to controlling *Cre* expression. Transcription of *Cre* itself can be induced, or Cre fusion-proteins can be created that involve the addition of a synthetic ligand in order to regulate Cre activity.

Expression of *Cre* is regulated in the *AhCre* mouse strain. The expression of the *Cre* gene is inducible from a cytochrome P450 promoter element. This promoter is activated by the binding of a high-affinity DNA binding protein. The binding of a lipophilic xenobiotic such as β-napthoflavone to a cytoplasmic aryl hydrocarbon (Ah) receptor causes the receptor to translocate to the nucleus where it complexes with other factors to create a high-affinity DNA binding protein. Addition of β-napthoflavone to the *AhCre* system therefore causes expression of *Cre* and leads to recombination events (Figure 6.2). A reporter strain has show that *AhCre* is active in the stomach and transit-amplifying cells of the intestine amongst other tissues (Ireland et al., 2004). This strain shows spontaneous recombination events in the absence of β-napthoflavone in some tissues with occasional spontaneous recombination occurring in the glandular stomach, small intestine and colon (Kemp et al., 2004).

Figure 6.2 The *AhCre* system. The *Cre* gene is positioned under the transcriptional regulation of the cytochrome P450 promoter element. Upon the addition of β-napthoflavone, the xenobiotic binds to a cytoplasmic aryl hydrocarbon (Ah) receptor, allowing it to translocate to the nucleus and complex with other factors to form a high-affinity DNA binding protein. This protein activates the cytochrome P450 promoter element, driving transcription of *Cre.* Cre-mediated recombination between *lox*P sites then occurs.

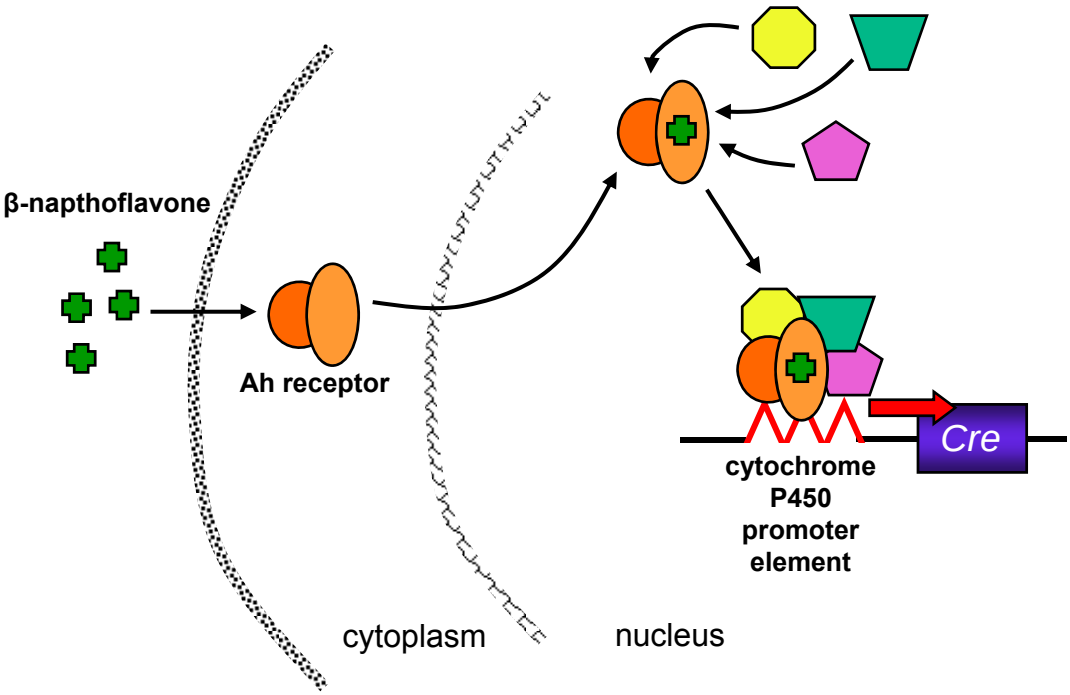

The *Cre-ER^{TM}* mouse strain utilises a Cre-fusion protein technique. This strain relies on 4-hydroxytamoxifen (4-OHT), the active metabolite of Tamoxifen (TM), to induce expression of a *Cre* fusion protein (Feil et al., 1996, Danielian et al., 1998). Either TM or 4-OHT can be administered to mice as TM will be metabolised to 4-OHT. The Cre-fusion protein was created by fusing the coding sequence for *Cre* to a mutant form of the ligand-binding domain of the oestrogen receptor (ER^{TM}). The mutation of the amino acid at position 525 from glycine to arginine prevents the natural ligand, 17-β-estradiol, from binding and instead binds 4-OHT (Danielian et al., 1993, Littlewood et al., 1995). The fusion of Cre with ER^{TM} leads to ER^{TM} dependent sequestering of Cre by heat shock protein 90 (Hsp90). This prevents Cre entering the nucleus. The binding of 4-OHT to ER^{TM} in the protein complex disrupts the Hsp90 interaction and so Cre-ER^{TM} translocates to the nucleus and initiates recombination (Figure 6.3) (Picard, 1994).

A strain of *Cre-ER^{TM}* mice has been established in which the fusion gene is under the control of a chimeric promoter of the cytomegalovirus immediate-early enhancer and chicken β-actin promoter/enhancer (CAGG). Cre-ER^{TM} was found to be ubiquitously expressed in these *CAGGCre-ER^{TM}* mice, with expression reported in the intestine (Hayashi and McMahon, 2002). Cre-mediated recombination can be induced in *CAGGCre-ER^{TM}* adults by intraperitoneal (IP) administration of 4-OHT. IP injection of 4-OHT in pregnant mothers causes recombination in *CAGGCre-ER^{TM}* embryos and so different embryonic stages can also be targeted for gene loss (Hayashi and McMahon, 2002). IP administration of 4-OHT is the preferred route, but other methods are possible to permit spatial control of recombination events. In *CAGGCre-ER^{TM}* embryos, 0.1% of cells underwent spontaneous recombination in the absence of 4-OHT. This 'leakiness' was also seen in adults, but the number of cells undergoing spontaneous recombination remained low, indicating tight regulation of Cre activity over many cell divisions (Hayashi and McMahon, 2002).

In some situations, any spontaneous recombination events can be undesirable. In order to prevent these random occurrences, the control of *Cre* expression can be placed under a dual system involving control over both *Cre* transcription and Cre activity. The Ah*cre*ER^{T} mouse strain contains such a system (Kemp et al., 2004). The

Figure 6.3 The *Cre*ER^{TM} system. Cre is expressed as a fusion protein with a mutated form of the oestrogen receptor. The mutated receptor (glycine at position 525 mutated to arginine) will only bind 4-OHT. In the absence of 4-OHT, the fusion protein binds Hsp90 via the oestrogen receptor. This sequesters Cre away from the nucleus where it is required to function. Following addition of 4-OHT, Hsp90 binding is disrupted and Cre translocates to the nucleus where it mediates recombination at the *lox*P sites.

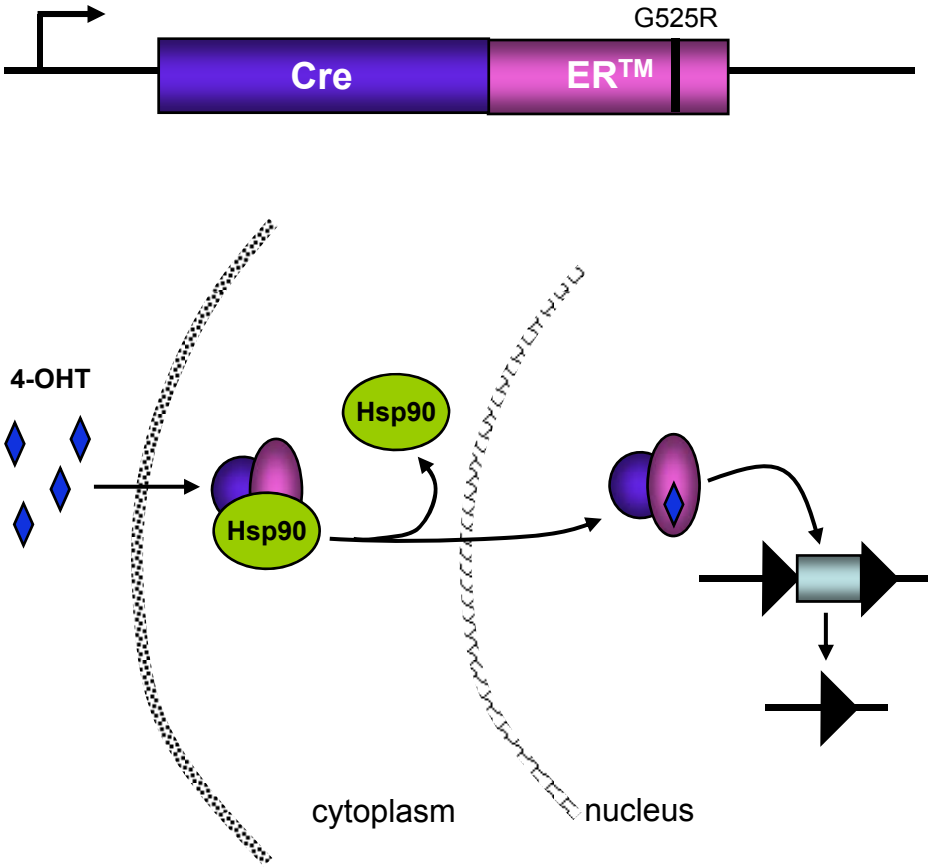

expression of *Cre* is controlled by the *Ah* promoter and therefore requires β-napthoflavone for activation of the promoter as found in the *AhCre* mouse strain (Ireland et al., 2004). Only in the presence of β-napthoflavone does the *Ah* promoter drive expression of the fusion protein CreER^{TM}. This complex remains inactive until the addition of 4-OHT, as found in *CreER^{TM}* mice (Feil et al., 1996, Danielian et al., 1998). Spontaneous recombination events do not occur in the stomach, small intestine and colon of these mice due to the tight regulation of Cre activity. It was found however that inducible recombination events were not as frequent in these mice as in the *AhCre* strain, possibly because the fusion protein is not as efficient as the native Cre (Kemp et al., 2004).

Upon activation, all the above mouse strains express inducible *Cre* or a Cre fusion protein ubiquitously. In the situation of the *Cdx2* conditional knock-out, the stage at which stem cell potential becomes restricted in the intestine will be under investigation. If this occurs postnatally, ubiquitous expression of *Cre* will not cause a problem as *Cdx2* is only expressed in the intestine at this stage. If this restriction occurs embryonically however, ubiquitous deletion of Cdx2 at this stage may cause a lethal phenotype due to the requirement of *Cdx2* for other developmental processes. Intestine-specific expression of *Cre* would target recombination and therefore Cdx2 deletion to the intestine. The villin-*Cre* mouse strain targets *Cre* expression to the intestinal epithelium (el Marjou et al., 2004). In these mice the expression of *Cre* was placed under the control of the villin regulatory region. Villin is expressed in the epithelial cells and progenitors of the small and large intestine from 12.5dpc onwards into adulthood. The *villin*-Cre strain, expressing *Cre* constitutively, was crossed with the *ROSA26* reporter strain (see below). In these mice, recombination was detected from 9dpc in visceral endoderm, leading to expression in the entire intestinal epithelium from 12.5dpc into adulthood. The expression of the 4-OHT dependent Cre-fusion protein was also placed under control of this region (villin-*Cre*ER^{T2} mice) although this system was not tested in embryos (el Marjou et al., 2004). Subsequently, villin-*Cre*ER^{T2} mice were crossed to *Gata4$^{Flox/Flox}$* mice; administration of tamoxifen daily for five days to time-mated mothers from 12.5dpc onwards led to inactivation of *Gata4* in the embryos by 17.5dpc. The villin-*Cre*ER^{T2} expression system is therefore functional embryonically (Bosse et al., 2007).

Another system that permits inducible intestine-specific *Cre* expression is the *Fabp*-rtTA/*tet*O-P_{hCMV}-Cre mouse strain (Saam and Gordon, 1999). *Cre* expression was originally placed under the control of a rat fatty acid-binding protein (*Fabp*) regulatory region to determine spatial and temporal activity of this region. A reporter strain crossed to these *Fabp*-Cre mice indicated that this regulatory region was active in the intestine from 13.5dpc onwards and remained active in all epithelial cells of the distal adult small intestine and the large intestine and colon. The expression of a reverse tetracycline-regulated transactivator (rtTA) was therefore placed under the control of the same *Fabp* regulatory region in order to target rtTA expression to the intestine. In the same mouse strain, the expression of *Cre* was placed under the control of a *tet* operator sequence (tet*O*) and a minimal promoter from human cytomegalovirus (P_{hCMV}). This generated the *Fabp*-rtTA/*tet*O-P_{hCMV}-Cre mouse strain. The rtTA expressed in the intestine of these mice is activated by the administration of doxycycline. The rtTA then binds to the Tet*O* system and activates it, causing expression of *Cre* (Saam and Gordon, 1999) (Figure 6.4). This *Fabp* driven inducible system has not been tested in embryos. A similar system involved the expression of rtTA in the retina; the rtTA required activation by doxycycline (Gimenez et al., 2004). Pregnant mothers were administered doxycycline via drinking water from 7dpc onwards; the presence of doxycycline did not hinder development or cause embryonic death (Gimenez et al., 2004). There is no reason therefore, why the rtTA/*tet*O-P_{hCMV}-Cre system cannot be used in embryos in to induce *Cre* expression from 13.5dpc onwards, leading to the knock-out of *Cdx2* in the intestinal epithelium only.

The point at which the potency of the intestinal stem cell appears to alter will dictate the choice of *Cre* expressing mouse strain that will be used to cause the knock-out of *Cdx2*. In the adult, a ubiquitous promoter will be used as *Cdx2* is only expressed in the intestine; the Ah*cre*ER^T strain is most suitable as it is the only strain not to report 'leakiness' in the intestine. In the embryo, the villin-*Cre*ER^{T2} or *Fabp*-rtTA/*tet*O-P_{hCMV}-Cre strain may be used to limit loss of Cdx2 protein to the intestine and avoid causing embryonic lethality. One disadvantage of these strains is that *Cre* expression occurs from 13.5dpc onwards; the stem cells may lose potency prior to this as the gut tube is formed at 9.5dpc.

Figure 6.4 The *Fabp*-rtTA/*tet*O-PhCMV-Cre system. Expression of the reverse tetracycline-regulated transactivator (rtTA) is driven by the intestinal epithelium-specific *Fabp* promoter. In the presence of doxycycline, the rtTA binds to and activates the Tet*O* sequence adjacent to a minimal promoter from human cytomegalovirus (P_{hCMV}). The *Cre* gene is positioned downstream of this sequence and expression is therefore induced following the binding of the rtTA in the presence of doxycycline.

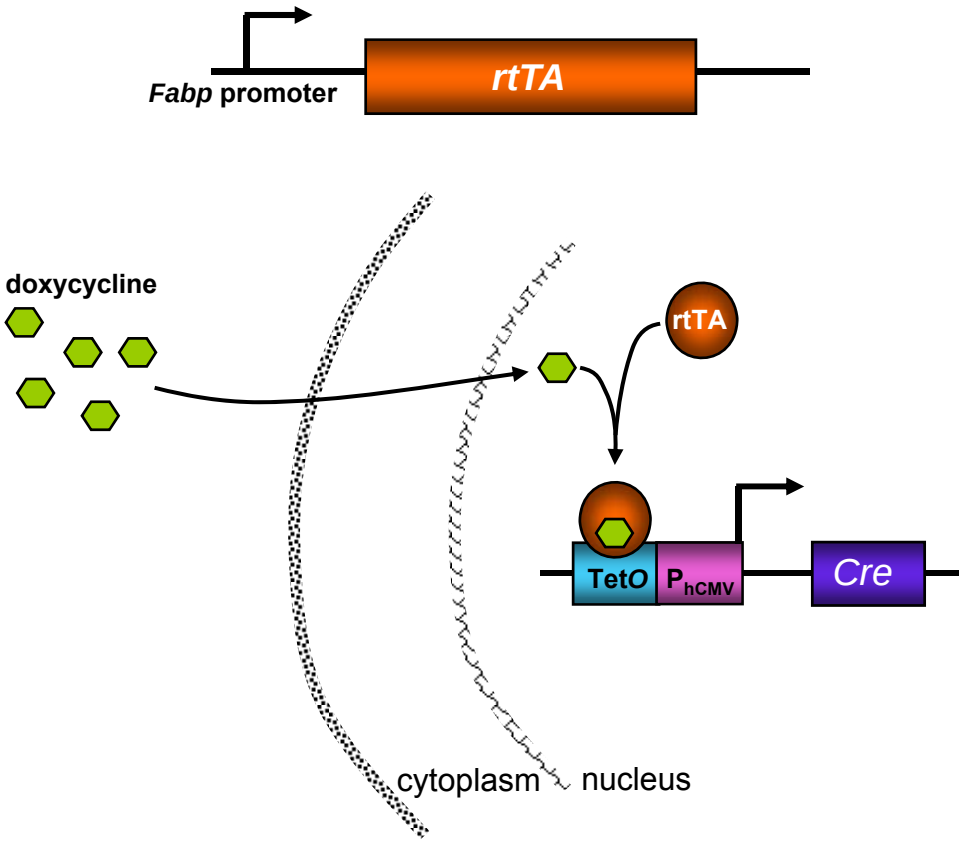

Once it has been determined when the intestinal stem cell loses potency (if at all), then the loss of *Cdx2* expression can be targeted to the different sets of stem cells. As discussed in section 1.5.1, two populations of stem cells are thought to exist; an *Lgr5*-expressing set which appear to be rapidly proliferating (Barker et al., 2007), and a *Bmi1*-expressing set that appear to be more quiescent (Sangiorgi and Capecchi, 2008). The *Lgr5-EGFP-IRES-creERT2* mouse strain expresses *Cre* from the *Lgr5* promoter. In the *Bmi1*-IRES-*Cre-ER* mouse strain, *Cre* expression is under the control of the *Bmi1* promoter (Barker et al., 2007, Sangiorgi and Capecchi, 2008). Both forms of Cre are activated by the administration of 4-OHT. The *Cdx2* conditional mouse strain can be crossed to the *Lgr5-EGFP-IRES-creERT2* mouse strain to target the loss of *Cdx2* to the rapidly proliferating stem cells. The crossing of the *Bmi1*-IRES-*Cre-ER* mouse strain to the *Cdx2* conditional line may not be as useful because *Bmi1* is expressed in the proximal small intestine while *Cdx2* expression is more distal. Some overlap may however be evident and so some response to *Cdx2* loss may be detected. Overall, it is hoped that the crossing of the *Cdx2* conditional mouse line to these *Cre*-expressing mouse strains will allow the loss of *Cdx2* expression to be targeted to the different stem cell populations and the response studied. This will provide insight into the role of the two stem cell populations with regard to the differentiation of the intestinal epithelium.

6.1.2.3 Reporter mouse strains

Mouse strains are available that 'report' upon Cre activity. These 'reporter strains' can be used to determine the spatial and temporal expression of *Cre* and the subsequent recombination event. These strains are also useful in demonstrating spontaneous recombination events due to 'leaky' Cre activity. Most reporter strains rely upon the expression of a LacZ reporter cassette containing the β-galactosidase (*β-gal*) gene. This cassette is transcribed following Cre-mediated recombination to remove an inhibitory region flanked by *lox*P sites.

Ideally, ubiquitous and constitutive expression of the promoter upstream of the LacZ cassette is required in order to determine precisely where and when *Cre* expression is occurring. One such strain is the ROSA26 reporter (*R26R*) (Soriano, 1999). In these mice, a neo^R cassette, flanked by *lox*P sites, is positioned upstream of the

LacZ reporter cassette. The *neo*^{R} cassette contains a triple polyadenylation sequence at the 3' end to prevent read through to the LacZ cassette. The whole sequence is under transcriptional control of the ROSA26 promoter. Upon *Cre* expression, recombination occurs to remove the *neo*^{R} cassette and so expression of LacZ occurs that can be monitored by X-Gal staining (Soriano, 1999) (Figure 6.5). The ROSA26 promoter is active from preimplantation in all cells and so *Cre* expression can be determined spatially and temporally from very early stages in development (Zambrowicz et al., 1997).

One problem with a system such as that in the *R26R* strain is that the presence of LacZ is the only evidence of recombination. A dual system reports upon both presence and absence of Cre, removing any doubt about enzyme activity. A reporter mouse strain, *Z/EG* (*LacZ/EGFP*), has therefore been created that contains a double reporter system. *β-gal* is flanked by *lox*P sites, under the control of the constitutive CAGG promoter. The *β-gal* gene is followed by a triple polyadenylation site to stop transcriptional read-through. This is followed by an enhanced green fluorescent protein (*EGFP*) reporter gene. *LacZ* is expressed in the absence of Cre. In the presence of Cre, *EGFP* is expressed (Figure 6.6) (Novak et al., 2000). This system therefore conclusively identifies regions of Cre activity. One problem with this strain however is that the husbandry of these mice when on a C57/Bl6 background is difficult; offspring need to be fostered to other mothers in order to survive.

A disadvantage of a reporter system that is separate to the Cre/*lox*P system of the target gene is that it will only indicate regions of *Cre* expression; this does not mean that the gene under investigation has also undergone Cre-mediated recombination. The positioning of a promoterless reporter gene downstream of the gene under investigation will report upon Cre-mediated excision of the gene. This approach was used in the creation of β1 integrin conditional knock-out mice. The entire coding region of the β1 integrin gene was flanked by *lox*P sites, with a promoterless lacZ reporter gene downstream of the second *lox*P site. Following Cre-mediated excision of β1 integrin, the *lacZ* reporter cassette was expressed under the control of the β1 integrin promoter. Cells in which conditional knock-out of β1 integrin had occurred could therefore be detected by LacZ activity (Brakebusch et al., 2000).

Figure 6.5 The ROSA26 reporter system. The ROSA26 promoter is ubiquitously active from preimplantation. (A) In the absence of Cre, transcription terminates at the triple polyadenylation site, prior to expression of *LacZ*. (B) In the presence of Cre, the construct undergoes Cre-mediated recombination between the *lox*P sites. The loss of the *neo*^{R} cassette and polyadenylation site permits expression of *LacZ;* this expression can be monitored by X-Gal staining.

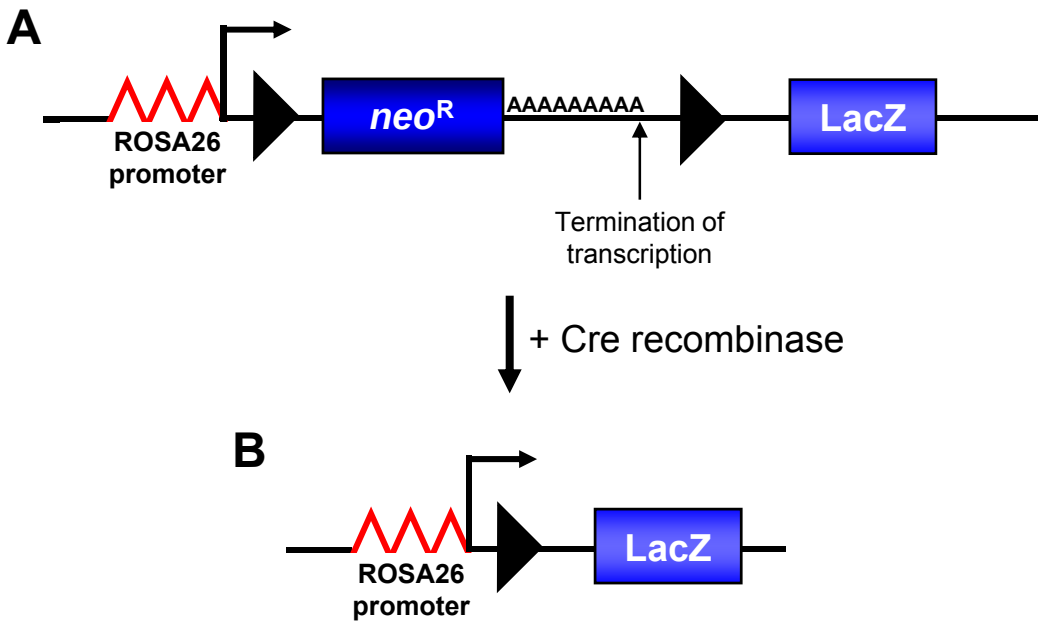

Figure 6.6 The Z/EG system. The CAGG promoter is constitutively active. (A) In the absence of Cre, the *LacZ* reporter cassette is expressed and transcription terminates at the triple polyadenylation site. This expression can be monitored by X-Gal staining. (B) In the presence of Cre, the construct undergoes Cre-mediated recombination between the *lox*P sites. The loss of the *LacZ* cassette and polyadenylation site permits expression of *EGFP;* this expression can be monitored under fluorescent light.

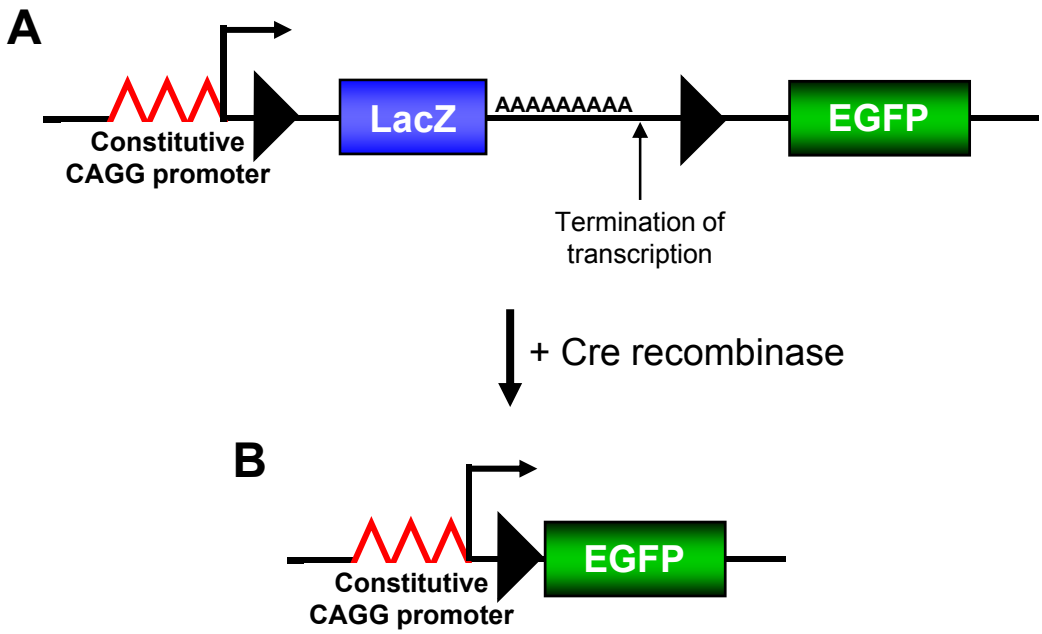

6.1.2.4 The Flp-FRT system

As discussed in section 1.10.2, the Flp-*FRT* system is an alternative to the Cre-*LoxP* technique. Some targeting vectors contain two regions that need to be deleted. The use of a single system alone makes deletion of the undesirable region (such as a positive selection cassette) more difficult due to different outcomes, including the loss of function of the targeted gene. Utilising both Flp/*FRT* and Cre/*lox*P systems during a genetic strategy allows the ubiquitous deletion of an undesirable region (such as a positive selection cassette) with the addition of Flippase whilst ensuring the targeted gene remains intact until addition of Cre recombinase.

The Flp-*FRT* system was first shown to be functional in mice in 1996 (Dymecki, 1996). This system was based upon *β-gal* being positioned downstream of a stop codon flanked by *FRT* sites, under the control of a strong ubiquitous promoter. The *Flp* gene was placed under the control of the same promoter. *Flp* expression in mice was found to be non-toxic and the subsequent double mutant mice were found to express LacZ due to Flp-driven recombination between the *FRT* sites (Dymecki, 1996).

FLPeR ('Flipper') mice utilise this system (Farley et al., 2000). These mice contain an enhanced version of the site specific recombinase Flp (FLPe) (Buchholz et al., 1998, Rodriguez et al., 2000). The *FLPe* cassette was targeted to the *ROSA26* locus to produce a strain in which FLPe was broadly active; the *FLPeR* strain. These mice were crossed to a reporter strain containing an *FRT*-disrupted LacZ transgene driven by the mouse hydroxymethylglutaryl-coenzyme A reductase (*HMGCR*) promoter (Rodriguez et al., 2000). They showed extensive Flp-mediated recombination had occurred and only recombined DNA was transmitted germline (Farley et al., 2000). This system will therefore efficiently and permanently remove redundant reporter cassettes.

6.1.2.5 Reported use of the Cre/LoxP and Flp/FRT recombination systems

Meyers et al created a mouse line ($Fgf8^{Neo}$) in which Fgf8 was 'allelogenic'. This means that the same mouse line can generate three other mouse lines carrying a

different version of the targeted allele. This mouse line utilised both the Cre/*LoxP* and Flp*/FRT* systems (Meyers et al., 1998).

The *neo*^{R} cassette, used as a positive selection marker, was flanked by *FRT* sites and positioned in the intron between exon 1 and 2 of *Fgf8*. It was found that the presence of the *neo*^{R} cassette caused *Fgf8* to become hypomorphic (impairment of gene expression but not abolition). This was because the *neo*^{R} cassette contains cryptic splice acceptor and donor sites and so both WT and hybrid *Fgf8* RNA was produced (Meyers et al., 1998). In the absence of Cre and Flp, *Fgf8* expression was therefore hypomorphic (*Fgf8*^{Neo} mice). Addition of Flp removed the *neo*^{R} cassette and returned *Fgf8* expression to normal (*Fgf8*^{Flox} mice). Exons 2 and 3 of *Fgf8* were flanked by *lox*P sites as these are the functional exons. Addition of Cre therefore led to generation of a null allele (*Fgf8*$^{\Delta 2,3n}$ mice) (Meyers et al., 1998).

Fgf8$^{Neo/+}$ mice were crossed to a Cre strain to produce *Fgf8*$^{\Delta 2,3n/+}$ offspring. These were intercrossed to produce phenotypically abnormal *Fgf8*$^{\Delta 2,3n}$ homozygotes that reabsorbed by 10.5dpc due to a failure of gastrulation. The importance of an inducible *Fgf8* null allele was therefore highlighted (Meyers et al., 1998). *Fgf8*$^{Neo/+}$ mice were intercrossed. The *Fgf8*^{Neo}/*Fgf8*^{Neo} embryos survived to term but died within a day of birth. These animals showed severe defects of the brain due to hypomorphism of *Fgf8.* *Fgf8*^{Neo}/*Fgf8*$^{\Delta 2,3n}$ compound mutations showed an even greater phenotype due to increased severity of the hypomorphism (Meyers et al., 1998). The hypomorphism was effectively reversed by crossing *Fgf8*$^{Neo/+}$ with an Flp expressing mouse strain. The resultant *Fgf8*$^{Flox/+}$ offspring were intercrossed. The *Fgf8*^{Flox}/*Fgf8*^{Flox} mice showed no defects and appeared as normal. The mating of *Fgf8*$^{Flox/+}$ with *Fgf8*$^{\Delta 2,3n/+}$ mice resulted in compound *Fgf8*^{Flox}/ *Fgf8*$^{\Delta 2,3n}$ offspring that also appeared normal and so it was deduced that a single functional *Fgf8* allele was sufficient to support normal development (Meyers et al., 1998). *Fgf8*^{Flox} homozygotes were crossed to *Cre* expressing mice. Some of the progeny carried the *Fgf8*$^{\Delta 2,3n}$ allele, indicating that a single allele can be modified by both Cre and Flp-mediated recombination (Meyers et al., 1998).

6.2 Aims

The *Cdx2* mutant mouse models currently available contain a constitutive *Cdx2* mutation. These mice demonstrate intestinal lesions of gastric-type epithelium with underlying mesoderm expressing a stomach-specific gene. Previous observations suggest that the mice do not develop lesions postnatally as they are born with all the heterotopic lesions they ever exhibit. Two possible explanations for this observation are either that Cdx2 function is not downregulated to the level of haploinsufficiency in the adult intestine or the stem cells progressively lose potency during development and are therefore not responsive to postnatal downregulation of Cdx2 function. The causes of the downregulation of Cdx2 function from the remaining wild type allele are unknown, but are thought to be due to epigenetic and environmental factors. It is likely that these factors continue to occur into adulthood and therefore that postnatal loss of Cdx2 function does occur. It is hypothesised, therefore, that the intestinal stem cells may alter in potential at some stage of development to no longer respond to a decrease in *Cdx2*.

The aim of this chapter was to generate a mouse line containing a conditional knock-out of *Cdx2*. This mouse line will be fundamental in investigating the potential of adult stem cells. If the adult mice are shown to develop heterotopias upon the conditional loss of *Cdx2* then it will suggest that the intestinal stem cells do not lose potency; the factors causing the loss of Cdx2 in the *Cdx2*$^{+/-}$ mice must only occur embryonically. If the conditional loss of *Cdx2* does not result in heterotopias forming in the adult, then the mice can be used to determine the point at which the intestinal stem cells alter in potency to no longer respond to a loss of *Cdx2*.

6.3 Results

6.3.1 The Cdx2 conditional knock-out strategy

Cdx2 is a homeobox gene; the protein therefore contains a homeodomain, allowing Cdx2 to act as a transcription factor. Exon 2 of the gene codes for the homeodomain and is therefore the functional region of *Cdx2*. Deletion of exon 2 will render *Cdx2* non-functional i.e. knocked out.

The *Cdx2* conditional knock-out vector was therefore designed so that exon 2 was positioned between *lox*P sites (Figure 6.7). Expression of *Cre* would cause excision of exon 2. Once created, the construct would have to be electroporated into ES cells in an attempt to achieve homologous recombination; a neo^R selection cassette was therefore required. This would have to be removed before the *Cdx2* allele would be functional in mice and so this was flanked by *FRT* sites to allow Flp mediated recombination (Figure 6.7). As previously discussed in Chapter 1, the use of both *lox*P/Cre and *FRT*/Flp systems are preferential to *lox*P/Cre alone.

The construct (pGKCdx2) was therefore designed to contain three sections (arms). The middle arm contained the sequence for exon 2, flanked by *lox*P sites. The left and right arms contained the *Cdx2* sequence adjacent to that contained in the middle arm (Figure 6.7). These arms needed to be as long as possible to increase the chances of homologous recombination occurring at these sites, whilst not hindering the cloning events. The length of the right arm had to be limited, however, because the 3' end of the *Cdx2* sequence has not yet been cloned, possibly due to an element of the sequence being toxic to bacteria. This region is therefore not yet sequenced.

A positive control vector was required to be used as a PCR control for the screening of homologous recombination events between pGKCdx2 and ES cell DNA following electroporation. This vector was designed so that the insert to be used was longer than the LA in pGKCdx2. This arm was cloned into the same vector as that used for pGKCdx2. The forward primer (OES30) annealed within the arm of the positive control but outside the left arm of pGKCdx2. The reverse primer (OES31) annealed within both pGKCdx2 and the positive control. A PCR product was therefore detected following random recombination of the positive control into ES cells; this ES cell DNA was subsequently used as a positive control for the PCR reaction. Only a homologous recombination event within ES cells electroporated with pGKCdx2 would produce a band following a PCR using OES30 and OES31 (Figure 6.8).

Once the construct had undergone homologous recombination into ES cells, a selected clone would be injected into blastocysts to create chimeras. Once the chimeras had been used to achieve germline transmission of the *Cdx2* conditional

Figure 6.7 Designing the *Cdx2* conditional knock-out vector (pGKCdx2). The left, middle and right arms are indicated on the *Cdx2* allele in relation to the exons. The position of these arms in the pGKCdx2 vector are shown. Exon 2 (the functional region) is located within the middle arm, flanked by *lox*P sites. The *neo*^{R} cassette is flanked by *FRT* sites. The 3' end of the *Cdx2* allele has not been sequenced (indicated by hatched box). (LA; left arm, RA; right arm, MA; middle arm). Diagrams were created using Vector NTI (Invitrogen).

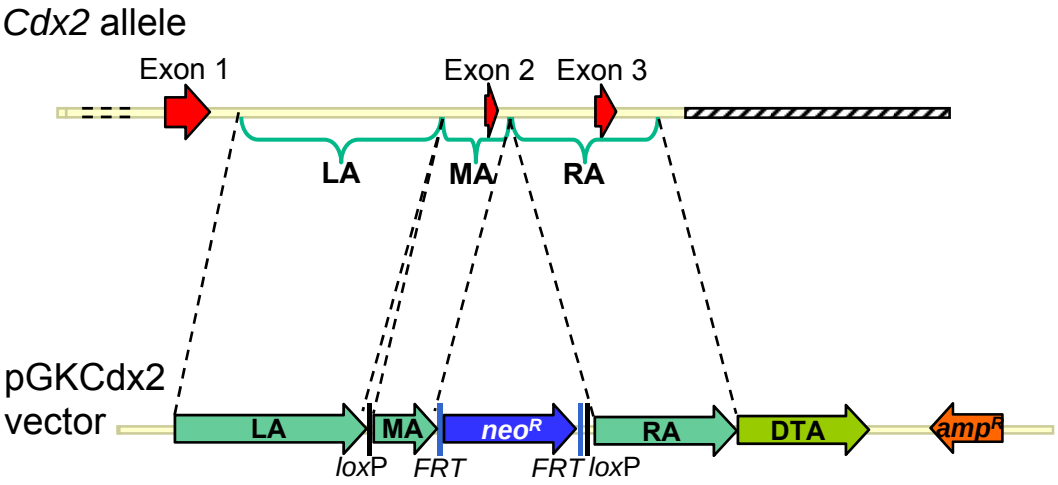

Figure 6.8 Primers used to screen for homologous recombination of the LA. The reverse primer (OES31) anneals between the arm and the *lox*P site in both the pGKCdx2 construct and positive control. The forward primer (OES30) anneals in the endogenous *Cdx2* DNA and also the positive arm. Random recombination of the positive arm anywhere in the genome therefore produces a band of 2.6Kb following PCR using the primers OES30 and OES31. A band of the same size will only be seen in ES clones electroporated with pGKCdx2 if the construct has undergone homologous recombination at the left arm. Diagrams were adapted from Vector NTI (Invitrogen).

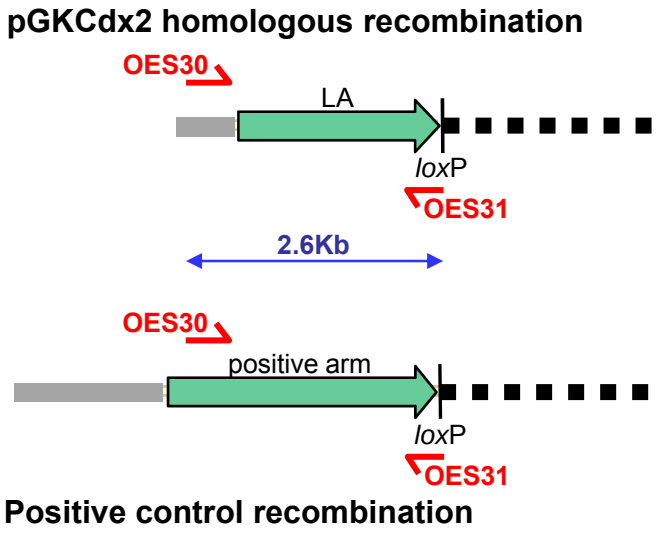

construct, the *neo*^{R} cassette would be removed by crossing the heterozygous mice (*Cdx2*$^{WT/LoxFRT}$) to mice ubiquitously expressing Flp (Figure 6.9). The resultant *Cdx2*$^{WT/Lox}$ mice would be crossed to create *Cdx2*$^{Lox/Lox}$ mice. The mating of this line to a chosen inducible *Cre*-expressing line would allow conditional knock-out of *Cdx2* (*Cdx2*$^{-/-}$) (Figure 6.9).

6.3.2 The pGKNeoF2L2DTA vector

The vector used to create the construct pGKCdx2 was pGKNeoF2L2DTA. This vector contains both *FRT* and *lox*P sites (Figure 6.10). The positive selection cassette is positioned between *FRT* sites and so Flp recombinase can be used to delete the cassette without concern for the undesirable deletion of the floxed region of *Cdx2*. The vector also contains a diphtheria toxin A (DTA) fragment; this aids the removal of clones containing unwanted random recombination events involving the DTA cassette (see section 1.9.2).

The pGKNeoF2L2DTA vector contains two *EcoR* I sites. The cloning strategy required insertion of the middle arm of the construct into one of the *EcoR* I sites and so the pGKNeoF2L2DTA vector was first digested with *Nco* I and re-ligated in order to remove a fragment of the vector containing the additional *EcoR* I site (Figure 6.11). The pGKNeoΔNcoI vector was supplied by S. Munson (Geneta, University of Leicester, Leicester).

6.3.3 Generating the arms of the construct

Mouse genomic DNA (supplied by S. Munson, Geneta, University of Leicester, Leicester) was used as a template for creating the arms. The primers used were as follows; Left arm (LA): OES10 and OES11, Middle arm (MA): OES5 and OES9, Right arm (RA): OES7 and OES12 (Figure 6.12). OES5 and OES11 were adjacent but did not overlap; this is also the same for OES7 and OES9. The primers were designed so that the PCR products would contain the appropriate restriction enzyme sites for cloning into the vector.

Figure 6.9 The *Cdx2* conditional knock-out strategy. Crossing the *Cdx2*$^{WT/LoxFRT}$ mouse strain to an Flp-recombinase expressing strain will remove the *neo*^{R} cassette flanked by *FRT* sites to produce the *Cdx2*$^{WT/Lox}$ strain. These mice will be crossed to a *Cre* expressing strain before being intercrossed to produce the *Cdx2*$^{Lox/Lox}$ strain. The expression of *Cre* can then be induced at the desired spatial and temporal point to remove exon 2 of *Cdx2*, effectively knocking out the gene.

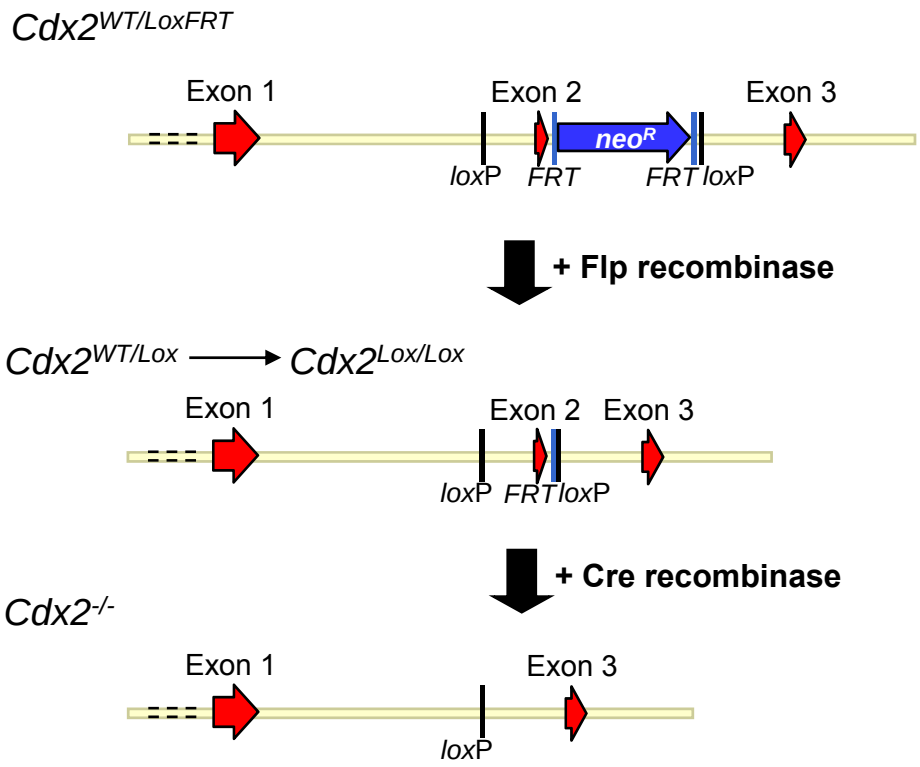

Figure 6.10 The vector pGKNeoF2L2DTA. The vector contains a positive selection cassette (*neo*^{R}) flanked by *FRT* sites. This entire region is flanked by *lox*P sites. The vector also has a DTA cassette for negative selection and is ampicillin resistant for growth in bacteria. The vector contains two *EcoR* I and *Nco* I sites. Diagram was created using Vector NTI (Invitrogen).

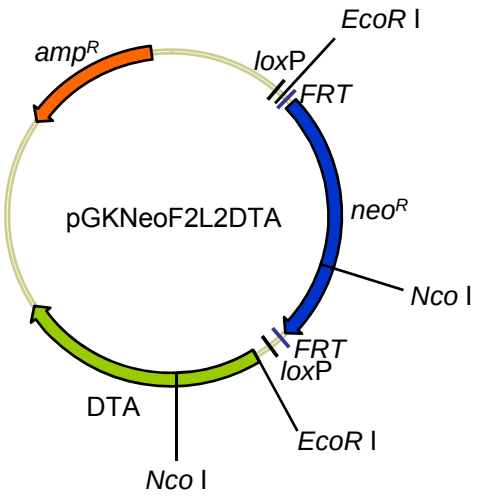

Figure 6.11 The vector pGKNeoΔNcoI. The vector shown in Figure 6.10 was digested with *Nco* I and re-ligated in order to remove the additional *EcoR* I site. This vector was used for the cloning of the middle arm into the remaining *EcoR* I site. Diagram was created using Vector NTI (Invitrogen).

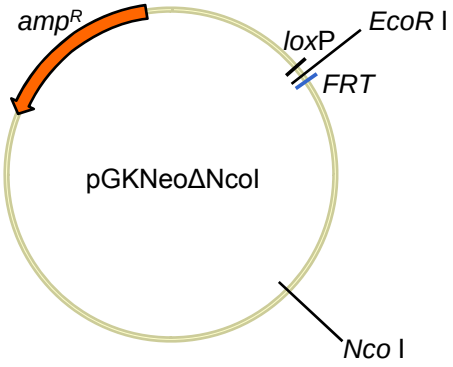

Figure 6.12 Primers for creating the arms of pGKCdx2. Primer pairs were designed for the left (red), middle (blue) and right (green) arms. The primers annealed to the *Cdx2* gene (exons indicated by red arrows). The PCR products were electrophoresed and produced bands of 2306bp, 760bp and 1706bp. The diagram was created using Vector NTI (Invitrogen).

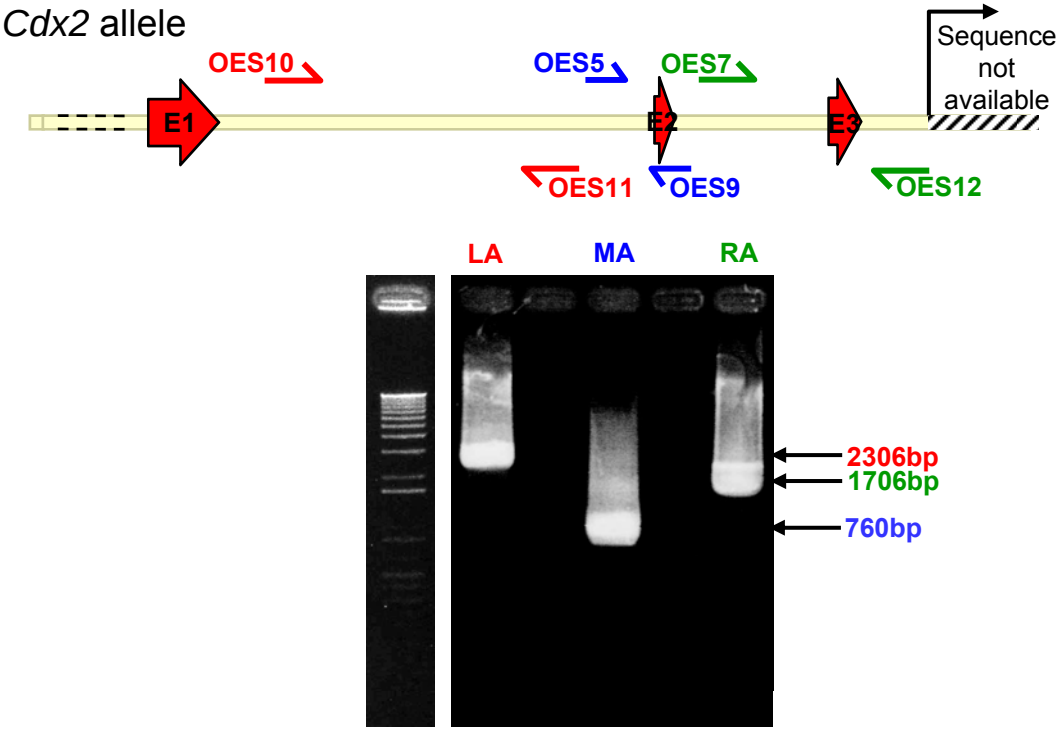

6.3.4 Cloning of the middle arm into pGKNeoF2L2DTA

The MA was first cloned into pBluescriptSKII+ at the *EcoR* I site. This was a straightforward cloning step and facilitated subsequent cloning into the pGKNeoΔNcoI vector. The ligation mixture was transformed into DH5α. DNA was extracted from the subsequent colonies by minipreparation and digested with *EcoR* I. (data not shown). The successful cloning event was confirmed by sequencing using T7 and T3 DNA polymerase.

Following a large-scale preparation of plasmid DNA, a restriction enzyme digest using *EcoR* I was performed to sub-clone the MA insert into pGKNeoΔNcoI at the one remaining *EcoR* I site to create pGKNeoΔNcoI(MA). Following transformation, DNA extracted from colonies was screened by restriction enzyme digest using *EcoR* I. Two colonies indicated that they contained an insert of 760bp (data not shown). The DNA from these colonies was then double-digested with *Spe* I and *BsrG* I to indicate the orientation of the MA. One colony appeared to contain the insert in the correct orientation (Figure 6.13A and 6.13B). The successful cloning event was confirmed by DNA sequencing using the primers OES5 and OCP66 (Figure 6.13C).

pGKNeoΔNcoI(MA) was double restriction enzyme digested with *Not* I and *Xma* I as was pGKNeoF2L2DTA. The fragment containing the MA from pGKNeoΔNcoI(MA) was ligated to the digested pGKNeoF2L2DTA (Figure 6.14). This was transformed into bacteria and the colonies screened using a restriction enzyme digest with *Nco* I. The two colonies produced a band of the correct size to indicate the presence of MA (data not shown). Further restriction enzyme digests of the DNA from one colony indicated that pGKCdx2(MA) had been successfully cloned (Figure 6.15A). The successful cloning of pGKCdx2(MA) was confirmed by DNA sequencing using the primers OES5 and OCP66. The annealing sites for these primers are indicated in Figure 6.15B.

6.3.5 Cloning of the left arm into pGKCdx2(MA)

The left arm was first cloned into pBluescriptSKII+ (pBSSKII+) using *Not* I. To detect colonies containing pBS(LA), minipreparations of DNA were made and restriction enzyme digested with *Not* I. The DNA from one colony was digested with further

Figure 6.13 Determination of MA orientation in pGKNeoΔNcoI(MA) using restriction enzyme digests and DNA sequencing. (A) MA in the incorrect orientation. The DNA bands expected from restriction enzyme digest of this construct are indicated in the table below. One clone was electrophoresed and although not all bands can be visualised, it was sufficient to determine incorrect MA orientation. (B) MA in the correct orientation. The expected size of the DNA bands following restriction enzyme digest of this construct are indicated in the table below. One clone was electrophoresed and produced bands of this size on the gel. N.B: A band of 1190bp can be seen due to inefficient digestion with *BsrG* I. (C) Positions of primer annealing sites used for DNA sequencing to confirm the successful cloning event. Diagrams were created using Vector NTI (Invitrogen).

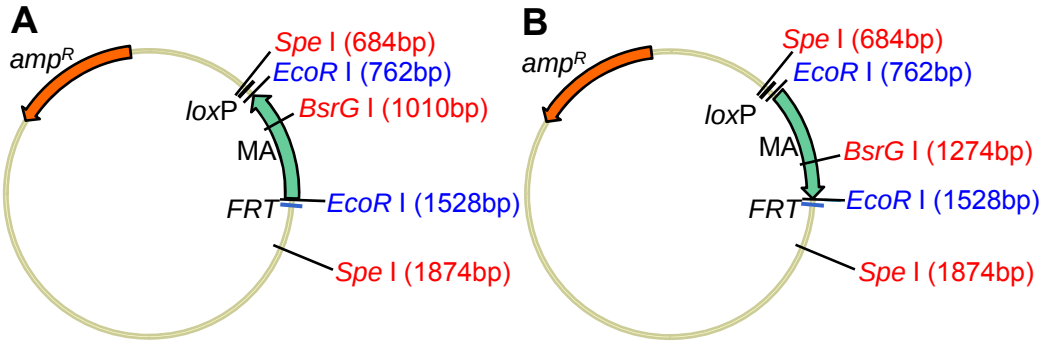

Restriction digest	Band size (bp)
EcoR I	766
Spe I/ *BsrG* I	326, 864, 4793

Restriction digest	Band size (bp)
EcoR I	766
Spe I/ *BsrG* I	590, 600, 4793

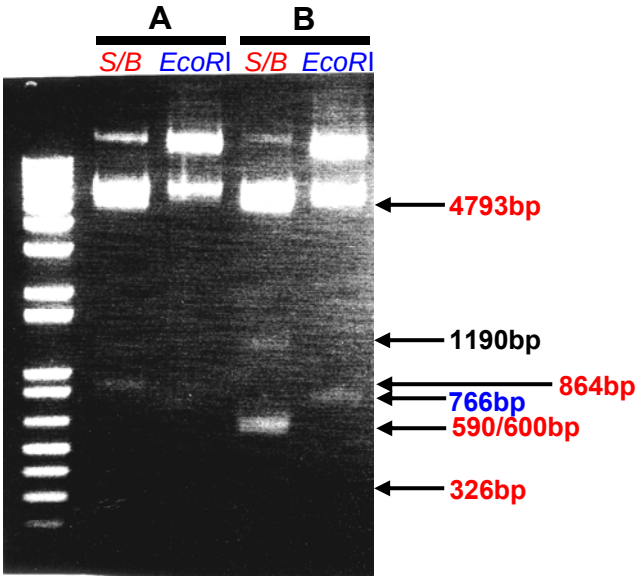

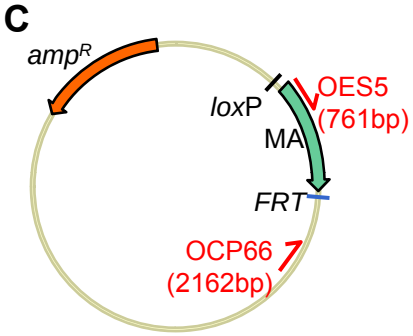

Figure 6.14 Cloning of the MA into pGKNeoF2L2DTA. (A) pGKNeoΔNcoI(MA) was restriction enzyme digested with *Not* I and *Xma* I. The fragments were electrophoresed and the MA fragment extracted from the gel. (B) pGKNeoF2L2DTA was digested with the same restriction enzymes and cleaned up on a column to retain the large fragment. (C) The two fragments were ligated to create pGKCdx2(MA). Diagrams were created using Vector NTI (Invitrogen).

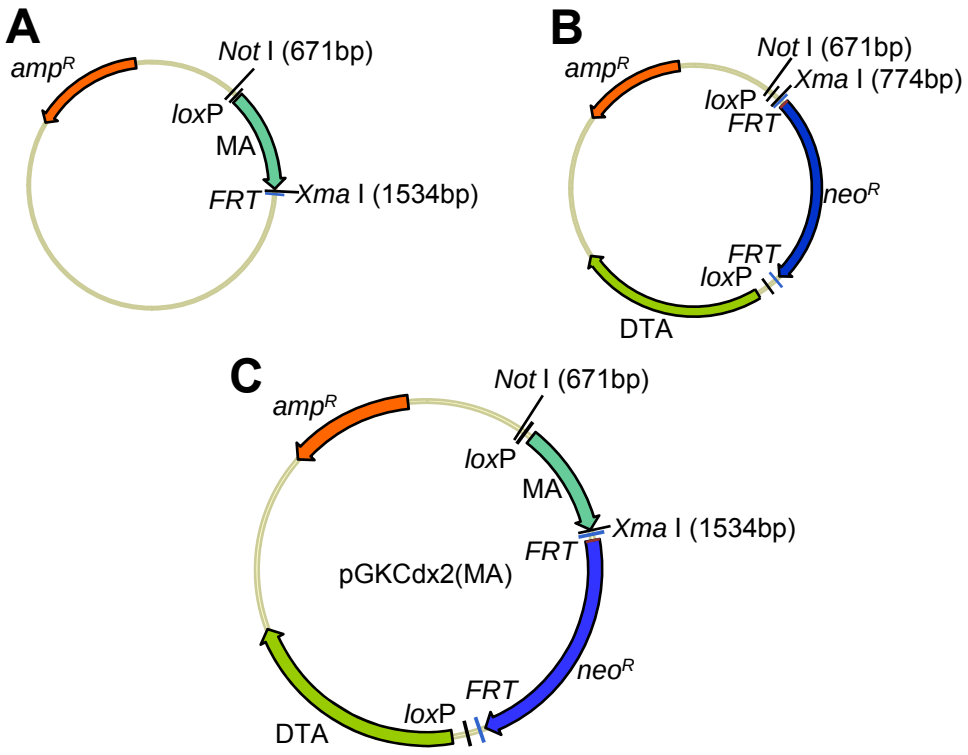

Figure 6.15 Determining successful cloning of pGKCdx2(MA). (A) The DNA of a clone thought to contain pGKCdx2(MA) was restriction enzyme digested with *EcoR* I (E), *Not* I (No) and *Nco* I (Nc). The resultant fragments were electrophoresed alongside uncut DNA (U). The gel indicated DNA bands of the expected sizes following restriction enzyme digest of pGKCdx2(MA). (B) The clone was sent for sequencing with OES5 and OCP66; the annealing sites for these primers are indicated. Diagrams were created using Vector NTI (Invitrogen).

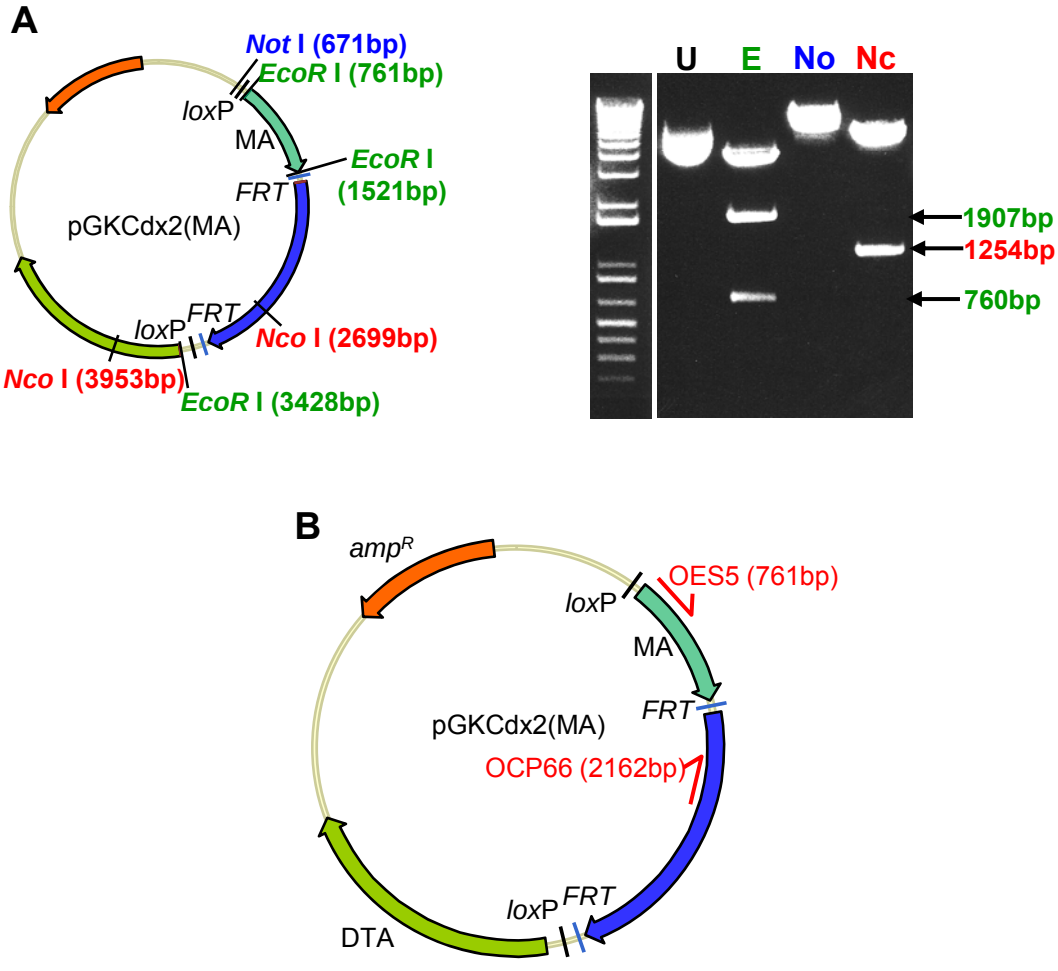

restriction enzymes to ensure that pBS(LA) had been successfully cloned before sending the colony for sequencing (data not shown). The sequencing was performed using T7 and T3 DNA polymerase, confirming the successful cloning of pBS(LA).

pBS(LA) was then digested with *Not* I as was pGKCdx2(MA). Following ligation of the LA into pGCdx2(MA), subsequent colonies were screened by restriction enzyme digest of minipreparations of DNA, using *Not* I to identify colonies containing the LA insert (Figure 6.16A). The DNA from one clone identified as containing pGKCdx2(MA/LA) was digested with *Not* I, *Nco* I, *Bgl* II, *Xma* I and *Afl* III to confirm this (Figure 6.16B). The DNA was also sent for sequencing with OES9 and OCP66 to confirm successful cloning to create pGKCdx2(MA/LA).

6.3.6 Cloning of the right arm into pGKCdx2(MA/LA)

The right arm was first cloned into pBluescriptSKII+ (pBSSKII+) using *Hind* III. DNA was prepared from the transformed colonies and digested with *EcoR* I to linearise the plasmid. This was then electrophoresed to identify any DNA bands bigger than 3Kb (the size of pBluescriptSKII+ without additional inserts) (data not shown). Any DNA samples that produced a band of approximately 4.5Kb were also digested with *Hind* III to determine the size of the insert (data not shown). A single colony containing a successful cloning event was sequenced using T7 and T3 DNA polymerase in order to confirm this.

The insert was then subcloned into pGKCdx2(MA/LA) using *Hind* III restriction sites. The ligation was transformed into DH5α and minipreparations of DNA were performed upon subsequent colonies. These were digested with *Hind* III to detect the insert. A number of colonies were identified as producing a band of the correct size (Figure 6.17). Various enzyme digests were performed to ensure that all the arms were present and in the correct orientation (Figure 6.18 and 6.19A); the fragments produced indicated that pGKCdx2 had been created correctly. Sequencing of the construct with DNA polymerase T7 and primers OES9, OES11, OES12, and OES29 confirmed this (Figure 6.19B).

Figure 6.16 Restriction enzyme digest to confirm successful cloning of pGKCdx2(MA/LA). (A) The DNA of numerous colonies was digested with *Not* I. A number of samples produced bands of 2306bp in size, indicative of successful cloning of the left arm into pGKCdx2(MA). (B) One of the colonies shown in (A) was further digested with *Not* I (No), *Nco* I (Nc), *Xma* I (X), *Afl* II (A) and *Hind* III (H). The digested fragments were electrophoresed alongside uncut DNA (U). The DNA bands produced were as expected following digest of pGLCdx2(MA/LA). Diagrams were created using Vector NTI (Invitrogen).

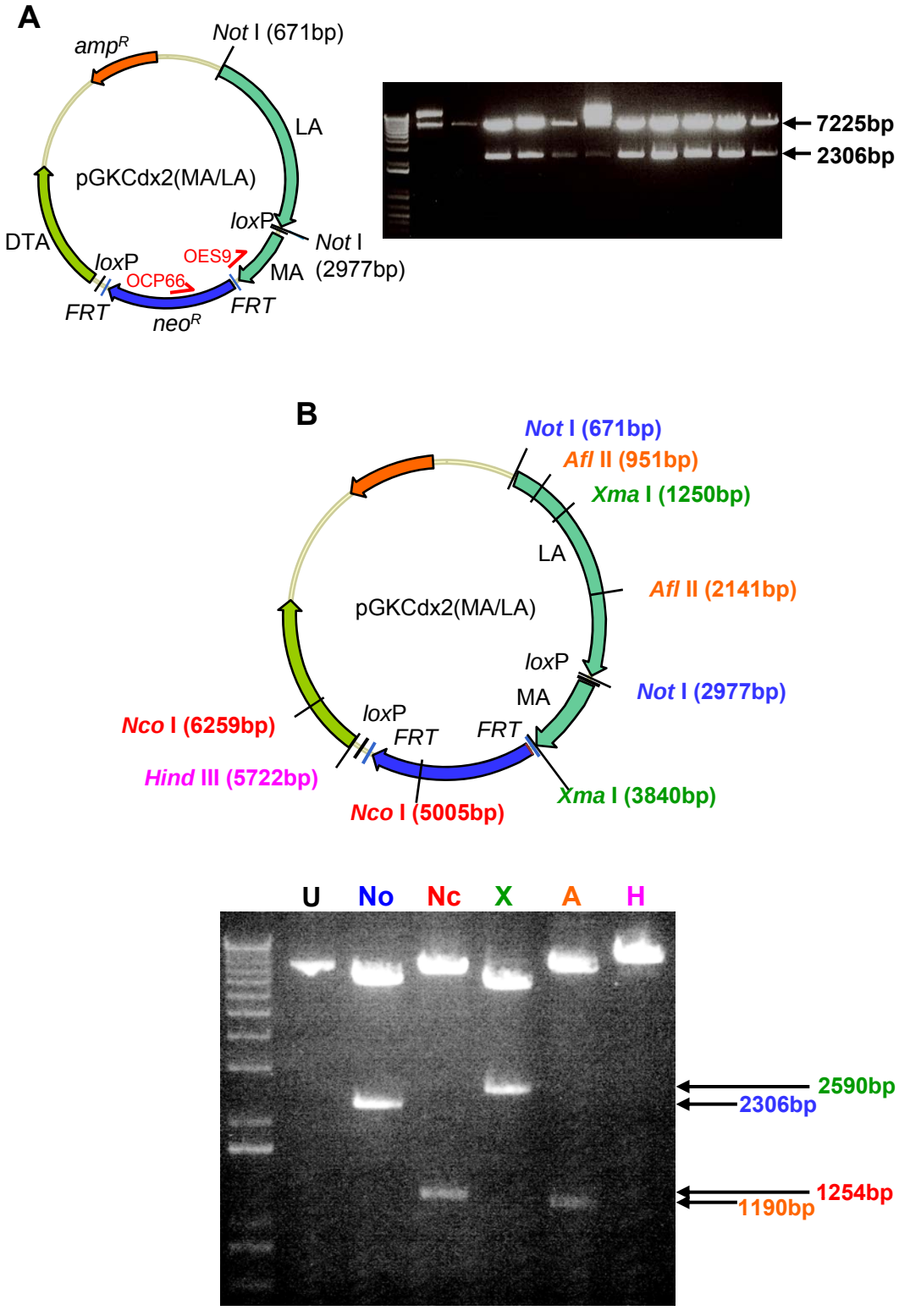

Figure 6.17 Restriction enzyme digest to confirm cloning of pGKCdx2. The DNA from numerous clones was digested with *Hind* III. The digested fragments were electrophoresed to identify any DNA bands at 1706bp, indicative of the RA. Numerous colonies were found to contain the construct. Diagram was created using Vector NTI (Invitrogen).

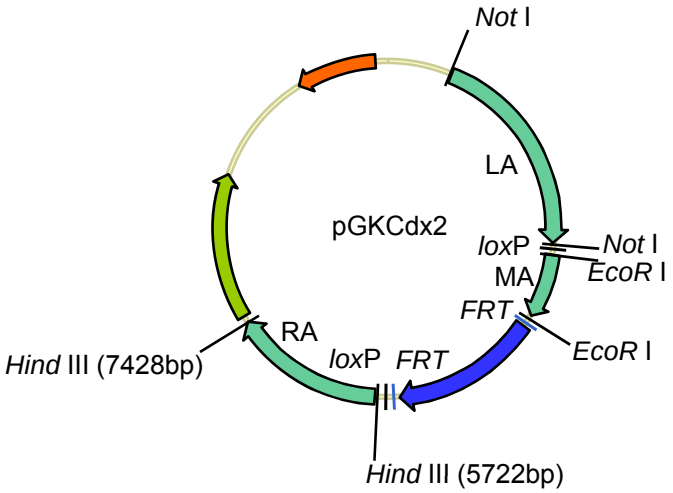

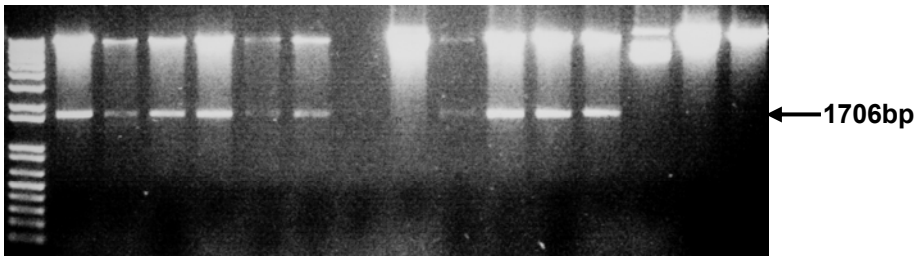

Figure 6.18 Confirmation of the orientation of the RA in pGKCdx2. Following restriction enzyme digest with *Nco* I, if the RA was in the correct orientation, then DNA bands of 2167bp and 805bp were seen on the gel (A). If the RA was in the incorrect orientation, then bands of 2337bp and 623bp were seen on the gel (B). Diagrams were created using Vector NTI (Invitrogen).

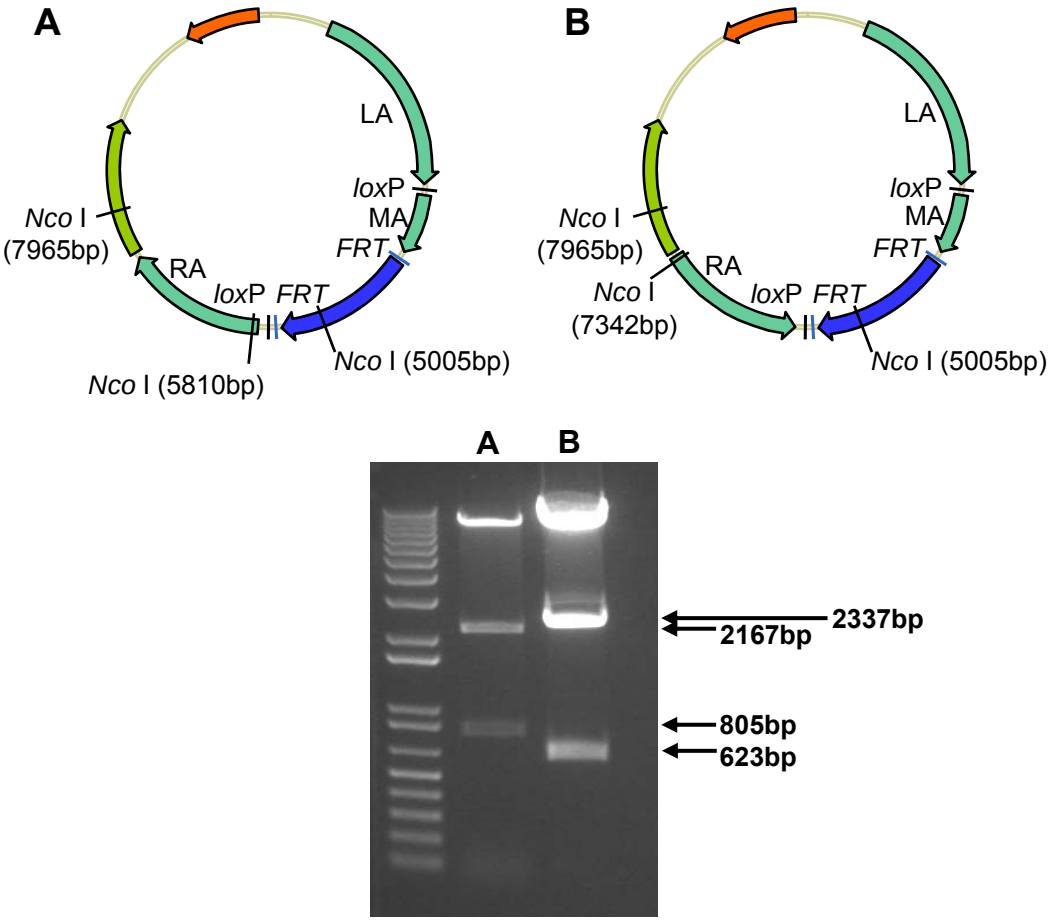

Figure 6.19 Determining the successful cloning of pGKCdx2. (A) The DNA from the clone was digested with *Not* I (No), *EcoR* I (E), *Nco* I (Nc), *Hind* III (H) and *EcoR* V (Ev). The bands seen on the gel were of the correct size to indicate that pGKCdx2 had been successfully cloned. (B) Sequencing with OES9, OES11, OES12, OES29 and T7 polymerase confirmed successful creation of pGKCdx2. Diagram was created using Vector NTI (Invitrogen).

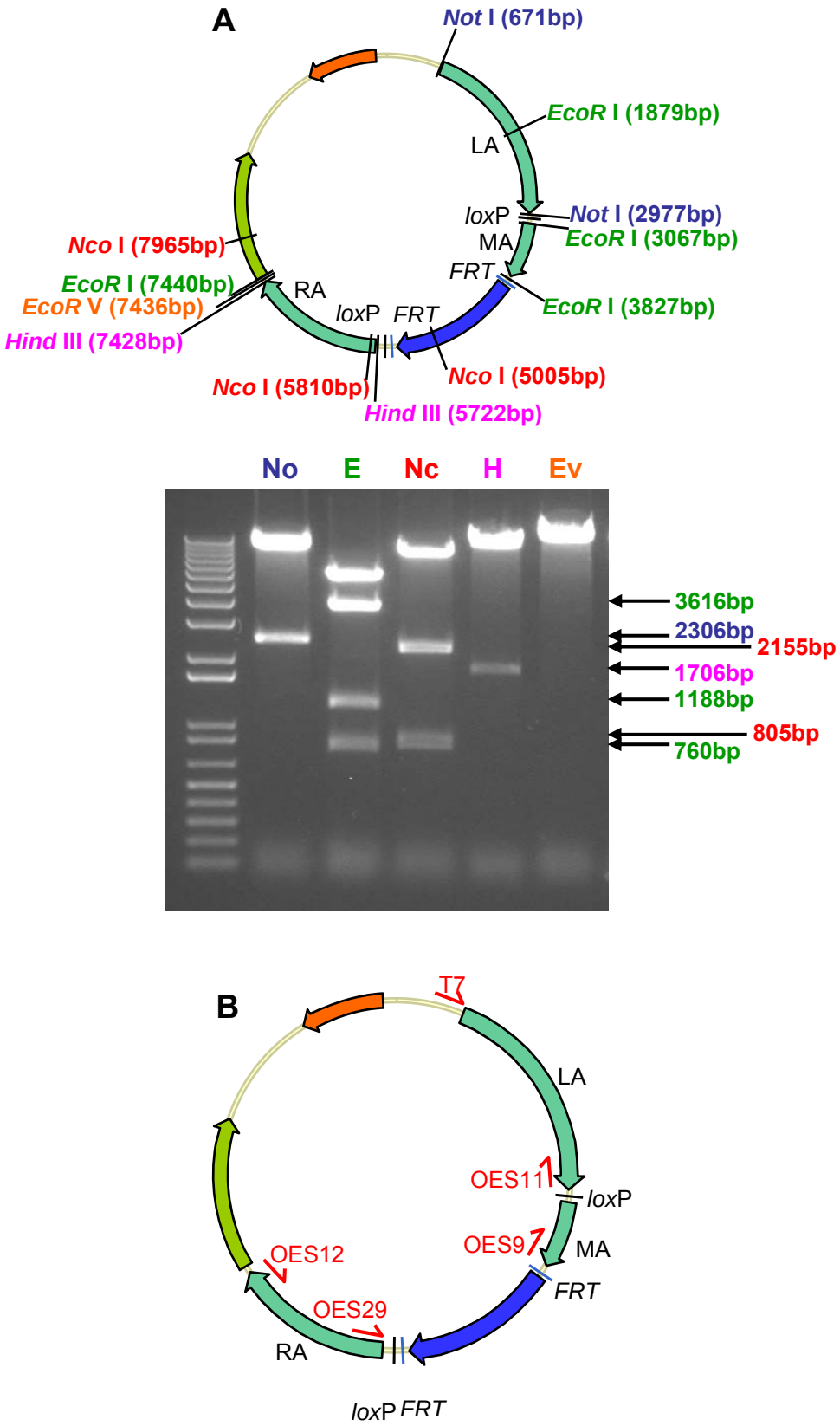

6.3.7 Creation of a positive control

The principles involved in the designing of the positive control were explained in section 6.3.1. The primers used for creating the positive arm were OES2 and OES11 (Figure 6.20). These primers also contained *Not* I restriction enzyme sites to allow this arm to be directly cloned into pGKNeoF2L2DTA. Following ligation of the *Not* I digested insert and vector, DNA was prepared from transformed clones. The DNA was digested with *Not* I to indicate the presence of the positive arm (data not shown). Restriction enzyme digest of this colony with *Afl* III indicated the correct orientation of the positive arm (Figure 6.21), confirmed by sequencing with primers OES2 and OCP66.

6.3.8 Large scale DNA preparation of pGKCdx2

The positive control plasmid, as with other constructs, was prepared using a standard caesium chloride method to generate large amounts of plasmid DNA. The pGKCdx2 plasmid, however, failed to successfully amplify using this technique. An EndoFree Plasmid Maxi Kit (Qiagen) was then used in an attempt to amplify the DNA and again this failed to produce sufficient DNA of a suitable quality. It was found that the bacterial life span appeared to be limited in broth when the plasmid was present; the reason for this is unknown, but the bacteria survived as expected when grown on plates. To overcome this problem, XL10-GoldR Ultracompetent Cells (Stratagene) were used for the transformation and subsequent clones were grown in Terrific Broth. The bacteria survived well when seeded into 5 ml aliquots of Terrific Broth and grown overnight, but beyond this the bacteria would not seed any further aliquots. To circumvent this problem and generate enough bacterial culture for use with the EndoFree kit, numerous colonies were seeded into 5 ml aliquots, grown overnight and then small scale DNA preparations performed to find the best quality bacterial broths. These were pooled for use with the EndoFree kit.

6.3.9 Confirmation of Cre-mediated recombination

The positive control and pGKCdx2 were linearised with *Xho* I (Figure 6.22) ready for electroporation into ES cells. The integrity of the *lox*P sites needed to first be tested, prior to homologous recombination in ES cells, to ensure that Cre-mediated recombination would be successful. A small amount of pGKCdx2 was therefore

Figure 6.20 Position of primer annealing sites used to create a positive control. OES11 was used to create the LA of the pGKCdx2 construct. It was used in combination with OES2 to generate an arm longer than the original LA. Diagrams created using Vector NTI (Invitrogen).

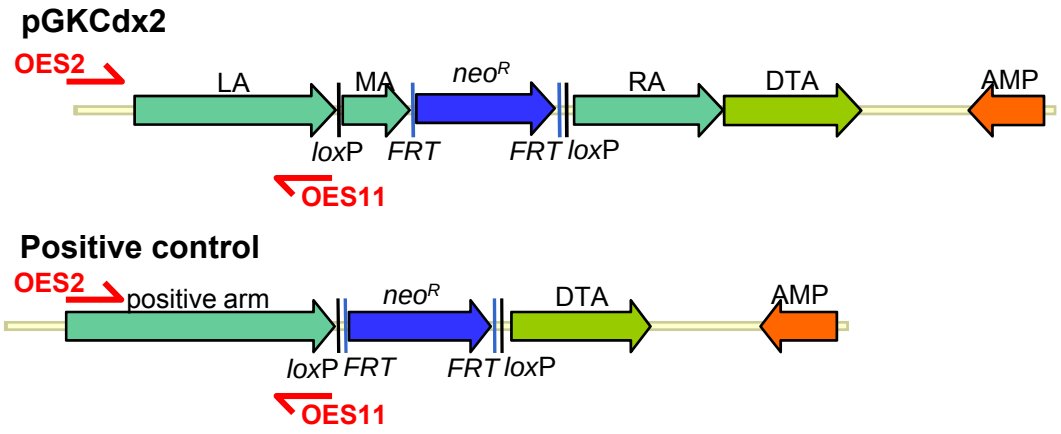

Figure 6.21 *Afl* III restriction enzyme digest to determine orientation of positive control arm in pGKNeoF2L2DTA. (A) positive arm in the correct orientation, indicating *Afl* III sites and the expected bands on the gel. (B) positive arm in the incorrect orientation, with *Afl* III sites indicated. The gel shows a colony following *Afl* III digest, with the insert in the correct orientation as shown in (A) (grey arrows and labels indicate the size of the bands expected following digest of the construct shown in (B)). Diagrams were created using Vector NTI (Invitrogen).

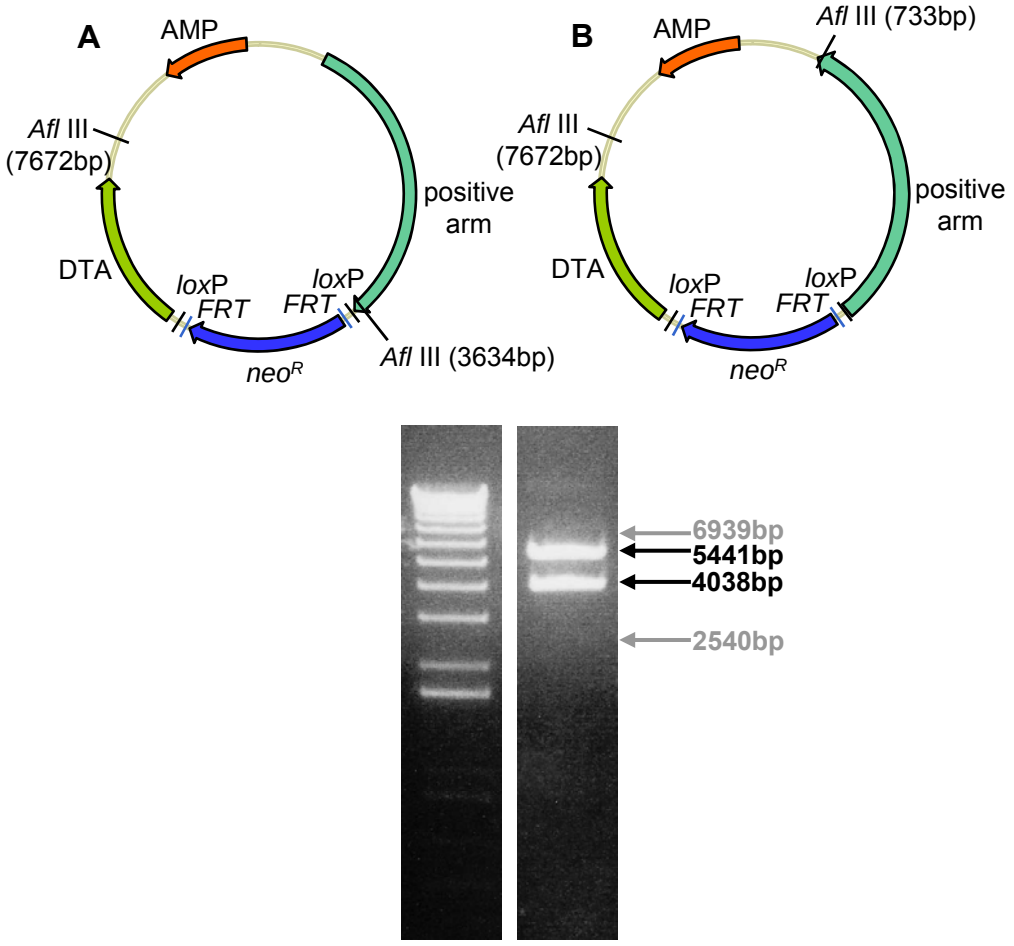

Figure 6.22 *Xho* I restriction enzyme sites in (A) positive control and (B) pGKCdx2. Both constructs contained a single *Xho* I site, in a position suitable to linearise the plasmid for electroporation into ES cells. Diagrams were created using Vector NTI (Invitrogen).

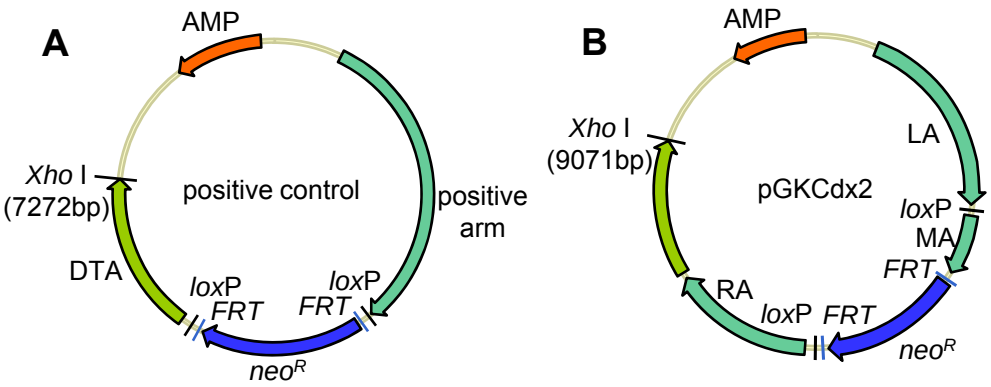

treated with Cre recombinase to ensure that the *lox*P sites were working effectively (Figure 6.23).

6.3.10 Electroporation and selection of ES Cells

The linearised constructs were electroporated into ES cells and G418 selection applied to select for clones containing the *neo*^{R} region of the construct. Any clones undergoing random recombination including the DTA cassette did not survive. This positive and negative selection reduced the number of surviving clones containing random recombinations and therefore increased the probability of selecting clones containing homologous recombination events (Figure 6.24). Prior experience involving electroporation of a previous *Cdx2* floxed construct in ES cells had indicated that homologous recombination events with *Cdx2* are notoriously rare and so 600 colonies were picked and screened to maximise the chances of finding recombinants. For the positive control, 50 colonies were picked. The PCR used for screening for homologous recombination was performed upon the first five of these positive control colonies; a band of the correct size was produced and so these samples were suitable as a positive control.

6.3.11 PCR screening of ES clones

The purpose of the positive control was as a confirmation of a successful PCR reaction when screening the ES cell clones for homologous recombination at the LA using OES30 and OES31. The strategy for the use of these primers was explained in section 6.3.1. A PCR product of 2.6Kb was produced with OES30 and OES31 only when the ES cell clones had undergone homologous recombination with pGKCdx2 in the left arm. Of the 600 colonies screened, only one contained a homologous recombination event at the left arm (designated clone pGKCdx2+) (Figure 6.25).

6.3.12 Analysis of pGKCdx2+

Having identified a clone that had undergone homologous recombination at the left arm, it had to be ensured that the floxed MA was also intact. Primers OES34 and OES35 were designed so that OES34 annealed to the construct between the *neo*^{R} cassette and the *FRT* site and OES35 annealed to the endogenous *Cdx2* DNA. A

Figure 6.23 Addition of Cre recombinase to pGKCdx2. Both gel images are the same gel, exposed at different levels. (A) Uncut pGKCdx2. (B) Linearised pGKCdx2. The linearised plasmid ran at 11.2Kb as expected. (C) Addition of Cre recombinase to pGKCdx2. A band of approximately 1.8Kb could be seen on the gel; this is the region of the plasmid between *lox*P sites, containing the MA, excised due to Cre-mediated recombination. This band appeared smaller than the expected 2665bp because this fragment was circular and so migrated quickly through the gel. An extremely dense band could also be seen in this lane; this contained both the linearised plasmid and the 8619bp fragment. An equilibrium exists between the linearised plasmid and the two products following addition of Cre recombinase and so a large amount of DNA was loaded to visualise the small circular fragment. Diagrams were created using Vector NTI (Invitrogen).

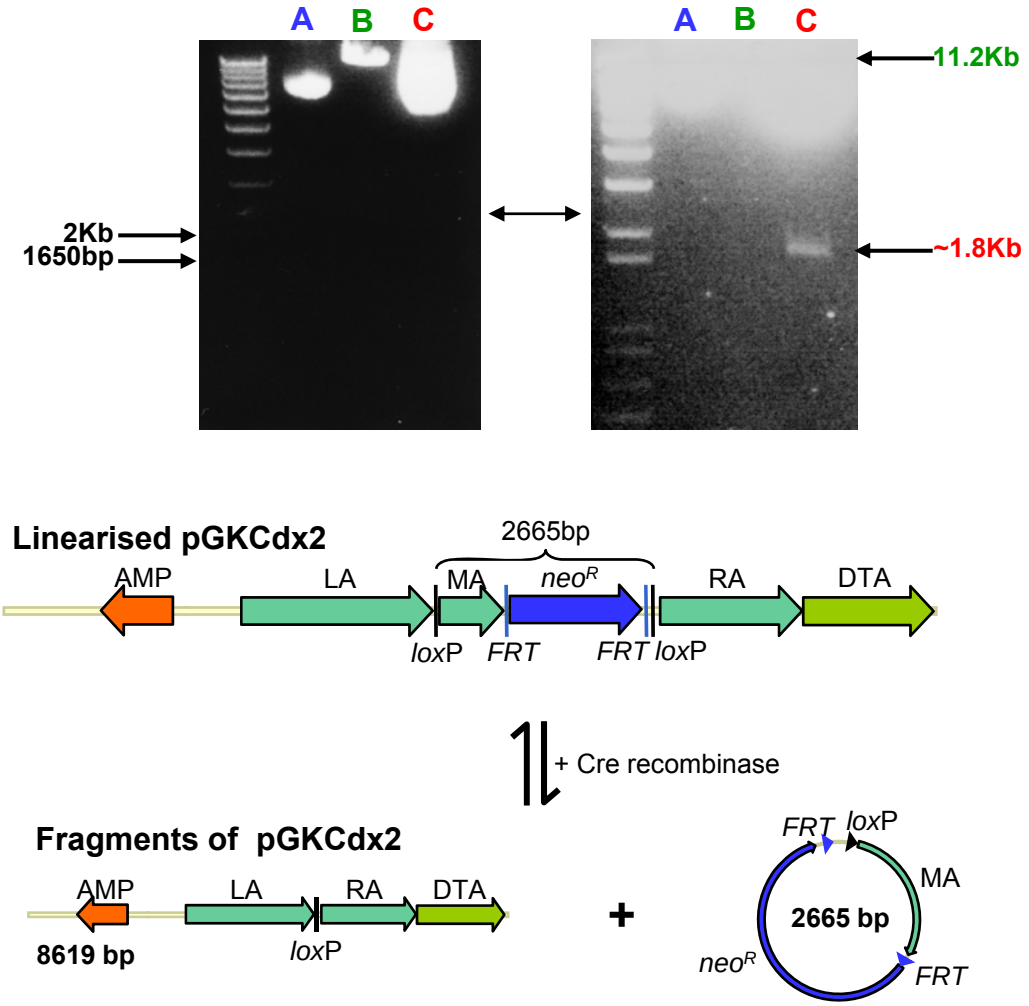

Figure 6.24 Homologous recombination of pGKCdx2 into ES cells. Recombination occurs between the LA and RA of pGKCdx2 and the endogenous *Cdx2* allele where the regions are homologous to each other (indicated by 'X'). This homologous recombination of the *Cdx2* allele results in the flanking of exon 2 with *lox*P sites and the loss of the DTA cassette. The *neo*^{R} cassette is retained however for positive selection of ES cell clones. Diagrams were adapted from Vector NTI (Invitrogen).

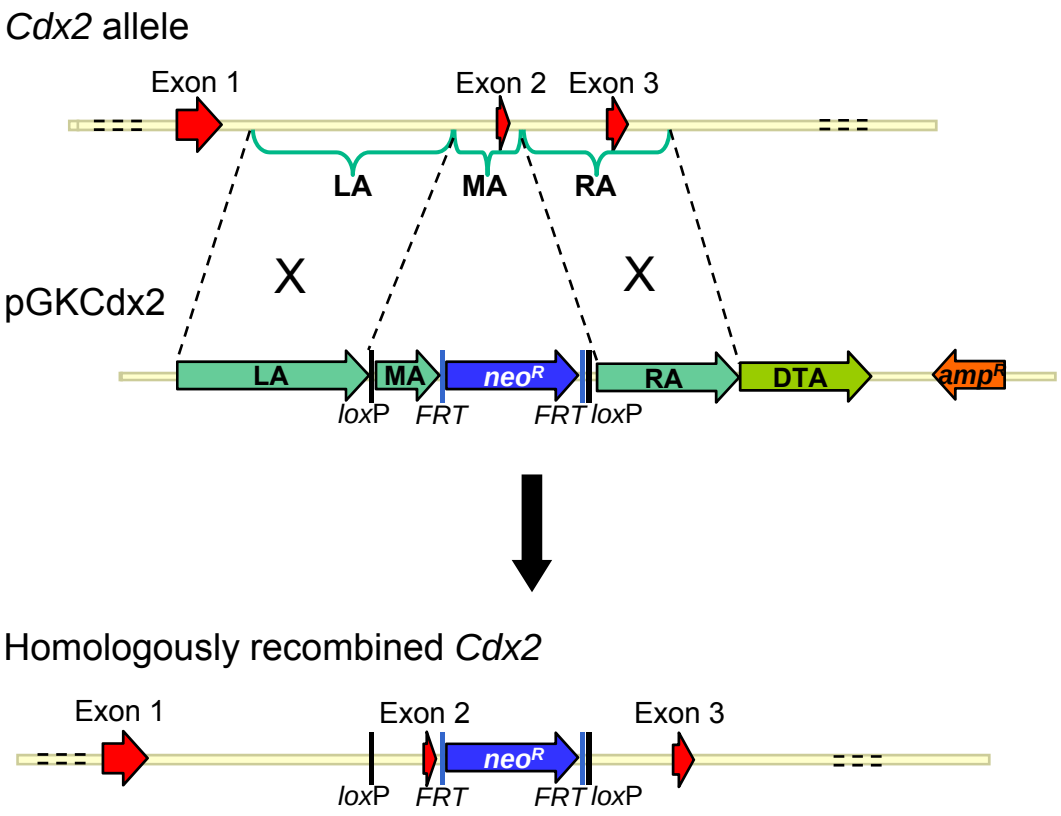

Figure 6.25 PCR screening for left arm homologous recombination. Primers OES30 and OES31 were used to screen DNA from clones picked following electroporation. The positive control was used to confirm success of the PCR reaction. Following screening of 600 colonies, only a single colony indicated left arm homologous recombination.

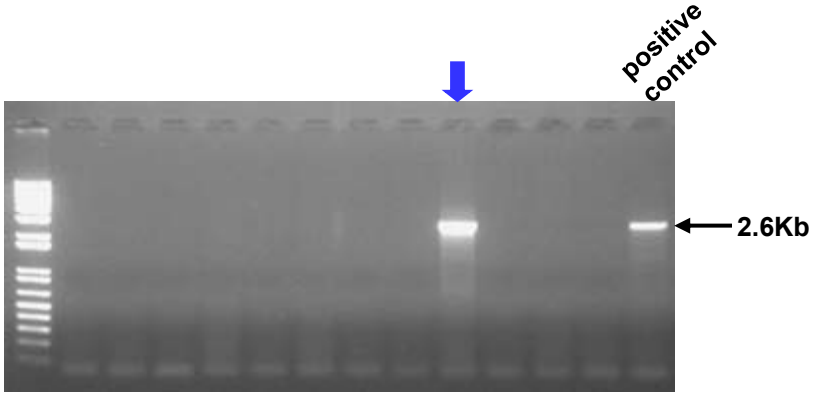

PCR product of 2.4Kb confirmed that the full construct was present with homologous recombination between the right arm and *Cdx2* (Figure 6.26).

Prior to injection of the pGKCdx2+ cells into blastocysts, a Southern blot was performed to provide some indication as to the number of non-homologously recombined events that had also occurred. A probe for the *neo*^{R} cassette was used. Restriction enzyme sites within the homologously recombined *Cdx2* gene were investigated. The purpose of this was to find a restriction enzyme that would digest the DNA to produce a fragment (containing the *neo*^{R} cassette) of a suitable size for detection by Southern blot. *Hind* III was determined to be suitable for this purpose (Figure 6.27). The pGKCdx2+ ES cell DNA was therefore digested with *Hind* III and the subsequent DNA fragments hybridised with the *neo*^{R} probe. A band of 10.1Kb was expected following exposure of the membrane to film.

Following development of the film, a band of 10.1Kb was detected, confirming the homologous recombination event. However, one other band was also present which indicated the presence of a random recombination event in this clone (Figure 6.28). Despite the presence of this other integration, this ES clone pGKCdx2+ was used to make mice.

6.3.13 Injection of blastocysts

pGKCdx2+ was injected into blastocysts despite the additional recombination event detected by Southern blot. Following injection of the pGKCdx2+ ES cell clone into blastocysts, three offspring were produced. Unfortunately these were all WT in coat colour with no evidence of chimerism.

The pGKCdx2+ ES cell clone was also sent to another laboratory (J. Deschamps, Hubrecht Laboratory, Utrecht, The Netherlands) where it was injected into blastocysts. From a total of 134 injected blastocysts, only six pups were born. One pup was found dead in the cage and two others were found to be chimeras. Of these two chimeras, one did not breed and the other failed to produce any germline offspring. This suggests an inherent problem with the pGKCdx2+ cells (see discussion).

Figure 6.26 PCR to determine homologous recombination at the right arm in pGKCdx2+. A PCR was performed upon DNA extracted from the ES cell clone containing pGKCdx2 homologously recombined at the LA. The primers used were OES34 (anneals to pGKCdx2) and OES35 (anneals to endogenous DNA). A band of the correct size was produced, indicating homologous recombination at the right arm.

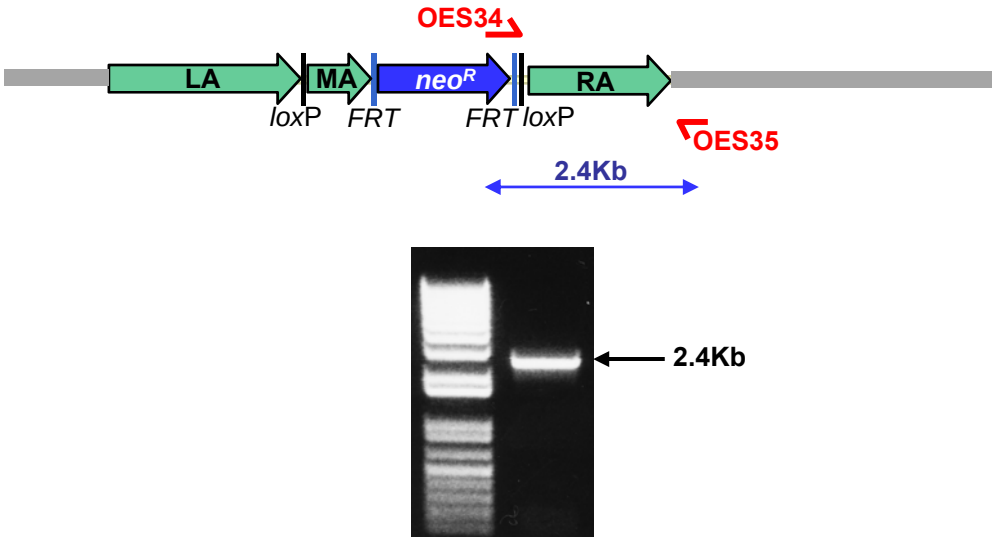

Figure 6.27 Position of *Hind* III sites in relation to *neo*^{R} probe in pGKCdx2+ clone. (A) The diagram indicates the position of the pGKCdx2 construct within the endogenous *Cdx2* DNA. On either side of this is the rest of chromosome 5 (indicated in grey). Within the pGKCdx2/endogenous *Cdx2* sequence, there is one *Hind* III site. Further sites are located in chromosome 5, outside of the *Cdx2* gene. Following *Hind* III digest of the DNA and hybridisation with a radioactive *neo*^{R} probe (shown in red) a fragment of 10.1Kb is indicative of the homologous recombination event. Any additional bands indicate recombination of the region of the construct containing the *neo*^{R} cassette, into other regions of the genome. (B) The WT *Cdx2* allele is shown within chromosome 5 (again indicated by grey lines). There are no *Hind* III sites within the *Cdx2* allele. Diagrams were created using Vector NTI (Invitrogen).

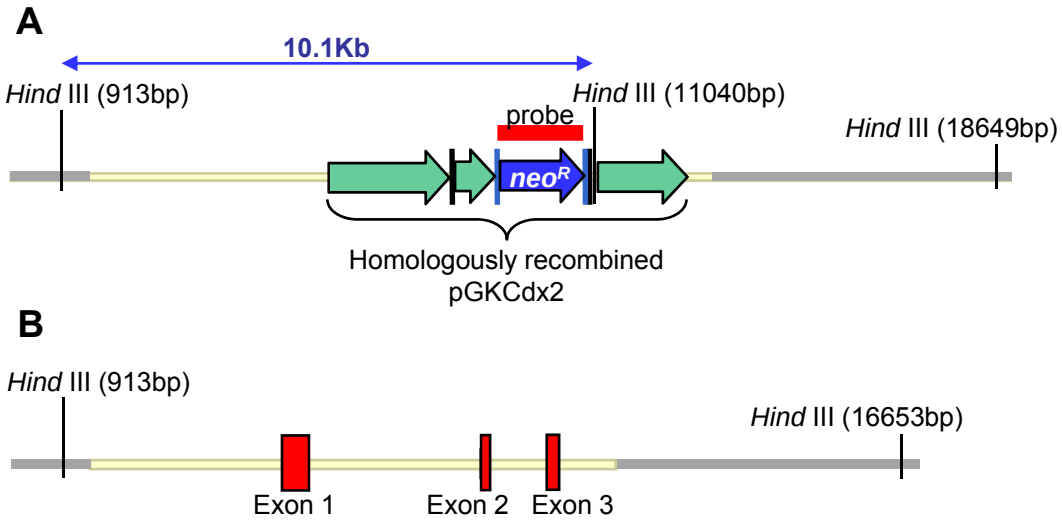

Figure 6.28 Southern blot of ES cell DNA. The *Hind* III digested DNA was hybridised with a *neo*^{R} probe. The ES cell clones in lanes 1 and 2 were random recombinants. Lane 3 contains the pGKCdx2+ ES cell clone. A band can be seen at approximately 10.1Kb (black arrow), indicative of the targeted allele. The pGKCdx2+ ES cell clone also contained another random recombination event containing the *neo*^{R} cassette, as indicated by the other *Hind* III fragment, which produced a strong band for unknown reasons (grey arrow).

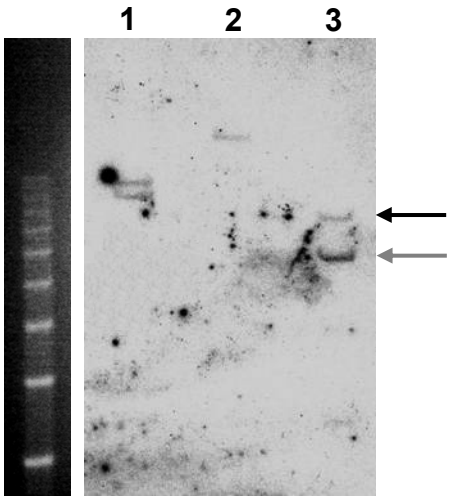

With this in mind, the same laboratory also re-electroporated pGKCdx2 into more ES cells in the hope of finding further homologous recombinants; this was successful and a further three clones were identified from 400+ colonies. A Southern blot was performed upon these clones, again using a *neo*^{R} probe, alongside pGKCdx2+ (Figure 6.29). Again, the pGKCdx2+ clone produced a 10.1Kb band alongside a darker band at 8Kb. The newly identified homologously recombined clones (Figure 6.29: lanes 2-4) produced a single band at 10.1Kb. Two of the clones (Figure 6.29: lanes 2 and 3) were injected into blastocysts (lane 2: 39 blastocysts, lane 3: 36 blastocysts). From these injections, 9 chimeras out of 14 pups were recovered from the clone shown in lane 2 and 5 chimeras out of 10 pups were recovered from the clone shown in lane 3. These chimeras were crossed to FVB mice. Two males have indicated successful germline transmission; the offspring are currently being crossed to *FLPeR* mice to remove the *Neo*^{R} cassette.

6.4 Conclusion

The creation of a conditional *Cdx2* mouse line has been attempted for the past 5-6 years; this is now close to being achieved. A *Cdx2* conditional construct utilising just the *lox*P system existed prior to me starting in the lab but had failed to successfully undergo homologous recombination, possibly because the left and right arms were not long enough for a recombination event to occur within them.

Due to this and the availability of a dual system involving both *lox*P and *FRT* sites, a whole new cloning strategy was designed. The designing of the construct was however extremely difficult. The 3' end of *Cdx2* contains regions resistant to cloning and so is not fully sequenced. The length of the right arm therefore had to be shorter than it was originally hoped. The *Cdx2* gene also contains a vast number of restriction enzyme sites making the choice of restriction enzymes for cloning extremely limited. This meant that the cloning strategy involved many unavoidable cloning steps and the occasional use of inefficient enzymes; the whole process was therefore extremely time consuming. Fortunately, the amplification of the three arms was reasonably straightforward, as was the cloning of these inserts into pBluescriptSKII+. The cloning of the MA into pGKNeoΔNcoI and subsequent cloning of the MA fragment into pGKNeoF2L2DTA was performed without significant

Figure 6.29 Southern blot performed upon new homologous recombinants obtained at the Hubrecht Laboratory. pGKCdx2 was re-electroporated into ES cells in the Hubrecht Laboratory and a Southern blot performed upon three possible homologous recombinants. The DNA was digested with *Hind* III and a *neo*^{R} probe was used; a 10.1Kb band is indicative of the homologously recombined allele. Lane 1 contains the original pGKCdx2+ ES cell clone, lanes 2, 3 and 4 contain the new recombinants. Southern blot performed by T. Young, Hubrecht Laboratory, Utrecht, The Netherlands.

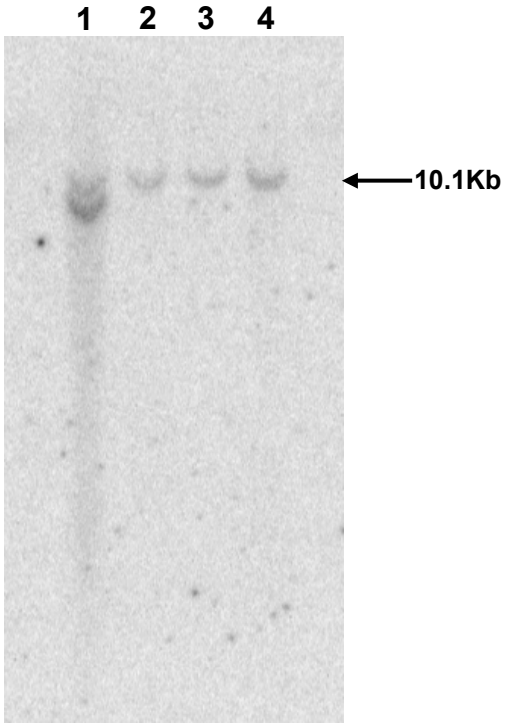

problems. The cloning of the LA into this construct also occurred with relative ease. The cloning of the RA however, proved to be extremely difficult; pGKCdx2(MA/LA) and the RA failed to ligate and transform bacteria for many weeks. For unknown reasons, one transformation proved to be extremely fruitful and so creation of the pGKCdx2 construct was experimentally completed, although large-scale preparation of the plasmid was also challenging.

Since the pGKCdx2 cloning strategy commenced, the use of recombination-mediated genetic engineering (recombineering) has become more frequently used. This system is based on homologous recombination occurring in bacteria, caused by the temperature sensitive expression of recombination proteins derived from phage. The recombineering strategy is useful when conventional cloning techniques are limited by the availability of suitable restriction enzyme sites. The linear DNA arms to be introduced into the plasmid backbone are designed so that they are flanked by regions homologous to the backbone vector. The bacterial expression of the recombination proteins in the presence of the linear DNA arm causes homologous recombination of the arm into the vector without the use of restriction enzymes. If the strategy to create the *Cdx2* conditional knock-out construct was designed now, this approach would possibly be taken.

Due to the technical difficulties of manipulating this construct, it was decided that the neo^R cassette would be left intact until the ES cells successfully underwent germline transmission in mice. One problem with this is that the neo^R cassette may disrupt the transcription/translation of *Cdx2* of this allele. Only one allele is targeted and so the other allele is unaffected. The mice will therefore effectively be heterozygous and therefore capable of survival and breeding as seen in the conventional $Cdx2^{+/-}$ mice. The neo^R cassette will then be deleted by crossing the mice to a Flp-expressing strain and so the conditional *Cdx2* allele will be functional in the offspring.

Following electroporation of pGKCdx2 into ES cells and PCR screening of the resultant colonies, only one clone contained a successful homologous recombination event. A subsequent Southern blot indicated a random recombination event in this pGKCdx2+ ES cell clone. This could have occurred in a gene required for embryonic

survival and so normally, when various clones are available, the clones containing the least number of random recombinations are used for blastocyst injection. In this project, only one pGKCdx2+ ES cell clone was achieved and the lack of chimeric offspring following the injection of blastocysts in this laboratory suggested that a random recombination event had possibly caused disruption of a gene essential for embryonic survival. Chimeras generally only contain relatively few mutant cells within a WT host and so embryonic lethality of chimeras is not expected. The fact that only two chimeras were obtained in the Hubrecht Laboratory and both of these were extremely small and weak suggests that the number of incorporated pGKCdx2+ cells may dictate whether embryonic lethality occurs or whether the level of mutant cells is low enough to permit survival of a weak specimen.

Due to the apparent inherent problem with the pGKCdx2+ clone, pGKCdx2 was electroporated into ES cells in the Hubrecht Laboratory. Three homologously recombined clones were identified and two of these were injected into blastocysts. The resultant chimeras have been crossed to FVB mice to achieve germline transmission to create the *Cdx2*$^{WT/LoxFRT}$ mouse strain. These mice are now being crossed to Flp-expressing mice (the *FLPeR* strain) to remove the *neo*^{R} cassette (Figure 6.30A). The resultant *Cdx2*$^{WT/Lox}$ mice will most likely be crossed to the Ah*cre*ER^{T} strain (Figure 6.30B). Subsequent crosses of the resultant *Cdx2*$^{WT/Lox}$/Ah*cre*ER^{T}/WT mice with *Cdx2*$^{WT/Lox}$ mice will produce mice homozygous for the *Cdx2* conditional allele and heterozygous for the Ah*cre*ER^{T} allele (*Cdx2*$^{Lox/Lox}$/Ah*cre*ER^{T}/WT) (Figure 6.30C). The mice must be homozygous for the conditional allele as *Cdx2*$^{Lox/-}$ mice will demonstrate a phenotype prior to expression of *Cre* as they will be functionally heterozygous. *Cdx2* can be conditionally knocked out in the *Cdx2*$^{Lox/Lox}$/Ah*cre*ER^{T}/WT mice on the addition of β-napthoflavone and 4-OHT. The crossing of these mice to *R26R* can provide some indication as to where *Cre* expression is occurring and therefore the regions hopefully undergoing conditional *Cdx2* knock-out. The Cdx2 conditional knock-out mice will be instrumental in addressing the potency of the intestinal stem cells.

The entire process, from the creation of the pGKCdx2 construct to injection of blastocysts, was a major undertaking. This aspect of the project took half the total

Figure 6.30 Breeding strategy to achieve *Cdx2* conditional knock-out mice. (A) The crossing of the *Cdx2*$^{WT/LoxFRT}$ to FLPeR will cause excision of the *neo*^{R} cassette. (B) The offspring can then be crossed with an inducible *Cre*-expressing strain such as Ah*cre*ER^{T}. (C) The *Cdx2*$^{WT/Lox}$/Ah*cre*/WT offspring can then be crossed to *Cdx2*$^{WT/Lox}$ mice to produce *Cdx2*$^{Lox/Lox}$ mice that are also carrying the Ah*cre*ER^{T} allele. *Cdx2* can be conditionally knocked-out in these mice upon the addition of β-napthoflavone and 4-OHT. The ratio of mice produced of the required genotype, based on Mendelian inheritance, is shown in brackets.

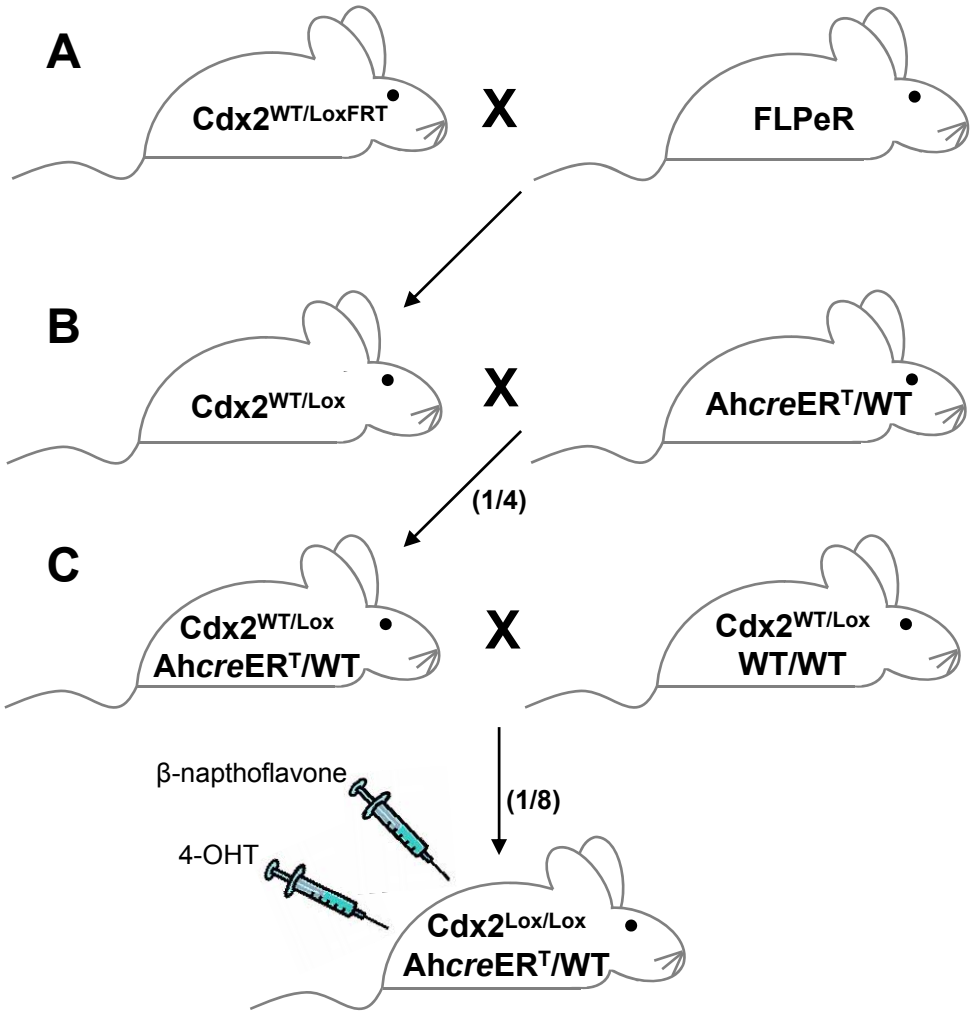

time spent in the laboratory and so the importance of this *Cdx2* conditional mouse line cannot be underestimated. The conditional knock out will allow the investigation of the ability of both the epithelium and mesoderm to respond to the loss of expression of a gene so fundamentally involved in specifying tissue type. The point at which the stem cells may loose potential can be investigated by knocking out *Cdx2* at different developmental stages and the response investigated.

7. Summary and Discussion

7.1 Investigating endoderm to mesodermal signalling

7.1.1 Project background

Information regarding endoderm-mesodermal signalling in the intestine is limited; it was not previously known whether the mesoderm responds to fundamental endodermal signals prior to cytodifferentiation occurring in the gut epithelium. One of the principal aims of this project was to address this. Two possibilities were considered here; either the mesoderm responds to signals from the overlying endoderm or it relies on signals from adjacent regions of mesoderm to specify position along the gastro-intestinal tract. It may also be possible that a combination of these events occurs.

The *Cdx2* mutant mouse models provide a useful approach to investigate whether the endoderm and mesoderm interact. These mice develop gastric-epithelium type tissue in the intestine (Beck et al., 2003). This was shown to be due to a loss of endodermal *Cdx2*. This project therefore investigated whether an alteration in endodermal gene expression resulted in a response in the underlying mesoderm.

The mesoderm underlying the gastric heterotopia could not be determined histologically at early developmental stages to be of stomach or intestinal type; expression of markers had to be investigated. Gene expression within the mesoderm is more likely to be stomach or intestine-specific during development when tissue type is being determined. For this reason, the expression of endodermal and mesodermal genes was investigated at the embryonic stage.

7.1.2 Identifying gastric heterotopias

The gastric heterotopias could not be detected histologically during early development. The nature of the developing heterotopias first had to be investigated to determine the developmental stage and region of the intestine that was optimal for investigating mesodermal gene expression. A marker for stomach endoderm was therefore required in order to detect developing gastric heterotopias in embryonic

intestine; it was hypothesised that *Sox2* would be a suitable marker (Que et al., 2007). This was proved to be correct, as shown in Chapter 3; *Sox2* was used to identify the regions of gastric endodermal heterotopia developing in the intestine of *Cdx2* mutant embryos. These regions were mostly clustered around the paracaecal area and appeared from 12.5dpc onwards. The distribution of embryonic heterotopias generally reflected that seen in the *Cdx2* mutant adults, although some regions were located more proximally than expected. It was deemed that 14.5dpc was the ideal stage at which to investigate gene expression in the underlying mesoderm.

7.1.3 Investigating mesodermal gene expression underlying gastric heterotopias

It was hypothesised that the mesoderm underlying the gastric heterotopias of the *Cdx2* mutant intestine may respond to overlying endodermal signals. Initially a PCR approach was undertaken to screen samples of *Cdx2* mutant caecum for stomach-mesoderm specific gene expression. *Barx1*, an example of such a gene (Kim et al., 2005), was found to be expressed in some of these samples, as shown in Chapter 4. *In-situ* hybridisation was then performed using DIG-labelled *Barx1* probes, as shown in Chapter 5. The distribution and frequency of regions expressing *Barx1* reflected that seen using *Sox2* probes. The data suggests that the hypothesis may be correct; the mesoderm appeared to be responding to endodermal stomach-specific signals.

To confirm the occurrence of cross-talk between the endoderm and mesoderm, *Sox2* and *Barx1* expression was co-localised on serial sections in both *Cdx2*$^{+/-}$ and *Cdx2*$^{-/-}$ //WT samples. This indicated that areas of the mesoderm underlying the *Sox2* expressing gastric endoderm were expressing stomach specific *Barx1.* Some regions appeared to express *Sox2* without underlying *Barx1* expression; this is thought to reflect the fact that *Barx1* expression may be regional within the stomach and therefore regional within the intercalated heterotopias. The regions found to be expressing *Sox2* were developing in the absence of Cdx2, as shown by the use of a Cdx2 antibody upon sections from the *Cdx2*$^{-/-}$//WT sample.

From these findings it can be concluded that the hypothesis was correct; the mesoderm responds to fundamental signals received from the endoderm (Figure 7.1).

7.1.4 Further Work

This project has addressed the expression of three genes in different tissue layers; *Cdx2* is mutually exclusive to *Barx1* and *Sox2*. It is not known what signalling factors are involved in maintaining this mutual exclusivity (Figure 7.1), although from this project it has been shown that *Cdx2* expression must result in the expression of signalling factors that repress expression of *Barx1*. It is also not known how *Sox2* is involved in this signalling pathway; *Sox2* expression is either downstream of *Barx1* or *Cdx2* represses *Sox2* expression more directly without the involvement of the mesoderm (Figure 7.1). These two questions can be studied further by different approaches.

To study the signalling pathways involved between the endoderm and mesoderm further, a microarray screen could be used to highlight any changes in gene expression between WT and *Cdx2* mutant caecum. Gene ontology could then be used to identify any possible candidate genes involved in endoderm-mesoderm signalling for further investigation. One such candidate gene may be *Bmp4*. This soluble factor has been shown to repress *Barx1* expression in the jaw (Tucker et al., 1998) and is known to be expressed in the intestine (Roberts et al., 1995, Kaestner et al., 1997). There appears to be no data directly linking *Cdx2* expression and Bmp4 so this could be of potential interest. Further investigation of these signalling pathways may also provide indications as to why the *Barx1* expression seen underlying *Sox2* expression in the heterotopias was regional; the intercalation normally seen in the gastric heterotopias of the *Cdx2* mutant may be the result of different levels of *Sox2* expression thus causing signalling gradients within which *Barx1* is expressed.

To further study the level at which *Sox2* expression is controlled, *Cdx2* expression could be induced in appropriate *Sox2* expressing epithelial cells. If *Sox2* expression is repressed, this will indicate that *Sox2* repression occurs due to endodermal signals

Figure 7.1 Diagram illustrating the project findings in relation to the original hypothesis. It was known, from studies of *Barx1*$^{-/-}$ mice that the mesoderm signals to the endoderm (red arrows). It was hypothesised that the initial signal (*Cdx2*) originates in the intestinal endoderm and the mesoderm responds to this expression. This project has shown that a loss of endodermal Cdx2 results in the expression of stomach-mesoderm specific *Barx1*, i.e. the hypothesis was proven (blue arrows). *Sox2* has been shown to be expressed in the endoderm in the regions not expressing *Cdx2*, although it is not known whether *Sox2* expression is downstream or upstream of the endoderm-mesodermal interactions involving *Barx1* (the two possible signalling pathways leading to *Sox2* expression are shown by green arrows). This project has not addressed the genes involved in the intestinal endoderm-mesodermal interactions (shown by the yellow box) nor has the stomach signalling pathway been exhaustively studied; these issues form part of the future work for this project.

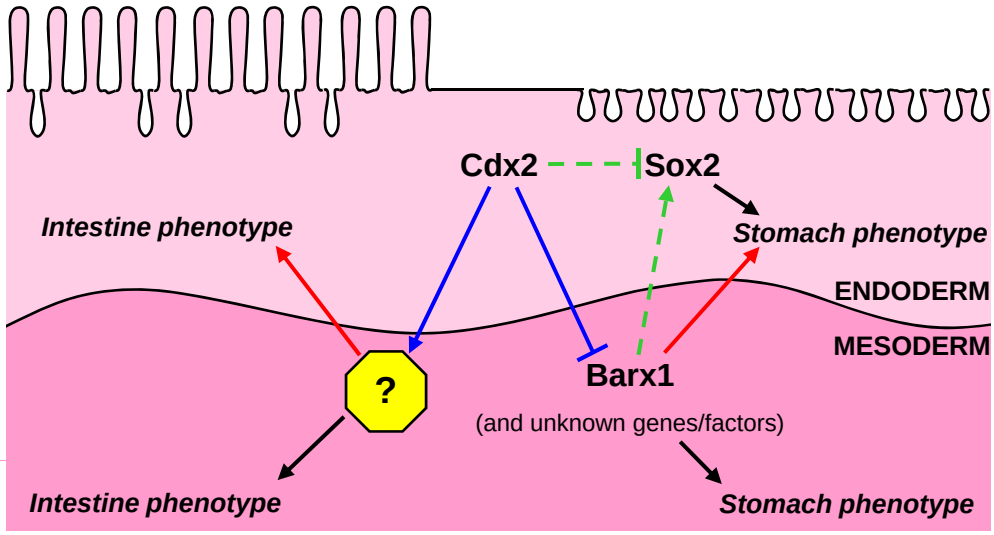

originating from *Cdx2* expression. If *Sox2* expression remains unaltered, then it is more likely that mesodermal factors are required in the signalling cascade and that *Sox2* expression is possibly downstream of *Barx1*.

7.2 Creation of a conditional *Cdx2* transgenic mouse line

7.2.1 Project background

Previous evidence has suggested that *Cdx2*$^{+/-}$ mice do not develop additional heterotopic lesions postnatally (Beck et al., 1999). This was a significant observation because the epigenetic factors and random mutations thought to cause the haploinsufficiency of *Cdx2* expression are also thought to continue into adulthood. The stem cells from which the intestinal epithelium arises may have therefore become committed down an intestinal lineage, despite the loss of instructive *Cdx2* expression.

What causes this possible alteration and the point at which it occurs is currently unknown, as is the level of determination of these adult intestinal stem cells. This information may have major implications for the use of intestinal stem cells for regeneration of adult tissue. The ability to conditionally knock-out *Cdx2* in the intestine at different developmental stages will allow these unknown factors to be investigated.

7.2.2 Design and creation of the Cdx2 conditional mouse line

A number of conditional targeting vectors had already been attempted both in this laboratory and others; all appeared to have failed to undergo homologous recombination. It was decided to design a new targeting vector utilising both *lox*P and *FRT* sites; this approach would make the downstream removal of the selection cassette much easier than the use of *lox*P sites alone.

The vector was designed so that the functional region of *Cdx2* was flanked by *lox*P sites. The subsequent mouse strain could then be crossed to a *Cre* expressing strain to conditionally knock-out *Cdx2*. The regions designed to undergo homologous recombination with the endogenous *Cdx2* gene (i.e. the left arm and right arm) were

designed so that they were as long as possible to hopefully overcome the lack of homologous recombination events experienced previously.

The creation of the targeting vector, pGKCdx2, proved to be a major undertaking, comprising half the total time spent on this project. The complexity of the construct meant that numerous cloning stages were involved; the most difficult being those involving the right arm, for unknown reasons. Once successfully cloned, it was found that pGKCdx2 does not amplify well in bacteria, again for unknown reasons. Despite this, the construct was successfully made and amplified ready for electroporation into ES cells. A total of 600 ES cell colonies were screened; one indicated homologous recombination at the left arm. Subsequent investigation confirmed the entire targeting vector had recombined into the endogenous *Cdx2* gene, but a random integration was also present.

The targeted ES cell clone was injected into blastocysts both in Leicester and The Hubrecht Laboratory. The clone failed to successfully produce chimeras from which germline transmission could be achieved. Following re-electroporation in The Hubrecht Laboratory, a further three homologous recombinants were obtained. Injection of two of these clones into blastocysts has resulted in chimeras that have been bred for germline transmission. The resultant mice are now being crossed to *FLPeR* mice to remove the *Neo*^{R} cassette. The *Cdx2* conditional knock-out mouse line has therefore been successfully achieved.

7.2.3 Further Work

The potential uses of a conditional *Cdx2* transgenic mouse line are quite varied. Within this laboratory, as discussed earlier in the chapter, the mice will be used to identify the stage and degree to which embryonic intestinal stem cells lose potency and become restricted. These mice will also be used, in collaboration with J-N Freund (Inserm, Strasbourg), to investigate the progression of intestinal tumours into a malignant phenotype, upon the loss of *Cdx2*; this will mimic the situation reported in human colon cancer and hopefully provide a realistic mouse model for the disease. The role of *Cdx2* in cancer is largely unknown, as discussed in chapter 1 and so these mice will be of vital importance in this study. This conditional mouse line can

also be used to investigate the roles of *Cdx2* beyond the requirement of the gene for trophoblast development. The universal loss of *Cdx2* in the placental-stage embryo has never previously been studied.

7.3 Conclusion

Cdx2 mutant mouse models have been used to demonstrate that the intestinal mesoderm responds to overlying endodermal signals. An alteration in expression of an endodermal gene fundamentally involved in midgut development (*Cdx2*) leads to expression of a mesodermal gene fundamentally involved in stomach development (*Barx1*). It has therefore been concluded that the mesoderm is responsive to endodermal signals and that *Cdx2* represses *Barx1* expression. It is not currently known what factors are involved in the interaction of the two genes; this would be the subject of further work.

The *Cdx2* mouse models used in this study have limitations. The mice are not ubiquitously null for the gene; they are haploinsufficient or chimeric as null mice die at implantation (Chawengsaksophak et al., 1997). The use of tetraploid fusion techniques only supported embryonic *Cdx2*$^{-/-}$ survival until 11.5dpc; the point at which *Cdx2* is required for normal placental development (Chawengsaksophak et al., 2004). The universal loss of *Cdx2* cannot therefore be studied beyond the placental-stage with these current models. The creation of a *Cdx2* conditional knockout mouse line will permit the manipulation of *Cdx2*. Expression of the gene can be spatially and temporally turned off to allow the role of *Cdx2* to be investigated in various processes. These studies include investigation of intestinal stem cell potential and creation of mouse models for colon cancer.

References

AMANN, J. M., CHYLA, B. J., ELLIS, T. C., MARTINEZ, A., MOORE, A. C., FRANKLIN, J. L., MCGHEE, L., MEYERS, S., OHM, J. E., LUCE, K. S., OUELETTE, A. J., WASHINGTON, M. K., THOMPSON, M. A., KING, D., GAUTAM, S., COFFEY, R. J., WHITEHEAD, R. H. & HIEBERT, S. W. (2005) Mtgr1 is a transcriptional corepressor that is required for maintenance of the secretory cell lineage in the small intestine. Mol Cell Biol, 25, 9576-85.

ANDREU, P., COLNOT, S., GODARD, C., GAD, S., CHAFEY, P., NIWA-KAWAKITA, M., LAURENT-PUIG, P., KAHN, A., ROBINE, S., PERRET, C. & ROMAGNOLO, B. (2005) Crypt-restricted proliferation and commitment to the Paneth cell lineage following Apc loss in the mouse intestine. Development, 132, 1443-51.

ANG, S. L. & ROSSANT, J. (1994) HNF-3 beta is essential for node and notochord formation in mouse development. Cell, 78, 561-74.

AOKI, K., TAMAI, Y., HORIIKE, S., OSHIMA, M. & TAKETO, M. M. (2003) Colonic polyposis caused by mTOR-mediated chromosomal instability in Apc+/Delta716 Cdx2+/- compound mutant mice. Nat Genet., 35, 323-30.

AULEHLA, A., WEHRLE, C., BRAND-SABERI, B., KEMLER, R., GOSSLER, A., KANZLER, B. & HERRMANN, B. G. (2003) Wnt3a plays a major role in the segmentation clock controlling somitogenesis. Dev Cell, 4, 395-406.

AVILION, A. A., NICOLIS, S. K., PEVNY, L. H., PEREZ, L., VIVIAN, N. & LOVELL-BADGE, R. (2003) Multipotent cell lineages in early mouse development depend on SOX2 function. *Genes Dev,* 17**,** 126-40.

AYABE, T., SATCHELL, D. P., WILSON, C. L., PARKS, W. C., SELSTED, M. E. & OUELLETTE, A. J. (2000) Secretion of microbicidal alpha-defensins by intestinal Paneth cells in response to bacteria. Nat Immunol, 1, 113-8.

BARKER, N., VAN ES, J. H., KUIPERS, J., KUJALA, P., VAN DEN BORN, M., COZIJNSEN, M., HAEGEBARTH, A., KORVING, J., BEGTHEL, H., PETERS, P. J. & CLEVERS, H. (2007) Identification of stem cells in small intestine and colon by marker gene Lgr5. Nature, 449, 1003-7.

BATLLE, E., HENDERSON, J. T., BEGHTEL, H., VAN DEN BORN, M. M., SANCHO, E., HULS, G., MEELDIJK, J., ROBERTSON, J., VAN DE WETERING, M., PAWSON, T. & CLEVERS, H. (2002) Beta-catenin and TCF mediate cell positioning in the intestinal epithelium by controlling the expression of EphB/ephrinB. Cell, 111, 251-63.

BECK, F. (2002) Homeobox genes in gut development. Gut, 51, 450-4.

BECK, F., CHAWENGSAKSOPHAK, K., LUCKETT, J., GIBLETT, S., TUCCI, J., BROWN, J., POULSOM, R., JEFFERY, R. & WRIGHT, N. A. (2003) A study of regional gut endoderm potency by analysis of Cdx2 null mutant chimaeric mice. Dev Biol, 255, 399-406.

BECK, F., CHAWENGSAKSOPHAK, K., WARING, P., PLAYFORD, R. J. & FURNESS, J. B. (1999) Reprogramming of intestinal differentiation and intercalary regeneration in Cdx2 mutant mice. Proc Natl Acad Sci U S A, 96, 7318-23.

BECK, F., ERLER, T., RUSSELL, A. & JAMES, R. (1995) Expression of Cdx-2 in the mouse embryo and placenta: possible role in patterning of the extra-embryonic membranes. Dev Dyn, 204, 219-27.

BECK, F., MOFFAT, D. B. & DAVIS, D. P. (1985) Human Embryology. Blackwell Scientific Publications, Second Edition.

BECK, F., TATA, F. & CHAWENGSAKSOPHAK, K. (2000) Homeobox genes and gut development. Bioessays, 22, 431-41.

BEDDINGTON, R. S. & ROBERTSON, E. J. (1999) Axis development and early asymmetry in mammals. Cell, 96, 195-209.

BIENZ, M. & CLEVERS, H. (2000) Linking colorectal cancer to Wnt signaling. Cell, 103, 311-20.

BJERKNES, M. & CHENG, H. (1981) The stem-cell zone of the small intestinal epithelium. III. Evidence from columnar, enteroendocrine, and mucous cells in the adult mouse. Am J Anat, 160, 77-91.

BJERKNES, M. & CHENG, H. (1999) Clonal analysis of mouse intestinal epithelial progenitors. Gastroenterology, 116, 7-14.

BLACHE, P., VAN DE WETERING, M., DULUC, I., DOMON, C., BERTA, P., FREUND, J. N., CLEVERS, H. & JAY, P. (2004) SOX9 is an intestine crypt transcription factor, is regulated by the Wnt pathway, and represses the CDX2 and MUC2 genes. J Cell Biol, 166, 37-47.

BONHOMME, C., DULUC, I., MARTIN, E., CHAWENGSAKSOPHAK, K., CHENARD, M. P., KEDINGER, M., BECK, F., FREUND, J. N. & DOMON-DELL, C. (2003) The Cdx2 homeobox gene has a tumour suppressor function in the distal colon in addition to a homeotic role during gut development. Gut, 52, 1465-71.

BOOTH, C. & POTTEN, C. S. (2000) Gut instincts: thoughts on intestinal epithelial stem cells. J Clin Invest., 105, 1493-9.

BOSSE, T., FIALKOVICH, J. J., PIASECKYJ, C. M., BEULING, E., BROEKMAN, H., GRAND, R. J., MONTGOMERY, R. K. & KRASINSKI, S. D. (2007) Gata4 and Hnf1alpha are partially required for the expression of specific intestinal genes during development. *Am J Physiol Gastrointest Liver Physiol,* 292**,** G1302-14.

BOSSE, T., PIASECKYJ, C. M., BURGHARD, E., FIALKOVICH, J. J., RAJAGOPAL, S., PU, W. T. & KRASINSKI, S. D. (2006) Gata4 is essential for the maintenance of jejunal-ileal identities in the adult mouse small intestine. Mol Cell Biol, 26, 9060-70.

BOULANGER, J., VEZINA, A., MONGRAIN, S., BOUDREAU, F., PERREAULT, N., AUCLAIR, B. A., LAINE, J., ASSELIN, C. & RIVARD, N. (2005) Cdk2-dependent phosphorylation of homeobox transcription factor CDX2 regulates its nuclear translocation and proteasome-mediated degradation in human intestinal epithelial cells. J Biol Chem, 280, 18095-107.

BOUWMEESTER, T., KIM, S., SASAI, Y., LU, B. & DE ROBERTIS, E. M. (1996) Cerberus is a head-inducing secreted factor expressed in the anterior endoderm of Spemann's organizer. Nature, 382, 595-601.

BRADLEY, A., EVANS, M., KAUFMAN, M. H. & ROBERTSON, E. (1984) Formation of germ-line chimaeras from embryo-derived teratocarcinoma cell lines. Nature, 309, 255-6.

BRAKEBUSCH, C., GROSE, R., QUONDAMATTEO, F., RAMIREZ, A., JORCANO, J. L., PIRRO, A., SVENSSON, M., HERKEN, R., SASAKI, T., TIMPL, R., WERNER, S. & FASSLER, R. (2000) Skin and hair follicle integrity is crucially dependent on beta 1 integrin expression on keratinocytes. *Embo J,* 19**,** 3990-4003.

BRITTAN, M. & WRIGHT, N. A. (2004) The gastrointestinal stem cell. Cell Prolif, 37, 35-53.

BUCHBERGER, A., PABST, O., BRAND, T., SEIDL, K. & ARNOLD, H. H. (1996) Chick NKx-2.3 represents a novel family member of vertebrate homologues to the Drosophila homeobox gene tinman: differential expression of cNKx-2.3 and cNKx-2.5 during heart and gut development. *Mech Dev,* 56**,** 151-63.

BUCHHOLZ, F., ANGRAND, P. O. & STEWART, A. F. (1998) Improved properties of FLP recombinase evolved by cycling mutagenesis. *Nat Biotechnol,* 16**,** 657-62.

CALON, A., GROSS, I., LHERMITTE, B., MARTIN, E., BECK, F., DUCLOS, B., KEDINGER, M., DULUC, I., DOMON-DELL, C. & FREUND, J. N. (2007) Different effects of the Cdx1 and Cdx2 homeobox genes in a murine model of intestinal inflammation. Gut, 56, 1688-95.

CHAWENGSAKSOPHAK, K. & BECK, F. (1996) Chromosomal localization of cdx2, a murine homologue of the Drosophila gene caudal, to mouse chromosome 5. Genomics, 34, 270-1.

CHAWENGSAKSOPHAK, K., DE GRAAFF, W., ROSSANT, J., DESCHAMPS, J. & BECK, F. (2004) Cdx2 is essential for axial elongation in mouse development. Proc Natl Acad Sci U S A, 101, 7641-5.

CHAWENGSAKSOPHAK, K., JAMES, R., HAMMOND, V. E., KONTGEN, F. & BECK, F. (1997) Homeosis and intestinal tumours in Cdx2 mutant mice. Nature, 386, 84-7.

COLLIER, R. J. & KANDEL, J. (1971) Structure and activity of diphtheria toxin. I. Thiol-dependent dissociation of a fraction of toxin into enzymically active and inactive fragments. J Biol Chem, 246, 1496-503.

COLNOT, S., ROMAGNOLO, B., LAMBERT, M., CLUZEAUD, F., PORTEU, A., VANDEWALLE, A., THOMASSET, M., KAHN, A. & PERRET, C. (1998) Intestinal expression of the calbindin-D9K gene in transgenic mice. Requirement for a Cdx2-binding site in a distal activator region. J Biol Chem, 273, 31939-46.

CONLON, F. L., LYONS, K. M., TAKAESU, N., BARTH, K. S., KISPERT, A., HERRMANN, B. & ROBERTSON, E. J. (1994) A primary requirement for nodal in the formation and maintenance of the primitive streak in the mouse. Development, 120, 1919-28.

DANIELIAN, P. S., MUCCINO, D., ROWITCH, D. H., MICHAEL, S. K. & MCMAHON, A. P. (1998) Modification of gene activity in mouse embryos in utero by a tamoxifen-inducible form of Cre recombinase. *Curr Biol,* 8**,** 1323-6.

DANIELIAN, P. S., WHITE, R., HOARE, S. A., FAWELL, S. E. & PARKER, M. G. (1993) Identification of residues in the estrogen receptor that confer differential sensitivity to estrogen and hydroxytamoxifen. *Mol Endocrinol,* 7**,** 232-40.

DAUCA, M., BOUZIGES, F., COLIN, S., KEDINGER, M., KELLER, M. K., SCHILT, J., SIMON-ASSMANN, P. & HAFFEN, K. (1990) Development of the vertebrate small intestine and mechanisms of cell differentiation. Int J Dev Biol, 34, 205-18.

DESCHAMPS, J. & VAN NES, J. (2005) Developmental regulation of the Hox genes during axial morphogenesis in the mouse. Development, 132, 2931-42.

DESSIMOZ, J., OPOKA, R., KORDICH, J. J., GRAPIN-BOTTON, A. & WELLS, J. M. (2006) FGF signaling is necessary for establishing gut tube domains along the anterior-posterior axis in vivo. Mech Dev, 123, 42-55.

DRUMMOND, F., SOWDEN, J., MORRISON, K. & EDWARDS, Y. H. (1996) The caudal-type homeobox protein Cdx-2 binds to the colon promoter of the carbonic anhydrase 1 gene. Eur J Biochem, 236, 670-81.

DUBRULLE, J. & POURQUIE, O. (2004) Coupling segmentation to axis formation. Development, 131, 5783-93.

DULUC, I., FREUND, J. N., LEBERQUIER, C. & KEDINGER, M. (1994) Fetal endoderm primarily holds the temporal and positional information required for mammalian intestinal development. J Cell Biol, 126, 211-21.

DULUC, I., LORENTZ, O., FRITSCH, C., LEBERQUIER, C., KEDINGER, M. & FREUND, J. N. (1997) Changing intestinal connective tissue interactions alters homeobox gene expression in epithelial cells. Journal of Cell Science, 110, 1317-24.

DUPREY, P., CHOWDHURY, K., DRESSLER, G. R., BALLING, R., SIMON, D., GUENET, J. L. & GRUSS, P. (1988) A mouse gene homologous to the Drosophila gene caudal is expressed in epithelial cells from the embryonic intestine. Genes Dev, 2, 1647-54.

DYMECKI, S. M. (1996) Flp recombinase promotes site-specific DNA recombination in embryonic stem cells and transgenic mice. *Proc Natl Acad Sci U S A,* 93**,** 6191-6.

EE, H. C., ERLER, T., BHATHAL, P. S., YOUNG, G. P. & JAMES, R. J. (1995) Cdx-2 homeodomain protein expression in human and rat colorectal adenoma and carcinoma. Am J Pathol, 147, 586-92.

EGLITIS, M. A. & MEZEY, E. (1997) Hematopoietic cells differentiate into both microglia and macroglia in the brains of adult mice. Proc Natl Acad Sci U S A., 94, 4080-5.

EL MARJOU, F., JANSSEN, K. P., CHANG, B. H., LI, M., HINDIE, V., CHAN, L., LOUVARD, D., CHAMBON, P., METZGER, D. & ROBINE, S. (2004) Tissue-specific and inducible Cre-mediated recombination in the gut epithelium. *Genesis,* 39**,** 186-93.

ESCAFFIT, F., PARE, F., GAUTHIER, R., RIVARD, N., BOUDREAU, F. & BEAULIEU, J. F. (2006) Cdx2 modulates proliferation in normal human intestinal epithelial crypt cells. Biochem Biophys Res Commun, 342, 66-72.

EVANS, M. J. & KAUFMAN, M. H. (1981) Establishment in culture of pluripotential cells from mouse embryos. Nature, 292, 154-6.

FANG, R., OLDS, L. C. & SIBLEY, E. (2006) Spatio-temporal patterns of intestine-specific transcription factor expression during postnatal mouse gut development. Gene Expr Patterns, 6, 426-32.

FARLEY, F. W., SORIANO, P., STEFFEN, L. S. & DYMECKI, S. M. (2000) Widespread recombinase expression using FLPeR (flipper) mice. *Genesis,* 28**,** 106-10.

FAWCETT, D. W. (1986) Bloom + Fawcett, A Textbook of Histology. W.B. Saunders, 11th Edition.

FEIL, R., BROCARD, J., MASCREZ, B., LEMEUR, M., METZGER, D. & CHAMBON, P. (1996) Ligand-activated site-specific recombination in mice. *Proc Natl Acad Sci U S A,* 93**,** 10887-90.

FERGUSON, C. A., TUCKER, A. S. & SHARPE, P. T. (2000) Temporospatial cell interactions regulating mandibular and maxillary arch patterning. *Development,* 127**,** 403-12.

FERRARI, G., CUSELLA-DE ANGELIS, G., COLETTA, M., PAOLUCCI, E., STORNAIUOLO, A., COSSU, G. & MAVILIO, F. (1998) Muscle regeneration by bone marrow-derived myogenic progenitors. Science., 279, 1528-30.

FRE, S., HUYGHE, M., MOURIKIS, P., ROBINE, S., LOUVARD, D. & ARTAVANIS-TSAKONAS, S. (2005) Notch signals control the fate of immature progenitor cells in the intestine. Nature, 435, 964-8.

FREUND, J. N., DULUC, I., FOLTZER-JOURDAINNE, C., GOSSE, F. & RAUL, F. (1990) Specific expression of lactase in the jejunum and colon during postnatal development and hormone treatments in the rat. Biochem J, 268, 99-103.

GAMER, L. W. & WRIGHT, C. V. (1993) Murine Cdx-4 bears striking similarities to the Drosophila caudal gene in its homeodomain sequence and early expression pattern. Mech Dev, 43, 71-81.

GARTNER, L. & HIATT, J. (2000) Color Atlas of Histology. Lippincott Williams and Wilkins, Third Edition.

GILL, D. M. & DINIUS, L. L. (1971) Observations on the structure of diphtheria toxin. J Biol Chem, 246, 1485-91.

GIMENEZ, E., LAVADO, A., GIRALDO, P., COZAR, P., JEFFERY, G. & MONTOLIU, L. (2004) A transgenic mouse model with inducible Tyrosinase gene expression using the tetracycline (Tet-on) system allows regulated rescue of abnormal chiasmatic projections found in albinism. *Pigment Cell Res,* 17**,** 363-70.

GREGORIEFF, A., GROSSCHEDL, R. & CLEVERS, H. (2004) Hindgut defects and transformation of the gastro-intestinal tract in Tcf4(-/-)/Tcf1(-/-) embryos. EMBO J, 23, 1825-33.

GROSS, I., DULUC, I., BENAMEUR, T., CALON, A., MARTIN, E., BRABLETZ, T., KEDINGER, M., DOMON-DELL, C. & FREUND, J. N. (2007) The intestine-specific homeobox gene Cdx2 decreases mobility and antagonizes dissemination of colon cancer cells. Oncogene.

GROSS, I., LHERMITTE, B., DOMON-DELL, C., DULUC, I., MARTIN, E., GAIDDON, C., KEDINGER, M. & FREUND, J. N. (2005) Phosphorylation of the homeotic tumor suppressor Cdx2 mediates its ubiquitin-dependent proteasome degradation. Oncogene, 24, 7955-63.

HARVEY, R. P. (1996) NK-2 homeobox genes and heart development. *Dev Biol,* 178**,** 203-16.

HAYASHI, S. & MCMAHON, A. P. (2002) Efficient recombination in diverse tissues by a tamoxifen-inducible form of Cre: a tool for temporally regulated gene activation/inactivation in the mouse. *Dev Biol,* 244**,** 305-18.

HAYASHI, K., YASUGI, S. & MIZUNO, T. (1988) Pepsinogen gene transcription induced in heterologous epithelial-mesenchymal recombinations of chicken endoderms and glandular stomach mesenchyme. Development, 103, 725-31.

HE, X. C., ZHANG, J. & LI, L. (2005) Cellular and molecular regulation of hematopoietic and intestinal stem cell behavior. Ann N Y Acad Sci, 1049, 28-38.

HEATH, J. P. (1996) Epithelial cell migration in the intestine. Cell Biol Int., 20, 139-46.

HENDRY, J. H., POTTEN, C. S., GHAFOOR, A., MOORE, J. V., ROBERTS, S. A. & WILLIAMS, P. C. (1989) The response of murine intestinal crypts to short-range promethium-147 beta irradiation: deductions concerning clonogenic cell numbers and positions. Radiat Res, 118, 364-74.

HENNING, S. J. (1981) Postnatal development: coordination of feeding, digestion, and metabolism. Am J Physiol., 241, G199-214.

HENTSCH, B., LYONS, I., LI, R., HARTLEY, L., LINTS, T. J., ADAMS, J. M. & HARVEY, R. P. (1996) Hlx homeo box gene is essential for an inductive tissue interaction that drives expansion of embryonic liver and gut. Genes Dev, 10, 70-9.

HOESS, R. H. & ABREMSKI, K. (1984) Interaction of the bacteriophage P1 recombinase Cre with the recombining site loxP. Proc Natl Acad Sci U S A, 81, 1026-9.

HOESS, R. H., ZIESE, M. & STERNBERG, N. (1982) P1 site-specific recombination: nucleotide sequence of the recombining sites. Proc Natl Acad Sci U S A, 79, 3398-402.

HORN, J. M. & ASHWORTH, A. (1995) A member of the caudal family of homeobox genes maps to the X-inactivation centre region of the mouse and human X chromosomes. Hum Mol Genet, 4, 1041-7.

HOUDE, M., LAPRISE, P., JEAN, D., BLAIS, M., ASSELIN, C. & RIVARD, N. (2001) Intestinal epithelial cell differentiation involves activation of p38 mitogen-activated protein kinase that regulates the homeobox transcription factor CDX2. J Biol Chem, 276, 21885-94.

IKEYA, M. & TAKADA, S. (2001) Wnt-3a is required for somite specification along the anteroposterior axis of the mouse embryo and for regulation of cdx-1 expression. Mech Dev, 103, 27-33.

IRATNI, R., YAN, Y. T., CHEN, C., DING, J., ZHANG, Y., PRICE, S. M., REINBERG, D. & SHEN, M. M. (2002) Inhibition of excess nodal signaling during mouse gastrulation by the transcriptional corepressor DRAP1. Science, 298, 1996-9.

IRELAND, H., KEMP, R., HOUGHTON, C., HOWARD, L., CLARKE, A. R., SANSOM, O. J. & WINTON, D. J. (2004) Inducible Cre-mediated control of gene expression in the murine gastrointestinal tract: effect of loss of beta-catenin. Gastroenterology, 126, 1236-46.

ISHII, Y., REX, M., SCOTTING, P. J. & YASUGI, S. (1998) Region-specific expression of chicken Sox2 in the developing gut and lung epithelium: regulation by epithelial-mesenchymal interactions. *Dev Dyn,* 213**,** 464-75.

JAMES, R., ERLER, T. & KAZENWADEL, J. (1994) Structure of the murine homeobox gene cdx-2. Expression in embryonic and adult intestinal epithelium. J Biol Chem, 269, 15229-37.

JAMES, R. & KAZENWADEL, J. (1991) Homeobox gene expression in the intestinal epithelium of adult mice. J Biol Chem, 266, 3246-51.

JENNY, M., UHL, C., ROCHE, C., DULUC, I., GUILLERMIN, V., GUILLEMOT, F., JENSEN, J., KEDINGER, M. & GRADWOHL, G. (2002) Neurogenin3 is differentially required for endocrine cell fate specification in the intestinal and gastric epithelium. Embo J, 21, 6338-47.

JENSEN, J., PEDERSEN, E. E., GALANTE, P., HALD, J., HELLER, R. S., ISHIBASHI, M., KAGEYAMA, R., GUILLEMOT, F., SERUP, P. & MADSEN, O. D. (2000) Control of endodermal endocrine development by Hes-1. Nat Genet, 24, 36-44.

JIN, T. & LI, H. (2001) Pou homeodomain protein OCT1 is implicated in the expression of the caudal-related homeobox gene Cdx-2. J Biol Chem, 276, 14752-8.

JOHNSON, K. R. & DAVISSON, M. T. (1992) A multipoint genetic linkage map of mouse chromosome 18. Genomics, 13, 1143-9.

KAESTNER, K. H., SILBERG, D. G., TRABER, P. G. & SCHUTZ, G. (1997) The mesenchymal winged helix transcription factor Fkh6 is required for the control of gastrointestinal proliferation and differentiation. Genes Dev, 11, 1583-95.

KAIMAKTCHIEV, V., TERRACCIANO, L., TORNILLO, L., SPICHTIN, H., STOIOS, D., BUNDI, M., KORCHEVA, V., MIRLACHER, M., LODA, M., SAUTER, G. & CORLESS, C. L. (2004) The homeobox intestinal differentiation factor CDX2 is selectively expressed in gastrointestinal adenocarcinomas. Mod Pathol, 17, 1392-9.

KARAM, S. M., LI, Q. & GORDON, J. I. (1997) Gastric epithelial morphogenesis in normal and transgenic mice. Am J Physiol, 272, G1209-20.

KATZ, J. P., PERREAULT, N., GOLDSTEIN, B. G., LEE, C. S., LABOSKY, P. A., YANG, V. W. & KAESTNER, K. H. (2002) The zinc-finger transcription factor Klf4 is required for terminal differentiation of goblet cells in the colon. Development, 129, 2619-28.

KAUFMAN, M. H. & BARD, J. B. L. (1999) The Anatomical Basis of Mouse Development, London, Academic Press.

KAWAZOE, Y., SEKIMOTO, T., ARAKI, M., TAKAGI, K., ARAKI, K. & YAMAMURA, K. (2002) Region-specific gastrointestinal Hox code during murine embryonal gut development. Dev Growth Differ., 44, 77-84.

KEDINGER, M., DULUC, I., FRITSCH, C., LORENTZ, O., PLATEROTI, M. & FREUND, J. N. (1998) Intestinal epithelial-mesenchymal cell interactions. Ann N Y Acad Sci, 859, 1-17.

KEMP, R., IRELAND, H., CLAYTON, E., HOUGHTON, C., HOWARD, L. & WINTON, D. J. (2004) Elimination of background recombination: somatic induction of Cre by combined transcriptional regulation and hormone binding affinity. *Nucleic Acids Res,* 32**,** e92.

KIM, B. M., BUCHNER, G., MILETICH, I., SHARPE, P. T. & SHIVDASANI, R. A. (2005) The stomach mesenchymal transcription factor Barx1 specifies gastric epithelial identity through inhibition of transient Wnt signaling. Dev Cell, 8, 611-22.

KIM, B. M., MAO, J., TAKETO, M. M. & SHIVDASANI, R. A. (2007a) Phases of canonical Wnt signaling during the development of mouse intestinal epithelium. Gastroenterology, 133, 529-38.

KIM, B. M., MILETICH, I., MAO, J., MCMAHON, A. P., SHARPE, P. A. & SHIVDASANI, R. A. (2007b) Independent functions and mechanisms for homeobox gene Barx1 in patterning mouse stomach and spleen. Development, 134, 3603-13.

KINDER, S. J., TSANG, T. E., ANG, S. L., BEHRINGER, R. R. & TAM, P. P. (2001) Defects of the body plan of mutant embryos lacking Lim1, Otx2 or Hnf3beta activity. Int J Dev Biol, 45, 347-55.

KORINEK, V., BARKER, N., MOERER, P., VAN DONSELAAR, E., HULS, G., PETERS, P. J. & CLEVERS, H. (1998) Depletion of epithelial stem-cell compartments in the small intestine of mice lacking Tcf-4. Nat Genet, 19, 379-83.

KOSINSKI, C., LI, V. S., CHAN, A. S., ZHANG, J., HO, C., TSUI, W. Y., CHAN, T. L., MIFFLIN, R. C., POWELL, D. W., YUEN, S. T., LEUNG, S. Y. & CHEN, X. (2007) Gene expression patterns of human colon tops and basal crypts and BMP antagonists as intestinal stem cell niche factors. Proc Natl Acad Sci U S A, 104, 15418-23.

KRASINSKI, S. D., VAN WERING, H. M., TANNEMAAT, M. R. & GRAND, R. J. (2001) Differential activation of intestinal gene promoters: functional interactions between GATA-5 and HNF-1 alpha. Am J Physiol Gastrointest Liver Physiol, 281, G69-84.

LAMBERT, M., COLNOT, S., SUH, E., L'HORSET, F., BLIN, C., CALLIOT, M. E., RAYMONDJEAN, M., THOMASSET, M., TRABER, P. G. & PERRET, C. (1996) cis-Acting elements and transcription factors involved in the intestinal specific expression of the rat calbindin-D9K gene: binding of the intestine-specific transcription factor Cdx-2 to the TATA box. Eur J Biochem, 236, 778-88.

LAWSON, K. A. & PEDERSEN, R. A. (1987) Cell fate, morphogenetic movement and population kinetics of embryonic endoderm at the time of germ layer formation in the mouse. Development., 101, 627-52.

LEWIS, S. L. & TAM, P. P. (2006) Definitive endoderm of the mouse embryo: formation, cell fates, and morphogenetic function. Dev Dyn., 235, 2315-29.

LI, Y. Q., ROBERTS, S. A., PAULUS, U., LOEFFLER, M. & POTTEN, C. S. (1994) The crypt cycle in mouse small intestinal epithelium. J Cell Sci., 107, 3271-9.

LICKERT, H., DOMON, C., HULS, G., WEHRLE, C., DULUC, I., CLEVERS, H., MEYER, B. I., FREUND, J. N. & KEMLER, R. (2000) Wnt/(beta)-catenin signaling regulates the expression of the homeobox gene Cdx1 in embryonic intestine. Development, 127, 3805-13.

LINTS, T. J., HARTLEY, L., PARSONS, L. M. & HARVEY, R. P. (1996) Mesoderm-specific expression of the divergent homeobox gene Hlx during murine embryogenesis. Dev Dyn, 205, 457-70.

LINTS, T. J., PARSONS, L. M., HARTLEY, L., LYONS, I. & HARVEY, R. P. (1993) Nkx-2.5: a novel murine homeobox gene expressed in early heart progenitor cells and their myogenic descendants. *Development,* 119**,** 419-31.

LIPSCOMB, K., SCHMITT, C., SABLYAK, A., YODER, J. A. & NASCONE-YODER, N. (2006) Role for retinoid signaling in left-right asymmetric digestive organ morphogenesis. Dev Dyn, 235, 2266-75.

LITTLEWOOD, T. D., HANCOCK, D. C., DANIELIAN, P. S., PARKER, M. G. & EVAN, G. I. (1995) A modified oestrogen receptor ligand-binding domain as an improved switch for the regulation of heterologous proteins. *Nucleic Acids Res,* 23**,** 1686-90.

LIU, P., WAKAMIYA, M., SHEA, M. J., ALBRECHT, U., BEHRINGER, R. R. & BRADLEY, A. (1999) Requirement for Wnt3 in vertebrate axis formation. Nat Genet, 22, 361-5.

LIU, Y., FESTING, M., THOMPSON, J. C., HESTER, M., RANKIN, S., EL-HODIRI, H. M., ZORN, A. M. & WEINSTEIN, M. (2004) Smad2 and Smad3 coordinately regulate craniofacial and endodermal development. Dev Biol, 270, 411-26.

LOEFFLER, M., BRATKE, T., PAULUS, U., LI, Y. Q. & POTTEN, C. S. (1997) Clonality and life cycles of intestinal crypts explained by a state dependent stochastic model of epithelial stem cell organization. J Theor Biol, 186, 41-54.

LORENTZ, O., DULUC, I., ARCANGELIS, A. D., SIMON-ASSMANN, P., KEDINGER, M. & FREUND, J. N. (1997) Key role of the Cdx2 homeobox gene in extracellular matrix-mediated intestinal cell differentiation. J Cell Biol, 139, 1553-65.

LORENTZ, O., SUH, E. R., TAYLOR, J. K., BOUDREAU, F. & TRABER, P. G. (1999) CREB-binding [corrected] protein interacts with the homeodomain protein Cdx2 and enhances transcriptional activity. J Biol Chem, 274, 7196-9.

LOWE, L. A., YAMADA, S. & KUEHN, M. R. (2001) Genetic dissection of nodal function in patterning the mouse embryo. Development, 128, 1831-43.

MARSHMAN, E., BOOTH, C. & POTTEN, C. S. (2002) The intestinal epithelial stem cell. Bioessays, 24, 91-8.

MARTIN, G. R. (1981) Isolation of a pluripotent cell line from early mouse embryos cultured in medium conditioned by teratocarcinoma stem cells. Proc Natl Acad Sci U S A, 78, 7634-8.

MARTIN, K., KIRKWOOD, T. B. & POTTEN, C. S. (1998a) Age changes in stem cells of murine small intestinal crypts. Exp Cell Res., 241, 316-23.

MARTIN, K., POTTEN, C. S., ROBERTS, S. A. & KIRKWOOD, T. B. (1998b) Altered stem cell regeneration in irradiated intestinal crypts of senescent mice. J Cell Sci., 111, 2297-303.

MCGINNIS, W. & KRUMLAUF, R. (1992) Homeobox genes and axial patterning. Cell, 68, 283-302.

MCLEOD, M., CRAFT, S. & BROACH, J. R. (1986) Identification of the crossover site during FLP-mediated recombination in the Saccharomyces cerevisiae plasmid 2 microns circle. Mol Cell Biol, 6, 3357-67.

MERRITT, A. J., POTTEN, C. S., KEMP, C. J., HICKMAN, J. A., BALMAIN, A., LANE, D. P. & HALL, P. A. (1994) The role of p53 in spontaneous and radiation-induced apoptosis in the gastrointestinal tract of normal and p53-deficient mice. Cancer Res., 54, 614-7.

MERRITT, A. J., POTTEN, C. S., WATSON, A. J., LOH, D. Y., NAKAYAMA, K. & HICKMAN, J. A. (1995) Differential expression of bcl-2 in intestinal epithelia. Correlation with attenuation of apoptosis in colonic crypts and the incidence of colonic neoplasia. J Cell Sci, 108, 2261-71.

MEYER, B. I. & GRUSS, P. (1993) Mouse Cdx-1 expression during gastrulation. Development, 117, 191-203.

MEYERS, E. N., LEWANDOSKI, M. & MARTIN, G. R. (1998) An Fgf8 mutant allelic series generated by Cre- and Flp-mediated recombination. *Nat Genet,* 18**,** 136-41.

MITCHELMORE, C., TROELSEN, J. T., SPODSBERG, N., SJOSTROM, H. & NOREN, O. (2000) Interaction between the homeodomain proteins Cdx2 and HNF1alpha mediates expression of the lactase-phlorizin hydrolase gene. Biochem J, 346 Pt 2, 529-35.

MORI-AKIYAMA, Y., VAN DEN BORN, M., VAN ES, J. H., HAMILTON, S. R., ADAMS, H. P., ZHANG, J., CLEVERS, H. & DE CROMBRUGGHE, B. (2007) SOX9 is required for the differentiation of paneth cells in the intestinal epithelium. Gastroenterology, 133, 539-46.

MORIN, P. J., SPARKS, A. B., KORINEK, V., BARKER, N., CLEVERS, H., VOGELSTEIN, B. & KINZLER, K. W. (1997) Activation of beta-catenin-Tcf signaling in colon cancer by mutations in beta-catenin or APC. Science, 275, 1787-90.

MOSES, K. A., DEMAYO, F., BRAUN, R. M., REECY, J. L. & SCHWARTZ, R. J. (2001) Embryonic expression of an Nkx2-5/Cre gene using ROSA26 reporter mice. *Genesis,* 31**,** 176-80.

MUTOH, H., HAKAMATA, Y., SATO, K., EDA, A., YANAKA, I., HONDA, S., OSAWA, H., KANEKO, Y. & SUGANO, K. (2002) Conversion of gastric mucosa to intestinal metaplasia in Cdx2-expressing transgenic mice. Biochem Biophys Res Commun, 294, 470-9.

MUTOH, H., SAKURAI, S., SATOH, K., OSAWA, H., HAKAMATA, Y., TAKEUCHI, T. & SUGANO, K. (2004a) Cdx1 induced intestinal metaplasia in the transgenic mouse stomach: comparative study with Cdx2 transgenic mice. Gut, 53, 1416-23.

MUTOH, H., SAKURAI, S., SATOH, K., TAMADA, K., KITA, H., OSAWA, H., TOMIYAMA, T., SATO, Y., YAMAMOTO, H., ISODA, N., YOSHIDA, T., IDO, K. & SUGANO, K. (2004b) Development of gastric carcinoma from intestinal metaplasia in Cdx2-transgenic mice. Cancer Res, 64, 7740-7.

NAGY, A. (2000) Cre recombinase: the universal reagent for genome tailoring. Genesis, 26, 99-109.

NG, A. Y., WARING, P., RISTEVSKI, S., WANG, C., WILSON, T., PRITCHARD, M., HERTZOG, P. & KOLA, I. (2002) Inactivation of the transcription factor Elf3 in mice results in dysmorphogenesis and altered differentiation of intestinal epithelium. Gastroenterology, 122, 1455-66.

NOVAK, A., GUO, C., YANG, W., NAGY, A. & LOBE, C. G. (2000) Z/EG, a double reporter mouse line that expresses enhanced green fluorescent protein upon Cre-mediated excision. *Genesis,* 28**,** 147-55.

PABST, O., SCHNEIDER, A., BRAND, T. & ARNOLD, H. H. (1997) The mouse Nkx2-3 homeodomain gene is expressed in gut mesenchyme during pre- and postnatal mouse development. Dev Dyn, 209, 29-35.

PABST, O., ZWEIGERDT, R. & ARNOLD, H. H. (1999) Targeted disruption of the homeobox transcription factor Nkx2-3 in mice results in postnatal lethality and abnormal development of small intestine and spleen. Development, 126, 2215-25.

PALMER, S., GROVES, N., SCHINDELER, A., YEOH, T., BIBEN, C., WANG, C. C., SPARROW, D. B., BARNETT, L., JENKINS, N. A., COPELAND, N. G., KOENTGEN, F., MOHUN, T. & HARVEY, R. P. (2001) The small muscle-specific protein Csl modifies cell shape and promotes myocyte fusion in an insulin-like growth factor 1-dependent manner. *J Cell Biol,* 153**,** 985-98.

PARTANEN, J., SCHWARTZ, L. & ROSSANT, J. (1998) Opposite phenotypes of hypomorphic and Y766 phosphorylation site mutations reveal a function for Fgfr1 in anteroposterior patterning of mouse embryos. Genes Dev, 12, 2332-44.

PETERSEN, B. E., BOWEN, W. C., PATRENE, K. D., MARS, W. M., SULLIVAN, A. K., MURASE, N., BOGGS, S. S., GREENBERGER, J. S. & GOFF, J. P. (1999) Bone marrow as a potential source of hepatic oval cells. Science., 284, 1168-70.

PICARD, D. (1994) Regulation of protein function through expression of chimaeric proteins. *Curr Opin Biotechnol,* 5**,** 511-5.

PINTO, D., GREGORIEFF, A., BEGTHEL, H. & CLEVERS, H. (2003) Canonical Wnt signals are essential for homeostasis of the intestinal epithelium. Genes Dev, 17, 1709-13.

PITTENGER, M. F., MACKAY, A. M., BECK, S. C., JAISWAL, R. K., DOUGLAS, R., MOSCA, J. D., MOORMAN, M. A., SIMONETTI, D. W., CRAIG, S. & MARSHAK, D. R. (1999) Multilineage potential of adult human mesenchymal stem cells. Science., 284, 143-7.

POLLARD, S. L. & HOLLAND, P. W. (2000) Evidence for 14 homeobox gene clusters in human genome ancestry. Curr Biol, 10, 1059-62.

POTTEN, C. S. (1998) Stem cells in gastrointestinal epithelium: numbers, characteristics and death. Philos Trans R Soc Lond B Biol Sci., 353, 821-30.

POTTEN, C. S., BOOTH, C. & PRITCHARD, D. M. (1997) The intestinal epithelial stem cell: the mucosal governor. Int J Exp Pathol, 78, 219-43.

POTTEN, C. S., HUME, W. J., REID, P. & CAIRNS, J. (1978) The segregation of DNA in epithelial stem cells. Cell, 15, 899-906.

POTTEN, C. S. & LOEFFLER, M. (1990) Stem cells: attributes, cycles, spirals, pitfalls and uncertainties. Lessons for and from the crypt. Development., 110, 1001-20.

POTTEN, C. S., OWEN, G. & BOOTH, D. (2002) Intestinal stem cells protect their genome by selective segregation of template DNA strands. J Cell Sci, 115, 2381-8.

QUE, J., OKUBO, T., GOLDENRING, J. R., NAM, K. T., KUROTANI, R., MORRISEY, E. E., TARANOVA, O., PEVNY, L. H. & HOGAN, B. L. (2007) Multiple dose-dependent roles for Sox2 in the patterning and differentiation of anterior foregut endoderm. *Development.,* 134**,** 2521-31.

RADTKE, F. & CLEVERS, H. (2005) Self-renewal and cancer of the gut: two sides of a coin. Science, 307, 1904-9.

REISS, M., JASTREBOFF, M. M., BERTINO, J. R. & NARAYANAN, R. (1986) DNA-mediated gene transfer into epidermal cells using electroporation. Biochem Biophys Res Commun, 137, 244-9.

RINGS, E. H., BOUDREAU, F., TAYLOR, J. K., MOFFETT, J., SUH, E. R. & TRABER, P. G. (2001) Phosphorylation of the serine 60 residue within the Cdx2 activation domain mediates its transactivation capacity. Gastroenterology, 121, 1437-50.

ROBERTS, D. J., JOHNSON, R. L., BURKE, A. C., NELSON, C. E., MORGAN, B. A. & TABIN, C. J. (1995) Sonic hedgehog is an endodermal signal inducing Bmp-4 and Hox genes during induction and regionalization of the chick hindgut. Development, 121, 3163-74.

ROBERTS, D. J., SMITH, D. M., GOFF, D. J. & TABIN, C. J. (1998) Epithelial-mesenchymal signaling during the regionalization of the chick gut. Development, 125, 2791-801.

RODRIGUEZ, C. I., BUCHHOLZ, F., GALLOWAY, J., SEQUERRA, R., KASPER, J., AYALA, R., STEWART, A. F. & DYMECKI, S. M. (2000) High-efficiency deleter mice show that FLPe is an alternative to Cre-loxP. *Nat Genet,* 25**,** 139-40.

SAAM, J. R. & GORDON, J. I. (1999) Inducible gene knockouts in the small intestinal and colonic epithelium. *J Biol Chem,* 274**,** 38071-82.

SANCHO, E., BATLLE, E. & CLEVERS, H. (2003) Live and let die in the intestinal epithelium. Curr Opin Cell Biol, 15, 763-70.

SANGIORGI, E. & CAPECCHI, M. R. (2008) Bmi1 is expressed in vivo in intestinal stem cells. Nat Genet., 40, 915-20.

SCHMIDT, G. H., WINTON, D. J. & PONDER, B. A. (1988) Development of the pattern of cell renewal in the crypt-villus unit of chimaeric mouse small intestine. Development., 103, 785-90.

SCOTT, M. P. (1993) A rational nomenclature for vertebrate homeobox (HOX) genes. Nucleic Acids Res, 21, 1687-8.

SCOTT, M. P., TAMKUN, J. W. & HARTZELL, G. W., 3RD (1989) The structure and function of the homeodomain. Biochim Biophys Acta, 989, 25-48.

SEKIMOTO, T., YOSHINOBU, K., YOSHIDA, M., KURATANI, S., FUJIMOTO, S., ARAKI, M., TAJIMA, N., ARAKI, K. & YAMAMURA, K. (1998) Region-specific expression of murine Hox genes implies the Hox code-mediated patterning of the digestive tract. Genes Cells, 3, 51-64.

SILBERG, D. G., SULLIVAN, J., KANG, E., SWAIN, G. P., MOFFETT, J., SUND, N. J., SACKETT, S. D. & KAESTNER, K. H. (2002) Cdx2 ectopic expression induces gastric intestinal metaplasia in transgenic mice. Gastroenterology, 122, 689-96.

SILBERG, D. G., SWAIN, G. P., SUH, E. R. & TRABER, P. G. (2000) Cdx1 and cdx2 expression during intestinal development Gastroenterology, 119, 961-71.

SMITH, A. G., HEATH, J. K., DONALDSON, D. D., WONG, G. G., MOREAU, J., STAHL, M. & ROGERS, D. (1988) Inhibition of pluripotential embryonic stem cell differentiation by purified polypeptides. Nature, 336, 688-90.

SMITH, D. M., GRASTY, R. C., THEODOSIOU, N. A., TABIN, C. J. & NASCONE-YODER, N. M. (2000) Evolutionary relationships between the amphibian, avian, and mammalian stomachs. Evol Dev, 2, 348-59.

SMITH, D. M., NIELSEN, C., TABIN, C. J. & ROBERTS, D. J. (2000) Roles of BMP signaling and Nkx2.5 in patterning at the chick midgut-foregut boundary. *Development,* 127**,** 3671-81.

SMITH, D. M. & TABIN, C. J. (1999) BMP signalling specifies the pyloric sphincter. *Nature,* 402**,** 748-9.

SORIANO, P. (1999) Generalized lacZ expression with the ROSA26 Cre reporter strain. *Nat Genet,* 21**,** 70-1.

STAINIER, D. Y. (2005) No organ left behind: tales of gut development and evolution. Science, 307, 1902-4.

STALOCH, L. J., DIVINE, J. K., WITTEN, J. T. & SIMON, T. C. (2005) C/EBP and Cdx family factors regulate liver fatty acid binding protein transgene expression in the small intestinal epithelium. Biochim Biophys Acta, 1731, 168-78.

STRUMPF, D., MAO, C. A., YAMANAKA, Y., RALSTON, A., CHAWENGSAKSOPHAK, K., BECK, F. & ROSSANT, J. (2005) Cdx2 is required for correct cell fate specification and differentiation of trophectoderm in the mouse blastocyst. Development, 132, 2093-102.

STUDER, M., GAVALAS, A., MARSHALL, H., ARIZA-MCNAUGHTON, L., RIJLI, F. M., CHAMBON, P. & KRUMLAUF, R. (1998) Genetic interactions between Hoxa1 and Hoxb1 reveal new roles in regulation of early hindbrain patterning. *Development,* 125**,** 1025-36.

SUBRAMANIAN, V., MEYER, B. & EVANS, G. S. (1998) The murine Cdx1 gene product localises to the proliferative compartment in the developing and regenerating intestinal epithelium. Differentiation, 64, 11-8.

SUBRAMANIAN, V., MEYER, B. I. & GRUSS, P. (1995) Disruption of the murine homeobox gene Cdx1 affects axial skeletal identities by altering the mesodermal expression domains of Hox genes. Cell, 83, 641-53.

SUBTIL, C., GUERIN, E., SCHNEIDER, A., CHENARD, M. P., MARTIN, E., DOMON-DELL, C., DULUC, I., BRABLETZ, T., KEDINGER, M., DUCLOS, B., GAUB, M. P. & FREUND, J. N. (2007) Frequent rearrangements and amplification of the CDX2 homeobox gene in human sporadic colorectal cancers with chromosomal instability. Cancer Lett, 247, 197-203.

SUH, E., CHEN, L., TAYLOR, J. & TRABER, P. G. (1994) A homeodomain protein related to caudal regulates intestine-specific gene transcription. Mol Cell Biol, 14, 7340-51.

TADA, S., ERA, T., FURUSAWA, C., SAKURAI, H., NISHIKAWA, S., KINOSHITA, M., NAKAO, K., CHIBA, T. & NISHIKAWA, S. (2005) Characterization of mesendoderm: a diverging point of the definitive endoderm and mesoderm in embryonic stem cell differentiation culture. Development, 132, 4363-74.

TAKAHASHI, Y., IMANAKA, T. & TAKANO, T. (1998) Spatial pattern of smooth muscle differentiation is specified by the epithelium in the stomach of mouse embryo. Dev Dyn, 212, 448-60.

TAM, P. P. & BEDDINGTON, R. S. (1987) The formation of mesodermal tissues in the mouse embryo during gastrulation and early organogenesis. Development, 99, 109-26.

TAM, P. P., KHOO, P. L., LEWIS, S. L., BILDSOE, H., WONG, N., TSANG, T. E., GAD, J. M. & ROBB, L. (2007) Sequential allocation and global pattern of

movement of the definitive endoderm in the mouse embryo during gastrulation. Development, 134, 251-60.

TAYLOR, J. K., LEVY, T., SUH, E. R. & TRABER, P. G. (1997) Activation of enhancer elements by the homeobox gene Cdx2 is cell line specific. Nucleic Acids Res, 25, 2293-300.

THEODOSIOU, N. A. & TABIN, C. J. (2005) Sox9 and Nkx2.5 determine the pyloric sphincter epithelium under the control of BMP signaling. *Dev Biol,* 279**,** 481-90.

THOMAS, P. & BEDDINGTON, R. S. (1996) Anterior primitive endoderm may be responsible for patterning the anterior neural plate in the mouse embryo. Curr Biol, 6, 1487-96.

THOMSON, J. A., ITSKOVITZ-ELDOR, J., SHAPIRO, S. S., WAKNITZ, M. A., SWIERGIEL, J. J., MARSHALL, V. S. & JONES, J. M. (1998) Embryonic stem cell lines derived from human blastocysts. Science., 282, 1145-7.

TISSIER-SETA, J. P., MUCCHIELLI, M. L., MARK, M., MATTEI, M. G., GORIDIS, C. & BRUNET, J. F. (1995) Barx1, a new mouse homeodomain transcription factor expressed in cranio-facial ectomesenchyme and the stomach. *Mech Dev,* 51**,** 3-15.

TORRES, R. M. & KUHN, R. (1997) Laboratory Protocols for Conditional Gene Targeting, Oxford University Press.

TROELSEN, J. T., MITCHELMORE, C., SPODSBERG, N., JENSEN, A. M., NOREN, O. & SJOSTROM, H. (1997) Regulation of lactase-phlorizin hydrolase gene expression by the caudal-related homoeodomain protein Cdx-2. Biochem J, 322 (Pt 3), 833-8.

TUCKER, A. & SHARPE, P. (2004) The cutting-edge of mammalian development; how the embryo makes teeth. *Nat Rev Genet,* 5**,** 499-508.

TUCKER, A. S., MATTHEWS, K. L. & SHARPE, P. T. (1998) Transformation of tooth type induced by inhibition of BMP signaling. *Science,* 282**,** 1136-8.

TUCKER, A. S., YAMADA, G., GRIGORIOU, M., PACHNIS, V. & SHARPE, P. T. (1999) Fgf-8 determines rostral-caudal polarity in the first branchial arch. *Development,* 126**,** 51-61.

UESAKA, T., KAGEYAMA, N. & WATANABE, H. (2004) Identifying target genes regulated downstream of Cdx2 by microarray analysis. J Mol Biol, 337, 647-60.

VALLBOHMER, D., DEMEESTER, S. R., PETERS, J. H., OH, D. S., KURAMOCHI, H., SHIMIZU, D., HAGEN, J. A., DANENBERG, K. D., DANENBERG, P. V., DEMEESTER, T. R. & CHANDRASOMA, P. T. (2006) Cdx-2 expression in squamous and metaplastic columnar epithelia of the esophagus. Dis Esophagus, 19, 260-6.

VAN DE WETERING, M., SANCHO, E., VERWEIJ, C., DE LAU, W., OVING, I., HURLSTONE, A., VAN DER HORN, K., BATLLE, E., COUDREUSE, D., HARAMIS, A. P., TJON-PON-FONG, M., MOERER, P., VAN DEN BORN, M., SOETE, G., PALS, S., EILERS, M., MEDEMA, R. & CLEVERS, H. (2002) The beta-catenin/TCF-4 complex imposes a crypt progenitor phenotype on colorectal cancer cells. Cell, 111, 241-50.

VAN ES, J. H., VAN GIJN, M. E., RICCIO, O., VAN DEN BORN, M., VOOIJS, M., BEGTHEL, H., COZIJNSEN, M., ROBINE, S., WINTON, D. J., RADTKE, F. & CLEVERS, H. (2005) Notch/gamma-secretase inhibition turns proliferative cells in intestinal crypts and adenomas into goblet cells. Nature, 435, 959-63.

VAN NES, J., DE GRAAFF, W., LEBRIN, F., GERHARD, M., BECK, F. & DESCHAMPS, J. (2006) The Cdx4 mutation affects axial development and

reveals an essential role of Cdx genes in the ontogenesis of the placental labyrinth in mice. Development, 133, 419-28.

VAN NOORT, M., MEELDIJK, J., VAN DER ZEE, R., DESTREE, O. & CLEVERS, H. (2002) Wnt signaling controls the phosphorylation status of beta-catenin. J Biol Chem, 277, 17901-5.

WELLS, J. M. & MELTON, D. A. (1999) Vertebrate endoderm development. Annu Rev Cell Dev Biol 15, 393-410.

WELLS, J. M. & MELTON, D. A. (2000) Early mouse endoderm is patterned by soluble factors from adjacent germ layers. *Development,* 127**,** 1563-72.

WINTON, D. J., BLOUNT, M. A. & PONDER, B. A. (1988) A clonal marker induced by mutation in mouse intestinal epithelium. Nature, 333, 463-6.

WISLET-GENDEBIEN, S., HANS, G., LEPRINCE, P., RIGO, J. M., MOONEN, G. & ROGISTER, B. (2005) Plasticity of cultured mesenchymal stem cells: switch from nestin-positive to excitable neuron-like phenotype. *Stem Cells,* 23**,** 392-402.

WOLPERT, L., BEDDINGTON, R., BROCKES, J., JESSELL, T., LAWRENCE, P. & MEYEROWITZ, E. (1998) Principles of Development, London, Current Biology Ltd.

XU, F., LI, H. & JIN, T. (1999) Cell type-specific autoregulation of the Caudal-related homeobox gene Cdx-2/3. J Biol Chem, 274, 34310-6.

YAMAMOTO, H., MIYAMOTO, K., LI, B., TAKETANI, Y., KITANO, M., INOUE, Y., MORITA, K., PIKE, J. W. & TAKEDA, E. (1999) The caudal-related homeodomain protein Cdx-2 regulates vitamin D receptor gene expression in the small intestine. J Bone Miner Res, 14, 240-7.

YANG, Q., BERMINGHAM, N. A., FINEGOLD, M. J. & ZOGHBI, H. Y. (2001) Requirement of Math1 for secretory cell lineage commitment in the mouse intestine. Science, 294, 2155-8.

ZAMBROWICZ, B. P., IMAMOTO, A., FIERING, S., HERZENBERG, L. A., KERR, W. G. & SORIANO, P. (1997) Disruption of overlapping transcripts in the ROSA beta geo 26 gene trap strain leads to widespread expression of beta-galactosidase in mouse embryos and hematopoietic cells. *Proc Natl Acad Sci U S A,* 94**,** 3789-94.

ZHU, X. D., PAN, G., LUETKE, K. & SADOWSKI, P. D. (1995) Homology requirements for ligation and strand exchange by the FLP recombinase. J Biol Chem, 270, 11646-53.

Appendix

Publications

- Stringer, E.J., Pritchard, C.A.., Beck, F., (2008) '**Cdx2 initiates histodifferentiation of the midgut endoderm',** *FEBS Letters,* 582, 2555-2560

FEBS Letters 582 (2008) 2555–2560

Cdx2 initiates histodifferentiation of the midgut endoderm

Emma J. Stringer, Catrin A. Pritchard, Felix Beck*

Department of Biochemistry, Henry Wellcome Building, University of Leicester, Lancaster Road, Leicester LE1 7RH, UK

Received 7 April 2008; revised 6 June 2008; accepted 16 June 2008

Available online 23 June 2008

Edited by Paul Bertone

Abstract **Null mutation or haploinsufficiency of *Cdx2* results in the development of heterotopic lesions with a gastric phenotype in the midgut endoderm. Conversely transgenic expression of *Cdx2* in the stomach causes the endoderm to differentiate into intestinal-type mucosa. We demonstrate that the mesoderm adjacent to intestinal heterotopic areas expresses stomach specific *Barx1* while the surrounding mesoderm is *Barx1* negative. We conclude that the initiation of gut histodifferentiation lies in the endodermal expression of *Cdx2* and that endodermal/mesodermal cross-talk involving *Barx1* with appropriate feedback loops results in the development of the postnatal gut phenotype.**

Keywords: Gut histodifferentiation; *Cdx2*; *Barx1*; *Sox2*

1. Introduction

Cdx2 is expressed throughout the endoderm of the intestine distal to the developing stomach from the appearance of the head and tail folds [1]. It persists throughout life and is found at highest levels just distal to the apex of the midgut loop diminishing both cranially and caudally but never appearing in the stomach.

In vivo knock out [2] and overexpression studies [3] indicate that the gene is involved in morphogenesis of the intestinal epithelium. Chimaeric mice bearing $Cdx2^{-/-}$ cells in wild-type hosts, develop intestinal patches of organotypically normal stomach epithelium [4] and in $Cdx2^{+/-}$ animals areas of stomach mucosa develop in the paracaecal region [5], this being the area in which the gene is normally required at its highest level for normal development and therefore that in which haploinsufficiency is most likely to manifest. Clonal analysis in male wild-type animals bearing female $Cdx2^{-/-}$ lesions shows that the gastric heteroses are of chimaeric (female) origin while the underlying stroma is of host (male) origin [4]. Thus, *Cdx2* is required for the histogenesis of intestinal epithelium and in its absence or haploinsufficiency development along a 'default' pathway results in the formation of a region of stomach mucosa.

This model allows study of the epithelial/mesenchymal interaction necessary for normal intestinal morphogenesis. Mucosal intestinal recombination experiments have yielded conflicting results. For example, recombination of E14 distal endoderm with proximal mesoderm in mouse foetal tissue results in a small intestinal phenotype but conversely proximal endoderm recombined with distal mesoderm continues to differentiate as small intestine [6,7]. In the present experiments, we ask whether the mesoderm underlying areas of paracaecal gastric heteroses expresses genes normally absent from the mesenchyme of the small intestine but present in the stomach mesoderm. The demonstration of such gene expression would prove the existence of mesenchymal responsiveness to overlying gastric endodermal signals and indicate that the primary signal for gut differentiation is of endodermal origin.

We have chosen the gene *Barx1* as a marker of gastric mesoderm since it is involved in defining the stomach phenotype. Kim et al. [8] have shown that it is expressed in the mesoderm of the developing stomach and not in that of the intestine. Furthermore, null mutation of *Barx1* results in underdevelopment and malrotation of the stomach together with a disorganisation of the gastric mucosa and an anterior homeotic shift of the duodenum [9].

2. Materials and methods

2.1. Animals

$Cdx2^{+/-}$ embryos were obtained from matings of $Cdx2^{+/-}$ [10] males with C57BL6 females and timed from the morning of the day when a vaginal plug was found. $Cdx2^{-/-}$ chimaeric embryos were obtained as described previously [4].

2.2. RT-PCR

Intestines were dissected and RNA extracted using an RNeasy kit (Qiagen). RNA was reverse transcribed using oligo-(dT) and Superscript™ III reverse transcriptase (Invitrogen). Reddy mix (AB gene) was used for the amplification of *Barx1* and *Gapdh* and PuRe Taq Ready-To-Go™ PCR Beads (GE Healthcare) for *Sox2* amplification. Primers were; *Barx1*: 5′-GCCTGAGCCAGTTACAGGTG-3′ and 5′-TGTCTCTTCGGTCGCCTCTG-3′, *Sox2*: 5′-TAGCACTTGTTGCCAGAACG-3′ and 5′-CCTTTTCTCTTCTCGCCGAA-3′ [11], *Gapdh*: 5′-AGGTCGGTGTGAACGGATTTG-3′ and 5′-ACTGGAGTTGATGTACCAGATGT-3′. Cycling parameters were: 35 cycles of 95 °C (30 s), 61.1 °C (*Barx1* and *Sox2*) or 55 °C (*Gapdh*; 30 s) and 72 °C (1 min).

2.3. In situ hybridisation and immunohistochemistry

Whole mount in situ hybridisation with digoxigenin probes was as described [12]. *Sox2* probes were generated from an I.M.A.G.E. clone (MRC Geneservice: I.D. 6413283) and the *Barx1* probes from a plasmid donated by Prof. P. Sharpe. Sections following DIG labelling were counterstained with Nuclear Fast Red or Haematoxylin and Eosin (H&E). For radiolabelling, embryonic intestines were fixed in 4% paraformaldehyde or methacarn, embedded in 2% agarose and subsequently in paraffin, and serial sectioned at 8 μm. Adjacent sections were hybridised with *Sox2* or *Barx1* ^{35}S-UTP-radiolabelled probes. Slides were dipped in Ilford K5 Nuclear Emulsion (Agar Scientific)

*Corresponding author. Fax: +44 (0)116 2297018.
E-mail address: fb22@le.ac.uk (F. Beck).

0014-5793/$34.00
doi:10.1016/j.febslet.2008.06.024

and left in the dark for 10 days before development in Kodak D-19 developer. Slides were counterstained with 1:100 Giemsa solution for 1 min. Adjacent sections were processed for immunohistochemistry with a Cdx2 antibody as described [1,13].

3. Results

3.1. Nascent areas of heterotopic endoderm can be localised using Sox2 as a marker

Sox2 is expressed in the stomach of the embryo [14]. Within the stomach, *Sox2* expression initially extends up to, but not including, the duodenum. Heterotopic lesions of stomach endoderm in the paracaecal region of the E12–E16 embryos cannot be detected histologically. *Sox2* was therefore used to determine their position. Whole mount in situ hybridisation was chosen for this purpose because it allowed the entire gut to be investigated at once. Hybridisation of the embryonic stomach indicated the specificity of the Sox2 probe (see Fig. S1 in the supplementary material). In $Cdx2^{+/-}$ gut at E12.5, E14.5 and E16.5 we detected on average 8 circumscribed regions of *Sox2* expression (Fig. 1A–D). We also detected discrete areas of *Sox2* expression in the midgut of an E12.5 $Cdx2^{-/-}$//WT chimaera (Fig. 1E).

3.2. Barx1 expression can be detected in the midgut of embryos expressing ectopic Sox2

Since *Sox2* expressing areas of heterotopia were detected in $Cdx2^{+/-}$ and $Cdx2^{-/-}$//*WT* embryos, the nature of the gut mesoderm was investigated. Using expression of the *Barx1* gene as a marker for stomach mesoderm, we first performed semi-quantitative RT-PCR. RNA was prepared from the paracaecal region of $Cdx2^{+/-}$ embryos at E14.5 and E16.5 and was subjected to RT-PCR using primers for *Sox2*, *Barx1* and *Gapdh* as a control. *Barx1* and *Sox2* transcripts were detected in E14.5 $Cdx2^{+/-}$ midgut (Fig. 2) and similar results were obtained in E16.5 $Cdx2^{+/-}$ midgut (data not shown). At these stages the heterotopic lesions are very small (Fig. 1) so negative PCR results were obtained in some embryos.

3.3. Barx1 expression mirrors Sox2 expression

To further investigate *Barx1* expression, whole mount in situ hybridisation with a *Barx1* DIG-labelled RNA probe was

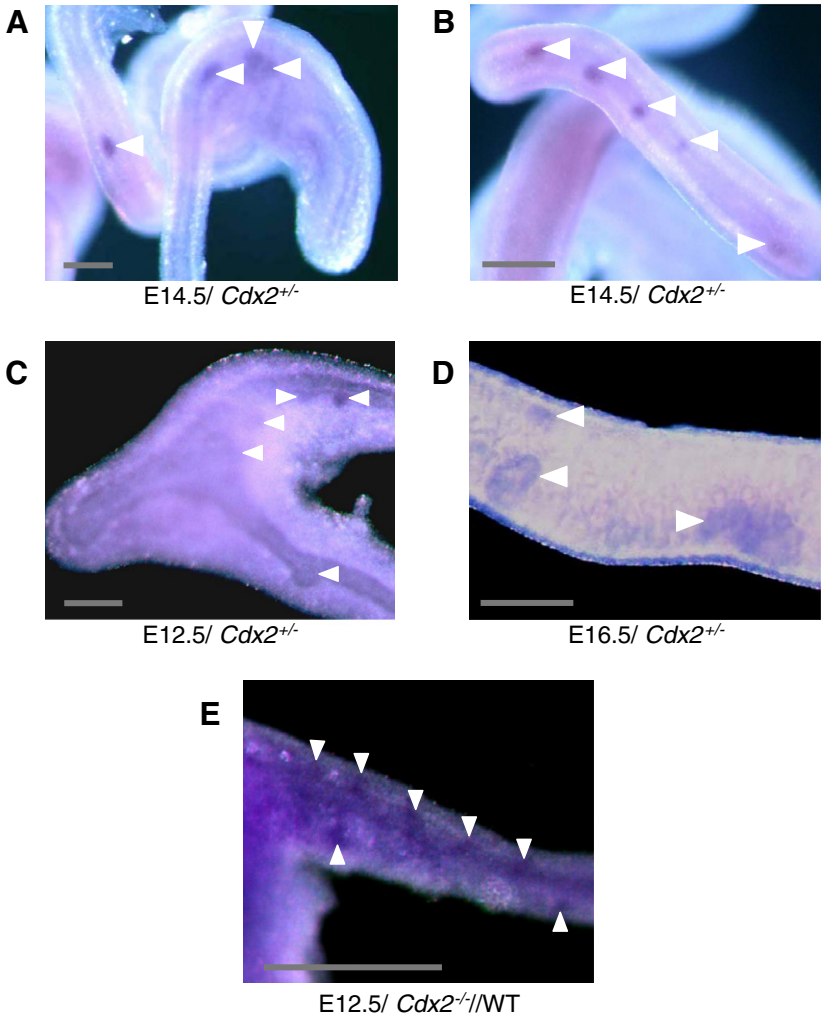

Fig. 1. Detection of areas of heterotopia using *Sox2*. Whole mount in situ hybridisation using a DIG-labelled *Sox2* antisense RNA probe to detect nascent areas of heterotopia. (A) E14.5 $Cdx2^{+/-}$ embryonic caecum; (B) E14.5 $Cdx2^{+/-}$ embryonic small intestine; (C) E12.5 $Cdx2^{+/-}$ embryonic caecum; (D) E16.5 $Cdx2^{+/-}$ embryonic small intestine; (E) E12.5 $Cdx2^{-/-}$//WT embryonic proximal colon. The arrows indicate regions of *Sox2* expression; these regions are deduced to be regions of stomach endoderm developing in the intestine. Scale bars = 500 μm.

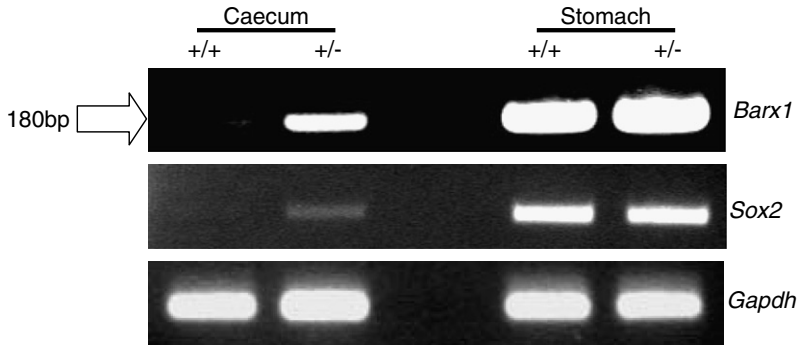

Fig. 2. RT-PCR to detect *Barx1* expression. The $Cdx2^{+/-}$ caecum expresses *Barx1*, whilst the $Cdx2^{+/+}$ caecum does not. Consistent with the results from Fig. 1, *Sox2* was also shown to be expressed in the $Cdx2^{+/-}$ caecum. RT-PCR for *Gapdh* confirmed all samples PCR amplified with equal efficiency and that there was equal gel loading. *Note:* The PCR primers for *Barx1* were more efficient than those for *Sox2*. Consequently, the *Sox2* band for the $Cdx2^{+/-}$ caecum sample is relatively faint, reflecting restricted areas of prospective gastric tissue intercalated into the normal paracaecal intestinal endoderm.

used. Hybridisation to stomach mesoderm to confirm specificity of the *Barx1* probe was consistent with the data of Kim et al. (2005) (see Fig. S2 in supplementary material). As with *Sox2*, *Barx1* expression was detected in a similar number of circumscribed sites in the midgut of E14.5 $Cdx2^{+/-}$ embryos (Fig. 3A and B). Similar results were obtained with embryos at E12.5 (not shown) and E16.5 (Fig. 3C). E14.5 and E16.5 $Cdx2^{-/-}$//WT embryos also contained regions of intestinal *Barx1* expression (Fig. 3D–F) in regions where engraftment of the $Cdx2^{-/-}$ cells had occurred. Generally, the intensity of staining with DIG-labelled probes was not strong enough for visualisation following sectioning. However, sections from one E14.5 $Cdx2^{-/-}$//WT embryo (Fig. 3E and F) enabled us to visualise the *Barx1* label and to demonstrate that staining was confined to the mesoderm (Fig. 3G and H).

3.4. Sox2 marks heterotopic endoderm and Barx1 marks heterotopic mesoderm

Having demonstrated areas of both *Sox2* and *Barx1* expression in the intestines of $Cdx2^{+/-}$ and $Cdx2^{-/-}$//WT embryos, we used ^{35}S-radiolabelled probes to demonstrate co-localisation of expression at a histological level. We tested the specificity of the radiolabelled probes by performing in situ hybridisation of sections prepared from embryonic stomach (see Fig. S3 in supplementary material) and confirmed confinement of *Sox2* expression to the stomach endoderm and *Barx1* expression to the stomach mesoderm. Random adjacent sections from caecal and paracaecal areas of an E16.5 $Cdx2^{+/-}$ embryo and an E14.5 $Cdx2^{+/-}$//WT embryo were then subjected to hybridisation either with the *Sox2* or *Barx1* probes. Co-localisation of *Barx1* and *Sox2* expression was clearly demonstrated in E16.5 $Cdx2^{+/-}$ gut (Fig. 4A) and in E14.5 $Cdx2^{-/-}$//WT gut (Fig. 4B). Sections from the chimaeric specimen were also stained with a Cdx2 antibody (Fig. 4B), demonstrating the absence of Cdx2 in the heterotopic endoderm together with normal expression of the protein in the surrounding normal intestinal tissue.

4. Discussion

The gut has not undergone histodifferentiation into stomach or intestinal morphology by E14, although changes in gene expression present at E12 suggest modulation as the basis of subsequent epithelial histogenesis [15]. In order to determine the position of heterotopic gut lesions prior to the development of overt histological changes we used *Sox2* as a marker. The gene is expressed throughout the embryonic mouse stomach endoderm at the stages investigated in this study but by E18.5 it becomes restricted to the forestomach region as histodifferentiation of the gastric corpus progresses [14]. It is therefore reasonable to assume that the lesions will be *Sox2* positive irrespective of their ultimate fate in terms of gastric differentiation.

Mesenchymally expressed *Barx1* is necessary for the differentiation of the overlying endoderm into a normal stomach phenotype [8]. The gene causes expression of the Wnt antagonists sFRP1 and 2 and the resulting downregulation of canonical Wnt signalling permits the development of stomach specific epithelium. Loss of Wnt expression probably results in downregulation of *Tcf1* and *Tcf4* and loss of *Cdx2* expression. In this connection, Gregorieff et al. [16] have shown that compound $Tcf4^{-/-}/Tcf1^{-/-}$ mutant embryos demonstrate intestinal defects and an anteriorisation of the gastro-intestinal tract, indicated by expression of *Sox2* and loss of expression of *Cdx2*. The demonstration of *Barx1* expression in the mesenchyme associated with the heterotopic lesions of $Cdx2^{-/-}$// WT chimaeras indicates that the absence of endodermal *Cdx2* expression initiates a cascade that allows mesenchymal *Barx1* expression. Kim et al. [9] showed expression of numerous intestinal genes including *Cdx2* in the disorganised distal region of the 'stomach' mucosa of *Barx1* null mutants indicating the existence of a negative feedback loop between mesenchymal *Barx1* and endodermal *Cdx2* expression that may explain the persistence of focal areas of gastric heterosis in the paracaecal region of $Cdx2^{+/-}$ heterozygotes. It may also account for the observation [5] that the number of such lesions does not increase post-natally since *Barx1* is reported to be downregulated in the stomach after E18.5 of gestation [8].

The events described here indicate some of the molecular events underlying the histogenesis of stomach and intestinal mucosa. It remains to be seen whether conditional inactivation of *Cdx2* in the adult gut results in the reactivation of mesenchymal *Barx1* expression in mesenchymal cells that might constitute a reservoir of undifferentiated cells that are capable of conferring a degree of plasticity in the adult.

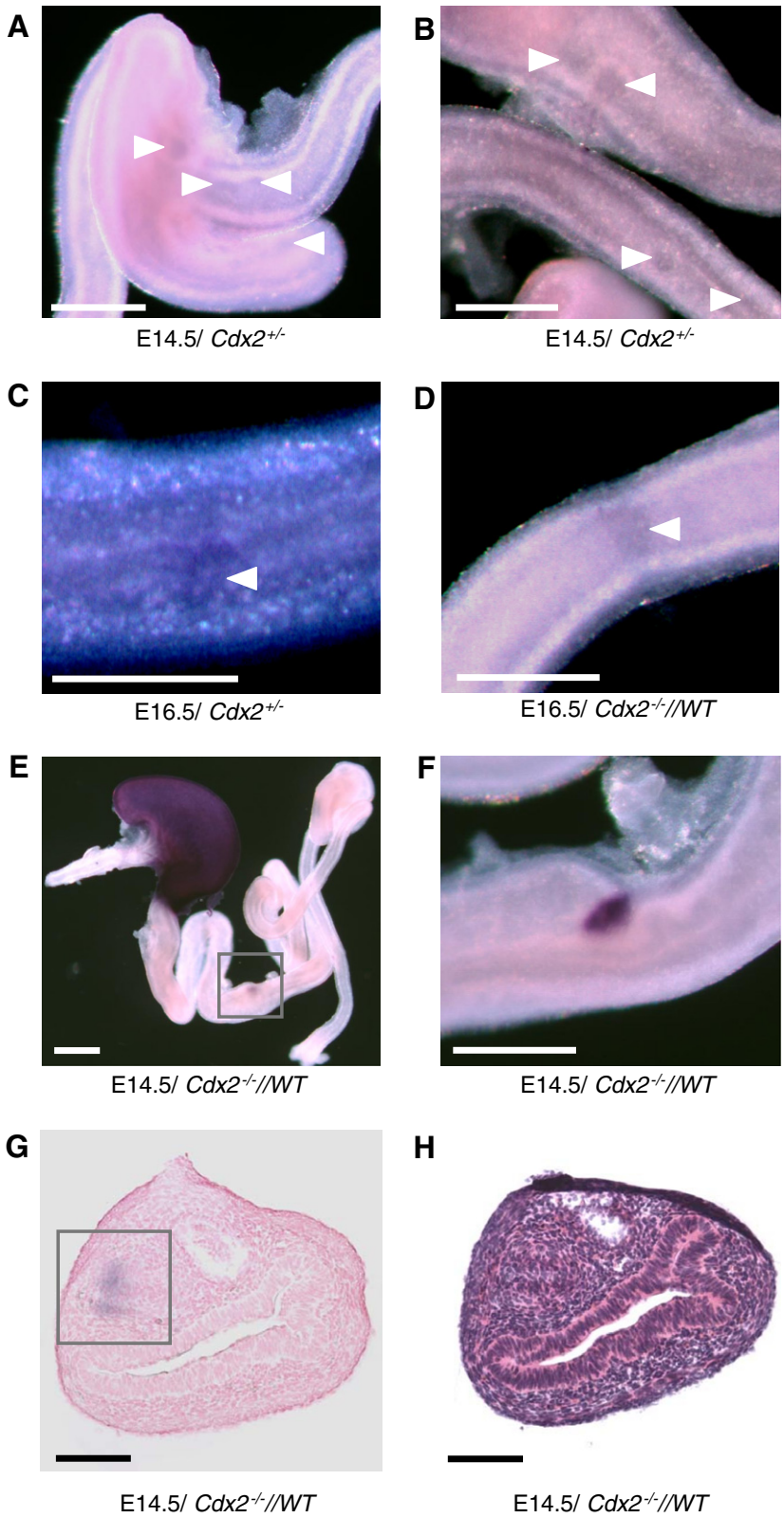

Fig. 3. *Barx1* labelling of embryonic gut. Whole mount in situ hybridisation using a DIG-labelled *Barx1* antisense RNA probe. (A and B) E14.5 $Cdx2^{+/-}$ embryonic gut. The *Barx1* probe labelled areas of the paracaecal region (A) and small intestine (B). (C) E16.5 $Cdx2^{+/-}$ small intestine. The *Barx1* probe detected a similar number of discrete regions to those shown with the *Sox2* antisense probe. (D) E16.5 $Cdx2^{-/-}$//*WT* small intestine showed one region of *Barx1* expression. The number of regions of gastric heterosis is dependent upon engraftment of $Cdx2^{-/-}$ cells into the gut. (E and F) E14.5 $Cdx2^{-/-}$//*WT* embryo showed one region of *Barx1* labelling in a thickened area midway along the small intestine. (G and H) The thickened intestinal region (E and F) was transversely sectioned through the *Barx1* labelled region and sections stained with Nuclear Fast Red (G) or H&E (H). The *Barx1* label is clearly confined to the mesoderm. (White scale bars = 500 μm; black scale bars = 100 μm.)

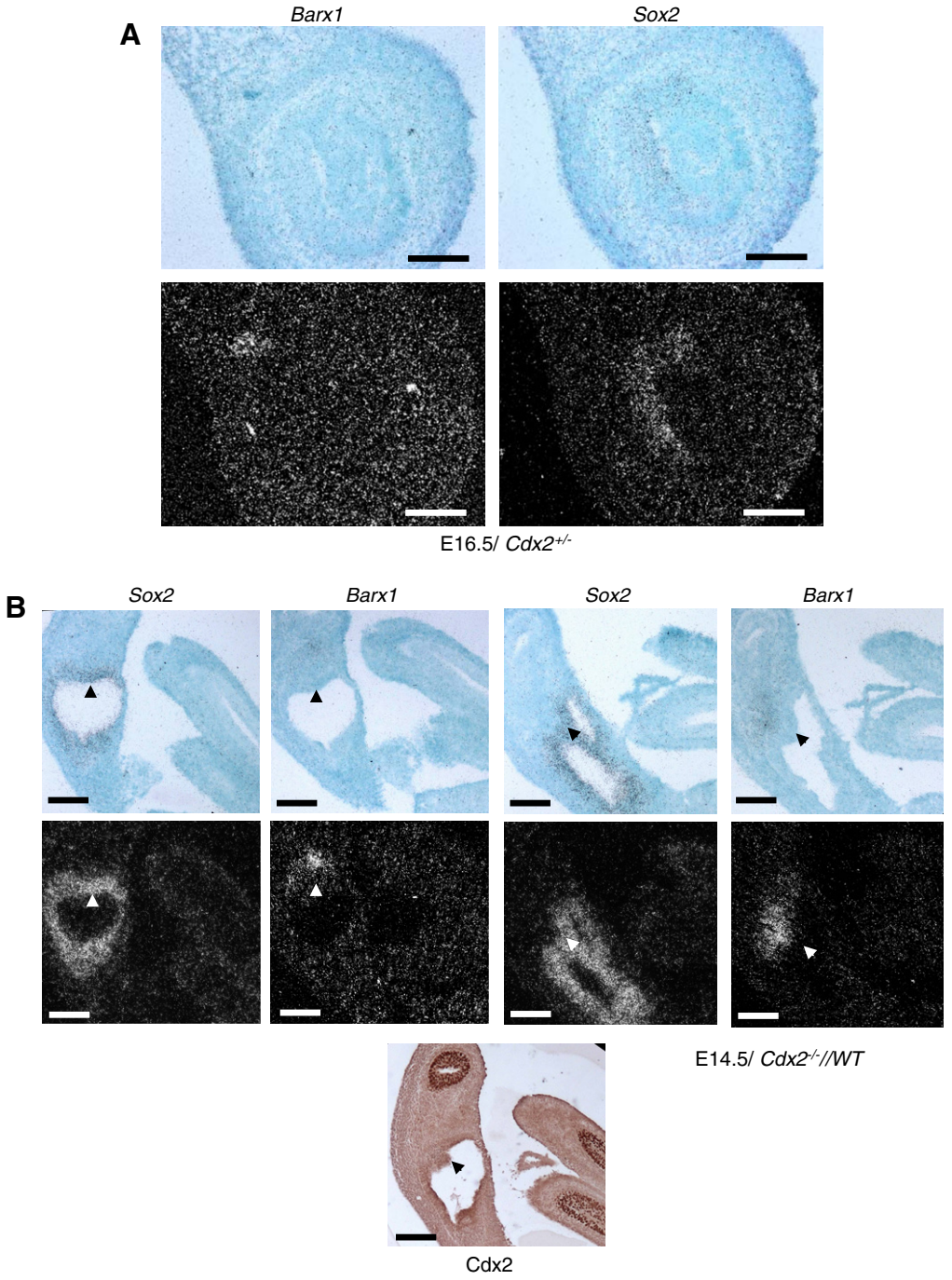

Fig. 4. *Barx1* and *Sox2* expression are co-localised in the *Cdx2* mutant embryonic gut. Sections were subjected to in situ hybridisation with *Sox2* or *Barx1* radiolabelled probes and visualised under brightfield (top panels) and darkfield (bottom panels). (A) E16.5 $Cdx2^{+/-}$ embryonic caecum. The position of the *Barx1* labelled region is adjacent to the *Sox2* labelled region. (B) E14.5dpc $Cdx2^{-/-}$//WT chimaeric caecum. Again, the position of the *Barx1* labelled region can be seen to be adjacent to the *Sox2* labelled region. A parallel section was also labelled with the *Cdx2* antibody (bottom panel) and the absence of *Cdx2* in the endoderm expressing *Sox2* indicates this region does not express *Cdx2* while adjacent endoderm does. Arrowheads indicate the same region, progressing through the serial sections. Scale bars = 100 μm.

We show that absence of *Cdx2* expression in the endoderm of the gut tube is associated with the expression of *Barx1* in the underlying mesoderm and the subsequent histodifferentiation of stomach mucosa. To this extent the primary signal for histodifferentiation of the gut mucosa is endodermal in origin. However, little is known about the initial A-P patterning of the endoderm prior to gut tube formation. Wells and Melton [17] have shown that FGF4 expressed in primitive streak mesoderm can induce differentiation of the adjacent endoderm in a concentration dependent manner and Dessimoz et al. [18] have shown that FGF signals establish initial gut tube domains along the A-P axis of the chick embryo. Cad homologues have been reported as downstream of FGF in all three germ layers and in numerous vertebrate species [2,19–21]. It seems

reasonable therefore to suggest that the mesodermal FGF gradient initiated at gastrulation might be involved in establishing the *Cdx2* expression domain in gut endoderm. In turn, endodermal Cdx2 protein then initiates a molecular cascade involving endodermal and mesodermal cross-talk leading to suppression of *Barx1* in the adjacent mesoderm and resulting in the final specification of intestinal mucosa.

Acknowledgements: E.J.S. is funded by a BBSRC PhD studentship. F.B. is in receipt of a project grant from AICR.

Supplementary material

Supplementary data associated with this article can be found, in the online version, at doi:10.1016/j.febslet.2008.06.024.

References

[1] Beck, F., Erler, T., Russell, A. and James, R. (1995) Expression of Cdx-2 in the mouse embryo and placenta: possible role in patterning of the extra-embryonic membranes. Dev. Dynam. 204, 219–227.
[2] Chawengsaksophak, K., de Graaff, W., Rossant, J., Deschamps, J. and Beck, F. (2004) Cdx2 is essential for axial elongation in mouse development. Proc. Natl. Acad. Sci. USA 101, 7641–7645.
[3] Mutoh, H. et al. (2002) Conversion of gastric mucosa to intestinal metaplasia in Cdx2-expressing transgenic mice. Biochem. Biophys. Res. Commun. 294, 470–479.
[4] Beck, F. et al. (2003) A study of regional gut endoderm potency by analysis of Cdx2 null mutant chimaeric mice. Dev. Biol. 255, 399–406.
[5] Beck, F., Chawengsaksophak, K., Waring, P., Playford, R.J. and Furness, J.B. (1999) Reprogramming of intestinal differentiation and intercalary regeneration in Cdx2 mutant mice. Proc. Natl. Acad. Sci. USA 96, 7318–7323.
[6] Kedinger, M., Duluc, I., Fritsch, C., Lorentz, O., Plateroti, M. and Freund, J.N. (1998) Intestinal epithelial–mesenchymal cell interactions. Ann. N.Y. Acad. Sci. 859, 1–17.
[7] Kedinger, M., Lefebvre, O., Duluc, I., Freund, J.N. and Simon-Assmann, P. (1998) Cellular and molecular partners involved in gut morphogenesis and differentiation. Philos. Trans. R. Soc. Lond. B: Biol. Sci. 353, 847–856.
[8] Kim, B.M., Buchner, G., Miletich, I., Sharpe, P.T. and Shivdasani, R.A. (2005) The stomach mesenchymal transcription factor Barx1 specifies gastric epithelial identity through inhibition of transient Wnt signaling. Dev. Cell 8, 611–622.
[9] Kim, B.M., Miletich, I., Mao, J., McMahon, A.P., Sharpe, P.A. and Shivdasani, R.A. (2007) Independent functions and mechanisms for homeobox gene Barx1 in patterning mouse stomach and spleen. Development 134, 3603–3613.
[10] Chawengsaksophak, K., James, R., Hammond, V.E., Kontgen, F. and Beck, F. (1997) Homeosis and intestinal tumours in Cdx2 mutant mice. Nature 386, 84–87.
[11] Wislet-Gendebien, S., Hans, G., Leprince, P., Rigo, J.M., Moonen, G. and Rogister, B. (2005) Plasticity of cultured mesenchymal stem cells: switch from nestin-positive to excitable neuron-like phenotype. Stem Cells 23, 392–402.
[12] Wilkinson, D. (1992) In Situ Hybridisation: A Practical Approach, IRL Press, Oxford, pp. 75–83.
[13] James, R., Erler, T. and Kazenwadel, J. (1994) Structure of the murine homeobox gene cdx-2. Expression in embryonic and adult intestinal epithelium. J. Biol. Chem. 269, 15229–15237.
[14] Que, J. et al. (2007) Multiple dose-dependent roles for Sox2 in the patterning and differentiation of anterior foregut endoderm. Development 134, 2521–2531.
[15] Hu, M. and Shivdasani, R. (2005) Overlapping gene expression in fetal mouse intestine development and human colorectal cancer. Cancer Res. 65, 8715–8722.
[16] Gregorieff, A., Grosschedl, R. and Clevers, H. (2004) Hindgut defects and transformation of the gastro-intestinal tract in Tcf4(−/−)/Tcf1(−/−) embryos. EMBO J. 23, 1825–1833.
[17] Wells, J.M. and Melton, D.A. (2000) Early mouse endoderm is patterned by soluble factors from adjacent germ layers. Development 127, 1563–1572.
[18] Dessimoz, J., Opoka, R., Kordich, J.J., Grapin-Botton, A. and Wells, J.M. (2006) FGF signaling is necessary for establishing gut tube domains along the anterior–posterior axis in vivo. Mech. Dev. 123, 42–55.
[19] Pownall, M., Tucker, A., Slack, J. and Isaacs, H. (1996) eFGF, Xcad3 and Hox genes form a molecular pathway that establishes the anteroposterior axis in Xenopus. Development 122, 3881–3892.
[20] Bel-Vialar, S., Itasaki, N. and Krumlauf, R. (2002) Initiating Hox gene expression: in the early chick neural tube differential sensitivity to FGF and RA signaling subdivides the HoxB genes in two distinct groups. Development 129, 5103–5115.
[21] Keenan, I.D., Sharrard, R.M. and Isaacs, H.V. (2006) FGF signal transduction and the regulation of Cdx gene expression. Dev. Biol. 299, 478–488.